# THE ROLE OF TUMOUR-ASSOCIATED MACROPHAGES IN PANCREATIC CANCER

**Dr Shanthini Crusz**

Thesis submitted for the degree of

**Doctor of Philosophy**

at the Queen Mary, University of London

Centre for Stem Cells in Cancer & Ageing
John Vane Science Centre
Barts Cancer Institute
Queen Mary University of London
EC1M 6BQ

# Abstract

Pancreatic ductal adenocarcinoma is a highly desmoplastic tumour, and non-malignant stromal cells contribute to progression and treatment resistance. Inflammatory cells in particular are known drivers of carcinogenesis, and macrophages are one of the most abundant inflammatory leucocytes. Therefore, exploring how macrophages drive tumour progression in pancreatic cancer would not only aid in understanding disease biology but could also offer insight to novel treatment strategies.

Results presented in this thesis show macrophages secrete factors that drive epithelial-to-mesenchymal transition, promote invasion and lead to expression of checkpoint inhibitors.

To determine what factors were driving this phenotype, the serine protease inhibitor SerpinB3 was initially explored, as it was highly upregulated in cancer cells cultured with conditioned media from macrophages. However, SerpinB3 gene overexpression and knockdown did not confirm a direct role for this gene in mediating migration and invasion.

Further investigation revealed macrophages were secreting the cytokine oncostatin M, which was driving a metastatic phenotype through activation of the STAT3 pathway. Expression of oncostatin M receptor was upregulated in cancer cells following culture with macrophage conditioned media and conferred a worse prognosis in patient samples. STAT3 pathway activation by oncostatin M led to increased invasion *in vitro*, particularly of the highly tumourigenic cancer stem cell population, and increased metastasis *in vivo*. Moreover, oncostatin M mediated expression of the immune 'checkpoint' inhibitors on the surface of pancreatic cancer cells. Using antibody and small molecule inhibitors, reversion of these signalling pathway effects were seen and preliminary data from *in vivo* assays showed decreased metastasis formation with cytokine receptor antibody inhibition.

Overall, the findings in this thesis contribute to emerging knowledge of how tumour associated macrophages drive tumour progression in pancreatic adenocarcinoma. Not only do they promote invasion and metastatic potential through oncostatin M secretion, but also potentiate inherent biological properties of cancer stem cells and assist in immune tolerance. In addition, results provide preliminary data to support a rationale for clinical targeting of macrophage-derived oncostatin M in pancreatic cancer.

# Statement of Originality

The work presented in this thesis is the original work of the author, Shanthini Crusz. Contributions by other persons have been acknowledged where necessary.

# Funding

This work was supported by a clinical research fellowship from Cancer Research UK.

# Acknowledgements


| | |
|---|---|
| **Supervisors** | |
| Professor Christopher Heeschen | Centre Lead, Centre for Stem Cells in Cancer & Ageing, Barts Cancer Institute. |
| Professor Frances Balkwill | Centre Lead, Centre for Cancer and Inflammation, Barts Cancer Institute. |
| Dr Sara Trabulo | Post-doctoral Research Assistance, Centre for Stem Cells in Cancer & Ageing |
| **Co-workers** | |
| Dr Patricia Sancho | Group Leader, IIS Aragón, Zaragoza, Spain. Assistance with *in vivo* experiments and guidance with scientific direction. |
| Mr Andrew Palfreeman | Lab Manager, Centre for Stem Cells in Cancer & Ageing. Assistance with macrophage culture, generation of conditioned media and ELISAs. |
| Dr Meng-Lay Lin | Post-doctoral Research Assistance, Centre for Stem Cells in Cancer & Ageing. Performed KEGG and TCGA data analysis. |
| Dr Matthieu Schoenhals | Post-doctoral Research Assistance, Centre for Stem Cells in Cancer & Ageing. Performed IPA analysis. |
| Dr Ming-hsin Yang | Clinical Research Fellow, Centre for Stem Cells in Cancer & Ageing. Acquired and cultured CTC cells. |
| Professor Hemant Kocher | Professor of Liver & Pancreas Surgery, Tumour Biology. Assistance with access to TMA and patient bloods samples. |
| Mr Ahmet Imrali | Research Assistance, Tumour Biology. Assistance with collection of patient bloods samples and ethics. |
| Mr Andrew Clear | Research Assistance, Centre for Haemato-Oncology. Performed staining and gave expert advice on Ariol Imaging Analysis of patient tissue. |
| Mr George Elia | Pathology Manager, Pathology Services. Performed IHC of *in vivo* tissue. |
| Dr Rebecca Pike | FACS Manager, Flow Cytometry Department. Performed live cell sorting. |
| **Collaborations** | |
| Professor Stephan Hahn | Professor of Molecular Gastrointestinal Oncology, Ruhr-University Bochum. Performed microarray gene analysis. |

# With special thanks

I would like to thank my supervisor, Professor Chris Heeschen, for offering me the opportunity to undertake this PhD project and for giving me the freedom to choose the direction of my research under his expert guidance. I would also like to thank my second supervisor, Professor Fran Balkwill, for providing feedback and advice throughout my project.

Special thanks to Dr Sara Trabulo, for her never-ending patience, kindness, support, dedication and scientific expertise that have enabled me to learn and develop as a scientist.

I would also like to thank everyone from the Centre for Stem Cells in Cancer & Ageing lab who have worked with me during the course of my PhD. In particular, Dr Patricia Sancho for her scientific discussions and advice, Mr Andrew Palfreeman for his assistance in experimental work and helpful feedback, Dr Tony Bou-Kheir for his scientific expertise and support and Dr Shinelle Menezes for her encouragement and discussions. In addition, I would like to thank my PhD colleagues, Ming-hsin Yang and Petra Jagušt, for their comradeship and support.

Finally, I would like to thank my family for the endless love and encouragement they provided me throughout my PhD.

# Dedication

I would like to dedicate this work to Dr Thomas Aquinas Marinus Crusz, who would have been very proud.

# Table of Contents

# List of Figures

# List of Tables

# Abbreviations

| | |
|---|---|
| 5-FU | 5-fluorouracil |
| ADEX | Aberrantly Differentiated Endocrine Exocrine |
| AJCC | American Joint Committee on Cancer |
| BRCA | Breast Cancer Early Onset |
| CA19-9 | Carbohydrate Antigen 19-9 |
| CCL | CC chemokine ligands |
| CCR | Chemokine Receptor |
| CDA | Cytidine Deaminase |
| CDKN2A | Cyclin-Dependent Kinase Inhibitor 2A |
| CDKN2B | Cyclin-Dependent Kinase Inhibitor 2B |
| CK | Cytokeratin |
| CNTF | Ciliary Neurotrophic Factor |
| CRAN | Comprehensive R Archive Network |
| CRP | C-reactive protein |
| CRUK | Cancer Research UK |
| CSC | Cancer Stem Cell |
| CSF1 | Colony Stimulatory Factor 1 |
| CSF1R | Colony-Stimulating Factor-1 Receptor |
| CT | Computer Tomography |
| CT1 | Cardiotrophin-1 |
| CTC | Circulating Tumour Cell derived xenografts |
| CTC | Circulating Tumour Cell |
| CTLA4 | Cytotoxic T-Lymphocyte-Associated Protein 4 |
| CXCR | C-X-C chemokine receptor |
| DC | Dendritic Cell |
| DFS | Disease Free Survival |
| DLBCL | Diffuse Large B Cell Lymphoma |
| ECM | Extracellular Matrix |
| ELISA | Enzyme linked immunosorbant assay |
| EMA | European Medicine Agency |
| EMT | Epithelial-to-Mesenchymal Transition |
| ERK | Extracellular Signal-Regulated Kinase |
| ESPAC | European Study Group for Pancreatic Cancer |
| EUS | Endoscopy Ultrasound |
| FBS | Fetal Bovine Serum |
| FDR | False Discovery Rate |
| FHIT | Fragile Histidine Triad |
| GEMM | Genetically Engineered Mouse Models |
| GMCSF | Granulocyte Macrophage Colony Stimulating Factor |
| GMCSF | Granulocyte Macrophage Colony Stimulating Factor |
| gp130 | Glycoprotein 130 |

| | |
|---|---|
| gp130R | Glycoprotein 130 receptor |
| GSEA | Gene Set Enrichment Analysis |
| hCAP-18 / LL37 | Human cathelicidin |
| HER2/ERBB2 | Neuro/glioblastoma Derived Oncogene Homolog |
| HR | Hazard Ratio |
| HSC | Haemopoietic Stem Cell |
| IFN | Interferon |
| IHC | Immunohistochemistry |
| IL | Interleukin |
| IL6R | Interleukin 6 receptor |
| IPA | Ingenuity Pathway Analysis |
| ISG15 | Interferon Stimulated Gene 15 |
| JAK | Janus Kinase |
| KPC | $Kras^{G12D/+}p53^{R172H/+}$Cre recombinase+ |
| KRAS | v-Ki-ras2 Kirsten rat sarcoma viral oncogene homolog |
| LIF | Leukaemia Inhibitory Factor |
| LIFR | Leukaemia Inhibitory Factor receptor |
| LPS | Lipopolysaccharide |
| mAb | Monocloncal Antibody |
| MCM | Macrophage Conditioned Media |
| MCSF | Macrophage Colony Stimulating Factor |
| MET | Mesenchymal-to-Epithelial Transition |
| MFI | Mean Fluorescent Intensity |
| MHC | Major Histocompatibility Complex |
| M-MDSC | Monocyte-Related Myeloid-Derived Suppressor Cell |
| MMP | Matrix Metalloproteinase |
| MOA | Mechanism of Action |
| MRI | Magnetic Resonance Imaging |
| nal-I | Nanoliposomal Irinotecan |
| NAMP | Nicotinamide Phosphoribosyltransferase |
| NCCN | National Comprehensive Cancer Network |
| NES | Normalised Enrichment Score |
| NICE | National Institute of Clinical Excellence |
| NSCLC | Non-Small Cell Lung Cancer |
| NP | Neuropoietin |
| ORR | Overall Response Rate |
| OS | Overall Survival |
| OSM | Oncostatin M |
| OSMR | Oncostatin M receptor |
| PanIN | Pancreatic Intraepithelial Neoplasia |
| PBMC | Peripheral Blood Monocyte |
| PD-1 | Programme Death 1 |
| PDAC | Pancreatic Adenocarcinoma |
| PDL-1 | Programme Death Ligand 1 |

| | |
|---|---|
| PDX | Patient-Derived Xenografts |
| PFA | Paraformaldehyde |
| PFS | Progression Free Survival |
| PI3K | Phosphoinositide 3-Kinase |
| PP | Pancreatic Polypeptide |
| RR | Response Rate |
| RT qPCR | Quantitative Reverse Transcription Polymerase Chain Reaction |
| SAGE | Serial Analysis of Gene Expression |
| SCC | Squamous Cell Carcinoma |
| SCCA | Squamous Cell Carcinoma Antigen |
| SD | Standard Deviation |
| SEER | Surveillance, Epidemiology, and End Results |
| SEM | Standard Error Mean |
| SH2 | Src Homology 2 |
| SMAD4 | SMAD Family Member 4 |
| STAT | Signal Transducer and Activator Transcription |
| TAM | Tumour Associated Macrophages |
| TCGA | The Cancer Genome Atlas |
| TGF | Transforming Growth Factor |
| TGS | Total Gene Signature |
| TLR | Toll-like Receptor |
| TME | Tumour Microenvironment |
| TP53 | Tumour Protein 53 |
| $T_{reg}$ | Regulatory T cells |
| UPR | Unfolded Protein Reaction |

# Publications

To date, the following papers have been published that relate to work described in this thesis:

Crusz SM, Balkwill FB (2015) *Inflammation and Cancer: Advances and New Agents.* Nat Rev Clin Oncol. 2015; 12(10):584-96

Lonardo E, Cioffi M, Sancho P, Crusz SM, Heeschen C (2015) *Studying Pancreatic Cancer Stem Cell Characteristics for Developing New Treatment Strategies.* J Vis Exp 2015; (100):e52801

# 1 CHAPTER ONE: INTRODUCTION

## 1.1 Pancreatic Cancer

Pancreatic cancer has a median overall survival (OS) of less than six months and 5-year survival of less than 5% (Vincent et al. 2011). Although surgery offers the prospect of long-term survival, only 20% of pancreatic cancer patients have resectable disease at diagnosis, and even these patients have a 5-year survival rate of 15-20% (Oettle et al. 2013).

Several factors influence poor outcomes in pancreatic cancer, including the tendency for late stage at diagnosis, lack of validated screening tests and biomarkers, tumour genetic heterogeneity, dense stroma contributing to rapid tumour progression and ineffective treatment strategies (Kleeff et al. 2016).

Pancreatic cancer is set to surpass breast, prostate and colorectal cancer to become the third common cause of cancer death by 2030 (Rahib et al. 2014). Accordingly, there is an urgent unmet need to overcome the significant challenges at both a biological and clinical level to improve our understanding and outcomes of this devastating disease.

### 1.1.1 Anatomy and Physiology of Normal Pancreas

The pancreas is a retroperitoneal organ and has major functions in both digestion and glucose metabolism. 80% of the pancreas is composed of exocrine tissue and the remaining 20% is endocrine in origin.

The exocrine functions of the pancreas rely on two types of cells: acinar and ductal. Acinar cells constitute the bulk of the organ and are organised into grape-like clusters that produce digestive enzymes (Figure 1.1). The ducts add mucus and bicarbonate to this enzyme mixture, and empty into the duodenum.

The endocrine pancreas consists of four cells types; α-, β-, PP (pancreatic polypeptide) and δ- cells. These cells are organised into compact islets within acinar tissue and secrete hormone into the blood stream that are then dispersed throughout the body. α-

and β- cells produce glucagon and insulin to regulate glucose levels. PP and δ- cells secrete PP and somatostatin to regulate the secretory properties of the other cell types (Figure 1.1).

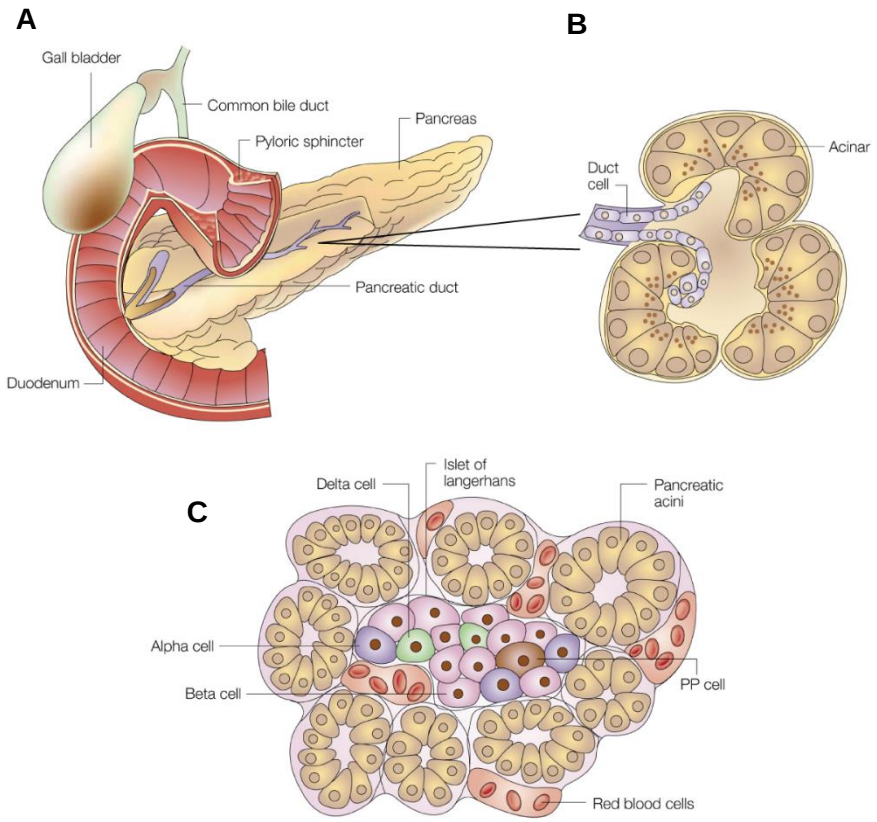


**Figure 1.1 Anatomy of the pancreas**
A) Anatomic location of the pancreas B) The exocrine pancreas composed of dutcal and acinar cells C) The endocrine pancreas composed of α-, β-, PP and δ- cells (taken from Bardeesy and DePinho, 2002).

### 1.1.2 Epidemiology and Risk Factors

Most recent figure estimates 8,319 new cases per year of pancreatic cancer in the UK (CRUK). Worldwide, the estimated 5-year prevalence of people living with pancreatic cancer is 4.1 per 100,000 (Ferlay et al. 2014). Incidence increases with age, and the peak in age-specific incidence rate is between 85-89 years (CRUK).

The vast majority of pancreatic tumours are sporadic (>80%), with only a minority associated with inherited germline mutations, BRCA2 being the most common (Ducreux et al. 2015). Several studies have established risk factors for pancreatic cancer, with smoking being the main acquired factor (overall relative risk 1.74), followed by obesity (Yeo 2015). Other risk factors associated include chronic pancreatitis and diabetes mellitus (Zavoral et al. 2011).

### 1.1.3 Histological Subtypes

Types of pancreatic cancers can be subdivided into the cell of origin, broadly exocrine vs. endocrine. The most common type is exocrine, and of these the overwhelming majority (90%) are adenocarcinomas. These cells originate from the epithelial cell lining of pancreatic duct and therefore form gland like structures. Mucinous tumours are the other exocrine subtype, accounting for <10% of all tumours. Endocrine pancreatic tumours are relatively uncommon, accounting for <5% of all pancreatic cancers (Fesinmeyer et al. 2005). Adenocarcinoma of the pancreas has the worst overall survival (Figure 1.2). As it is also the most common type of pancreatic tumour, focussing on pancreatic ductal adenocarcinoma (PDAC) is of great clinical importance to tackle poor outcomes.

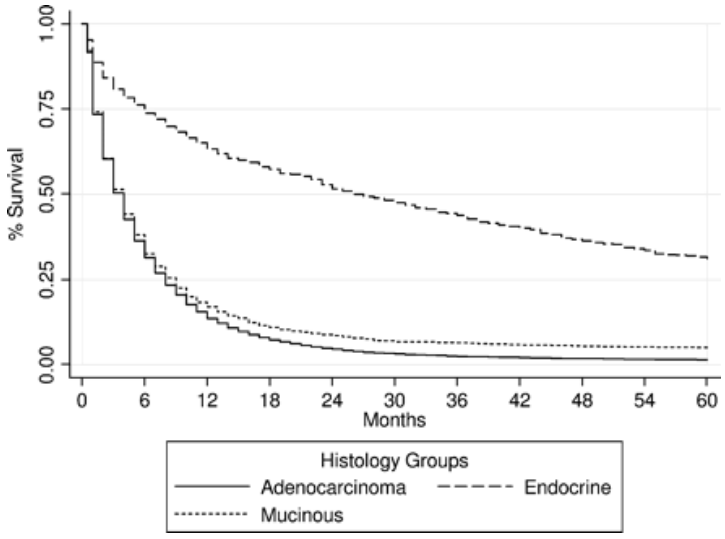


**Figure 1.2 Survival by histological subtype**
Kaplan Meier curves comparing 5-year survival in pancreatic histological subtypes; adenocarcinoma (n=31,357), mucinous (n=2,865) and endocrine (n=1,054) (taken from Feisimeyer *et al*.).

### 1.1.4 Molecular and Genomic Subtypes

There are commonly precursor lesions that develop prior to PDAC, which build an accumulation of mutations in both tumour suppressor and oncogenes that spur malignant progression. The most frequent precursors are microscopic pancreatic intraepithelial neoplasia (PanIN), which consist of microscopic (<5mm) mucinous-papillary lesions. These lesions eventually form invasive carcinoma through an adenoma-carcinoma sequence that leads to clonal expansion and subsequent acquisition of further mutations (Figure 1.3). The earliest activating mutation and most commonly mutated gene in PDAC is the KRAS oncogene (Li et al. 2004) (Table 1.1). Point mutations at codon 12 (from GGT to GAT or GTT, or more rarely CGT) occur in 75-97% of human PDAC (Almoguera et al. 1988).

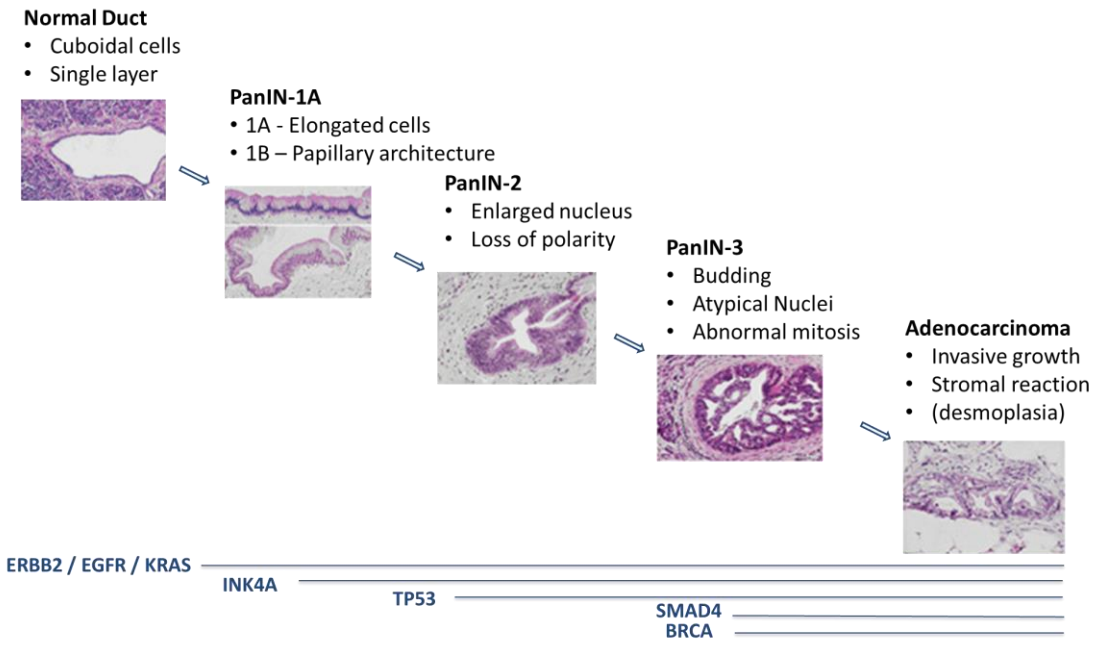


**Figure 1.3 Genetic progression model of PDAC**
(adapted from Biankin *et al*. 2012).

**Table 1.1 Common mutated genes in PDAC**
The most common genetic mutations in PDAC and frequency of mutation (modified from Li et al., 2004 and Bardeesy and DePinho, 2002).

| Gene | Type | Frequency |
|---|---|---|
| KRAS<br>(v-Ki-ras2 Kirsten rat sarcoma viral oncogene homolog) | Oncogene | 75-100% |
| HER2/ERBB2<br>(neuro/gliobastoma derived oncogene homolog) | Oncogene | 65-70% |
| TP53<br>(Tumour protein p53) | Tumour suppressor | 40-75% |
| SMAD4<br>(SMAD family member 4) | Tumour suppressor | 30% |
| CDKN2A<br>(cyclin-dependent kinase inhibitor 2A) | Tumour suppressor | 27-98% |
| CDKN2B<br>(cyclin-dependent kinase inhibitor 2B) | Tumour suppressor | 27-48% |
| BRCA<br>(breast cancer early onset) | Tumour suppressor | 7-10% |
| FHIT<br>(fragile histidine triad) | Tumour suppressor | 66-70% |

With rapid advancement in Next-Generation Sequencing technologies, it is now possible to compile whole-genome sequencing of established solid tumours to better analyse their mutational landscape. Several groups have undertaken whole genome sequencing in PDAC, revealing various molecular / genetic subtypes (Bailey et al. 2016; Collisson et al. 2011; Moffitt et al. 2015; Waddell et al. 2015). By identifying these new genetic subclasses, one can begin to understand patterns and biological behaviours in tumour subtypes, which may eventually lead to better prognostication and development of predictive therapies.

Two studies in particular have revealed important findings in relation to the tumour microenvironment (TME) and immune infiltrate in PDAC. Bailey *et al.* defined 4 PDAC subtypes: squamous, pancreatic progenitor, immunogenic and aberrantly differentiated endocrine exocrine (ADEX) (Bailey et al. 2016). Importantly, the immunogenic class of tumours was associated with a significant immune infiltrate, including macrophage gene signatures, which related to a worse OS (Figure 1.4). The immunogenic subclass of tumours demonstrated upregulation of immune related markers, such as programmed death-1 (PD-1) and cytotoxic T-lymphocyte-associated protein 4 (CTLA4), which relate to acquired tumour immune suppression pathways, inferring potential therapeutic targeting opportunities.

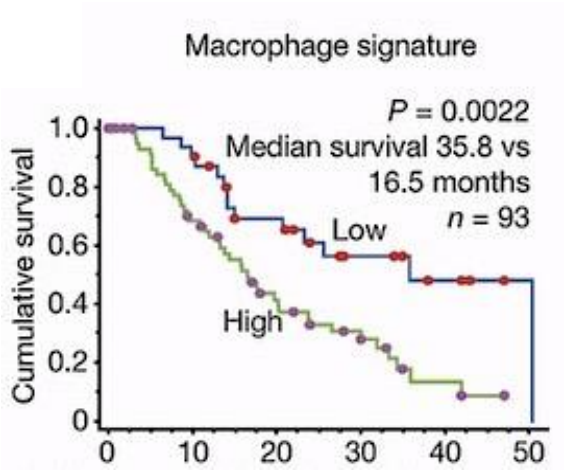


**Figure 1.4 Survival and macrophage gene signature in PDAC**
Kaplan Meier analysis comparing patients with high or low macrophage cell signature scores following integrated genomic analysis of 93 PDAC patients using combination of while-genome and deep-exome sequencing (taken from Bailey et al. 2016).

Moffit *et al.* performed microdissection of stromal vs. tumour tissue in individual patients to capture the precise involvement of each compartment relative to patient outcome. An 'activated' stromal subtype was found, which displayed diverse genes including those associated with macrophages, chemokine ligands, fibroblast activation genes and matrix metalloproteinases (MMPs). Importantly, when comparing patients with 'normal' or 'activated' stroma, the activated had a worse median survival compared to normal.

Both of these studies therefore imply that the non-cancer compartments of PDAC tumours, such as immune cells and stromal tissue, play an important role in clinical outcome and could allow for better-targeted therapies based on gene signature profiles.

### 1.1.5 Diagnosis and Staging

Early symptoms of pancreatic cancer commonly arise from mass effect. Primary tumours are situated either in the head, body or tail of the organ (Table 1.2), with head tumours likely to be diagnosed at an earlier stage due to bile duct / pancreatic duct obstruction causing jaundice (Ducreux et al. 2015). Other symptoms include abdominal pain, weight loss, steatorrhoea and new-onset diabetes.

**Table 1.2 Pancreatic tumour locations**

| Anatomic location | Frequency |
|---|---|
| Head | 60-70% |
| Body / Tail | 20-25% |
| Diffuse | 10-20% |

Various imaging modalities can be used to diagnose pancreatic cancer. Currently, the standard of care for investigation of a suspected pancreatic malignancy is computer tomography (CT) scan. Endoscopic ultrasound (EUS) can also be used for staging and biopsy. No clear benefit has been found for magnetic resonance imaging (MRI) over CT (Ducreux et al. 2015).

Blood tests are routinely carried out in a suspected diagnosis of pancreatic cancer. Serum carbohydrate antigen 19-9 (CA19-9) is increased in almost 80% of patients with advanced disease, and although prognostic (preoperative levels ≥500 IU/ml indicate worse prognosis after surgery), it is not reliable for diagnosis and is therefore not recommended as a marker for disease (Ducreux et al. 2015). As yet, there are no further biomarkers that aid diagnosis or prognostic outcomes.

Following confirmation of disease on cytology / histology, staging of pancreatic cancer is undertaken (Table 1.3). Staging is based on the size and extent of the primary tumour in relation to adjacent structures such as blood vessels, nodal involvement and distant metastasis. By staging disease, an assessment of whether it is resectable, borderline resectable or unresectable can be determined in a multidisciplinary setting. There are various definitions of what constitutes resectable disease, but broadly it is based on the absence of metastasis and the extent of blood vessel involvement;

tumours must have no contact with local arteries (coeliac axis, superior mesenteric artery or common hepatic) and have no or <180° contact with local veins (superior mesenteric vein or portal vein) (NCCN guidelines 2015).

**Table 1.3 American Joint Committee on Cancer (AJCC) staging of Pancreatic Cancer**

| | | |
|---|---|---|
| **Primary Tumour (T)** | **T0** | No evidence of primary tumour |
| | **Tis** | Carcinoma *in situ* |
| | **T1** | Tumour limited to the pancreas, ≤2 cm in greatest dimension |
| | **T2** | Tumour limited to the pancreas, >2 cm in greatest dimension |
| | **T3** | Tumour extends beyond the pancreas but without involvement of the coeliac axis or the superior mesenteric artery |
| | **T4** | Tumour involves the coeliac axis or the superior mesenteric artery |
| **Regional Lymph Nodes (N)** | **NX** | Regional lymph nodes cannot be assessed |
| | **N0** | No regional lymph node metastasis |
| | **N1** | Regional lymph node metastasis |
| **Distant Metastases (M)** | **M0** | No distant metastasis |
| | **M1** | Distant metastasis |

### 1.1.6 Treatment of Pancreatic Cancer

Once a pancreatic tumour has been deemed resectable, borderline resectable or unresectable, a treatment strategy can be formulated. Treatment is broadly divided into ‘curative’, in the case of resectable and borderline resectable disease, and ‘palliative’ in unresectable disease (Figure 1.5).

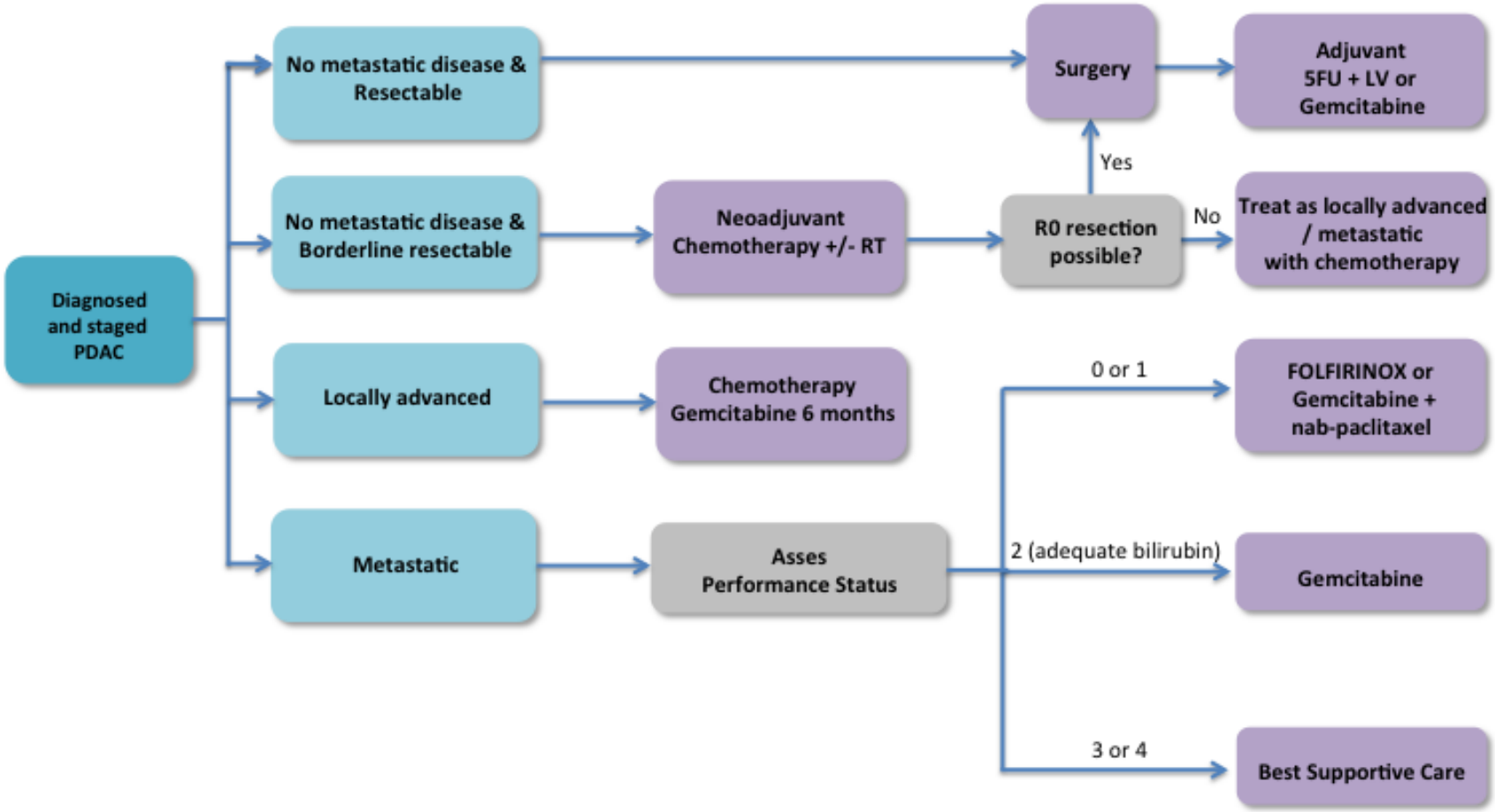


**Figure 1.5 Treatment strategy for pancreatic cancer**
Treatment of pancreatic cancer (based on ESMO guidelines - Ducreux et al. 2015). RT, radiotherapy; 5-FU, 5-fluorouracil; LV, leucovorin.

#### 1.1.6.1 Treatment of Resectable Disease

The only curative treatment of PDAC is surgical resection. Patients who have been assessed as having a high probability of R0 resection (i.e. resection margin negative) will proceed to surgery. Theoretically, neoadjuvant therapy could improve the prospect of an R0 resection by downstaging the primary tumour. However the benefits of neoadjuvant therapy in resectable disease remains unclear, especially as PDAC is a rapidly progressing cancer. One study has shown that 19% of patients classed as 'resectable' and given neoadjuvant therapy developed radiological metastatic disease by the end of treatment (White et al. 2001). Definitive answers to the questions surrounding neoadjuvant therapy for initially resectable disease will hopefully be answered by the Phase III NEOPA-study (NCT01900327), which is currently recruiting. This study aims to demonstrate an OS increase following neoadjuvant treatment (gemcitabine and radiation) vs. primary surgery alone in resectable non-metastatic patients.

The current standard practice for patients with resectable disease remains upfront surgery. Those with head of pancreas tumours undergo pancreatoduodenectomy (Whipple procedure). Patients with body or tail of pancreas tumours will undergo a distal pancreatectomy.

Several trials have investigated adjuvant treatment following surgery; The European Study Group for Pancreatic Cancer (ESPAC)-1 trial randomised patients following intended curative resection. Patients were assigned to one of four arms: exclusive adjuvant chemotherapy (bolus 5-fluorouracil (5-FU) and folinic acid), chemoradiation (split course 40Gy and 5-FU), chemoradiation followed by chemotherapy or surveillance alone (Neoptolemos et al. 2001). No significant differences were seen with adjuvant chemoradiation in patients who had undergone either R0 or R1 (i.e. positive resection margins following surgery) resections. However, a clear benefit of adjuvant chemotherapy was seen when taking R0 and R1 patients collectively, with a median survival of 19.7 months in the chemotherapy group compared to 14 months with no chemotherapy ($p=0.0005$). Following this study, CONKO-001 confirmed a benefit in disease free survival (DFS) with adjuvant chemotherapy. Patients receiving 6 months gemcitabine had a 13.4 month DFS compared to 6.7 months ($p<0.001$)

(Oettle et al. 2007). Subsequent follow up analysis of this study in 2013 proved a benefit in OS with adjuvant treatment, observing a 5-year OS of 20.7% in the treatment group compared to 10.4% in the control arm (p=0.01) (Oettle et al. 2013). Findings from these studies collectively support the use of adjuvant chemotherapy following surgical resection of localised disease.

When examining whether the type of adjuvant chemotherapy is important, ESPAC-3 compared gemcitabine or 5-FU and found no statistical differences between the two groups (Neoptolemos et al. 2010). However, the most recent data from ESPAC-4 has now determined a new standard of care of gemcitabine and capecitabine within 12 weeks of R0 and R1 surgery, as this regimen gave an improved OS compared to gemcitabine alone (Neoptolemos et al. 2017). Specifically in Japanese patients, the use of a novel chemotherapeutic agent, S-1, was shown to be superior to gemcitabine in the adjuvant setting (5-year OS of 24.5% with gemcitabine compared to 44.1% with S-1; $p<0.0001$). However, this agent has yet to be assessed in non-Asian patients. Results from adjuvant use of gemcitabine alone vs. gemcitabine with nab-paclitaxel are pending (NCT01964430).

Despite curative intent and benefits of adjuvant treatment, the outcome of patients with resectable disease remains extremely poor. There is a high chance of disease recurrence and the 5-year survival rate is 15-20% (Oettle et al. 2013). In addition, results from ESPAC-4 show at best a median survival of only 28 months with adjuvant treatment (Neoptolemos et al. 2017).

#### 1.1.6.2 Treatment of Borderline Resectable & Locally Advanced Disease

Limited data exists on the benefits of neoadjuvant treatment in patients with borderline resectable disease. The aim of this treatment is to limit residual disease after resection, reduce lymph node positive disease and treat micrometastasis. Two meta-analyses have explored outcome of pre-operative treatment in the form of chemotherapy, radiotherapy or chemoradiation (Assifi et al., 2011; Gillen et al. 2010). These analyses

could be criticised for including a heterogeneous mix of studies with both borderline resectable and resectable lesions included. However, despite this, improved R0 resections rates and promising survival rates were seen with neoadjuvant treatment in both studies. Therefore, although no clear consensus exists, patients with borderline resectable disease should be considered for chemotherapy followed by chemoradiation to downstage disease if they are unable to enrol in prospective clinical trials assessing neoadjuvant treatment.

Locally advanced tumours are those deemed unresectable in the absence of metastasis, and not potentially resectable with neoadjuvant treatments. The median OS for this group remains low (<1 year) and there is a lack of robust data to identify how best to treat this cohort of patients as no randomised prospective data exists. General consensus extrapolated from randomised trials in the metastatic setting is treatment with chemotherapy, either FOLFIRINOX or combination of gemcitabine+/-nab-paclitaxel (Conroy et al. 2011; Faris et al. 2013; Von Hoff et al. 2013). After response or stabilisation to chemotherapy is achieved, consolidation treatment with chemoradiation could be considered as a maintenance treatment in selected patients, especially following a capecitabine-based induction regimen (Mukherjee et al. 2013). In patients with good performance status and local progression only, locoregional treatment with chemoradiation or radiotherapy alone could be given if further chemotherapy (i.e. due to toxicity) is contraindicated (Salgado et al. 2017).

#### 1.1.6.3 Treatment of Metastatic Disease

The current therapeutic options for patients with Stage IV (i.e. metastatic) PDAC include single agent gemcitabine, gemcitabine in conjunction with nab-paclitaxel (abraxane) or combination FOLFIRINOX therapy.

Gemcitabine is a nucleoside analogue that competes with the naturally present deoxycytidine, a pyrimidine deoxynucleoside, to integrate into an elongating DNA chain. In advanced PDAC, gemcitabine improved OS compared to fluorouracil (5.6

vs. 4.4 months; p=0.002) and was thus used as standard of care for many years (Burris et al. 1997).

In 2010, the FOLFIRINOX schedule showed best-ever survival data in metastatic disease, with 11.1 months OS in the combination arm compared to 6.8 months with gemcitabine alone (hazard ratio (HR) 0.47; p<0.0001) (Conroy et al. 2011). However, despite an improved OS, progression free survival (PFS) and response rate (RR) compared to gemcitabine alone, this trial showed a less favourable toxicity profile, with significantly higher incidences of grade 3 or 4 toxicities. Consequently, although it showed the first real improvement in OS and PFS, this regimen is limited to younger patients with good performance state (0-1) only (Figure 1.5), and therefore only the minority of PDAC patients realistically receive it.

After many failed randomised trials with drugs in combination with gemcitabine alone, positive results were reported in 2013 when combining gemcitabine with nab-paclitaxel in metastatic patients (Von Hoff et al. 2013). Nab-paclitaxel in combination with gemcitabine compared to gemcitabine alone gave a better median OS (8.5 vs. 6.7 months HR 0.72; p<0.001), improved median PFS (5.5 vs. 3.7 months p<0.001) and a higher RR (23% vs. 7% p<0.001). Although neuropathy of grade 3 was greater in the combination group, this improved to grade 1 or lower in a median of 29 days. Therefore, this regime is also offered in the metastatic setting in place of single agent gemcitabine.

With regards to second-line treatment in the metastatic setting, the NAPOLI-1 study compared nanoliposomal irinotecan (nal-I), leucovorin, and infusional 5FU with leucovorin and infusional 5-FU alone and with nal-I alone following failure of gemcitabine-based chemotherapy. Combination treatment was better than single agent 5FU alone, with an improvement in OS from 4.2 to 6.1 months (HR, 0.67; P = 0.012) (Wang-Gillam et al. 2016). Therefore this treatment could be offered to fit patients following failure of first line therapy in the metastatic setting. This regime has gained approval from the European Medicine Agency (EMA) but has yet to receive NICE approval within the UK.

Despite advances in our understanding of chemotherapy, the median survival for patients with metastatic disease remains poor and at best 11.1 months (Conroy et al. 2011). Thus, the need for more effective therapies to prevent recurrence and treat metastatic progression in PDAC is required.

## 1.2 Cancer Metastasis

A metastasis is defined as colonisation of tumour cells from the primary site of cancer to a distant organ. For all tumour types, metastasis is arguably the greatest contributor to patient death (Steeg 2016). In PDAC, the vast majority of patients present with distant spread (SEER online data) defined as Stage IV disease (Figure 1.6). Median survival is 2-6 months and the 5-year survival rate is only 1-2% (CRUK). Even in the 5-25% of patients who present with resectable disease, there is a high chance of metastatic recurrence, with one study showing 46% of patients undergoing curative resection eventually presenting with distant metastasis (Fischer et al. 2012). These findings therefore suggest that even at the time of resection in localised disease, dissemination of cells from the primary site has occurred below the detection ability of imaging techniques, resulting in relapse and mortality. Adjuvant chemotherapy is given to reduce this occurrence, however the median survival in patients who undergo surgical resection remains only 12-20 months (Fischer et al. 2012), suggesting current therapies are inadequate.

Understanding the processes by which metastatic disease forms in PDAC is therefore vital. By doing so, new treatment strategies could be developed, particularly in the adjuvant setting, to improve the current poor survival outcomes.

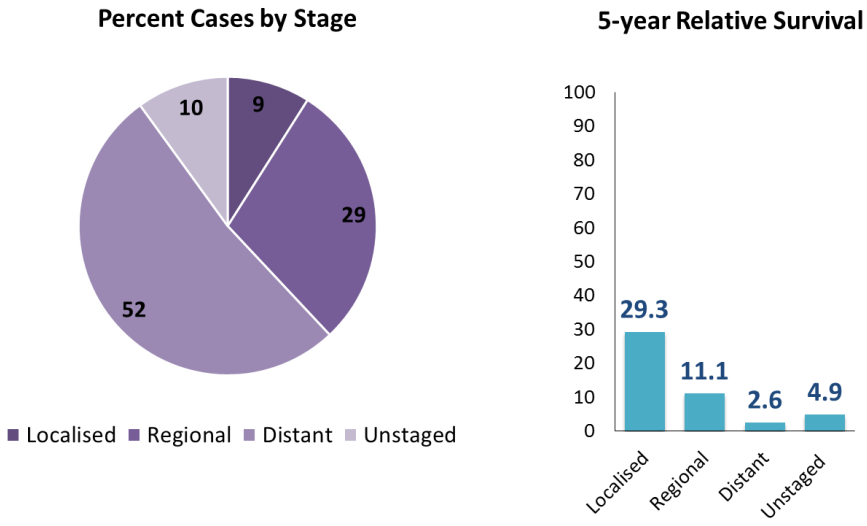


**Figure 1.6 Percentage and 5-year relative survival by stage at diagnosis**
Localised: confined to primary site; Regional: spread to regional lymph nodes; Distant: metastatic disease (adapted from SEER 18 2006-2012).

### 1.2.1 Invasion and Epithelial-to-Mesenchymal Transition

An important step in tumour progression to form metastasis is the acquisition of tumour invasion. Tumour cells initially invade the basement membrane to begin the process of metastasis. Invasion is therefore defined as proteolytic destruction of the ECM and increased motility. Once this initial step has taken place, tumour cells entering the bloodstream (either directly or via the lymphatic system) then extravasate the bloodstream to colonise distant sites. The original 'soil and seed' hypothesis was proposed by Paget 100 years ago (Paget 1889) and described how metastasis formed on the basis of 'seeds' (tumour cells) colonising 'congenial soil' (the metastatic microenvironment) to allow the progressive outgrowth of tumour cells at the distant site.

Many mechanistic pathways have been proposed for the initial 'seeding' and invasion of tumour cells from the primary site of disease. One of the most studied is epithelial-to-mesenchymal transition (EMT), a plastic biological process describing the loss of adherence and cell-cell junction in an epithelial cell towards a more mesenchymal cell phenotype, allowing motility. Within the field, this process has been described as critical for acquisition of malignant phenotype in epithelial cancer cells (Thiery 2002). EMT was first termed in the context of embryology, and subsequently three types are thought to exist; type 1 in embryogenesis, gastrulation and neural crest formation; type 2 is in tissue regeneration and wound healing; and type 3 in malignancy, invasion and metastasis (Kalluri and Weinberg 2009).

In type 3 EMT, there are extensive *in vitro* and *in vivo* data explaining the initiation of EMT by changes in regulatory pathways that lead to a loss of cellular adhesions, loss of apico-basal polarity, gain of front-rear polarity and detachment to allow the cells to locally invade. EMT is regulated by several 'master' regulator pathways, including signalling through transforming growth factor (TGF)-β, Notch and Wnt. Common to these pathways is the loss of E-cadherin and gain of transcription factors such as Twist1, Snail 1, Slug, Zeb1, Zeb2 and proteins such as Vimentin and Loxl2 (Craene and Berx 2013). Once activated, these transcription factors act pleiotropically to choreograph the EMT process and trigger a series of intracellular signalling networks involving, amongst others, ERK, MAPK, PI3K, Akt, Smads, RhoB, β-catenin,

lymphoid enhancer binding factor, Ras, and c-Fos as well as cell surface proteins such as β4 integrins, α5β1 integrin, and αVβ6 integrin (Tse and Kalluri 2007). Upregulation of enzymes that degrade the extracellular matrix (ECM) are induced, and cells undergo a robust reorganisation of the actin-cytoskeleton resulting in a change of shape. Despite a complex networking signalling, the key feature of EMT is the mesenchymal property of increased invasion and migration.

Some have argued that EMT is dispensable for metastasis in PDAC, given that genetic depletion of EMT-activators Snai1 or Twist1 had no effect in the $Kras^{G12D/+}p53^{R172H/+}$Cre recombinase+ (KPC) mouse model (Zheng et al. 2015). However, most recent data suggest that Zeb1 instead is the driving EMT transcription factor for this PDAC mouse model, as deletion of this gene led to less distant metastasis formation as well as reduced tumour grade and invasion (Krebs et al. 2017).

EMT cells are typically growth arrested, with several studies showing EMT-inducing transcription factors directly inhibiting proliferation (Brabletz et al. 2001; Thiery et al. 2009; Tsai et al. 2012). This EMT phenotype however is 'plastic', as cells need to resume their epithelial properties (such as proliferation) in order to colonise distant metastatic sites. This reversion has been demonstrated through findings that EMT-derived migratory cancer cells established as secondary colonies at distant sites histologically resemble the primary tumour from which they derived (Kalluri and Weinberg 2009). Thus, metastasised cells must shed their mesenchymal phenotype to form secondary tumours through mesenchymal-to-epithelial transition (MET). This step in metastasis formation in cancer is less well understood, and still requires direct experimental validation.

### 1.2.2 Cancer Stem Cells and Metastasis

Evidence supports the existence of a highly tumourigenic population of cancer cells that bear stem cell properties and represent an integral part of the development and maintenance of various human cancers, referred to as cancer stem cells (CSCs) (Clarke et al. 2006). Similar to normal stem cells, a hierarchical model of tumour development

lies in the ability of this subset of cells to undergo self-renewal and produce a heterogeneous lineage of cancer cells that form a tumour (Figure 1.7). Therefore based on this hypothesis, CSCs represent a population with tumour-initiating potential, not only forming the primary tumour but also capable of generating tumour metastases. This theory is one that is being explored in current literature, but difficult to prove in part due to the difficultly in identifying optimal markers that distinguish CSCs from non-CSCs and also due to variations in these markers between tumour types. Despite this, expression of certain cancer stem-like markers correlates with the occurrence of metastasis and reduced survival in patients (Kreso and Dick 2014), supporting their involvement in distant dissemination of disease. In PDAC, Hermann *et al.* have shown that the invasive front of pancreatic tumours contains a distinct subpopulation of CSCs defined by $CD133^{+}$ / C-X-C chemokine receptor (CXCR) $-4^{+}$, and depleting this subpopulation resulted in the loss of metastases *in vivo* (Hermann et al. 2007).

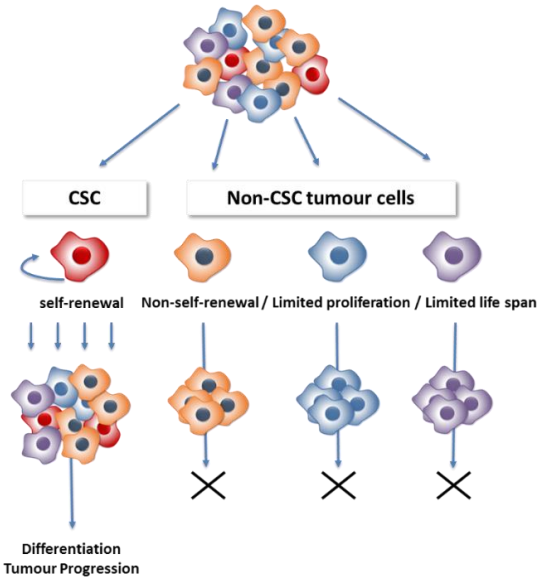


**Figure 1.7 The Cancer Stem Cell Model**

The cancer stem cell model describing tumours as heterogeneous in which only the cancer stem cell subset (CSC in red) has the anility to proliferate to form new tumours.

A link between stemness and EMT is debatable. Although not all cells undergoing EMT are stem cells, there is some evidence in breast cancer that EMT drives stem-like properties (i.e. de-differentiation); Mani *et al.* show that induction of EMT in human mammary epithelial cells by overexpression of transcription factors Snail and Twist

generates stem cell-like cells ($CD44^+/CD24^-$), and these cells give rise to metastasis (Mani et al. 2008). Similar results in breast cancer were found by Morel *et al.* (Morel et al. 2008), Dyck *et al* (Dyck et al. 1996) and Gupta *et al*. (Gupta et al. 2009). There is little data supporting this phenotype in PDAC, although Rhim *et al.* show circulating pancreatic cells expressing Zeb1 / lacking E-cadherin are enriched for $CD24^+$ / $CD44^+$ expression and exhibit stem cell properties, but no mechanistic link between the transcription factor and the stem phenotype is derived (Rhim et al. 2012).

As with normal stem cells, to some extent CSCs also require external signals for optimal balance between self-renewal, activation and differentiation. There is evidence that these could be derived from the TME, and has been termed the 'CSC niche' (Medema JP 2011). Thus, non-cancer cells are vital in influencing the cancer cell phenotype and tumour progression.

## 1.3 The Tumour Microenvironment

Cancer stroma is a highly complex environment containing malignant and host cells as well as non-cellular elements, including metabolites, ECM, fibres, ions, secreted proteins and free acids. In PDAC, the majority of tissue is stromal, which can form up to 70% of the tumour bulk (Bardeesy and DePinho 2002). PDAC is commonly resistant to treatment and it is postulated that one of the contributing factors to resistance is the intense stromal reaction serving not only as a barrier to chemotherapy but also to provide pro-tumourigenic signals (Rishi et al. 2015). Certainly, the once held cancer-cell-centric view in treating malignancy is now shifting to encompass the TME, with interest on targeting stromal components that play an active role in sustaining cancer growth, progression, invasion and metastasis to treat disease.

### 1.3.1 Cancer-associated Inflammation

Inflammatory cells are key components of the TME and are recognised as integral factors in contributing to carcinogenesis. Colotta *et al.* were the first to describe the link between inflammation and malignancy (Colotta et al. 2009), and it is now an established hallmark of cancer (Hanahan and Weinberg 2011). Epidemiological and experimental data indicate that a highly inflammatory TME within PDAC contributes to the development and progression of tumourigenesis (Rhim et al. 2012), for example chronic pancreatitis is known to increase the risk of developing pancreatic cancer (Guerra et al. 2007; Malka et al. 2002).

The relationship between immune cells and cancer within the TME is complex. Inflammatory cells and mediators, including cytokines, chemokines and prostaglandins, co-ordinate a milieu of pro-inflammatory responses which act in both an autocrine and paracrine manner on malignant and non-malignant cells (Mantovani et al. 2008). A chronic inflammatory state within the TME can drive tumour progression, for example by sustaining the immunosuppressive cell populations including regulatory T cells ($T_{reg}$), which suppress the anti-tumour immune response (Sakaguchi et al. 2001). In one *in vivo* study, using LSL-Kras$^{G12D/+;}$Pdx-1-Cre and

LSL-Kras$^{G12D/+}$;p48$^{Cre}$ mice models of PDAC, a prominent leucocyte infiltration was associated with low grade preinvasive lesions. A more immunosuppressive infiltrate, including immature myeloid cells (also known as myeloid-derived suppressor cells), tumour-associated macrophages (TAMs) and $T_{reg}$ cells then dominated the initial response and remained in invasive lesions (Clark et al. 2007). Thus, immune cell infiltrate may dictate the ability of PDAC cells to disseminate from the primary tumour site and consequently targeting inflammation in PDAC may lead to less metastasis. *In vivo*, this was demonstrated by Rhim *et al.* using the immunosupressive agent dexamethasone, which abolished circulating pancreatic cancer cells (Rhim et al. 2012). In conclusion, inflammation plays a role in driving PDAC tumourigenesis and pre-clinical data supports the concept of targeting this hallmark of cancer to inhibit tumour progression and dissemination.

## 1.4 Macrophages

Macrophages are one of the most abundant immune cells within the TME and are known to drive inflammation (Allavena et al. 2008). Therefore understanding the role of these immune cells in driving cancer may aid in developing a viable anti-inflammatory treatment strategy.

Macrophages are dominant immune cells that modulate tissue homeostasis and play a vital role in host inflammation and infection in response to pathogens and disease (Gordon and Taylor 2005). Their functions in normal states are to engulf invading bacteria and cell debris at inflamed and injured sites, secrete immunomodulatory cytokines, present antigen to T cells and act as accessory cells in lymphocytes activation. It is thought that two distinct populations of macrophages exist in homeostatic states; 'elicited' macrophages, recruited mainly from the bone marrow in response to inflammatory stimuli, and 'resident' macrophages, derived from embryonic (yolk sac) progenitors (Gordon and Taylor 2005). Elicited macrophages are derived from blood monocytes. Monocytes themselves originate in the bone marrow from haematopoetic stem cells (HSCs) and arise from a series of sequential differentiation stages (Figure 1.8).

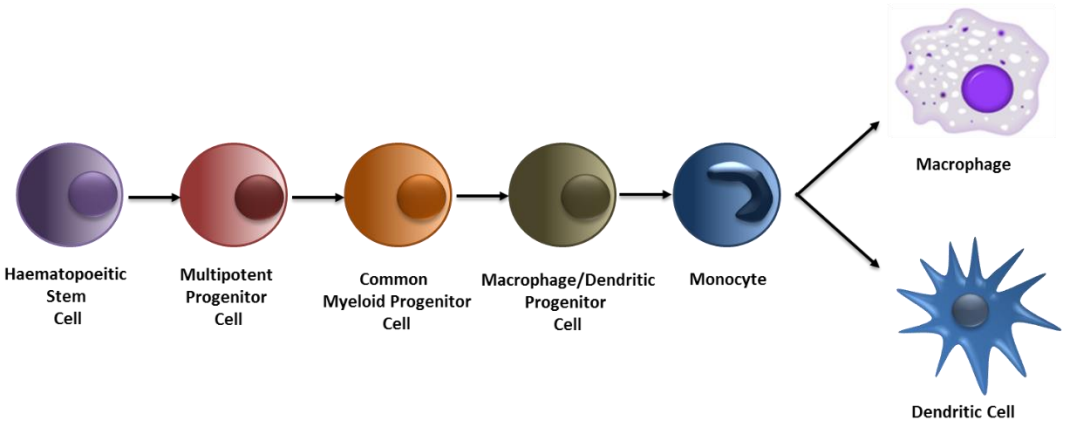


**Figure 1.8 Macrophage ontogeny**
Continuous generation of monocytes takes place within bone marrow from hematopoietic stem cells. Myeloid progenitors eventually give rise to monocytes, which function in tissue as macrophages or dendritic cells. Commitment to differentiation into a monocyte, macrophage or dendritic cell occurs as a macrophage / dendritic progenitor cell.

Monocytes are released into the circulation and within a few days they seed tissues by the process of extravastion through the endothelium. They eventually differentiate into either dendritic cells (DCs) or macrophages (Figure 1.8). Dependent on the tissue location and the inflammatory insult, there is evidence that both recruitment of monocytes / macrophages and local proliferation takes place to replenish and maintain the tissue-specific population of macrophages under normal pathological conditions (Gordon and Taylor 2005). 'Resident' embryonic macrophages on the other hand take residence in tissues prior to birth and maintain themselves within local tissue throughout adulthood independently of bone marrow derived precursors. Recently developed fate mapping techniques have enabled the identification and tracking of different embryonic macrophage populations into adulthood, and have revealed this population of macrophages to complex and heterogeneous (Epelman, Lavine, and Randolph 2014). In pancreatic cancer, heterogeneity in the ontogeny of TAMs has been demonstrated. Both monocytes and tissue-resident macrophages of embryonic origin are sources of TAMs in PDAC tissue. These populations display different phenotypes, with monocyte-derived TAMs being more potent at sampling tumour antigen and embryonic TAMs having higher expression of pro-fibrotic factors (Zhu et al. 2017). This appreciation of macrophage origin and heterogeneity is vital when exploring the effects of targeting the macrophage population within PDAC, for example the loss on the monocyte-derived macrophages had limited effects on tumour progression compared to loss of the tissue-resident population, which significantly reduced tumour progression.

### 1.4.1 Macrophage Phenotype and Activation

Macrophages are one of the most plastic cells of the haematopoietic system, showing great phenotypic and functional diversity. One way to classify tissue macrophages is according to their anatomical location, which then dictates functional phenotype. Well-described specialised resident macrophages include osteoclasts (bone), alveolar macrophages (lung), histiocytes (interstitial connective tissue) and Kuppfer cells (liver) (Murray and Wynn 2011).

Diversity of macrophage function is greatly influenced by the surrounding microenvironment. They respond not only to inflammatory stimuli but also to signals from antigen-specific immune cells and even macrophage-derived factors. Previously, the most commonly used classification of their activation state was the 'classically activated' M1 phenotype, and 'alternatively activated' M2 phenotype. This classification arose in the 1990s, when differential effects on macrophage gene expression were noted in response to external stimuli akin to the Th1/Th2 paradigm (Stein et al. 1992); M1 macrophages polarised in response to bacterial moieties such as lipolysaccharide (LPS) and the Th1 cytokine interferon (IFN)-γ, whilst M2 macrophages polarised in response to the Th2 cytokine interleukin (IL)-4. These findings have been since validated both *in vitro* with peripheral blood monocyte-derived macrophages, and *in vivo* (Biswas and Mantovani 2010) (Figure 1.9). Based on these two activation states, consistent differences in function, metabolism and subsequent cytokine production have been observed. M1 macrophages produce large quantities of pro-inflammatory cytokines (e.g. IL1β, IL12, and tumour necrosis factor (TNF)-α) that promote cell-mediated Th1 responses, have increased major histocompatibility complex class (MHC) class II expression, and are implicated in killing of pathogens and tumour cells (Gordon and Taylor 2005). In contrast, M2 macrophages secrete IL10 and other cytokines that mediate Th2 responses, moderate inflammatory responses and promote tissue re-modelling and repair (Gordon and Martinez 2010).

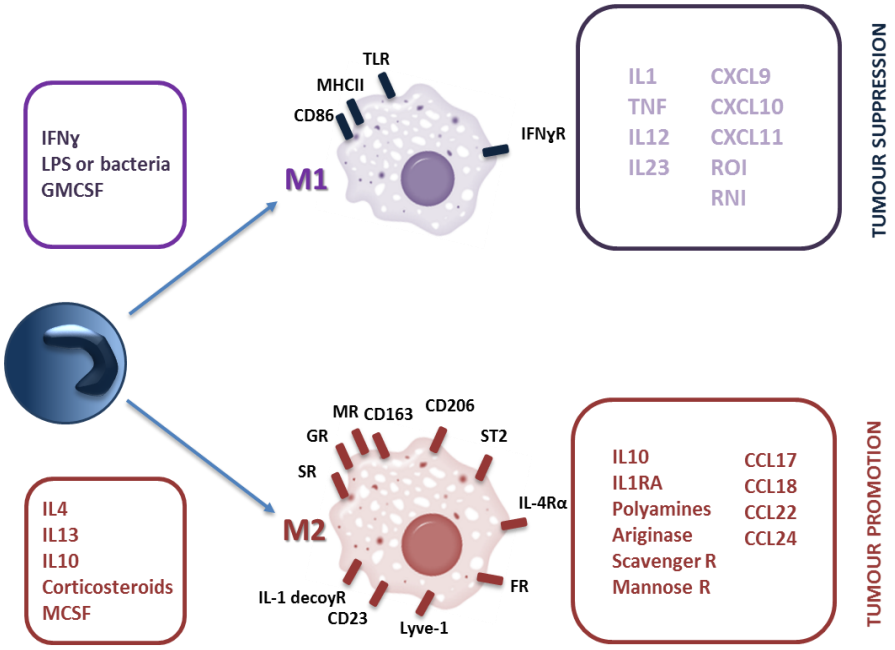


**Figure 1.9 The 'old' paradigm: differentiation pathways of 'classical' M1 & 'alternate' M2 macrophages**
FR, folate receptor; GR, galactose receptor; IFNγR, IFNγ receptor; IL1decoyR, IL1 decoy receptor; MHCII, major histocompatibility complex class II; MR, mannose receptor; SR, scavenging receptor; RNI, reactive nitrogen intermediate; ROI, reactive oxygen intermediate.

The concept of M1/M2 however has now been updated, with the old binary definition viewed as out-dated and oversimplified. Although this nomenclature is useful to describe the two extremes of population, expert consensus recognises the complexities in macrophage activation, phenotype and plasticity. The current view is that macrophages are most likely to exist in a spectrum of activation states depending on the exact composition of the activating signals present in the microenvironment rather than one or the other (Murray et al. 2014). Therefore instead of fitting within the constant and dualistic definition of M1/M2 as described in Figure 1.9, it is likely that the plasticity of macrophages within the tumour microenvironment leads to constant and complex changes in phenotype driven by gene and surface marker expression leading to a heterogeneous population at any given time.

Leading experts from the field of macrophage biology have therefore suggested the use of stimulators and activators to describe TAM polarisation, for example M(IL-4), M(LPS) and so forth (Martinez and Gordon 2014; Murray et al. 2014; Noy and Pollard 2014). Unfortunately, this nomenclature has yet to be fully taken up throughout the

field, and thus the M1/M2 classification is not only used in older publications, but still remains in use for some current publications referenced in this thesis. Therefore, in view of current consensus guidelines, where ‘M1’ or ‘M2’ is used in a publication to define a macrophage population, the polarisation method has also been stated.

### 1.4.2 Tumour Associated Macrophages

Macrophages are a major component in leucocyte infiltration of the TME, and their role in tumourigenesis is complex. Early studies into the role of TAMs initially reported that activation by bacterial moieties and cytokines enable tumour cell kill (Evans and Alexander 1970). However, it soon became apparent that they could also promote tumour growth and metastasis (Mantovani et al. 1979). Thus, early on in the investigation of TAMs, a dual function was demonstrated.

TAMs in tumour tissue are derived from tissue-resident macrophages, as demonstrated with microglial cells in glioma (Feng et al. 2015), and cytokine recruited blood monocytes and monocyte-related myeloid-derived suppressor cells (M-MDSCs) (Figure 1.10).

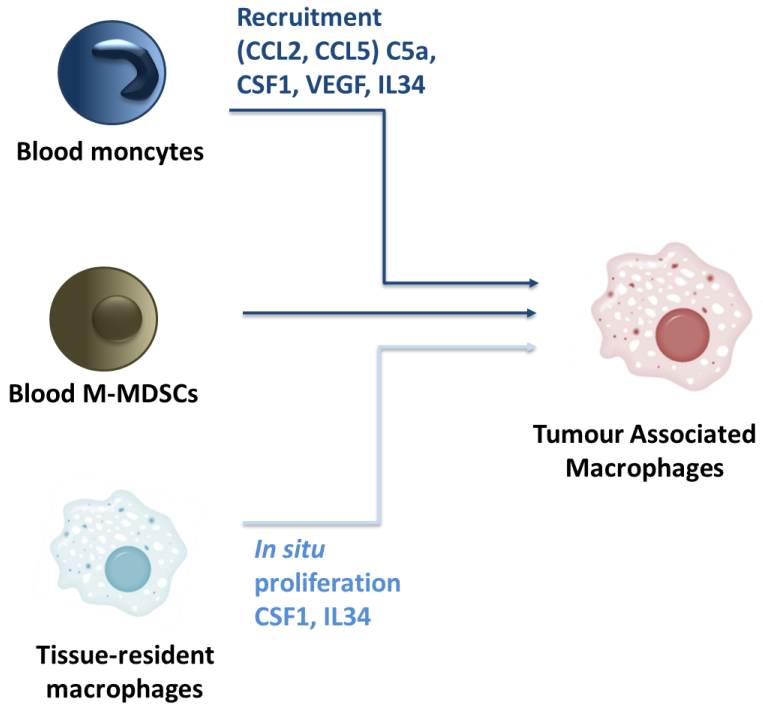


**Figure 1.10 Precursors of tumour-associated macrophages in cancer**
Monocytes and M-MDSCs from the blood are recruited in response to chemoattractant secreted from both tumour and host cells within the primary tumour. In some tumours, local tissue-resident macrophages (of embryonic origin) can contribute to the TAM population through *in situ* proliferation (adapted from Mantovani et al. 2017).

The dual supportive and inhibitory role of macrophages within tumours is largely driven by the TME (Beatty et al. 2011). Granulocyte macrophage colony stimulating factor (GMCSF) driven macrophages mediate an antitumour / cytotoxic effect, whilst IL4, IL13 and macrophage colony stimulating factor (MCSF) driven macrophages are typically pro-tumourigenic, supporting several hallmarks of cancer, including angiogenesis, cell invasion and migration, and suppression of anti-tumour immune responses (Ruffell and Coussens 2015) (Figure 1.9). The phenotype of TAMs is skewed by several different signals originating from tumour cells (e.g. chemokine secretion), B cells (immune complexes) and stromal cells (e.g. IL1), leading to a diverse and heterogeneous population of TAMs (Biswas and Mantovani 2010).

Despite the opposing functional populations of TAMs that exist within a primary tumour (pro- vs. anti- tumour), clinical data largely support a high density of

macrophages in tumours with poor prognosis as 80% of studies indicate a higher macrophage density is associated with inferior patient prognosis (Bingle, Brown, and Lewis 2002). In PDAC, TAMs are thought to be typically protumourigenic (as defined by CD163) and relate to progression and treatment resistance (Ino et al. 2013; Kurahara et al. 2013). This observation supports the widely accepted view that TAMs mainly promote several different aspects of tumour progression (Nielsen and Schmid 2017; Ruffell and Coussens 2015) (Figure 1.11).

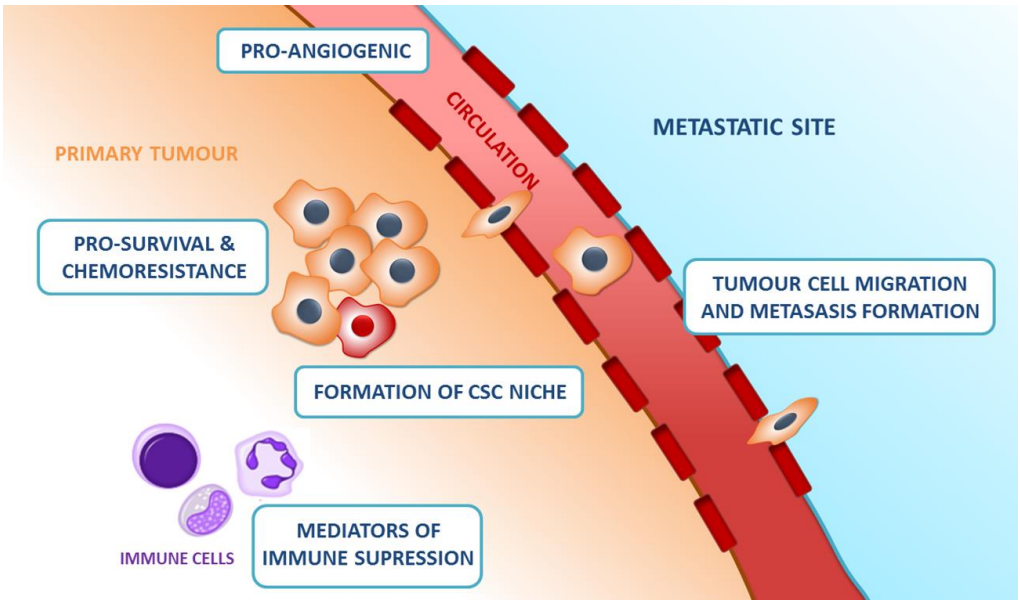


**Figure 1.11 The pro-tumourigenic effects of tumour associated macrophages**
Macrophages drive tumour progression within the primary tumour and in metastatic sites. These effects include supporting pro-survival and treatment resistance, evasion of immune cell cytotoxicity, supporting the expansion of the cancer stem cell (CSC) population, assisting in blood vessel formtaion, and initiating tumour cell invasion.

#### 1.4.2.1 Macrophages and Chemoresistance

Macrophages are important determinants of the efficacy of chemotherapeutic agents, but whether they enhance or counteract the anticancer effect is highly dependent on the drug used and tumour type (Mantovani et al. 2017).

In syngeneic orthotopic pancreatic tumour mouse models, direct targeting of macrophages through inhibition of either colony-stimulating factor-1 receptor (CSF1R) or chemokine receptor (CCR) 2 decreased the number of tumour-initiating cells, and thus improved gemcitabine efficacy (Mitchem et al. 2013). Similarly, using a transgenic mouse model with reduced macrophage recruitment and activation, Weizman *et al.* demonstrated improved response to gemcitabine treatment augmented by the CSF1R receptor antagonist, GW2580. The proposed method for driving chemoresistance in this study was upregulation of cytidine deaminase, the enzyme that metabolises gemcitabine following its transport into the cell (Weizman et al. 2014).

Interestingly, recent clinical data in PDAC suggest a dual prognostic significance of TAMs in the adjuvant setting; in patients not treated with chemotherapy, density of TAMs at the tumour-stroma interface (as defined by CD206, CD163 expression and IL10 expression) was associated with worse prognosis and distant metastasis (Di Caro et al. 2015). However, a high density was also associated with better prognosis for patients who received postsurgical adjuvant chemotherapy. *In vitro* data supported this finding, with gemcitabine treated macrophages becoming tumouricidal following treatment, implying chemotherapy ‘re-educated’ macrophages by inhibiting protumour functions and driving cytotoxic activity (Di Caro et al. 2015). This study implies therapeutic targeting of macrophages in the TME, especially in the adjuvant setting, should not only focus on decreasing TAMs density, but suggest developing agents that polarise macrophage function to improve outcomes by promoting their antitumourigenic functions.

#### 1.4.2.2 Macrophages and Cancer Stem Cells

Emerging data support a novel role for macrophages in supporting the 'CSC niche' in breast and PDAC, either through direct or indirect interaction with CSCs. Lu *et al*. demonstrate a juxtacrine (i.e. cell-cell) interaction between breast CSCs and monocytes / macrophages that drives and maintains stem-like properties such as sphere formation *in vitro* and tumour formation *in vivo* (Lu et al. 2014). Published data from our laboratory have shown that macrophages can drive CSC properties in PDAC through secreted factors, IFN-stimulated gene 15 (ISG15) and human cationic antimicrobial protein 18 (hCAP-18) / leucine leucine 17 (LL37). These factors reinforce pancreatic CSC self-renewal, expansion and tumourigenicity *in vitro* and *in vivo*. A 'crosstalk' between the cancer cells and macrophages was determined, with CSCs secreting TGFβ, nodal, activin and IFNβ leading to ISG15 and hCAP-18 secretion from the macrophages respectively (Sainz et al. 2014, 2015).

The ability of TAMs to drive stem-like properties in cancer would support the other pro-tumourigenic roles described, as the traits of CSCs are also associated with other TAM driven phenotypes such as metastases formation and treatment resistance (Hermann et al. 2007). Further understanding of what is driving this relationship is therefore of importance.

#### 1.4.2.3 Macrophages and Angiogenesis

Tumour angiogenesis is essential for allowing vessel growth to enable nutrient and oxygen supply to malignant tissue. TAMs play an essential role in driving the 'angiogenic switch', during which formation of high-density vessel networks leads to malignant transformation. This is observed in data from Lin *et al*. in which macrophage depletion, through homozygous null mutation of the macrophages growth factor CSF1, led to an attenuated angiogenic switch and a delay in malignant transformation (Lin et al. 2006).

One key contribution of macrophages to support angiogenesis is through cytokine secretion in response to hypoxic conditions, mainly vascular endothelial growth factor (VEGF). In mice depleted of macrophages, VEGF overexpression restored angiogenesis and accelerated malignant transformation (Lin et al. 2007).

A specific 'angiogenic' TAM subpopulation is likely to exist in cancers. For example, in RIP-Tag2 transgenic mice (in which pancreatic islets spontaneously develop adenomas and invasive adenocarcinomas), TIE2 expressing monocytes were shown to be recruited to tumour tissue and found in a perivascular location and this same population of cells mediated neovascularisation in a glioblastoma xenograft model (De Palma et al. 2005).

#### 1.4.2.4 Macrophages and Immune Suppression

Despite functioning in normal tissues to initiate and support adaptive immunity, TAMs within the TME are believed to play a mainly immunosuppressive role. TAMs do not behave as their regular homeostatic counterparts: they lack the capacity to present antigens, trigger anti-tumour responses from T and NK cells and lyse tumour cells (Lewis and Pollard, 2006). Several different mechanisms for how TAMs perform this function have been demonstrated, and can loosely be divide into either indirect effects, i.e. through secretion of factors that create an immunosuppressive environment, or direct effects i.e. by contact dependent immune cell interaction.

Several indirect immunosuppressive effects of macrophages are likely to exist in the TME. In murine lung carcinoma models, macrophages produced arginase which led to impaired T cell function within tumours (Rodriguez et al. 2004). In addition, TAMs have been shown to increase the presence of established immunosuppressive cytokines, such as IL10 in hepatocellular cancer patient tissue (Kuang et al. 2009), TGFβ and prostaglandin E(2) in breast cancer mouse models (Torroella-Kouri et al. 2009).

In order to self-regulate the immune system has developed 'checkpoints' which are receptors on specific immune cells that can be activated or inactivated to generate an immune reaction. Cells within the TME are known to manipulate this system, by

expressing ligands to these checkpoints that then inhibit immune cell function and thus allow tumour evasion from immune recognition. Macrophages themselves are known to express some of these ligands, such as programmed death ligand-1 (PDL-1). Binding of this ligand to PD-1 on T cells triggers loss of activity function. In the KPC mouse model of PDAC, TAMs have been shown to express very high levels of PDL-1 (Winograd et al. 2015). In turn, CSF1R blockade in syngeneic orthotopic PDAC mouse models led to upregulation of PDL-1 and another T-cell checkpoint inhibitor, CTLA4. The use of CSFR1 blockade and PD-1 and CTLA4 antagonists led to potent tumour regression, even in large established tumours, and thus provides a rationale for targeting of innate myeloid cell populations in PDAC to improve adaptive immune cell checkpoint inhibition (Zhu et al. 2014).

#### 1.4.2.5 Macrophages and Cancer Cell Migration and Invasion

TAMs are found in close proximity to migratory cells on the invasive edge of tumours (Wyckoff et al. 2004) and therefore implicated in the ability of cancer cells to form distant metastasis.

There are certainly data supporting the need for macrophages in metastasis formation. The most widely cited evidence is in breast cancer, using the PyMT mouse model. In this model, removal of macrophages, through a homozygous null mutation of CSF1, resulted not only in reduced rate of tumour progression but also less invasion and metastases (Nielsen and Schmid 2017). Conversely, overexpression in wild type tumours accelerated progression and metastatic potential (Lin et al. 2001).

As in breast cancer models, ablation of macrophages through CSF1R inhibition or inhibition of CCR2 results in decreased metastasis in pancreatic cancer mouse models (Mitchem et al. 2013). *In vitro* studies have shown that both GMCSF-polarised and MCSF-polarised macrophages can induce EMT in pancreatic cell lines (H6c7 and Colo357), but intriguingly the GMCSF-polarised cells became more MCSF-like (as characterised by greater CD163 expression) with subsequent co-culture (Helm et al. 2014), suggesting the MCSF phenotype is a closer representation of a tumour cell driven polarisation.

It is now understood that this pro-metastatic role of macrophages is likely to involve several different stages and interactions. TAMs not only promote the invasion and intravasation of tumour cells from the primary tumour site, but also promote survival within the circulation and eventually generate a metastatic niche at the site of dissemination (Nielsen and Schmid 2017).

The importance of EMT as an initial stage in metastasis has been previously discussed (section 1.2.1), and thus a likely pro-metastatic role of TAMs is an ability to induce this process in cancer cells residing in the primary tumour. There are data supporting this effect in several tumour types (Zhang et al. 2015), but how TAMs are initiating this process varies according the cell type and has yet to be fully elucidated in PDAC. One likely mechanism is through secretion of cytokines, which are produced in abundance by macrophages and are rich within the TME.

## 1.5 Cytokines

Cytokines are secreted or membrane-bound proteins that regulate growth, differentiation and activation of immune cells. In normal immunity, these proteins form a complex network with pleotropic effects. Within the TME, there is a rich mix of cytokines produced by malignant and non-malignant cells, and this network is often dysregulated. These secreted factors influence the malignant properties of cancer cells and non-cancer cells alike.

TAMs are one of the most prolific producers of cytokines within the TME. As described, TAMs can influence malignant cell behaviour through secretion of cytokines that activate oncogenic intracellular signalling pathways. But cytokines within the TME also influence macrophage activity, for example cytokines such as IL6, IL10 and TNF-α have been shown to regulate PDL-1 expression on macrophages (Kryczek et al. 2006; Kuang et al. 2009; Wang et al. 2017).

In pancreatic cancer, many different cytokines are present within the TME and are believed to drive tumour progression (Wörmann et al. 2014). One cytokine can influence many different cancer cell functions, thus inhibiting these small molecules poses an attractive therapeutic target

## 1.6 Targeting Immunity in Cancer

A paradigm shift in cancer treatment is emerging; instead of only targeting cancer cells, there is now a transition to target non-cancer cells that are supporting these cells and driving tumour progression. In particular, targeting immune cells has led to unprecedented outcomes in the treatment of metastatic disease. The intention of this strategy is to 'switch on', the immune system to recognise and kill cancer cells, thus providing long lasting immunity against the cancer, resulting in better long term outcomes compared to conventional chemotherapeutics.

In recent years, the use of immunotherapy in cancer has made exciting progress in several different cancer types. Current agents mainly focus on the adaptive immune system, most notably the immune checkpoint inhibitors in the form of antibodies against PDL-1, PD-1 and CTLA-4. These drugs have been extremely effective in clinical trials, with several gaining approval of use in the clinic (Table 1.4).

**Table 1.4 FDA approved immunotherapies in cancer**
CTLA-4 = cytotoxic T-lymphocyte-associated protein 4; mAb = monoclonal antibody; NSCLC = non–small-cell lung cancer; PD-1 = programmed death 1; PD-L1 = programmed death ligand 1.

| Agent | Mechanism of Action | FDA Approval Dates, Indications and related trial results |
|---|---|---|
| Atezolizumab | mAb targeting PD-L1 | March 15, 2016: previously treated locally advanced or metastatic NSCLC (Fehrenbacher et al. 2016)<br>May 18, 2016: first-line treatment locally advanced or metastatic urothelial carcinoma (Powles et al. 2014) |
| Avelumab | mAb targeting PD-L1 | May 9, 2017: locally advanced or metastatic bladder cancer after progression on platinum-containing chemotherapy (Heery et al. 2017) |
| Durvalumab | mAb targeting PD-L1 | 01 May 2017: locally advanced or metastatic bladder cancer whose disease has progressed during or after platinum-containing chemotherapy or within 12 months of neoadjuvant or adjuvant chemotherapy. |
| Ipilimumab | mAb targeting CTLA-4 | March 25, 2011: unresectable or metastatic melanoma (Hodi et al. 2010; Robert et al. 2011)<br>September 30, 2015: BRAF V600 wild-type unresectable or metastatic melanoma (in combination with nivolumab) (Postow et al. 2015)<br>October 28, 2015: adjuvant therapy to lower recurrence risk of stage III melanoma after surgery (Eggermont et al. 2015) |
| Pembrolizumab | mAb targeting PD-1 | September 4, 2014: advanced or unresectable melanoma (Hamid et al. 2013; Robert et al. 2014)<br>October 2, 2015: metastatic NSCLC with tumors that express PD-L1 and disease progression on or after platinum-containing chemotherapy (Garon et al. 2015)<br>December 18, 2015: First-line treatment of unresectable or metastatic melanoma (Robert et al. 2015)<br>May 18 2017: locally advance/ metastatic urothelial carcinoma progression after platinum chemotherapy<br>(Bellmunt et al. 2017) |
| Nivolumab | mAb targeting PD-1 | December 22, 2014: unresectable or metastatic melanoma that has progressed following ipilimumab and, if BRAF V600 mutation positive, a BRAF inhibitor (Weber et al. 2015)<br>March 4, 2015: metastatic squamous NSCLC with progression on or after platinum-based chemotherapy (Borghaei et al. 2015)<br>September 30, 2015: BRAF V600 wild-type unresectable or metastatic melanoma (in combination with ipilimumab) (Postow et al. 2015)<br>October 9, 2015: metastatic NSCLC that has progressed during or after platinum-based chemotherapy (Borghaei et al. 2015)<br>November 23, 2015: metastatic renal cell carcinoma after prior anti-angiogenic therapy (Motzer et al. 2015)<br>January 23, 2016: BRAF V600 wild-type and BRAF V600 mutation-positive unresectable/metastatic melanoma (in combination with ipilimumab) (Larkin et al. 2015)<br>February 02, 2017: Advanced bladder cancer (Plimack et al. 2017) |

However, studies involving immune checkpoint blockade have yet to be universally successful in all tumour types, and in PDAC this approach has shown no clinical efficacy thus far; Single agent ipilimumab, an anti–CTLA-4 therapeutic, in locally advanced or metastatic PDAC, showed no responses and only one "delayed" response (Royal et al. 2010). Anti–PD-L1 therapy had no efficacy in 14 PDAC patients treated in Phase I testing (Brahmer et al. 2010). One could argue these trials were limited by small patient numbers and therefore results from ongoing larger checkpoint trials will provide more conclusive evidence. Nonetheless, several reasons have been proposed for why immunotherapeutic agents may be ineffective in PDAC. One is a relatively low mutational load in PDAC tumours, leading to T cell exclusion due to a lack of antigen presentation (Bailey et al. 2016). Others have suggested that PDAC is a 'non-immunogenic cancer', insofar as the tumour-infiltrating effector T lymphocytes are not a histopathological hallmark of disease as in other tumour types (Von Bernstorff et al. 2001). Lack of T cell infiltration could be due to inhibition from the dense TME, for example by T cells (T regulatory), MDSCs, TAMs and inhibitory cytokines such as TGFβ and IL10 within the PDAC milieu (Byrne et al. 2015; Wachsmann, Pop, and Vitetta 2012). Most recent data show there may be a subpopulation of PDAC tumours with high cytolytic T cell activity despite low neoepitope load and that these tumours have a high expression of checkpoint inhibitors other than PDL-1 (Balli et al. 2017). Thus, targeting other immune regulators and cells to boost T cell activity as well as exploring inhibition of other checkpoint inhibitors in PDAC could prove successful in improving outcomes of immunotherapy.

### 1.6.1 Targeting Macrophages in Cancer

Due to the large infiltration of macrophages in cancers, their ability to influence adaptive immune cells, their association with poor prognosis and involvement in tumour progression, TAMs are emerging as targets of immunotherapy in cancer.

Existing chemotherapeutic agents may already have effects on TAMs, for example the chemotherapeutic drug trabectadin has been reported to have an additional action of selective cytotoxicity to human monocytes (Germano et al. 2010) as well as its direct

anti-cancer cell properties. In soft tissue sarcoma patients treated with trabectadin, decreased circulating monocytes and a reduction in TAMs were seen on biopsy specimens (Demetri et al. 2016). This drug is now approved for treatment of soft tissue sarcoma and is being tested in several other tumour types and thus its anti-macrophage properties may be further explored (Table 2).

An emerging target for direct macrophage toxicity is macrophage CSF1. The monoclonal antibody, RG7155, targets the CSF1 receptor and has shown a 74% objective clinical response in tenosynovial giant cell tumours (in which the CSF1 is overexpressed) (Ries et al. 2014). As part of this study, the use of RG7155 was extended to other solid malignancies, and a reduced macrophage infiltration on biopsy was correlated with an increased CD8+/CD4+ T cell ratio. This finding supports the combination of an adaptive and innate immunotherapy approach, and this agent is now being trialled in other solid malignancies (Table 1.5).

Specifically in PDAC, targeting TAMs pose a novel therapeutic strategy. Efficacy for this approach has been demonstrated in the Phase I setting, in which a CD40 agonist, CP-870,893, showed an overall response rate of 19% in patients with metastatic disease (Beatty et al. 2013). This drug works by up regulating co-stimulatory molecules on macrophages to shift them from pro-tumour to an anti-tumour phenotype, thus re-polarising TAMs towards an anti-tumour phenotype could be beneficial in treating cancer. In addition, a further Phase I trial has shown promising results in the adjuvant setting, through blocking recruitment of TAMs by targeting the CCL2-CCR2 axis using PF-04136309, a CCR2 inhibitor, in combination with FOLFIRINOX. In this study, primarily testing for safety and toxicity, 49% of patients in the combination arm underwent objective tumour response compared to 0% in the single arm group (Nywening et al. 2016).

**Table 1.5 Completed trials in agents targeting macrophages in cancer**

| Agent | Target | Mechanism of Actions | Study types / Tumour type |
|---|---|---|---|
| Trabectadin | TAM | Selective monocyte / macrophage cytotoxicity | Phase III Sarcoma (Demetri et al. 2016) |
| RG7155 / PLX3397 | CSF-1R | RG7155:Human CSF-1R specific antibodies<br>PLX3397: Small molecule inhibitor CSF1R and KIT | RG7155: Phase I Tenosynovial giant cell tumour (Ries et al. 2014), Phase I Diffuse-type tenosynovial giant cell tumour (Cassier et al. 2015)<br>PLX3397: Phase II GBM |
| CP-870,893 | CD-40 | Human CD40 agonist antibody | Phase I Pancreatic (Beatty et al. 2011, 2013) |
| PF-04136309 | CCR2 | Inhibition of CCL2-CCR2 recruitment | Phase Ib Pancreatic (Nywening et al. 2016) |
| Maraviroc | CCR5 | Antiretroviral CCR5 receptor antagonist | Pilot metastatic CRC (Halama et al. 2016) |

Despite these data, the clinical effectiveness of macrophage targeting agents has so far been modest in early phase trials, and they have yet to prove effective in the Phase III setting. Currently there are no approved therapeutic agents in clinical use that target TAMs specifically, and therefore further development is needed into novel ways to target the pro-tumourigenic functions of TAMs which may then translate to better clinically efficacy. Advancing our understanding of the relationship between TAMs and cancer cells could help identify better therapeutic approaches.

### 1.6.2 Targeting of Cytokines in Cancer

Due to the pleiotropic effects of inflammatory cytokines in tumour progression, selective inhibition of specific cytokines have been trialled, with the aim of disrupting the already dysregulated tumour cytokine network in cancer to achieve both systemic as well as tumour-specific therapeutic effects.

Several approved and novel agents targeting cytokines have been or are being tested in early phase cancer trials (Table 1.6). Some of these act on TAM function also, for example CCL2 inhibitors would limit macrophage recruitment (Brana et al. 2015; Pienta et al. 2013; Sandhu et al. 2013).

**Table 1.6 Completed trials in cytokine targeting agents in cancer**

| Target | Agent | Mechanism of Actions | Study types / Tumour type |
|---|---|---|---|
| TNFα | Infliximab | Chimeric TNF-specific antibody | Phase I/II RCC (Harrison et al. 2007; Larkin et al. 2010) |
| TNFα | Etanercept | Human TNFR2–Fc fusion protein | Phase II Breast (Madhusudan et al. 2004), Ovarian (Madhusudan et al. 2005); Phase I/II Pancreatic (Wu et al. 2013) |
| IL6 | Siltuximab | Chimeric anti-IL6 antibody | Phase I Castleman's disease (approved for use) (Kurzrock et al. 2013); Phase I/II advance solid tumours (Angevin et al. 2014), Prostate (Dorff et al. 2010; Hudes et al. 2013), RCC (Rossi et al. 2010); Phase II Ovarian (Coward et al. 2011) |
| CCL2 | Carlumab | Human anti-CCL2 antibody | Phase I (Sandhu et al. 2013); Phase 1b (Brana et al. 2015) Phase II prostate (Pienta et al. 2013) |
| IL1α | MABp1 | True human anti-IL2α antibody | Phase I (Hong et al. 2014); |

Cytokine targeting agents have been trialled in PDAC, but little benefit has been seen, with anti-TNFα (Wu et al. 2013) and anti-IL6 agents (Angevin et al. 2014). One of the reasons for lack of efficacy could be because these cytokines are not key players in driving PDAC tumour progression, and thus inhibiting their activity has little clinical efficacy. It may also be due to the stage of treatment, as giving a cytokine agent in the setting of metastatic disease could be ineffective due in an already established complex network of signalling pathways compared to giving it early (i.e. adjuvant setting).

## 1.7 Hypothesis

There is mounting evidence for the role of TAMs in driving tumour progression. Thus, understanding the functions they play in PDAC could provide a novel immune mediated therapeutic target to treat an otherwise devastating disease.

The basis of this project is formed on previous published data from our laboratory showing the ability of TAMs to create a pro-tumour paracrine niche for PDAC CSCs. Following microarray analysis of macrophages co-cultured with PDAC cells, two upregulated macrophage genes were investigated as important players in the crosstalk between the cell types: ISG15 and hCAP-18 / LL37 (Sainz et al. 2014, 2015).

ISG15, a protein normally secreted by cells to stimulate the production of type II IFN, was secreted by TAMs in response to IFNβ produced by PDAC cells. This factor enhanced the inherent stem cell-like properties of self-renewal and tumourigeneicity (Sainz et al. 2014). In turn, hCAP-18 (biologically active in its cleaved form of LL37) was found to be exclusively secreted by TAMs induced again by CSC derived factors (TGFβ, Nodal and Activin). LL37 similarly enhanced CSC properties and inhibition of its receptors (formyl peptide receptor 2 and purinoceptor 7 receptor) negatively impacted tumour growth and circulating tumour cell numbers.

The focus of these previous publications was that of the 'CSC-niche' promoting effects of macrophages derived factors. Results also demonstrated other potential pro-tumourigenic effects of TAMs on primary PDAC cells such as cell survival, migration and metastases formation; PDAC cells cultured with condition media from MCSF-polarised macrophages had upregulation of the pro-survival protein phospho-ERK, modulation of EMT-associated genes (E-cadherin, Zeb1 and Vimentin) and enhanced migratory capacity. In addition, cells treated with recombinant LL37 were found to have an increased CXCR4+ expression, which is a marker that defines a subpopulation of CSCs that drives metastasis (Hermann et al. 2007). Supporting this finding, cells pre-treated with LL37 generated more micrometastases *in vivo* (Sainz et al. 2015).

Although both ISG15 and LL37 were shown to be important in driving tumour progression through the mechanisms described, the basis of these findings were

determined through analysis of TAMs, and effects were mainly focussed on the CSCs. As yet, there are no clinical drugs to target macrophage-derived factors LL37 and ISG15 in patients; therefore clinical applications for inhibiting this pathway are not yet achievable.

Supporting the protumourigenic effects of TAMs in PDAC, our laboratory has also shown that conditioned media from macrophages can induce expression of the immune checkpoint inhibitor PDL-1 on the surface of treated PDAC cells, mediated by miR-93/106b. Thus, factors secreted by macrophages could also be inducing immune evasion in PDAC cells (Cioffi et al. 2017).

Therefore, the hypothesis of this thesis is that further factors induced by interaction with TAMs are driving PDAC progression. By analysing the effects of this interaction in PDAC cells specifically, these factors and their associated molecular pathways can be identified. In doing so, a better understanding of how TAMs drive tumour development can be achieved. Identifying novel approaches to inhibit these factors and pathways could lead to inhibition of PDAC tumour progression.

# 2 CHAPTER TWO: MATERIALS & METHODS

## 2.1 Cell Culture

### 2.1.1 Primary Pancreatic Cancer Cells

Human PDAC tissues were obtained with written informed consent from all patients. Primary tumours were processed and cultured *in vitro* and expanded *in vivo* as patient-derived xenografts (PDX) as previously described (Mueller et al. 2009) and are referred to herein as PDX derived primary PDAC culture cells (Panc185, Panc215, Panc253, Panc354, Panc10953, Panc12560 Panc140114). Circulating tumour cells (CTC) were collected using the IsoFlux System (Fluxion) using Dynabead selection, and acquired cells were processed and cultured *in vitro* and expanded *in vivo* as per PDX derived primary PDAC culture cells (M.Yang, *in submission*). CTC derived cultured are referred to herein as CDX derived primary PDAC culture cells (C75 and C76). Mutational characteristics for each cell type were defined through gene and protein analysis (Table 2.1).

**Table 2.1 Mutational characteristics of PDX and CDX cultured cells**
Mutational characteristics of Panc185, 215, 253 and 354 cells were determined through Serial Analysis of Gene Expression (SAGE) (Jones et al. 2008). Mutational characteristics of Panc10953, 12560, 140114, C75 and C76 were determined through digital PCR droplet analysis and western blot (M.Yang, *in submission*). WT, wild-type; uk, unknown.

| Cell Type | KRAS | SMAD4 | P53 |
|---|---|---|---|
| Panc185 | mutant | mutant | mutant |
| Panc215 | mutant | WT | mutant |
| Panc253 | mutant | WT | mutant |
| Panc354 | mutant | mutant | mutant |
| Panc10953 | uk | mutant | uk |
| Panc12560 | mutant | mutant | wt |
| Panc140114 | uk | uk | uk |
| C75 | mutant | mutant | wt |
| C76 | mutant | mutant | wt |

All cells were cultured at 37° in a humidified atmosphere of 5% $CO_2$. Cells were maintained in endotoxin free-RPMI (Gibco Life Technologies) supplemented with 10% heat-inactivated fetal bovine serum (FBS; Gibco Life Technologies) and 50 U/mL penicillin–streptomycin and used *in vitro* to passage 10 only.

Cells were maintained at 70% confluence, and for collection, flasks were treated with trypsin-EDTA 0.05% (Sigma) until the majority had detached and then quenched by the addition of equal volume RPMI containing FBS. Live cells were counted using trypan-blue staining at a ratio of 1:1 and seeded for experiments. When required, cells were pelleted by centrifugation for 5 minutes at 1500rpm. Cell were tested monthly for mycoplasma infection. For experiments with macrophage conditioned media, control media was DMEM:F12 (Gibco) supplemented with B-27 (Invitrogen), β-FGF (PeproTech), Penicillin-streptomycin (Sigma) and fungisome (Sigma).

### 2.1.2 Human Monocyte-derive Macrophages (and Differentiation)

In order to test the effects of tumour-associated macrophages on primary PDAC cultures, healthy donor monocytes were polarised to a more 'tumour-associated' phenotype *in vitro* using the methods stated below. The PBMCs used to generate these cells were from at least 10 different donors, ensuring heterogeneity in the macrophage populations, which was likely to better represent the clinical situation than using one donor alone.

Buffy coats of lymphocyte-rich peripheral blood from healthy volunteers were obtained from the National Blood Service (Tooting, London) (City and East London Research Ethics Committee 17/EE/0182). Leucocyte cones were stored at 4°C and used within 24 hours of delivery to maintain cell viability. In T175$cm^2$ flask (Corning) the combined 100ml volume of the two 'buffy coats' was added to 180mls of sterile PBS and mixed. 20mls of Ficoll-Paque PLUS (GE Healthcare) was added to eight 50ml capacity Falcon tubes (Corning). 35ml volumes of 'buffy coat' mixture were then slowly layered (with pipette controller set to gravity powered expulsion) onto the

Ficoll-Paque PLUS at an oblique angle. Samples were then spun at 2200rpm for 15 minutes with decelerate without a break.

Following centrifugation, separation occurred as per Figure 2.1. The lymphocyte–rich white layer (interphase) was collected and mixed with sterile PBS into 50ml Falcon tubes. The tubes were spun at 1500rpm for 10 minutes, supernatant aspirated and a repeat wash of the pellet with PBS was performed as per previous. The final cell pellet was then re-suspended in IMDM (Life Technologies) supplemented with 10% human serum (Sigma) for differentiation into mature macrophages. A density of approximately 5x $10^5$ PBMCs / $cm^2$ were cultured in T175 flasks.

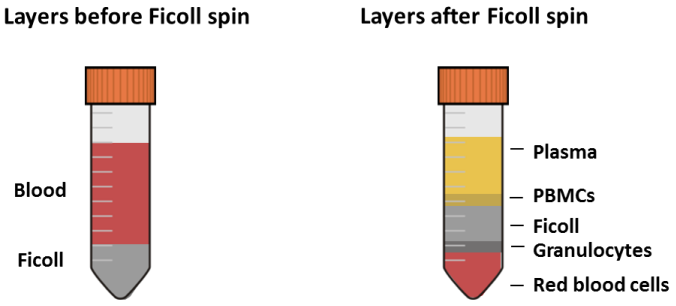


**Figure 2.1 Ficoll separation of blood PBMC, peripheral blood monocyte.**

For macrophages intended for co-culture with tumour cells, flasks were incubated for 4 days to allow full differentiation in IMDM and 10% human serum. After 4 days, cells were washed with PBS and gently detached using Accutase (Sigma). Viable mature macrophages were then counted ready for immediate use in co-culture experiments (section 2.1.3).

To generate ‘tumour associated’ monocyte-derived macrophages, PBMCs were polarised the day after initial seeding with 0.5ng/ml of macrophage colony-stimulating factor (MCSF; R&D). The rationale for using MCSF for polarisation stems from the typical elongated ‘TAM’ morphological appearance following treatment (Figure 2.2) (McWhorter et al. 2013) and based on expression of the classical TAM marker, CD163; MCSF treated macrophages have similar CD163 expression to macrophages

treated with media conditioned with PDX derived primary PDAC culture cells (Figure 2.3) (Sainz et al. 2014).

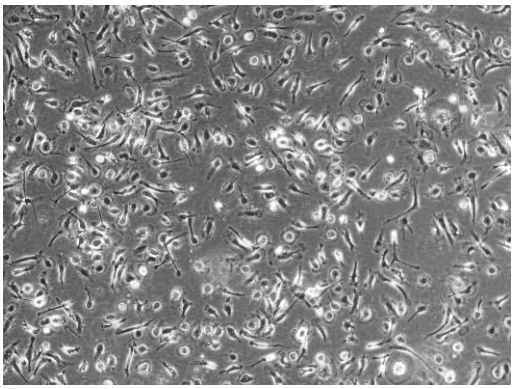

**Figure 2.2 MCSF-treated macrophage morphology**

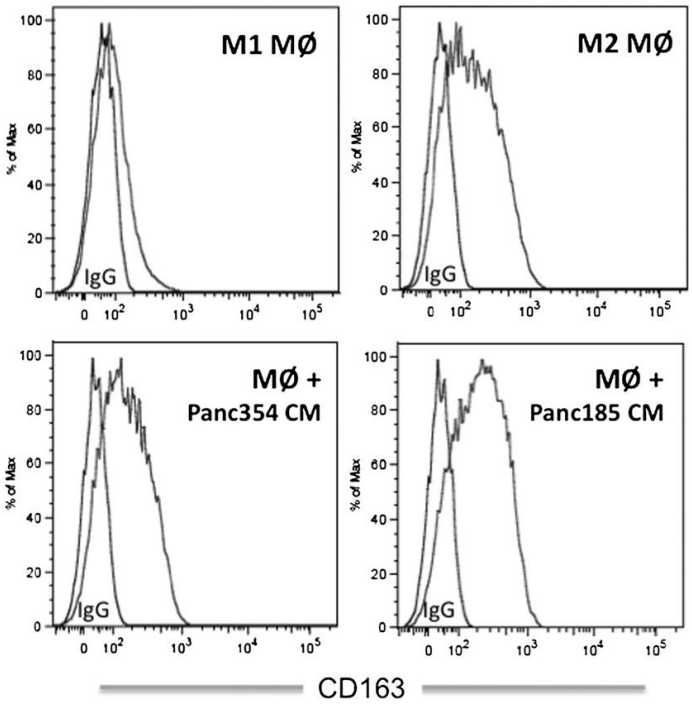


**Figure 2.3 CD163 expression of macrophage cultures**
Cytometric analysis of cell surface CD163 expression in PBMCs cultured in GMCSF (M1), MCSF (M2), Panc354 conditioned media and Panc185 conditioned media (taken from Sainz et al. 2014)

#### 2.1.2.1 Macrophage Conditioned Media (MCM)

After 4 days of culture in MCSF, macrophages were washed twice with PBS and media was replenished with DMEM:F12 (Gibco) supplemented with B-27 (Invitrogen) and β-FGF (PeproTech) to produce macrophage conditioned media (MCM). This media was collected after 48 hours, thus enriched with TAM secreted factors, and centrifuged at 1500rpm for 5 minutes to remove cell debris. Aliquots of MCM were stored at -80°C and defrosted to treat primary PDAC cells, using DMEM:F12 (Gibco) supplemented with B-27 (Invitrogen) and β-FGF (PeproTech) media alone as control.

#### 2.1.2.2 *In vitro* Macrophage Culture Experiments

5x $10^5$ mature macrophages were seeded per well to 6 well adherent plates in 2mls of IMDM (Gibco) supplemented with 10% Human Serum (Sigma). In parallel, 1.6x $10^5$ primary PDAC cells (i.e. ratio of 3:1) were seeded to pre-soaked 6 well 0.4μm permeable polycarbonate membrane transwell (Corning) in RPMI. Following attachment overnight, PDAC transwells were added to wells containing macrophages, and media was changed to control media (1ml top of transwell / 2ml below), or added alone to empty wells containing control media / MCM for comparison (Figure 2.4). After 4 days culture, cells were trypsinised and live cells counted. Cells were then seeded for further experiments, collected for flow cytometry (section 2.7), collected for RNA (section 2.5) or protein (section 2.6).

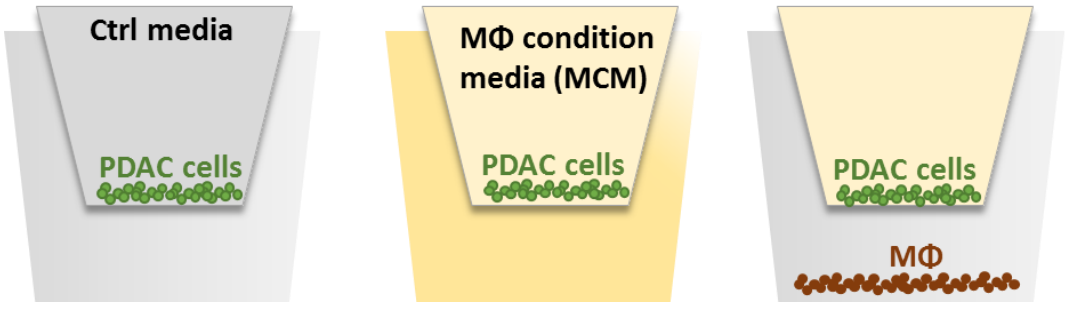


**Figure 2.4 Co-culture Experiments**

For macrophage phenotypes experiments, following 4 days of culture, 5x $10^5$ mature unpolarised macrophages were seeded per well to 6 well adherent plates in 2mls of IMDM (Gibco) supplemented with 10% Human Serum (Sigma). The next day, media was changed to either 0.5ng/ml of macrophage colony-stimulating factor (MCSF; R&D) or 1ng/µl transforming growth factor-β1 (TGFβ1; R&D).

### 2.1.3 3D-Matrix Culture

To assess cell morphology without the limitations of a monolayer cell culture, cells were grown in a three-dimensional model to better recapitulate the ECM and tissue organisation *in vivo*. This was based on methods used by Godinho *et al* (Godinho et al. 2014) whereby a matrix of Collagen-I (Invitrogen) supplemented with 62.5µl 10X FBS and 62.5µl 0.1M NaOH per 500µl Collagen-I, corrected to physiological pH of 7-7.5 was then mixed to Matrigel (Corning) at a 1:1 ratio to form an 'ECM'.

42µl of matrix was added to the center of each well in an 8-well chamber slide plate (Falcon), avoiding high meniscus on the border. Slides were incubated for 1 hour at 37°C to allow the matrix to set, and then cell suspension in 400µl assay medium containing 2% Matrigel was added to each chamber (4x $10^4$ cells per chamber) (Figure 2.5). Cells were incubated for 2-4 days at 37° in a humidified atmosphere of 5% $CO_2$. On completion of the experiment, cells were fixed in 5% Formalin (Sigma), permeabilised in 0.5% Triton X-100 PBS and immunofluorescence analysis was performed (section 2.9.2).

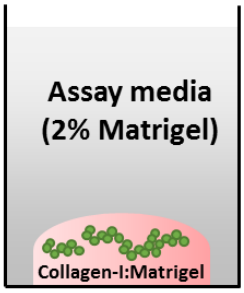


**Figure 2.5 3D Matrix Culture**

### 2.1.4 Sphere Formation

To test for enrichment of cancer stem cells, cell spheres were generated by culturing 1x $10^5$ PDX derived primary pancreatic cancer cells per ml of DMEM:F12 (Gibco) supplemented with B-27 (Invitrogen), βFGF (PeproTech), Penicillin-streptomycin (Sigma) and fungisome (Sigma) in anchorage-independent suspension conditions for 7 days. A CASY Cell Counter (Roche) was used to quantify spheres.

### 2.1.5 Treatments Used in Cell Culture

To determine the effects of soluble factors on PDAC cells, 100ng/ml and 200ng/ml of recombinant human serpinB3/SCCA1 (R&D systems), 100ng/ml of human recombinant oncostatin M (OSM) (PeproTech), 100ng/ml of human interleukin 6 (IL6) (PeproTech) and 100ng/ml of human recombinant leukaemia inhibitory factor (LIF) (PeproTech) were dissolved in control media.

To test agents disrupting the PDAC-TAM crosstalk, cells were cultured in for up to 48 hours in MCM or control media supplemented with soluble factors described above along with 10μg/ml of anti-OSM neutralising antibody (R&D systems), 2μg/ml of anti-gp130 human antibody (R&D systems) or 250nM of ruxolitinib (Sigma). In the case of anti-gp130 antibody, a pre-incubation of 30mins was performed prior to culture in experimental conditions.

For cytotoxicity assays, gemcitabine (Sigma) chemotherapy was added to selected media at a concentration of 300nM.

## 2.2 Cell viability

### 2.2.1 Crystal Violet Staining

Crystal violet staining is a method of quantifying survival cells based on cell staining in adherent conditions (Drysdale, Zacharchuk, and Shin 1983). 4x $10^3$ cells per well were seeded in 96 well plates and left to adhere overnight. The following day, cells were pre-treated with control media / MCM or OSM. Following 48 hours of treatment, media was supplemented with assay drug therapy if required. For collection on desired days (including a 'day 0' control), cells were fixed for 10 minutes in 100µl/well of 0.2% Crystal Violet and 20% Ethanol. Wells were then washed twice with water and photographed after drying. To read the crystal violet stain, 100-200µl/well of 1% Sodium Dodecyl Dulfate (SDS) was added simultaneously to each assay plate and left to dissolve. Optical density (at 570nm) was then read using the FLUOstar OPTIMA Microplate Reader (BMG labtech) and normalised to day 0 conditions.

## 2.3 Cell Migration and Invasion

### 2.3.1 Invasion Assay

Invasion assays were performed using 24-well 8.0µm PET membrane invasion chambers coated with growth factor reduced Matrigel (Corning 354483). Primary PDAC cells were pre-treated for 48 hours in adherent cultures. Following treatment, cells were trypsinised, live cells counted and re-suspended in serum free media (300µl per well) and seeded to coated inserts. 700µl of serum-free medium supplemented with 20% FBS was added to the lower chamber, creating a serum gradient to attract cells (Figure 2.6). Assay chambers were incubate for 12-24 hours at 37°C in a humidified atmosphere of 5% $CO_2$. Invaded cells were fixed with 4% paraformaldehyde (PFA), and matrigel coating was removed by wiping with cotton buds. Invaded cells were stained with DAPI and imaged on the Olympus Fluorescence microscope (model BX51). Cell number was analysed using automated ImageJ particle analysis software.

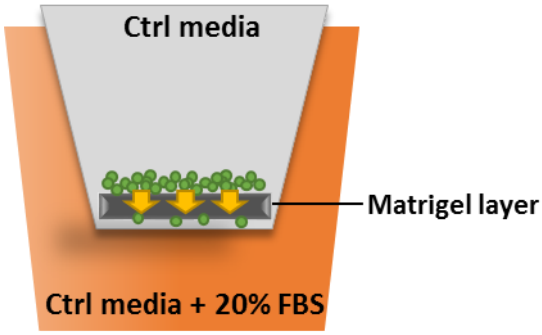


**Figure 2.6 Invasion Assay**

### 2.3.2 Scratch Wound Cell Migration Assay

*In vitro* scratch assay is an established method to study cell migration, based on creation of an artificial 'gap' in a confluent cell monolayer, leading to cell movement towards the opening to close the scratch and thus allowing determination of rate of cell migration (Liang, Park, and Guan 2007).

An automated system was used to perform this technique using IncuCyte ZOOM technology and analysis software (EssenBioscience). Cells were seeded in a 96-well plate ImageLock plate and incubated at 37°C, 5% CO2 until confluency was achieved. Following the WoundMaker protocol, wounding procedure was performed to simultaneously create precise and reproducible wounds in all wells. Wounds were washed twice with PBS and inspected. 100µl of control media or MCM (supplemented with 1:1000 doxycycline for experiments with SerpinB3 knockdown transduced cells) were added to corresponding wells. The plate was placed in the IncuCyte ZOOM and repeat scanning was scheduled for every hour using 10x objective. After 24hrs, wound density was determined using IncuCyte ZOOM Scratch Wound processing software.

## 2.4 Transfection and Transduction of Lentiviral Constructs

### 2.4.1 SerpinB3 shRNA Transfection

Three human SerpinB3-GFP lentiviral shRNA clones (pZIP-TREG3) and a non-targeting control were purchased from Transomic, USA (Figure 2.7A). Plasmids were recovered using the QIAGEN Plasmid Maxi kit (Qiagen - 12165). To make lentivirus, 293T cells were plated to 10cm dishes, and transfected at 80% confluence using Lipofectamine 2000 to deliver 22.5µg lentiviral shRNA construct, 14.6µg packing plasmid (Pax2) and 7.9µg envelope plasmid (pCNA3.1-VSVG). Virus-containing supernatant was collected 48 hours post transfection, filtered through a 0.45µm filter (BD Bioscience) and concentrated by centrifugation for 45 minutes at 1500rpm, aliquoted, frozen and subsequently titrated by flow cytometry analysis of GFP expression in 293T cells infected with increasing dilution of virus. Primary PDAC cells were infected in suspension and following expansion, doxycycline (1:1000) selection was carried out 48 hours prior to FAC sorting for GFP positivity to achieve >90% knock-down of gene expression.

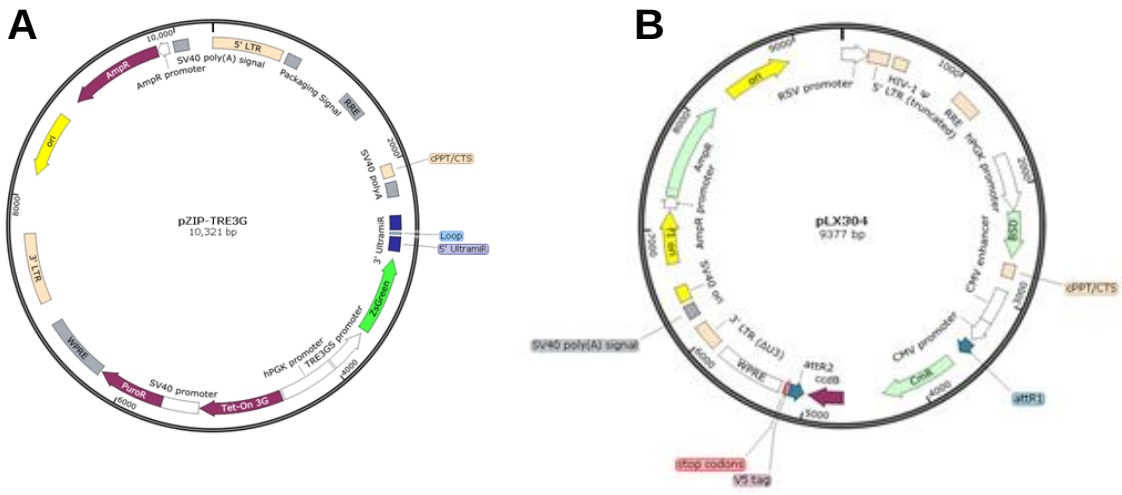


**Figure 2.7 SerpinB3 shRNA and overexpression constructs**
A) shRNA construct: TLHSU2300-6317 B) overexpression construct: TOLH-1515456 Human Lentiviral ORF clone

### 2.4.2 SerpinB3 Overexpression

Human SerpinB3 and empty vector lentiviral cDNA (pLX304) were purchased from Transomic USA (Figure 2.7B). Plasmids were recovered using the QIAGEN Plasmid Maxi kit. Transfection of 293T, virus production and infection of PDAC cells were carried out as per protocol section 2.4.1. Transfected cells were grown through blasticidin selection (using 2-4μg/ml).

## 2.5 Transcriptomics

### 2.5.1 RNA Extraction and Quantification

Cells were washed in PBS and TRI Reagent (Sigma-Aldrich T9424) added as per manufacturer's instructions. Samples were stored at -80°C until further use. Once defrosted, phase separation with 100µl chloroform per 500µl of TRI Reagent was performed; following vigorous shaking for 15 seconds, samples were centrifuged at 12000g for 30 minutes at 4°C. Phase separation resulted in: a red organic phase (containing protein), an interphase (containing DNA), and a colourless upper aqueous phase (containing RNA). The colourless aqueous phase was transferred to a fresh tube and 200µl isopropanol was added per 500µl of TRI Reagent. Samples were mixed and stored overnight at -20°C. The next day, samples were centrifuged at 12000g for 30 minutes at 4°C. The resultant RNA precipitate pellet was washed in 800µl of 80% ethanol and followed by 800µl of 100% ethanol. Following washes, the RNA pellet was left to air-dry for 15 minutes, ensuring the pellet did not completely dry. According to the cell pellet size, an appropriate volume of RNA-ase free water was added to dissolve (approximately 15-30µl).

Purity and quantity of RNA was analysed using the NanoDrop ND1000 UV-Vis spectrophotometer (Thermofisher, USA), measuring absorbance at 260 and 280 nm. Pure and contaminant free RNA was determined by 260/280 ratios of approximately 2 and concentration was determined by the software, which automatically calculates the nucleic acid concentration. For microarray analysis, RNA was run on the Bioanalyser for integrity and quality.

### 2.5.2 Complementary DNA (cDNA) Synthesis

Using the QuantiTect Reverse Transcription Kit (Qiagen - 205314), 1µg of total purified RNA diluted in RNA-se free water was used for cDNA synthesis as per manufacturer's instructions. For initial DNA wipeout: 2µl of DNAse was added per sample. Samples were then incubated for 5 minutes at 42ºC on the Eppendorf

Mastercycler Thermal Cycler (Eppendorf, UK).

Reverse transcriptase (RT) mastermix was prepared (containing 1µg Quantiscript Reverse Transcriptase, 4µg Quantiscript RT Buffer, 1µg RT Primer Mix per sample) and gently added to 1µg of sample. cDNA synthesis reaction was performed using the following thermal cycling conditions:

- Step 1: 95ºC for 20 minutes
- Step 2: 60ºC for 30 minutes
- Step 3: 95ºC for 15 minutes
- Step 4: 4ºC overnight

cDNA sample was diluted with 180µl RNA-ase free water, to give a final concentration of 5ng/µl.

### 2.5.3 Quantitative Real Time Polymerase Chain Reaction (qRT-PCR)

Real time qRT-PCR reactions were prepared to a 10µl volume by adding 10ng of cDNA to 8µl master mix per well (master mix 2.8µl RNAse free water; 5µl MasterMix PerfeCTa SBYR green (Applied Biosystems); 0.2µl of 10µM forward and reverse primer mix of gene of interest) (Table 1.1).

**Table 2.2 Primers List**

| Gene | Primer sense | Primer antisense |
|---|---|---|
| *HPRT* | TGACCTTGATTTATTTTGCATACC | CGAGCAAGACGTTCAGTCCT |
| *ubiquitin C* | AGTAGTCCCTTCTCGGCGAT | GCATTGTCAAGTGACGATCACAG |
| *zeb1* | GATGATGAATGCGAGTCAGATGC | CTGGTCCTCTTCAGGTGCC |
| *vimentin* | GACAATGCGTCTCTGGCACGTCTT | TCCTCCGCCTCCTGCAGGTTCTT |
| *slug* | ATGCCGCGCTCCTTCCT | TGTGTCCAGTTCGCT |
| *loxl2* | GGCACCGTGTGCGATGACGA | GCTGCAAGGGTCGCCTCGTT |
| *OSMR* | TACGCGTCAGAGTTTGCACT | GTGCTGTAATTCCCCACCCA |
| *IL6R* | ATCCCTGACGACAAAGGCTG | CTGGCAGGAGAACTTCTGGG |
| *LIFR* | GGGAGCGTACCGACTGACTG | CCAGAGGGTGCTTTCCAAGA |
| *KLF4* | TCTCCACGTTCGCGTCTGGC | TCCCGCCAGCGGTTATTCGG |
| *OCT 3/4* | CTTGCTGCAGAAGTGGGTGGAGGAA | CTGCAGTGTGGGTTTCGGGCA |
| *SOX2* | AGAACCCCAAGATGCACAAC | CGGGGCCGGTATTTATAATC |
| *serpinB3* | GCAAATGCTCCAGAAGAAAG | CGAGGCAAAATGAAAAGATG |

The reaction was set up in a MicroAmp optical 384-well reaction plate (Applied Biosystems 4309849) and amplified in QuantStudio 7 Flex System (Applied Biosystems, USA). Thermal cycling conditions were as follows:

- Step 1: 95°C for 20 seconds
- Step 2: 40 cycles of 95°C for 3 seconds / 60°C for 30 seconds
- Step 3: 95°C for 15 seconds
- Step 4: 60°C for 1 minute

Data were collected and analysed using the QuantStudio 7 Flex System software, version 1.0 in order to determine Ct (threshold cycle) values for each sample. Relative gene expression of each target gene was calculated using HPRT and Ubiqutin C as reference genes.

### 2.5.4 Microarray

RNA from treated Pan215, 253 and 354 cells were analysed by Professor Stephan Hahn, University of Bochum, Germany. In summary, 100ng of each total RNA sample were hybridized to Agilent whole genome expression microarrays (Human GE 4x44K, v2 G4845A, AMADID 026652, Agilent Technologies). Array data analysis was undertaken using the AFE algorithm to generate the total gene signal (TGS), which was then used for further data analyses using the GeneSpring GX software package version 11.0.2. AFE-TGS were normalised by the quantile method. Subsequently, data were filtered on normalized expression values. Only entities where at least 2 out of 4 samples had values within the selected cut-off (50th-100th percentile) were further included in the data analysis process. Differentially expressed genes were identified by pairwise comparison using the moderated t-test assuming equal variance, $p \leq 0.05$.

#### 2.5.4.1 Gene Set enrichment

The quantile-normalised expression dataset derived from Agilent whole genome microarrays and 186 gene sets derived from KEGG pathway database were used as input for Gene Set Enrichment Analysis (GSEA). Only those gene sets with significant enrichment levels (FDR $q < 0.25$) were considered.

### 2.5.5 Tissue Cancer Genome Atlas

To evaluate the expression activity level of genes in pancreatic cancer, the RNA seq database of pancreatic adenocarcinoma from The Cancer Genome Atlas (TCGA) was analysed by Dr Meng-Lay Ling (https://portal.gdc.cancer.gov/). Patient survival was estimated using R 3.3.3 software with the non-parametric product limit method (Kaplan-Meier). Additional software packages (survival 2.41.3 and survminer 0.4.0) were downloaded from the Comprehensive R Archive Network (CRAN). Gene expression data were categorised into high expression or low expression group, based on median cut off. A p-value $< 0.05$ was considered as significant.

## 2.6 Protein Analysis

### 2.6.1 Western Blotting

Cells grown in adherent 6-well plates were washed with PBS and placed on ice. 50µl of RIPA buffer (Sigma) supplemented with a protease inhibitor cocktail (Roche) was immediately added directly to washed cells. After 5 minutes on ice, cells were harvested using a cell scraper (BD Falcon) and collected to 1.5ml eppendorf tubes. Samples were vortexed for 1 minutes and placed on ice for 10 minutes, for a total of three times. Following the third vortex, samples were centrifuged at 14000g for 30 minutes at 4ºC to pellet cell debris. Supernatant was removed and stored at -20ºC until immunoblotting.

Protein standards of diluted albumin (BSA 2µg/l Sigma-Aldrich) were prepared at the following concentrations: 0, 0.1, 0.25, 0.5, 0.75, 1 and 2µg/µl protein, in RIPA buffer. Cell lysate samples were diluted 1 in 5 and 10µl of diluted sample or reagent were plated in triplicates in a 96 U-bottom plate well (Corning) plate. 200µl of Peirce BCA Protein Assay Reagent (Thermo Fisher Scientific 23225) was added to each well and incubated at 37ºC for 30 minutes. Samples were read using the FLUOstar OPTIMA microplate reader (BMG labtech) at 595nm and protein quantification was calculated against BSA protein controls.

15-30µg of sample protein diluted in distilled water was mixed with loading buffer (50µl β-mercaptoethanol in 1ml NuPAGE sample buffer (Invitrogen NP0007)) at a ratio of 1 to 4 (buffer to sample). Samples were denatured by heating at 95ºC for 10 minutes and then spun and cooled.

Protein was separated in pre-cast 4-12% Bis-Tris NuPAGE gels (Invitrogen NP0321) using 10µl of Novex Sharp Pre-stained Protein Standard (Invitrogen LC5800). Samples were run in 1X MOPS SDS buffer (Invitrogen NP0001) at 150V for 1 hour, or until bromophenol blue marker ran off the bottom of the gel.

Protein was transferred to nitrocellulose membranes (Amersham Pharmacia) using the wet transfer apparatus (Bio-Rad) and Tri-glycine with 20% ethanol transfer buffer

using pre-soaked Extra ThickBlot Paper (Bio-Rad).

Membranes were subsequently blocked with 1X TBS containing 5% BSA (w/v) and 0.05% Tween20 (v/v) for 1 hour at room temperature, and then incubated with primary antibody (see Table 2.3) overnight at 4ºC, followed by 3 washes with TBS containing 0.05% Tween20 (v/v). Incubation with horseradish peroxidase-conjugated secondary antibody at a concentration of 1:1000 was carried out at room temperature for 2 hours. Membranes were washed again with PBS and bound antibody complexes were detected with Enhanced Chemiluminescence Western Blotting Detection Reagent Kit (GE Healthcare RPN 2232).

**Table 2.3 Western Blot Antibodies**

| **Primary antibodies** | | | | |
|---|---|---|---|---|
| **Target** | **Host species** | **Clonality / Isotype** | **Supplier** | **Dilution used WB** |
| SerpinB3 | Mouse | Monoclonal IgG2 | Santa Cruz | 1:500 |
| Total STAT3 | Mouse | Monoclonal IgG2 | Cell Signalling | 1:1000 |
| Phospo-STAT3 | Mouse | Monoclonal IgG1 | Cell Signalling | 1:1000 |
| Vinculin | Mouse | Monoclonal IgG | Sigma | 1:1000 |
| Tubulin | Mouse | Monoclonal IgG | Sigma | 1:1000 |
| **Secondary antibodies** | | | | |
| **Target** | **Conjugate** | **Host species** | **Supplier** | **Dilution used** |
| Anti-Mouse IgG | HRP* | Rat | DAKO | 1:1000 |
| Anti-Rabbit IgG | HRP* | Donkey | DAKO | 1:1000 |

*Horseradish Peroxidase

### 2.6.2 Enzyme Linked Immunosorbent Assay (ELISA)

Enzyme linked immunosorbant assay (ELISA) for OSM cytokine was carried out using the DuoSet Development kit (R&D DY295) in 96-well plates.

#### 2.6.2.1 Plate Preparation

Mouse anti-human OSM capture antibody was prepared to the working concentration in PBS without carrier protein (1:180). A 96-well microplate was immediately coated with 100µl per well of the Diluted Capture Antibody, sealed and incubated overnight at room temperature.

Wells were aspirated and washed three times with Wash Buffer (0.05% Tween 20 in PBS) the following day. Plates were then blocked with 300µl/well Reagent Diluent (1% BSA in PBS) and left to incubate for 1 hour at room temperature. Following aspiration/wash, plates were then ready for sample addition.

### 2.6.3 Cell Supernatants

Cellular supernatants were collected and centrifuged at 1500rpm for 5 minutes to remove cellular debris. Samples were then snap frozen and stored at 80ºC until ELISA analysis as per protocol above.

### 2.6.4 Human Plasma / Serum

Blood samples of treatment naïve metastatic PDAC patients were obtained with consent according to the Barts Pancreatic Tissue Bank Protocol from treatment naïve patients treated at Barts NHS Trust Hospital (City and East London Research Ethics Committee 13/SC/0592). Following centrifugation of the EDTA samples for plasma (as per section 2.1.2), and clotting of blood in SSTII bottles for serum, samples were snap frozen and stored at -80ºC until ELISA analysis.

## 2.7 Flow Cytometry

Tumour cells were harvested using 1% trypsin-EDTA, centrifuged at 1500rpm for 5 minutes and washed with PBS. Cells were re-suspended in 1ml of immune globin intravenous (Human) flebogamma 5% (Grifols Biologics) and incubated at 4°C for 30 minutes. Cells were centrifuged at 1500rpm for 5 minutes and supernatant aspirated. Selected antibody was then added diluted in flebogamma 5% (Table 2.5). After incubation, cells were centrifuged and re-suspended in PBS with DAPI (1:1,000).

Specific antibody protocols were as follows; For AnnexinV, 400µl of AnnexinV binding buffer (eBiosciences 556454) was added per sample post antibody incubation. For Ki67, cells were vortexed and 5mls of cold 70% ethanol was added dropwise to each sample (1-5x$10^7$ cells). Cells were incubated overnight in ethanol at -20ºC, washed in PBS and incubated with antibody as per protocol above.

**Table 2.4 FACS antibody**

| Antibody | Fluorochrome | Volume (per 1x $10^6$ cells) | Incubation time (mins) |
|---|---|---|---|
| AnnexinV (550474 eBiosciences) | APC | 5µl | 30 |
| CD133 (Miltenyi 130-090-826) | APC | 0.2µl | 30 |
| Ki67 (556026 eBiosciences) | FITC | 20µl | 30 |
| CD274 (B7-H1, PD-L1) (Biolegend 329707) | APC | 0.2µl | 15 |

### 2.7.1 Cell Sorting

Cultured cells were harvested in trypsin-ETDA and pelleted at 1500rpm for 5 minutes. Cells were then re-suspended in PBS. Cells were re-suspended in 1ml of immune globin intravenous (Human) flebogamma 5% (Grifols Biologics) and incubated at 4°C for 30 minutes. Cells were then centrifuged at 1500rpm for 5 minutes, and supernatant aspirated. RFP / GFP positive cells proceeded straight to re-suspension in 100-200µl Sorting Buffer (1x PBS; 3% FBS (v/v); 3mM EDTA (v/v)) containing DAPI for the exclusion of dead cells (1:10,000). Cells requiring staining were incubated in appropriate antibody diluted in flebogamma at 4°C for 30 minutes (Table 2.5). Following antibody incubation, cells were re-suspended in Sorting Buffer and centrifuged. Samples were sorted using the BD FACS ARIA Fusion Cell Sorter (BD

Bioscience). Gates were created against unstained and isotype controls for accurate analysis. Samples were immediately re-suspended in cell culture medium and live cells counted prior to seeding for experiments.

### 2.7.2 FACS analysis

Samples were read using the BD LSR Fortessa Cell Analyser platform (BD Bioscience). All samples were analysed with unstained and isotype controls for accuracy, and compensation was performed with positive stained samples. Data was analysed using FlowJo 7.6.5 version software.

## 2.8 Animal Studies

### 2.8.1 Cell Culture

Firefly luciferase expressing human Panc354 cells were established by infecting cells with CMV-Luciferase-RFP-TK Lentivector system from BioCat GmbH (Heidelberg, German). Cells were sorted for RFP expression with FACS and expanded *in vitro* as per section 2.1.1 in adherent conditions.

For *in vivo* assays, cells were pre-treated for 48 hours in desired media (control / MCM / OSM) with or without 2μg/ml of human gp130 receptor antibody. Cells were then trypsinised and live cells counted. Cells for injection were suspended in 50μl of 1:1 growth factor reduced Matrigel and RPMI media.

### 2.8.2 Animals

Mice were housed in the Biological Services Unit of the Barts Cancer Institute, Queen Mary University of London. Animals were maintained in a pathogen-free environment according to institutional welfare guidelines under the authority of the UK Home Office Project License (70/8129) subjected to the Guidance on Operations of Animals scientific Procedures – Act 1986. Protocols and procedures were performed under the personal license number: IB7529564.

Wild-type C57Bl/6 mice, NSG (NOD.Cg-Prkdc$^{scid}$ Il2rgt$^{m1Wjl}$/SzJ) and NU-*Foxn1*$^{nu}$ nude mice were purchased from Charles Rivers (L'Arbresle, France). Mice used in experiments were at least 6 weeks old.

Three experimental set ups were used to assess metastases:

- For experiment ‘A’, 1x $10^5$ cells injected to NSG mice
- For experiment ‘B’, 0.5x $10^5$ cells injected to nude mice
- For experiment ‘C’, 0.5x $10^5$ cells injected to NSG mice

### 2.8.3 Metastasis Assay

Mice were anaesthetised with Isoflurane (Baxter Healthcare FDG9623) delivered at 2% v/v for induction and 1 % v/v for maintenance in oxygen.

Intrasplenic injections of cells suspended in 50µl ‘matrix’ were administered using a 0.3ml capacity syringe and 30-gauge needle (BD microlance).

7 days post injections, mice were anaesthetised as above, and splenectomy was performed (Figure 2.8).

Mice were checked and imaged weekly from week 6 post initial injection using IVIS Specturm Imaging System (Caliper Life Science, USA) as detailed in section 2.8.4.

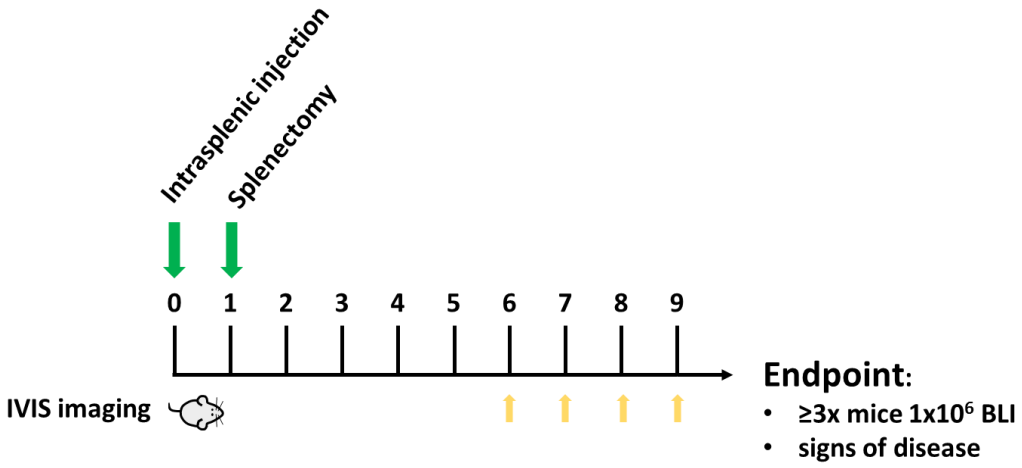


**Figure 2.8 Metastasis Assay Schematic**

### 2.8.4 Bioluminescence Imaging

IVIS Spectrum Imaging System was used for analysis of *in vivo* luciferase activity. Mice were anaesthetised and injected intraperitoneally with 150mg/kg of luciferin (Promega) diluted in PBS. Sequential images were obtained with mice positioned on the left (maximum light emission, ~ 16 and 21 minutes after luciferin injection). Luciferase activity was detected as photons per second per square centimetre per steradian (p/s -1 cm-2 sr-1). Living Image software (Caliper Life Sciences) was used for image analysis.

### 2.8.5 Sacrifice and Organ Removal

Once a minimum of $1x10^6$ ROI bioluminesce was achieved in at least 3 mice on IVIS imaging, or if signs of ascites developed in any mice (suggestive of liver decompensation), all experimental mice were sacrificed using $CO_2$ and cervical dislocation. Livers were harvested, imaged on collection and fixed in 4% PFA. Organs were then processed for immunohistochemical (IHC) analysis as per section.

## 2.9 Histology and Immunostaining

### 2.9.1 Immunohistochemistry

#### 2.9.1.1 *In vivo* Tissue Staining

Tissue staining for *in vivo* samples was undertaken with the assistance of Mr George Elia, Barts Cancer Institute UK. Formalin-fixed paraffin-embedded (FFPE) mice livers were serially sectioned (3μm thick). Sections were dewaxed in xylene and immersed in 100% ethanol for 5 minutes. Endogenous peroxidase was blocked using 100% methanol and 3% hydrogen peroxide for 10 minutes. Rehydration was then carried out using graded alcohols. Antigen retrieval was undertaken using microwaving in pre-heated 0.1M Citrate Buffer (2.84g Tri-sodium Citrate in 1L distilled water, pH 6) for 10 minutes. Sections were blocked using horse serum (1:75) for 15 minutes. CK19 antibody (Table 2.6) was applied for 1 hour at room temperature. After incubation, slides were washed in PBS and incubated with horseradish peroxidase-conjugated avidin (ABC Standard: Vector Laboratories). Antigen was visualised using 3,3'diaminobenzidine (DAB+) chromogen (DakoCytomation) for 2 minutes and then sections were counterstained in Mayer Haematoxylin for 2 minutes. Histological quantification of digitalised slides was performed using Panoramic Viewer (3DHistech). Following manual optimisation of antibody, automated staining was achieved using the Ventana Classic Automated system.

#### 2.9.1.2 Tissue Microarray Staining

Patients were consented for use of tissue biopsy samples under the Barts Pancreas Tissue Bank. Tissue microarrays (TMAs) of pancreatic tissues from hepto-pancreatico-biliary patients were constructed at Barts Health NHS Trust (City and East London Research Ethics Committee 07/0705/87). Following review for tissue core loss / inadequate staining, 33 PDAC tissue samples were available for analysis.

TMA staining was undertaken by Mr Andrew Clear, Barts Cancer Institute, UK and staining analysis was performed with his assistance. Paraffin sections were placed in a 60°C oven for 1 hour and then dewaxed in xylenes. Rehydration was undertaken in a series of graded alcohols to distilled water. Antigen retrieval was then performed; 10 minutes (high power) microwaving in citrate based Antigen Unmasking solution (Vector Laboratories), followed by cooling to room temperature. Endogenous peroxidase was quenched in 3% hydrogen peroxide for 10 minutes and rinsed in TBST. Tissue was then incubated with antibody for 40 minutes at room temperature (Table 2.6).

Prior to immunostaining, tissue was stained with hematoxylin followed by bluing in 0.5% ammonium. Serial rounds of staining on a single tissue section were optimised to ensure no loss of tissue antigenicity and were performed in order to maximise use of tissue cores and enable concurrent analysis of stained sections (Glass, Papin, and Mandell 2009). In addition, appropriate control sections were run in parallel with each round of staining. Sections were stained in the following order:

1. OSMR
2. CD68
3. CK19
4. pSTAT3

Each primary antibody detection was performed with the Biogenex Super sensitive polymer detection system and VIP (Vector Laboratories). Slides were coverslipped in DPX and imaged following each stain in high resolution using Ariol computerised imaging software (Leica Microsystems).

Destaining was undertaken by removing coverslips in xylene, and slides were then taken back to distilled water through a graded series of alcohols. Antibody and coloured reaction products from previous staining cycles were stripped by repeating the heat-induced epitope retrieval step (pressure cooking with citrate based Antigen Unmasking Solution). Complete stripping of antibody and chromogen was determined with comparison of non-stripped control sections and antibody omission controls.

Tissue was then re-stained, beginning with the primary antibody incubation step, as described previously.

**Table 2.5 Immunohistochemistry antibodies**

| Antibody | Concentration |
|---|---|
| CD68 (M0814 Dako) | 1:8000 |
| CK19 (ab9221 Abcam) | 1:2000 |
| pSTAT3 (9145 Cell Signalling) | 1:100 |
| OSMR (HPA017278 Sigma) | 1:250 |

#### 2.9.1.2.1 Microscopy and Image Analysis

Full-slide scans of stained tissue were obtained after each round of staining on the ARIOL imaging system (Leica Microsystems) and software was used to quantify antibody staining. For tissue analysis of CD68 staining, software was trained to automatically select and measure the area of purple (VIP) CD68 stained tissue per core. This was then calculated as a percentage of total tissue stained (i.e. coloured pixels above background white threshold) and a mean percentage area of CD68 staining was taken per patient, as per validated methodology (Greaves et al. 2013).

For staining of pSTAT3, software was first trained to detect and count the number of CK19 stained cells. Then, on linked images, software automatically counted cells positive for nuclear pSTAT3 within the previously determined CK19 stained area. pSTAT3 positive stained cells were then quantified as a percentage of the total CK19 cells and an average of the three cores per patient was calculated.

For OSMR staining, software quantified the pixel intensity of OSMR staining within the CK19 cell population per core. This value was then normalised to the number of CK19 positive cells per core and an average score was given for the triplicate cores per patient.

### 2.9.2 Immunofluorescence

Immunoflourescence was carried out cells in grown in adherent plates or embedded in three dimensional matrix. Following fixation and permeabilisation, cells were rinsed in IF Wash Buffer (PBS, 0.1% BSA; 0.2% Triton X-100; 0.05% Tween-20 pH 7.4) for 10 minutes at room temperature.

Samples were then blocked in Blocking Buffer (IF Wash Buffer with 10% goat serum) for 1 hour. Following blocking, antibody diluted in Blocking Buffer was added (Table 2.6) and incubation undertaken at room temperature. Antibody was then aspirated and 3x PBS washes completed. Hoechst (33342) diluted in Blocking Buffer 1:2500 was added to each chamber for 15 minutes. A final rinse with PBS was carried out. For 3D matrix samples, removal of chamber walls was carried out and slides were mounted using ProLong Antifade. Slides were stored in darkness at 4°C and imaged on the Zeiss LSM 510 Confocal Microscope.

**Table 2.6 Immunoflourescence antibodies**

| Antibody | Concentration | Incubation time (mins) |
|---|---|---|
| Phalloidin 488 (A12379 Life Technologies) | 5µl/ml | 15 |
| pSTAT3 (9145 Cell Signalling) | 1:50 | 60 |

## 2.10 Statistical Analysis

In general, all experiments were performed at least 3 independent times, unless stated. Statistical analyses were performed as an estimation of the associated probability to a student's t-test (95% confidence interval), or one-way analysis of variance (ANOVA) depending on the involved conditions. Fisher's exact test was used for analysis of *in vivo* studies to compare groups. Data were represented as means ± standard error of the mean (SEM) unless stated. In all cases statistical calculation was developed using Prism GraphPad version 5.04 software.

# 3 CHAPTER THREE: PRO-TUMOURIGENIC EFFECTS OF MACROPHAGES

## 3.1 Introduction and Aims

Published data support macrophage driven tumour progression in various tumour types and models (Nielsen and Schmid 2017; Ruffell and Coussens 2015). Data from our laboratory has focussed on TAMs aiding PDAC progression by creating a CSC niche, but also touched on other mechanisms such as promotion of cell survival and metastasis formation (Sainz et al. 2014, 2015). Therefore the initial aims of this thesis will be to explore these phenotypes further in both the CSC and non-CSC populations.

The majority of existing *in vitro* data exploring TAM driven tumourigenesis in PDAC from other groups has been carried out in cell line models. It is known that cell lines do not fully represent all tumour subtypes and these cultures loose heterogeneity over time as a result of major irreversible alterations in biological properties, including genetic gains and losses, growth and invasive properties and loss of specific cell populations (Gillet et al. 2011). Therefore by using primary cancer cells, both macrophages and PDAC cells, a more representative model could be applied for experimental testing that incorporates a more heterogeneous population of cells, resulting in more clinically relevant biological findings (Hidalgo et al. 2014) .

The aims of this chapter are:

- To explore the pro-tumourigenic effects of TAMs in the primary PDAC model
- To determine factors regulated by TAM interaction in primary PDAC cells

## 3.2 Results

### 3.2.1 EMT, Invasion and Metastases

To determine the effects of TAM secreted factors on primary PDAC cells, a panel of primary PDAC cells were cultured with standard control media (DMEM:F12 (Gibco) supplemented with B-27 (Invitrogen) and β-FGF (PeproTech)) or standard control media that had been conditioned by MCSF-polarised macrophages for 48 hours (MCM) (see methods section 2.1.2.1). PDAC cells were treated for 48hrs in 2D and matrix-based 3D conditions and compared to control media alone. It was noted that cells adopted a more myofibroblast-like morphology, with an elongated shape, and appeared detached / scattered, with less colony formation in MCM (Figure 3.1), suggestive of cells undergoing EMT.

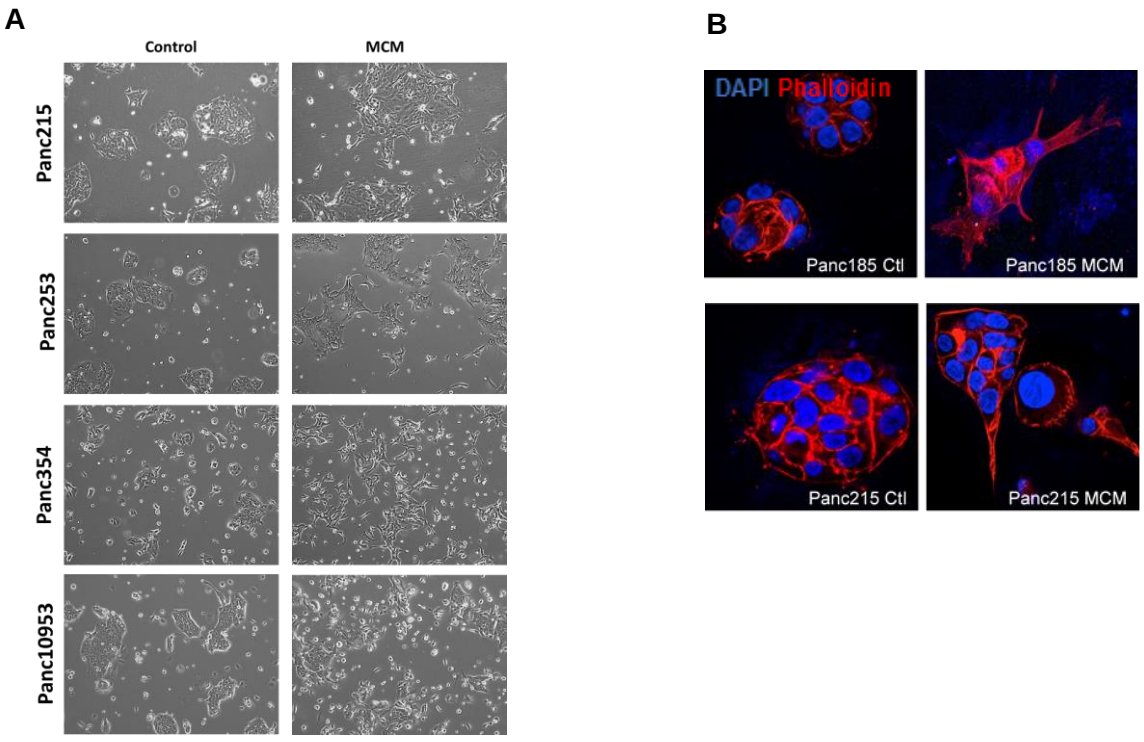


**Figure 3.1 Primary PDAC cell morphology in MCM**
A) Brightfield microscopy images of primary PDAC cells cultured in MCM or control media for 48hrs
B) Immunoflourescent images of primary PDAC cells grown in a 3D matrix in the presence of control and MCM media. Cells were stained with phalloidin to define cell morphology.

Morphological changes were confirmed to be transition from an epithelial to a mesenchymal state by RT-qPCR gene analysis of cells cultured in MCM. Consistent upregulation of mesenchymal-associated genes (zeb1, vimentin, loxl2 and slug) were seen in all cell types compared to treatment with control media alone (Figure 3.2). Of note, a difference in the degree and pattern of each gene upregulation between cell types was seen throughout the primary cell panel and when using different donor macrophages to generate conditioned media and through use of different *in vivo* and *in vitro* passages of primary PDAC cells. This was expected, as the cancer cells tested represent a group of heterogeneous primary PDAC tumours and primary macrophage were derived from different donors. This model would therefore be reflective of the heterogeneity likely to be seen in the 'real' PDAC tumour. Upregulation of EMT genes was consistent across all cell types despite heterogeneity of tumour and macrophage cells, thus indicating a true finding likely to be relevant to a heterogeneous patient population.

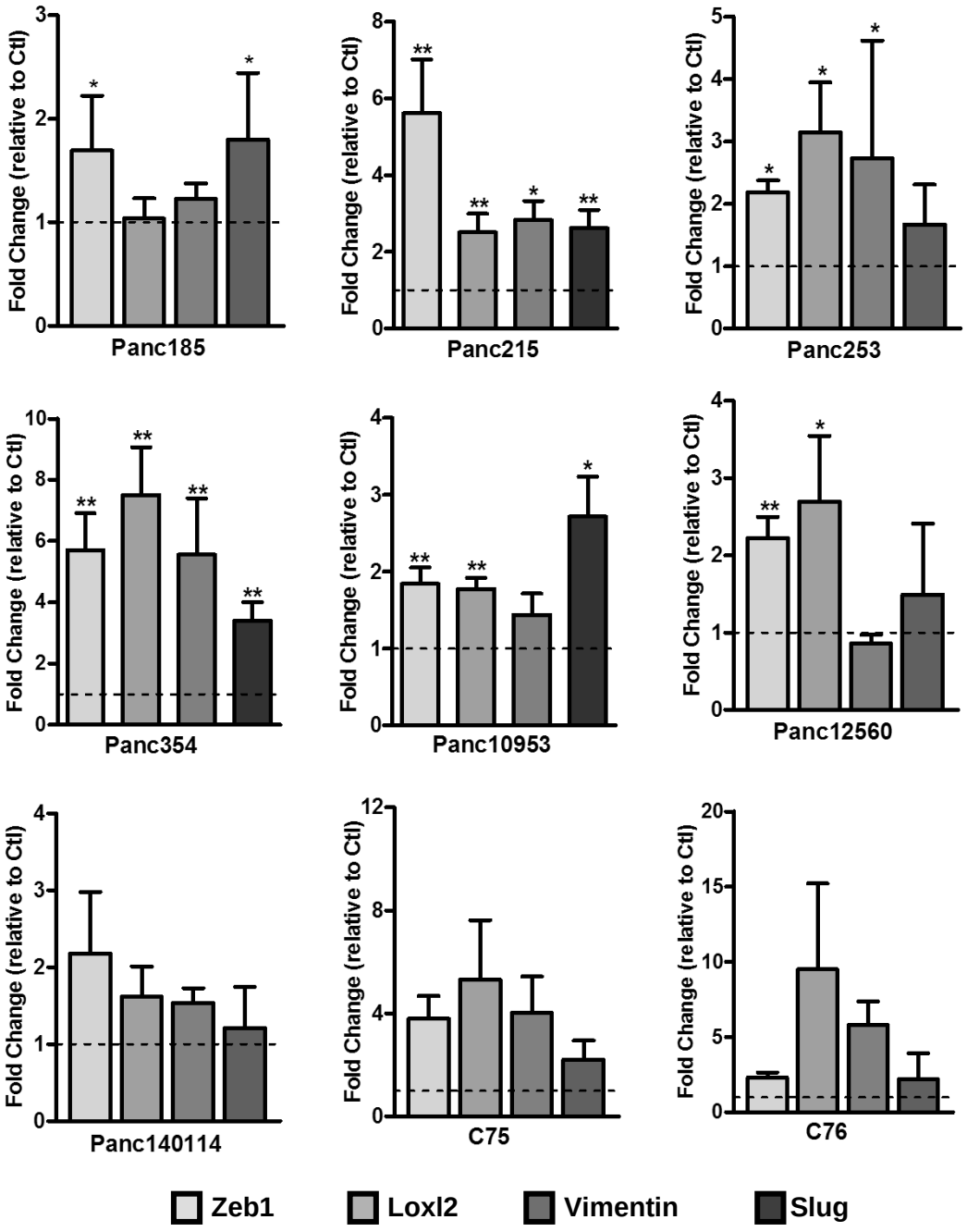


**Figure 3.2 EMT gene expression in MCM culture**
RT qPCR of Panc185, 215, 253, 354, 10953, 12560 (n=9 per cell type) and Panc140114, C75, C76 (n=4 per cell type) treated with MCM over 48hrs. Results represent a compilation of experiments normalised to control, with values representing the mean (+/- SEM). Statistical significance: Wilcoxian signed-rank test * = $p<0.05$, ** $p<0.005$

To confirm effects of TAMs on the induction of EMT in PDAC cells, a 'direct' co-culture of unpolarised macrophages was undertaken in Panc215, 354 and 10953 using transwell co-culture. These results confirmed upregulation of EMT genes in 'direct' co-culture as with MCM (Figure 3.3).

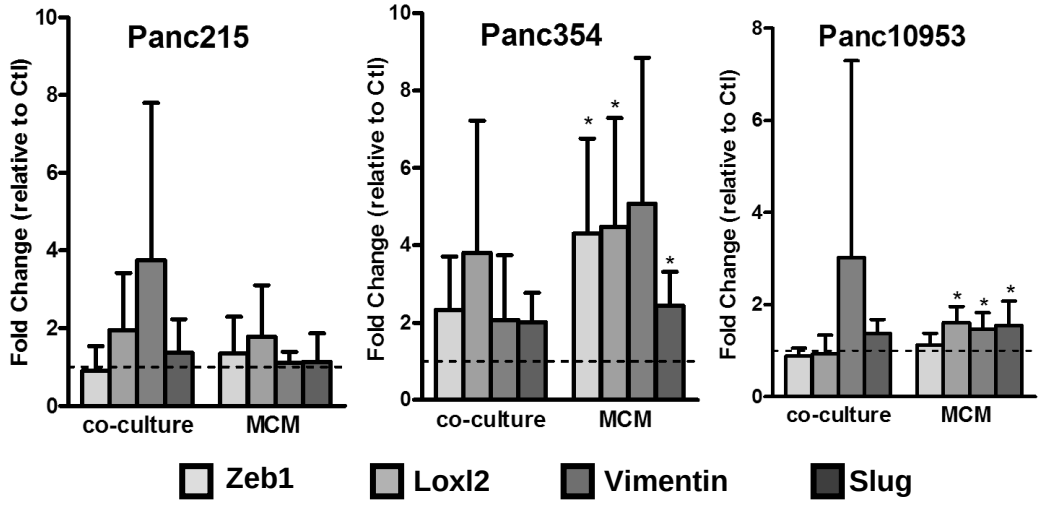


**Figure 3.3 EMT gene expression in 'direct' macrophage and MCM coculture**
RT qPCR of Panc215, 354, 10953, (n=6 per cell type) co-cultured with unpolarised donor macrophages or MCM for 72hrs. Results represent a compilation of experiments normalised to control, with values representing the mean (+/- SEM). Statistical significance: Wilcoxian signed-rank test * = $p<0.05$

Effects in direct culture were less pronounced than with MCM, for example *Zeb1* was not consistently upregulated as with experiments using MCM alone (Figure 3.2). This could be as a result of different PDX *in vivo* passages used for in each experiment or due to the different experimental set up: for cells tested in Figure 3.2, primary cultures were treated for 48hrs in adherent plates with either control media on MCM. For experiments using co-culture, cells were treated in transwells, either with MCM or with macrophages plated on inserts (as described in section 2.1.2.2). Thus for co-culture experiments, there was regulatory feedback between the two cell types when in direct culture that would not be present in conditioned media treating PDAC cells alone. As the cells types are in constant feedback with one another in co-culture, factors inducing EMT being secreted by macrophages could be regulated through a negative feedback loop when in direct culture, leading to lower EMT gene expression. Alternatively, the lesser effects could be explained by time points: macrophages used

in this experiment were ‘unpolarised’ at the time of seeding and only underwent ‘TAM’ polarisation once culture with PDAC cells began. Thus, in these conditions, the secretion of any EMT-inducing factors by TAMs may be delayed, unlike in MCM where the factors are present from the start. To try to compensate for this, both co-cultures were left for longer (72 hours) than the usual 48 hours with MCM alone. However, this presumes that polarisation of TAMs takes up to 72hrs in co-culture, and this has not been confirmed. One therefore cannot be certain of when the maximum ‘EMT’ inducing effects of the eventually polarised macrophages was taking place, and therefore it would have been better to perform a time course assay with cells in co-culture, first examining when macrophages were being polarised in direct culture with PDAC (for example using FACS analysis of CD163 or qPCR of ‘TAM’ gene expression in the macrophages) and then examining when the PDAC cells were undergoing EMT. By performing these kinetic experiments, time points could have been optimised more accurately.

Having now confirmed an EMT phenotype in PDAC as a result of TAM interaction, it was necessary to show functional effects. For all invasion assays, primary PDAC cultured cells were pre-treated with either non-conditioned control media (Ctl) or media conditioned by macrophages (MCM) for 48 hours and then seeded in transwell invasion assay (at least 2 transwells per condition per experiment). The number of invaded cells in each well was then counted and the mean number of cells per condition was calculated. The average number of invasive cells with MCM pre-treatment was then calculated as a fold-change against the average number of invasive cells with control media pre-treatment. Cells pre-treated with MCM showed consistent increased invasive ability towards serum-rich conditions compared to control treated cells (Figure 3.4). This finding indicated functional consequence that macrophage derived factors were activating invasion in PDAC cells, possibly through transition to a mesenchymal state.

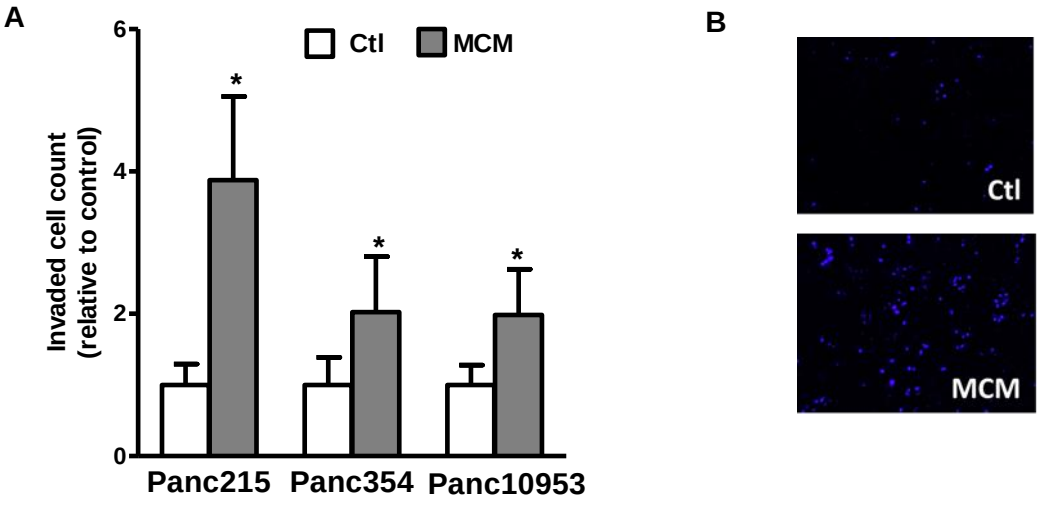


**Figure 3.4 Transwell invasion assay of MCM pre-treated cells**
A) Panc215, 354 and 10953 (n=6 experiments per cell type) cells cultured with macrophage conditioned media (MCM) or control media (Ctl) for 48hrs and seeded for transwell invasion assay. For each experiment, the average number of invaded cells with MCM pre-treatment was then calculated as a fold change compared to control treated cells. Results represent a compilation of experiments normalised to control, with values representing the mean (+/- SEM). Statistical significance: Wilcoxian signed-rank test * = $p<0.05$. B) Representative images of Panc354 cells invaded on transwell assay and stained with DAPI.

#### 3.2.1.1 EMT and Invasion in Cancer Stem Cells

Having now confirmed cells cultured with TAM secreted factors display an EMT phenotype and are more invasive, it was important to assess the effects of MCM on the cancer stem cell population specifically. Previous data from the laboratory has confirmed that factors within MCM enrich for cancer stem cells (Sainz et al. 2014, 2015). For the purpose of this thesis, differential effects of EMT and invasion between the CSC and non-CSC population were examined. Cancer stem cells were defined by sorting for the cancer stem cell marker, CD133 (Human prominin-1, PROM1). This protein is a transmembrane cell-surface protein that localises to the plasma membrane. CD133 is expressed in cancer progenitor cells, including pancreatic cancer cells, and is an essential marker for detecting and enriching for CSCs in PDAC (Hermann et al. 2007).

In the first instance, cells sorted for CD133 expression were cultured with control media or MCM for 48 hours and displayed differences in EMT gene regulation: at baseline (in control media) CD133+ cells had a significantly higher expression of the loxl2, and a trend for higher gene expression in zeb1 and vimentin (but not significant) (Figure 3.5). With MCM treatment, both the CD133- and CD133+ cells underwent a significant increase in all EMT genes, as seen in the 'bulk' mixed population of cells. Of interest, CD133+ cells had a significantly higher expression of zeb1, vimentin and loxl2 following MCM treatment when compared to upregulation of these genes in CD133- MCM treated cells. This finding would suggest that the invasive effects of CSCs were being potentiated by MCM, making them the most 'EMT' population within a mixed population of cells.

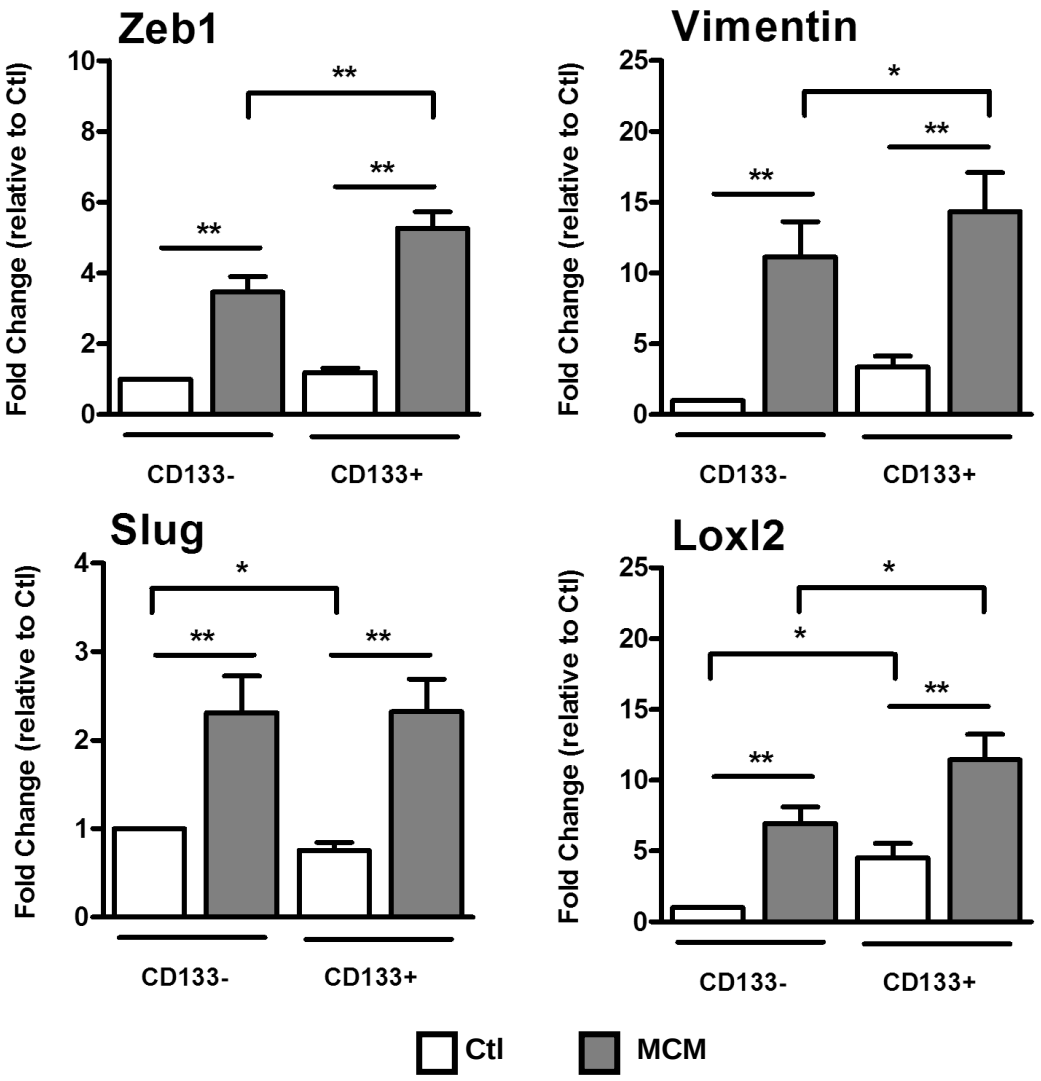


**Figure 3.5 EMT gene expression in CD133- & CD133+ Panc354 cells**
RT qPCR of CD133- and CD133+ Panc354 (n=8) cultured with MCM for 48hrs. Results represent a compilation of experiments normalised to control, with values representing the mean (+/-SEM). Statistical significance: Wilcoxian signed-rank test * = $p<0.05$ **=$p<0.005$

Confirming this result, CD133+ cells were more invasive at baseline compared to CD133- cells in invasion assay, but the most invasive population was the CD133+ MCM treated cells (Figure 3.6).

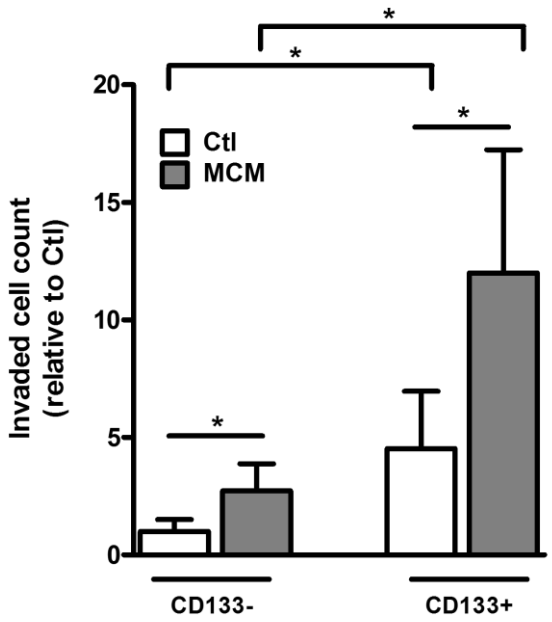


**Figure 3.6 Transwell invasion assay of CD133- and CD133+ Panc354**
Panc354 (n=6) cells cultured with MCM in transwell invasion assay. Results represent a compilation of experiments normalised to control, with values representing the mean (+/-SEM). Statistical significance: Wilcoxian signed-rank test * = $p<0.05$.

Thus, collective *in vitro* results confirmed activation of EMT and invasion in primary PDAC cells when exposed to TAM secreted factors. In particular, these factors had the effect of potentiating this phenotype in the CSC population specifically.

#### 1.8.1.1 *In vivo* metastasis

Following *in vitro* data supporting the invasive effects of MCM in the primary PDAC model, the systemic relevance of these effects were tested using the *in vivo* model.

Cells used for *in vivo* injection were Panc354 cells transduced with the CMV-Luciferase-RFP-TK Lentivirus. Prior to preparing cells for injection, the effects of MCM were tested on this cell type to ensure similar effects were seen as with non-transduced cells. Results confirmed typical changes in cell morphology and increased mesenchymal gene expression in Panc354-Luc cells following culture in MCM as seen with non-transduced cells (Figure 3.7).

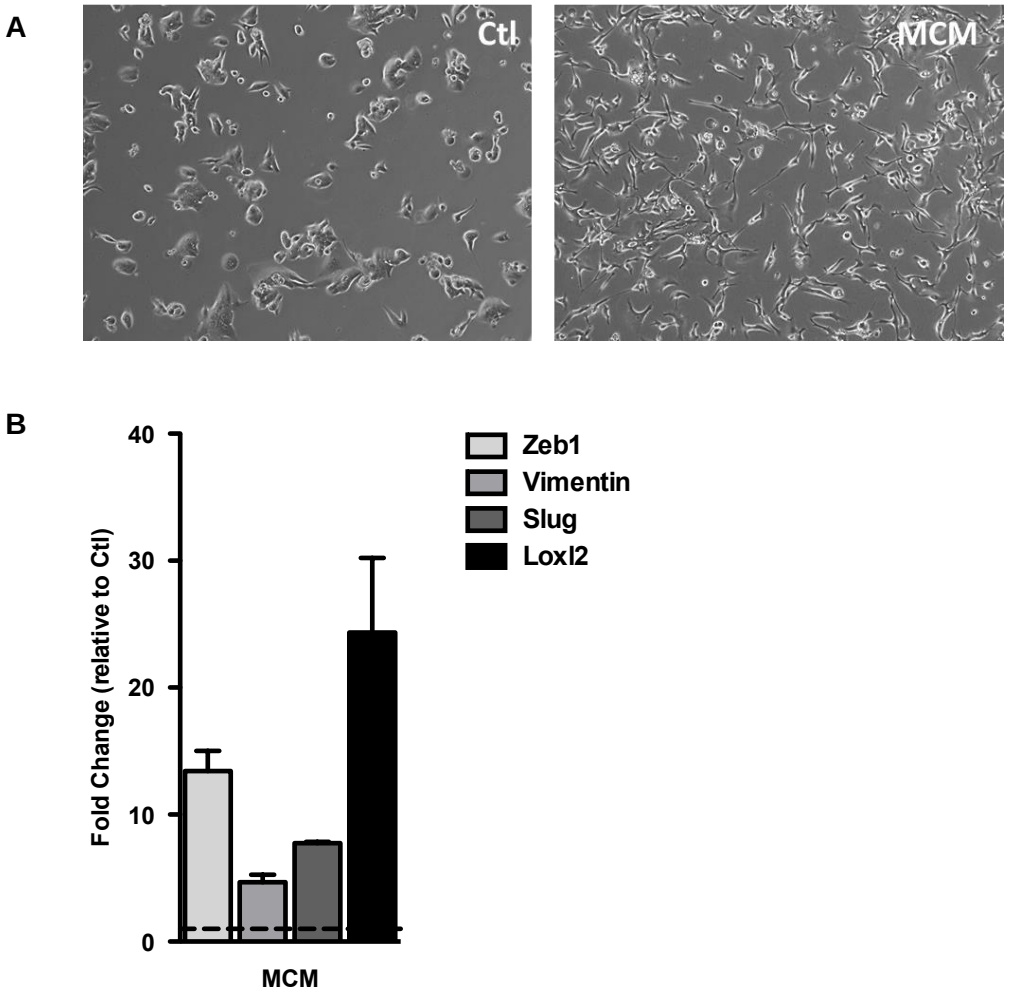


**Figure 3.7 Effects of MCM on Panc354-Luc cells**
A) Brightfield microscopy confirming EMT morphology in MCM cultured Panc354-Luc cells prior to *in vivo* injection B) RT qPCR of Panc354-Luc cells (n=2) cultured with MCM for 48hrs. Results represent a compilation of experiments normalised to control, with values representing the mean (+/- SEM).

*In vivo* experiment 'A' was performed using Panc354-Luc cells pre-treated with control media or MCM *in vitro* (see methods). Cells were then injected intrasplenically to mice after 48 hours. 1x $10^5$ cells were injected to NSG mice and splenectomy performed 1 week later. Animals were sacrificed at 6 weeks post injection, by which point the BLI signal was $1x10^6$ in 3 mice. Livers were dissected and imaged. Absence of metastatic spread was confirmed in livers with macrometastases by fixing organs and staining serial sections with CK19 antibody. On collection of organs, 3/5 livers treated with control media had macrometastasis and 5/5 in MCM pre-treated cells (Figure 3.8 and Table 3.1). The number of mice treated in this experiment was not enough to determine significant differences on the effects of metastases formation in MCM pre-treated cells compared to control media treated cells *in vivo*. Therefore, this experiment would need to be powered calculated and repeated in more animals in order to make definitive conclusions about the differences between the treated groups.

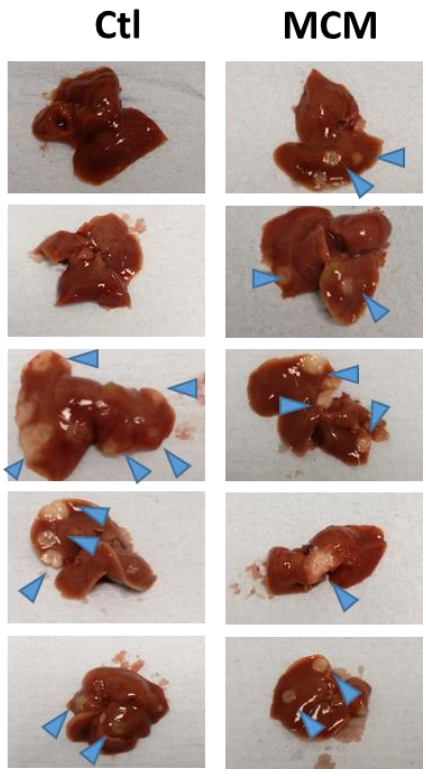


**Figure 3.8 Liver macrometastasis *in vivo***
Liver macrometastasis experiment 'A' following intrasplenic injection of 1x $10^5$ Panc354-Luc cells pretreated with control or MCM for 48hrs *in vitro*. Animals were sacrificed and livers imaged 6 weeks post injection.

**Table 3.1 Metastasis results *in vivo***

| Pre-treatment | Positive for liver metastasis / total number animals (%) |
|---|---|
| **Control** | **3/5 (60%)** |
| **MCM** | **5/5 (100%)** |

### 3.2.2 Proliferation

In order to further investigate the effects of TAM on PDAC progression, proliferative state was next assessed. Using FACS assessment of Ki67 staining, the percentage of positive stained cells (in G1 and S/G2-M phase) were quantified for both control media and MCM treated cells (Figure 3.9A). These results showed no significant difference between the percentage of Ki67 positive cells in control media or MCM treated cells (Figure 3.9B).

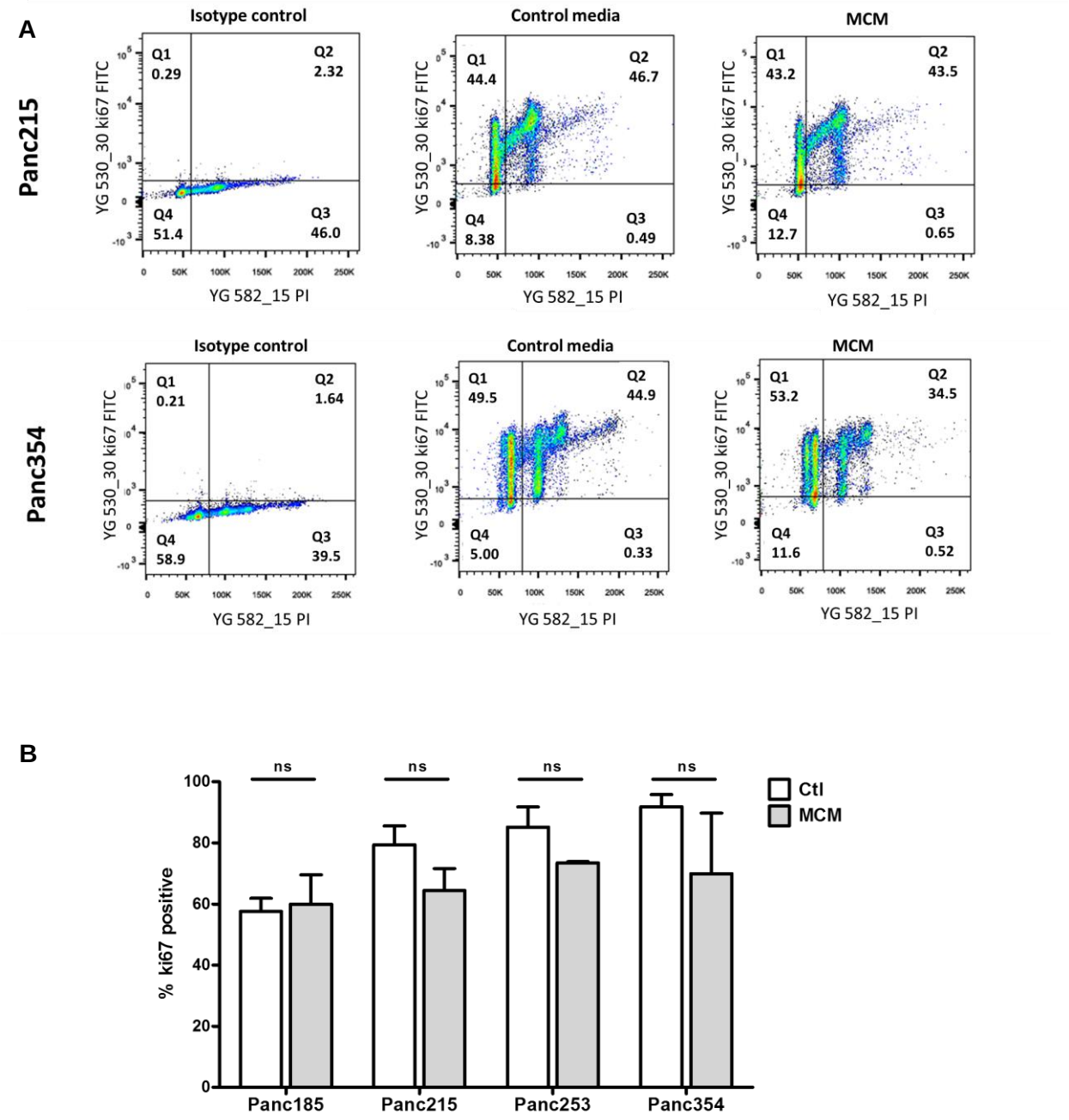


**Figure 3.9 Ki67 FACS analysis of MCM cultured cells**

A) Representative FACS plots of Panc215 and 354 stained with isotype control and Ki67 antibody after 48hrs of treatment in control media or MCM. Key: Q1=Ki67 +ve cells in G1 phase, Q2= Ki67 +ve cells in S/G2-M phase, Q4=Ki67 –ve cells. At least 10,000 events were recorded for each condition. B) Quantification of Panc185, 215, 253 and 354 positive cells (G1 and S/G2-M phase) in control media compared to MCM treated cells (n=3 per cell type). Results represent a compilation of experiments in each cell type normalised to control, with values representing the mean (+/- SD).

Crystal violet proliferation assay was also undertaken for culture over longer time periods. Following 4 days and 7 days treatment, there was again no significant difference in proliferation seen (Figure 3.10A and B).

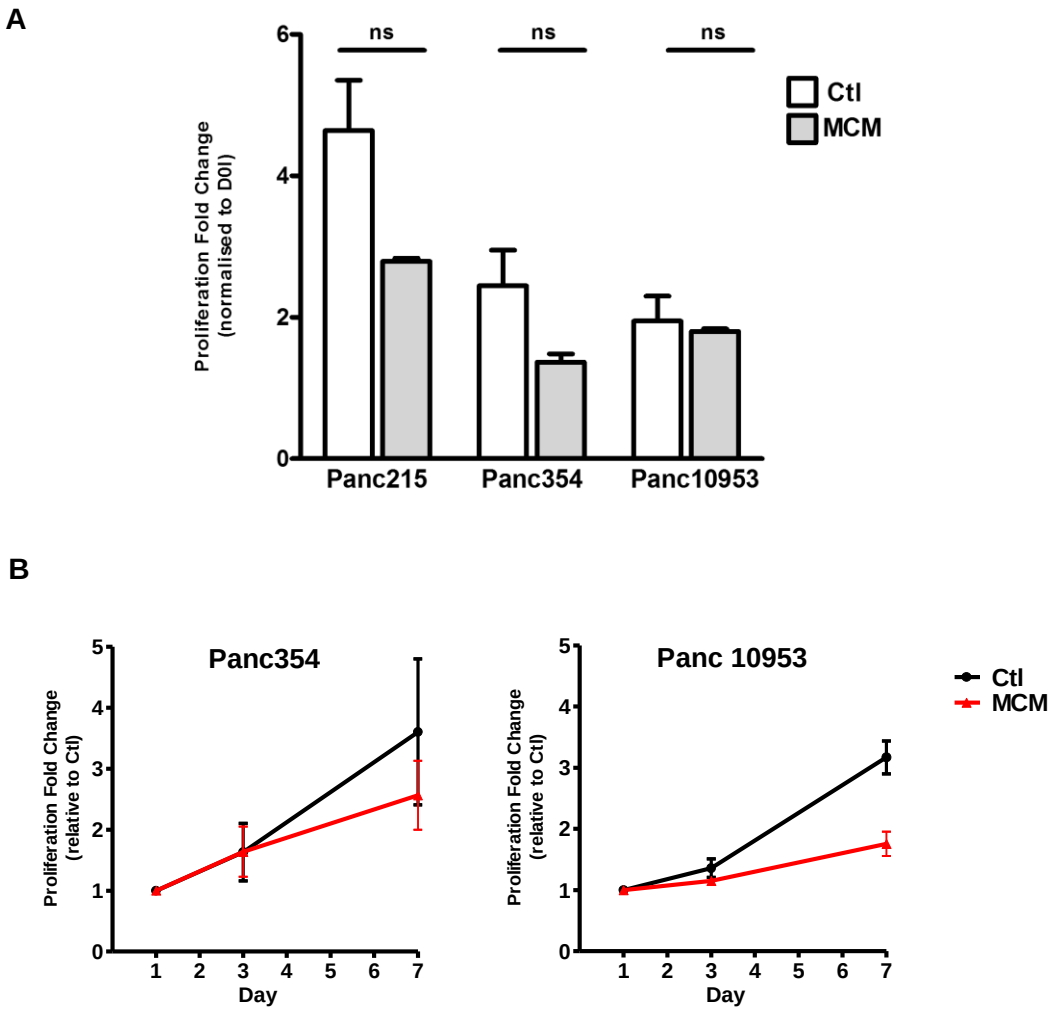


**Figure 3.10 Crystal violet proliferation of MCM cultured cells**
A) Crystal violet analysis of Panc215, 354 and 10953 treated with MCM for 4 days (n=3 per cell type). Staining of crystal violet was normalised to day 0 control (i.e. pre-treated cell density). B) Crystal violet analysis of Panc354 and 10953 treated with MCM for 3 and 7 days (n=2 per cell type). Staining of crystal violet was normalised to day 0 control (i.e. pre-treated cell density).

Cell death was next analysed using annexin V FACS staining of cells pre-treated in each condition. Quantification of live cells analysed using annexin V showed no significant difference in cell death following treatment with control or MCM (Figure 3.11).

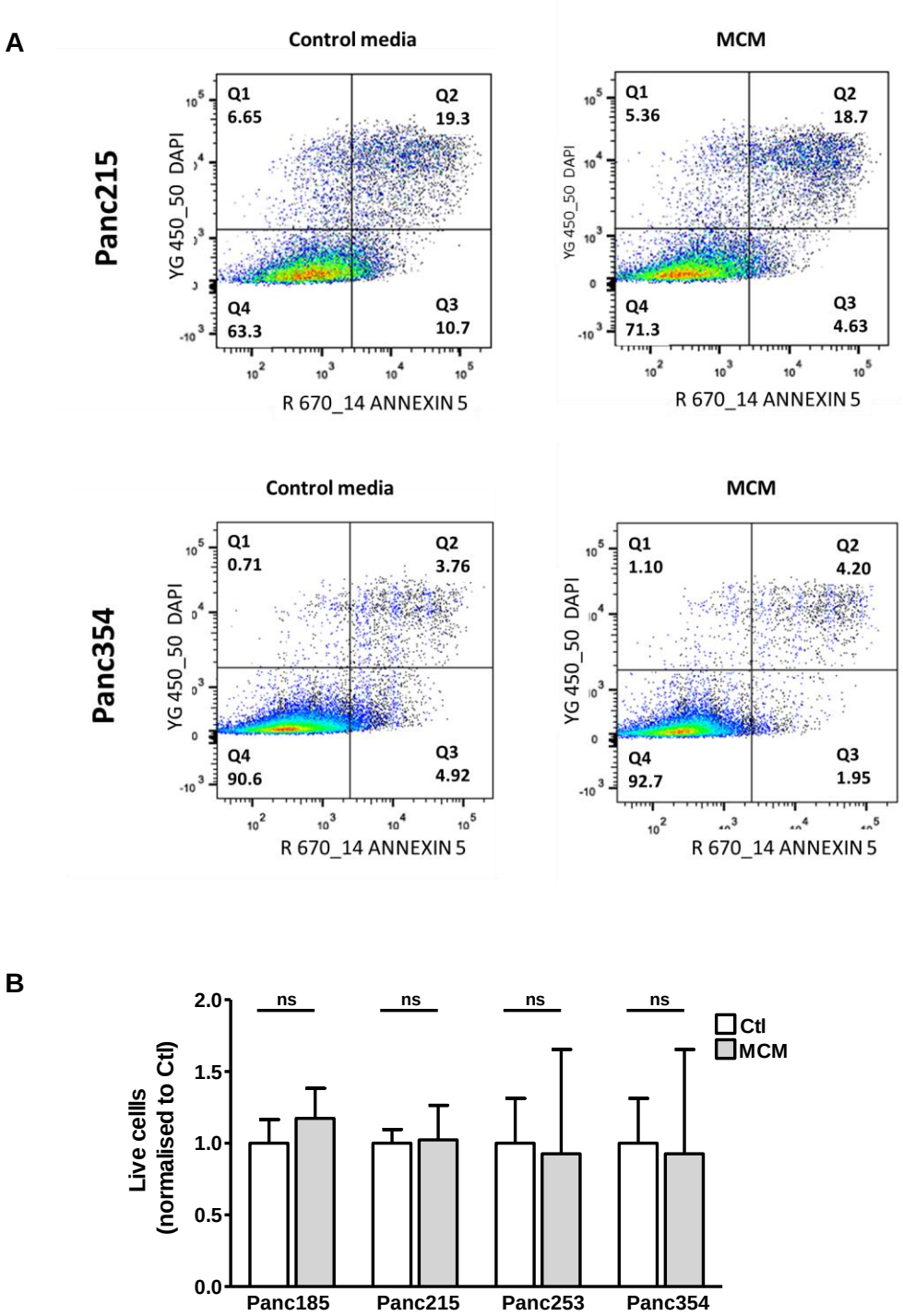


**Figure 3.11 Annexin V FACS staining of MCM cultured**

A) Representative FACS plot of Panc215 and 354 stained with Annexin V antibody after 48hrs of treatment in control media or MCM. Key: Q1=DAPI +ve dead cells +, Q2= DAPI+ve and annexin V +ve dead cells (apoptosis), Q3=annexin V + live cells (undergoing apoptosis), Q4= live cells. At least 10,000 events were recorded for each condition. B) Quantification of Panc185, 215, 253 and 354 live annexin V positive cells (Q4) in control media compared to MCM treated cells (n=4 per cell type). Results represent a compilation of experiments in normalised to control, with values representing the mean (+/- SD).

Thus, when cells were cultured in MCM, there was no differences seen in the number of cells undergoing cell death compared to control treated cells. Taken together, these results show factors within MCM do not confer a proliferative or survival advantage on PDAC cell growth in basal conditions.

### 3.2.3 Chemoresistance

Following data already published in PDAC (Di Caro et al. 2015; Mitchem et al. 2013; Weizman et al. 2014), it was pertinent to test the effects of MCM on cell survival in context of stress, particularly chemotherapy. As gemcitabine is the backbone of current therapy, cells were pre-conditioned with MCM or control media for 48 hours and media was then refreshed to contain 300nM of gemcitabine or no drug.

Analysis by crystal violet staining showed no survival advantage against chemotherapy with MCM pre-conditioning (Figure 3.12). No differences were noted between control and MCM gemcitabine treated cells, with an almost identical pattern of decreased crystal violet staining between the two conditions.

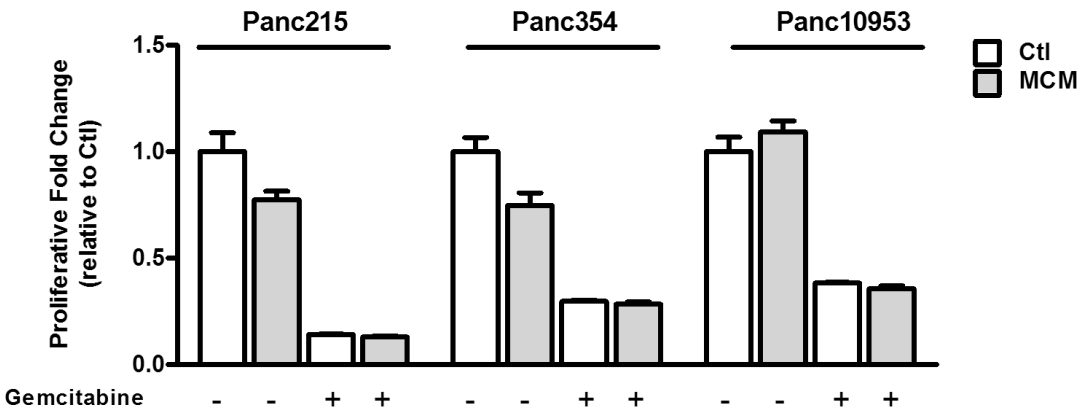


**Figure 3.12 Crystal violet analysis of gemcitabine treated cells**
Panc215, 354 and 10953 were pre-conditioned with MCM for 48hrs and then media was refreshed with the addition of 300nM gemcitabine. Cells were grown for a further 4 days. Results represent n=1 per cell types and values are normalised to day 0 control (i.e. pre-treatment cell density) and plotted relative to control treatment.

FACS analysis of annexin V staining was performed to determine cell death following treatment with gemcitabine. Again no significant differences were noted in MCM pre-treated cells (Figure 3.13).

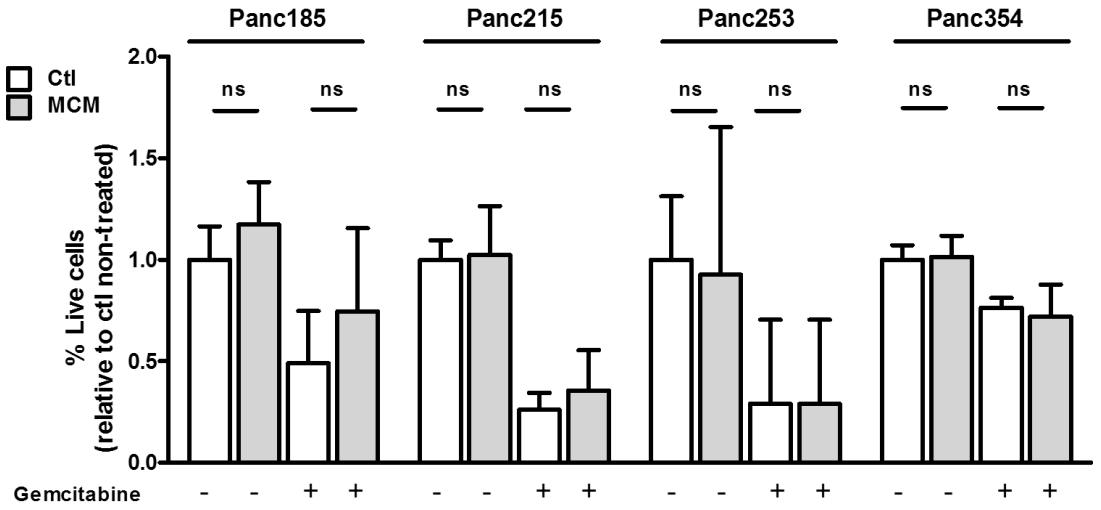


**Figure 3.13 Quantification of annexin V stained cells in MCM**
Quantification of Panc185, 215, 253 and 354 live annexin V positive cells (Q4) in control media compared to MCM pre-treated cells with gemcitabine treatment (n=4 per cell type). Results represent a compilation of experiments normalised to control, with values representing the mean (+/- SD).

Taken collectively, results indicate factors within MCM do not confer a survival advantage to PDAC cells treated with gemcitabine chemotherapy.

### 3.2.4 Microarray Gene Analysis of Panc253 and 354

Having determined that cells cultured with macrophage derived factors were driving epithelial-to-mesenchymal transition, leading to invasion *in vitro* and metastasis *in vivo*, the factors and pathways generating this phenotype in primary PDAC cells needed to be determined. To do this, Agilent microarray gene analysis of cells treated with MCM was performed in collaboration with Professor Stephan Hahn of the Ruhr-University Bochum, Germany. Initially, Panc253 and 354 were sent for analysis.

To validate microarray samples sent to collaborators, RT qPCR of the treated Panc253 and 354 was performed and confirmed upregulation of EMT genes (Figure 3.14).

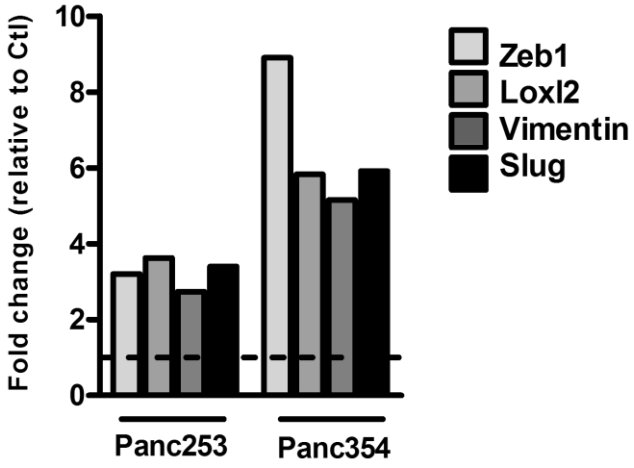


**Figure 3.14 EMT gene validation of microarray samples**
RT qPCR of EMT genes in Panc253 and 354 cells (n=1) cultured with MCM for 24hrs and sent for Agilent microarray analysis.

### 3.2.4.1 Gene Regulation

Microarray data were analysed as follows: fold change differences of gene expression in conditioned media compared to control treated cells was determined. Moderated t-test was applied and significant gene fold differences were determined ($p<0.05$). 159 genes were found to be significantly upregulated and 94 downregulated in Panc354. 41 genes were significantly upregulated and 34 downregulated in Panc253 (Figure 3.15).

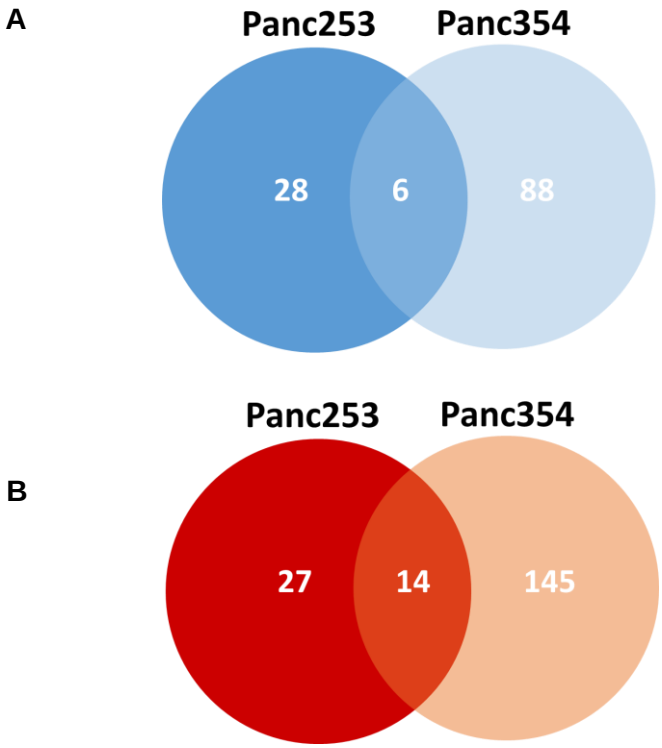


**Figure 3.15 Venn diagram of microarray gene expression**
Gene expression fold change profile in Panc253 and 354 comparing control media treated cells with conditioned media. A) Significantly downregulated genes B) Significantly upregulated genes. Statistical significance: moderated t-test $p<0.05$.

6 commonly downregulated genes in MCM culture were found between Panc253 and 354 (Figure 3.15 and 3.16).

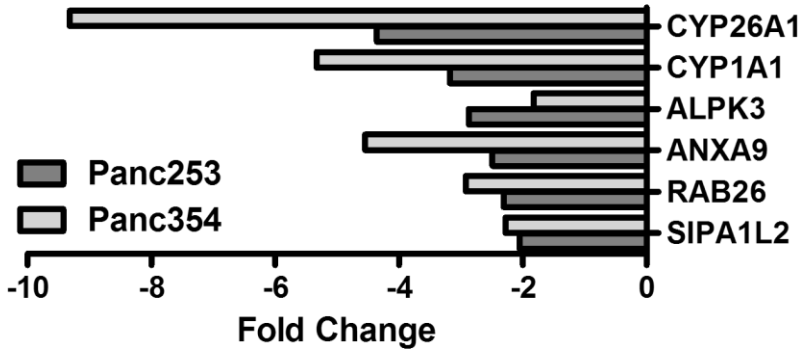


**Figure 3.16 Common downregulated genes on microarray**

14 commonly upregulated genes in culture with MCM were found between Panc253 and 354 (Figure 3.15 and 3.17). Of these genes, the serine proteases SerpinB3 and B4 were the most highly upregulated genes in both cell types.

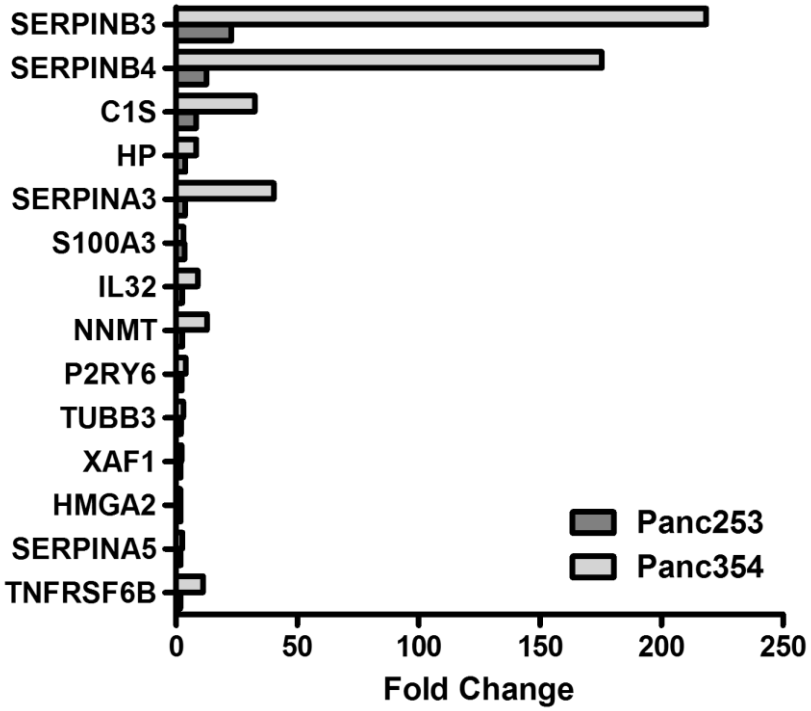


**Figure 3.17 Common upregulated genes on microarray**

#### 3.2.4.2 Gene Set Enrichment Analysis

To determine which pathways were likely to be activated by macrophage-derived factors, microarray data was analysed, with the assistance of Dr Meng-Lay Lin, using KEGG pathway mapping. Agilent microarray gene expression profiles were uploaded to software, and based on the transcriptomic profile of Panc253 and 354 cultured in MCM, 10 common gene sets were found to be significantly enriched between the two cell types (FDR q-val <0.25) (Table 3.2).

**Table 3.2 KEGG gene set enrichment Panc253 and 354**
(NES = normalised enrichment score. FDR= False Discovery Rate: p-val <0.25)

| KEGG GENE SET | Panc253 NES | Panc354 NES |
|---|---|---|
| COMPLEMENT_AND_COAGULATION_CASCADES | 1.4998453 | 1.7503108 |
| FOCAL_ADHESION | 1.5119898 | 1.3321809 |
| LEISHMANIA_INFECTION | 1.5941939 | 2.384698 |
| NOD_LIKE_RECEPTOR_SIGNALING_PATHWAY | 1.5958716 | 1.8420589 |
| CYTOSOLIC_DNA_SENSING_PATHWAY | 1.6120821 | 2.0001507 |
| CYTOKINE_CYTOKINE_RECEPTOR_INTERACTION | 1.6617507 | 2.2095013 |
| OLFACTORY_TRANSDUCTION | 1.6780441 | 1.600173 |
| JAK_STAT_SIGNALING_PATHWAY | 1.7079959 | 2.1062407 |
| ECM_RECEPTOR_INTERACTION | 1.7152467 | 1.7317232 |
| HEMATOPOIETIC_CELL_LINEAGE | 1.97643 | 2.1082714 |

Of these gene enrichment sets, two were noted to be of potential of interest: Cytokine receptor interaction was deemed important, as macrophages are known to be abundant producers of cytokines within the TME. In addition, the JAK-STAT signalling pathway was of interest, as this pathway is known to be activated by cytokines, dysregulated in many different cancers and relates to metastasis (Frank 2007).

Therefore, based on microarray analysis of Panc254 and 354, SerpinB3/B4 were determined as factors of interest and cytokine receptors / JAK-STAT signalling were gene sets of interest to take forward for investigation in relation to the invasive / metastatic phenotype seen following culture of PDAC cells with TAM secreted factors.

## 3.3 Discussion

When exploring the pro-tumourigenic effects of TAMs on primary PDAC cells, the most striking finding was that of TAMs inducing EMT, invasion and metastatic spread in primary PDAC cells. Results demonstrated an upregulation of mesenchymal genes associated with the process of EMT (zeb1, vimentin, loxl2 and slug) when primary cells were treated with conditioned media from MCSF-polarised macrophages. This finding was supported by transwell culture of the two cell types, confirming that this effect is seen in 'real-time' when macrophages are polarised through transwell interaction with the cancer cells rather than by MCSF. In keeping with transition from an epithelial-to-mesenchymal state, cells were more invasive *in vitro* and formed more metastases when injected *in vivo*.

Previous studies have published similar phenotypic changes in cancer cells following interaction with macrophages (summarised in section 1.4.2.5). In pancreatic cancer, Mitchem *et al.* first demonstrated a requirement for TAMs in metastatic spread. Focus of this study was on the effects of macrophage depletion on tumour initiating cells (i.e. a subpopulation of cells akin to CSCs), but when using orthotopic injections of mouse tumour cells, authors demonstrated a decrease in peritoneal metastases with two kinase inhibitors against the macrophage survival factor CSFR1 (PLX6134 and PLX3397) (Mitchem et al. 2013). No mechanism of action for how macrophages were inducing these metastatic effects was generated in this study, but these finding support our results that TAMs are important for tumour cell dissemination.

Our experimental model used conditioned media from MSCF-polarised macrophages and transwell co-culture, suggesting secreted factors from TAMs were likely to be driving EMT, leading to invasion and metastasis formation. Several publications have described TAM derived cytokines can mediate EMT and invasion in different cancer types (Table 3.3).

**Table 3.3 Macrophage derived cytokines inducing EMT**

| Cytokine | Cancer Type | Reference |
|---|---|---|
| CCL18 | Breast | (Chen et al. 2011; Su et al. 2014) |
| IL4, IL6, IL10, TNF-α and TGF-β1 | Cholangiocarcinoma | (Techasen et al. 2012) |
| TGF-β | Lung<br>Breast | (Gal et al. 2008; Bonde et al. 2012; Mikiko et al. 2012) |
| CCL18 | Pancreatic | (Meng et al. 2015) |
| IL10 | Pancreatic | (Liu et al. 2013) |
| CCL20 | Pancreatic | (Liu et al. 2016) |
| TGF-β | Gastric | (Shen et al. 2013) |

In pancreatic cancer cell line models, several cytokines have been implicated in driving EMT;

- IL10 induced EMT in Panc1 and BxPC3 cell lines, in response to activation of toll-like receptor (TLR) 4 in IL-4 polarised macrophages ( Liu et al. 2013).

- CCL18 derived from TAMs (using macrophage cell lines, U937 and THP-1) induced EMT in Panc1, BxPC3, Capan2 and SW1990 cells and was suggested as a potential clinical biomarker in PDAC, but no mechanism of action was implicated in this study (Meng et al. 2015).

- CCL20 expression in macrophages promoted EMT and invasion in pancreatic cancer cells lines Panc1, MiaPaCa2, and SW1990 and metastasis *in vivo*. RNA interference of its receptor in pancreatic cells, chemokine receptor 6 (CCR6), led to decreased invasion (Liu et al. 2016).

Therefore there are pre-clinical data implicating macrophage-secreted cytokines in the process of EMT and invasion in pancreatic cancer. These studies were predominantly undertaken in cell line models, although CCL18 was verified in clinical samples. When exploring data using patient derived cells, *in vitro* results of this chapter are validated by Helm *et al.* whereby transwell co-culture experiments were performed using both patient tissue derived TAMs and healthy donor GMCSF- and MCSF-polarised macrophages with PDAC cell lines (H6c7 = premalignant PDAC cell line, Colo357 = malignant PDAC cell line) (Helm et al. 2014). In the first instance, transwell co-culture using both patient tissue derived macrophages and healthy donor

macrophages revealed a change in PDAC cell lines to a more mesenchymal-like cell morphology along with increased RNA and protein expression of vimentin and the adhesion molecule L1CAM. In turn, Colo357 cells were more invasive following co-culture with both subsets of polarised macrophages. The authors did not deduce the specific cytokines or factors that could be inducing these effects, only speculated that it could be TGFβ1. These findings are in keeping with results from this chapter, which demonstrated increased expression of EMT genes (zeb1, vimentin, slug, loxl2) and invasion following exposure of primary PDAC cells to primary TAM secreted factors as well as transwell co-culture. The secreted factors inducing these changes in the primary culture model have yet to be identified.

In this first chapter, other published pro-tumourigenic effects of TAMs were explored. Proliferation and cell survival was assessed and showed no significant difference in cells treated with control media or conditioned media. Mitchem *et al*, showed inhibition of TAMs (through CSF1R and CCR2 inhibition) led to a decrease in orthotropic tumour burden, suggesting an effect on tumour cell proliferation *in vivo* through the loss of macrophages. However, the *in vivo* model used in this setting differs from our *in vitro* proliferation based platforms and it would be too simplistic to directly compare the two findings. TAMs have effects on pro-survival, angiogenesis and on the ECM, which effect the growth of tumours in the *in vivo* setting and not of cells grown *in vitro*. There are data to suggest cells undergoing EMT are less proliferative, .for example in colorectal tumour tissue, cells on the invasive front of tumours displaying a more mesenchymal profile were found to have less Ki67 staining as they were undergoing 'dedifferentiation' to invade and metastasise (Brabletz et al. 2001). However, we did not find a significant difference in proliferation rates in our cell cultures treated with macrophage conditioned media compared to control.

No survival advantage was demonstrated with chemotherapy in cells pre-treated with macrophage-secreted factors. Mitchem *et al.* showed better efficacy of gemcitabine *in vivo* when given concomitantly with TAM inhibitors (CSF1R and CCR2 inhibitors) (Mitchem et al. 2013). Weizman *et al.* have also tested the chemoprotective effects of TAMs and used similar *in vitro* assays to ours, whereby conditioned media from healthy donor 'TAM' macrophages was supplemented with gemcitabine and used to treat Panc01 cells. These data show a significant reduction in apoptosis and activation

of the caspase-3 pathway during gemcitabine treatment, and was supported by *in vivo* inhibition with the CSF1R antagonist GW2580. Smaller tumours were seen in mice treated with both gemcitabine and GW2580 compared to gemcitabine alone. Authors determined that TAMs were chemoprotective by inducing expression of the cytidine deaminase (CDA) gene in cancer cells, a gene responsible for resistance to gemcitabine and cisplatin, through paracrine signalling. It should be noted that the *in vitro* data for this study was limited to only one cell line (Panc01). Certainly from our limited data, FACS staining for annexin V showed a slight increase in live cells following gemcitabine treatment in Panc185 and 215 cells pre-treated with MCM, although this was not a significant increase. This finding could suggest heterogeneity of responses dependent on PDAC cell type, possibly due to differences in CDA expression in different cell types. However, our results are too limited to definitively conclude chemoprotective effects of macrophages in the primary PDAC model and would require further testing *in vitro* and *in vivo* on a wider panel of cell types.

The second aim of this chapter was to determine factors regulated by TAM interaction in primary PDAC cells. In microarray gene analysis of Panc253 and 354, the highest upregulated factors were protease inhibitors, SerpinB3 and B4. These genes encode for proteins known as squamous cell carcinoma antigens (SCCAs) and form part of the clade B subset of serpins. They bind to enzymes such as cathepsins via an irreversible interaction. The first variant of the SCCAs to be identified was SerpinB3 (aka SCCA1), which was elevated in squamous cell carcinoma (Kato and Torigoe 1977) and has since been proven to be highly expressed in several other cancers including lung, head and neck and liver (Vidalino et al. 2009). SerpinB3 drives EMT and invasion in hepatocellular carcinoma and breast cancer (Quarta et al. 2010; Sheshadri et al. 2014). In pancreatic cancer, SerpinB3 is expressed at higher levels in malignant tissue compared to non-malignant, and expression relates to the progression of cancer (Catanzaro et al. 2014). A function for this protein has yet to be established in PDAC. It would therefore be of interest to explore SerpinB3 in the context of macrophage induced expression in our primary models in the context of the metastatic phenotype identified.

As well as exploring specific genes of interest, activated signalling pathways in PDAC cells driven by TAM interaction were generated using microarray data. The JAK-

STAT and cytokine receptor pathways were noted to be enriched based on GSEA. The signal transducer and activator transcription (STAT) family comprises of seven genes; STAT1, STAT2, STAT3, STAT4, STAT5A, STAT5B and STAT6. Activation of these transcription factors crucially require phosphorylation by Janus kianses (JAKs). These tyrosine kinases are frequently coupled with receptors upstream of STATs and their kinase activity initiates downstream intracellular signalling. More than 40 different polypeptide ligands cause STAT phosporylation, either through cytokine receptor association with JAK kinases or growth factors acting through intrinsic receptor tyrosine kinase activity. Hence, it would not be unexpected that the JAK-STAT and cytokine receptor gene sets were both found to be enriched on GSEA as they are likely share similar genes in their assosciated expression profiles.

Of the seven different STAT family members, STAT3 is the most commonly described in cancer and is itself recognised as an oncogene (Bromberg et al. 1999). This STAT is commonly associated with inflammatory transcription pathways and is mediated by cytokine receptor activation (Figure 3.18).

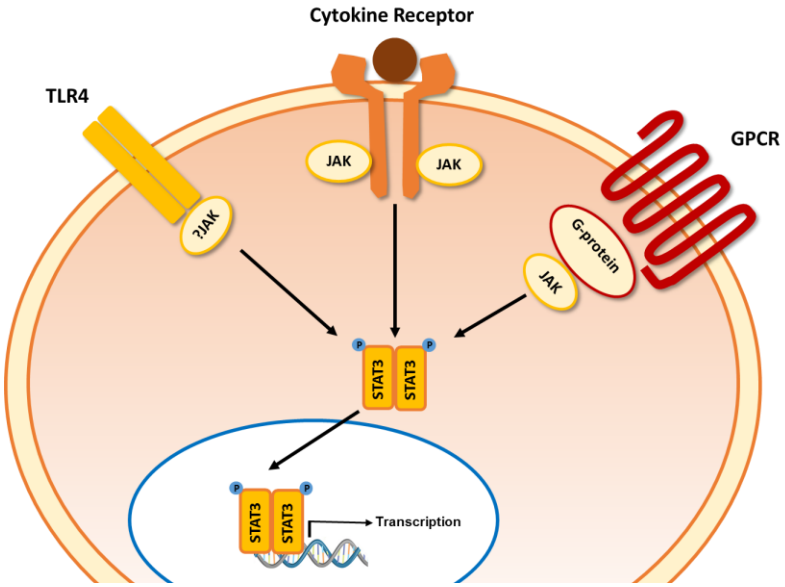


**Figure 3.18 STAT3 activation and translocation**
Under basal conditions, cytoplasmic STAT3 is activated by phosphorylation on a single tyrosine kinase residue 705 (Y705) in the C-terminal domain of STAT3. Phosphorylation of the STAT3 Y705 residue can be induced by cytokines, growth factors via non-receptor tyrosine kinases (such as JAK and Src). Following phosphorylation, STAT3 homodimers (or heterodimers with STAT1) translocate to the cell nucleus. Once in the nucleus, dimerised STAT3 binds to DNA, recognising bases in the major groove, and binds specific DNA response elements in the promoter regions of target genes.

STAT3 protein is constitutively activated in many cancers without mutation of the gene itself (Yu et al. 2014), is associated with cancer related inflammation (Yu et al. 2014) and plays an activate role in pancreatic tumourigensis (Scholz et al. 2003). Pioneering work by Lesina *at el.* has demonstrted the vital role of STAT3 in progression of PaNIN to PDAC, and linked activation fo this transcription factor to the inflammatory cytokine interleukin-6 (IL6) (Lesina et al. 2011). The downstream target effects of STAT3 in other cancers are many, and vary according to tissue type. Experimental data of the direct binding targets of STAT3 demonstrate involvement in a large variety of potential cancer pathways (Carpenter and Lo 2014). Based on direct binding alone, STAT3 is implicated in tumour metastases and mediates transcription of several genes involved in metastasis formation, including EMT (Zeb1, Twist, Vimentin), ECM degradation (MMPs) and cell survival (Bcl-2, Survivn, Bcl-x) (Carpenter and Lo 2014). Therefore, investigating further how activation of STAT3 may play a role in PDAC tumour progression as a result of TAM interaction would be of interest in determining the intracellular mechanisms that could then be targeted for therapeutic intervention.

# 4 CHAPTER FOUR: THE FUNCTION OF SERPINB3

## 4.1 Introduction and Aims

Microarray gene analysis of primary PDAC cells revealed SerpinB3 and B4 as the highest upregulated genes in Panc253 and 354 in the presence of macrophage conditioned media. There is a high degree of homology between the two proteins, however there are important differences in function, with analysis showing SerpinB3 as a potent cross-class inhibitor of papain-like cysteine proteinases such as cathepsins L, S and K, whereas SerpinB4 is an inhibitor of chymotrypsin-like serine proteinases such as cathepsin G and mast cell chymase and derp1 and 2 (Schick et al. 1998).

In both cell types, microarray analysis showed SerpinB3 to be the highest expressed following MCM treatment: in Panc253, the gene was upregulated 23 times more in conditioned media than control media ($p=0.000867$) and in Panc354 upregulation was 218 times higher ($p=0.003938$). In addition, SerpinB3 has been described as playing a role in regulating epithelial-to-mesenchymal state and invasion in other tumour types (Quarta et al. 2010; Sheshadri et al. 2014; Sueoka et al. 2005), a phenotype similar to that induced by MCM culture in this PDAC model. How this protein directly induces invasion and migration specifically has yet to be characterised. In HCC, a direct mechanism of action has not been proven, but SerpinB3 transfected cells have down-regulation of E-cadherin and upregulation of β-catenins, which are both known to be linked to the process of EMT, thus leading authors to speculate that these proteins could be playing a role. There is also upregulation of MMP activity in transfected cells, therefore SerpinB3 could also be regulating these enzymes resulting in more invasion (Quarta et al. 2010). In PDAC, SerpinB3 has already been identified as a marker of progression (Catanzaro et al. 2014).

Overexpression of the SerpinB3 gene results in an EMT phenotype in HCC (Quarta et al. 2010). As macrophage-conditioned media is upregulating this gene in PDAC treated cells, we hypothesised that expression of SerpinB3 in PDAC cells following MCM treatment could be directly regulating the resultant EMT phenotype. Therefore, expression of SerpinB3 will be investigated in the setting of the TAM/PDAC cross talk.

The aims of this chapter are:

- To confirm upregulation of SerpinB3 in PDAC cells treated with media conditioned by macrophages
- To characterise the role of SerpinB3 expression following TAM interaction with PDAC cells in the context of EMT, migration and invasion

## 4.2 Results

Although the aim of this chapter was to determine the function of SerpinB3 in the context of PDAC tumour progression, there was not enough experimental evidence to define its role. Several of the experiments in this chapter were initially performed 1-2 times in the three cell types respectively to test for an overall trend across cell types prior to further investigation. However, these preliminary experiments showed a lack of consistent findings across all cells types, therefore I stopped pursuing the role of SerpinB3 in PDAC. Conclusions presented are therefore speculative and it would require further investigation to definitively understand if the upregulation of SerpinB3 in response to macrophage secreted factors helps drive PDAC progression.

### 4.2.1 SerpinB3 upregulation

In order to confirm SerpinB3 gene was upregulated in MCM treated PDAC cells, RT qPCR was performed on a selection of primary PDAC cells treated for 48 hours (Figure 4.1). When normalising to control media, a consistent increase of SerpinB3 was seen across all cell types using several donor macrophages to generate MCSF-polarised macrophage conditioned media. These findings confirmed the microarray results and showed effects were consistent using different macrophage donors and different primary PDAC cells types.

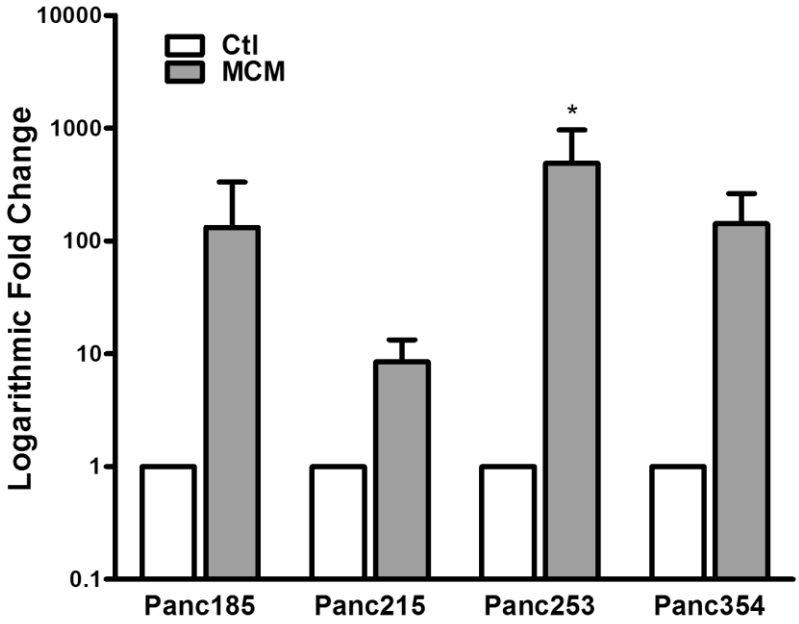


**Figure 4.1 Gene expression of SerpinB3**
SerpinB3 mRNA through RT qPCR of Panc185, 215, 253 and 354 cells cultured with MCM from 4 different donors over 48hrs (n=4 per cell type). Results represent a compilation of experiments in each cell type was normalised to control, with values representing the mean (+/- SD). Statistical significance: Wilcoxian signed-rank t test * = $p<0.05$.

Increased expression at the protein level was demonstrated on one western blot only of Panc354 cell lysate using anti-SerpinB3 antibody (Figure 4.2). This result could not be repeated, and this could relate either to lesser protein expression levels in subsequent cell lysates or due to suboptimal antibody detection methods (e.g. polyclonal antibody rather than monoclonal). Therefore further optimisation or investigation into alternative antibody for detection would be required to prove this result further.

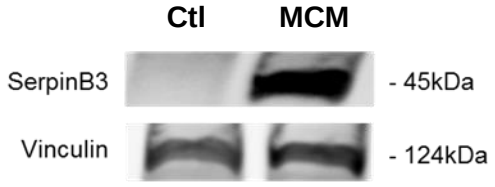


**Figure 4.2 Protein expression of SerpinB3**
SerpinB3 protein expression in Panc354 cells treated with MCM for 48hrs. Western blot was cut following transfer and incubate with relative antibody simultaneously.

### 4.2.2 Effects of recombinant SerpinB3

In relation to EMT and invasion, Quarta *et al.* have previously linked SerpinB3 to increased invasion and migration, as well as proliferation, in the HepG2 cell line following treatment with recombinant protein (Quarta et al. 2010). Thus, initial testing to determine the effects of SerpinB3 in PDAC were undertaken using recombinant human SerpinB3 (rhSerpinB3). Based on experimental data from Quarta *et al*, 100ng/ml and 200ng/ml were used to treat Panc185 and Panc354 cells.

After 48 hours of treatment, no difference in cell morphology was noted (Figure 4.3), and no consistent changes in EMT gene expression were seen (Figure 4.4).

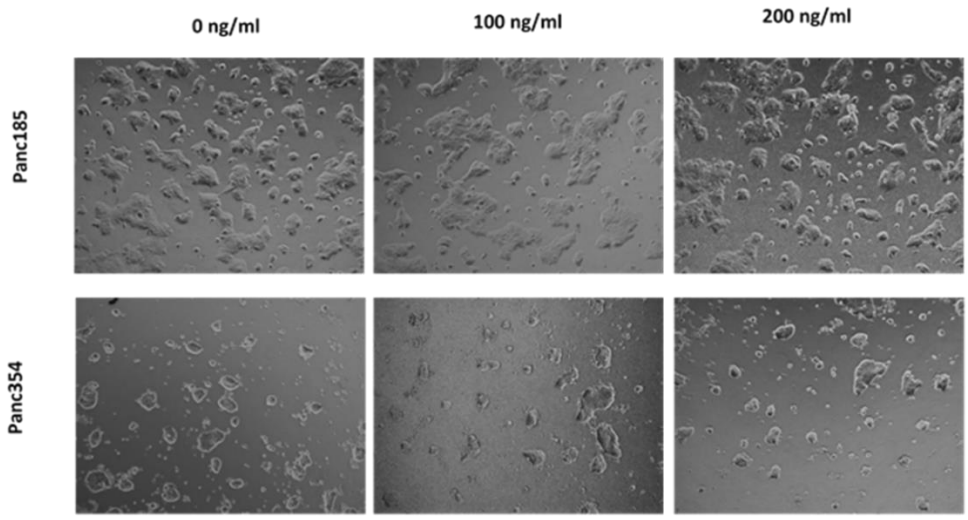


**Figure 4.3 Cell morphology with recombinant human SerpinB3**
Panc185 and Panc354 cells treated with 0ng/ml, 100ng/ml and 200ng/ml of recombinant SerpinB3 for 48hrs and imaged using brightfield microscopy.

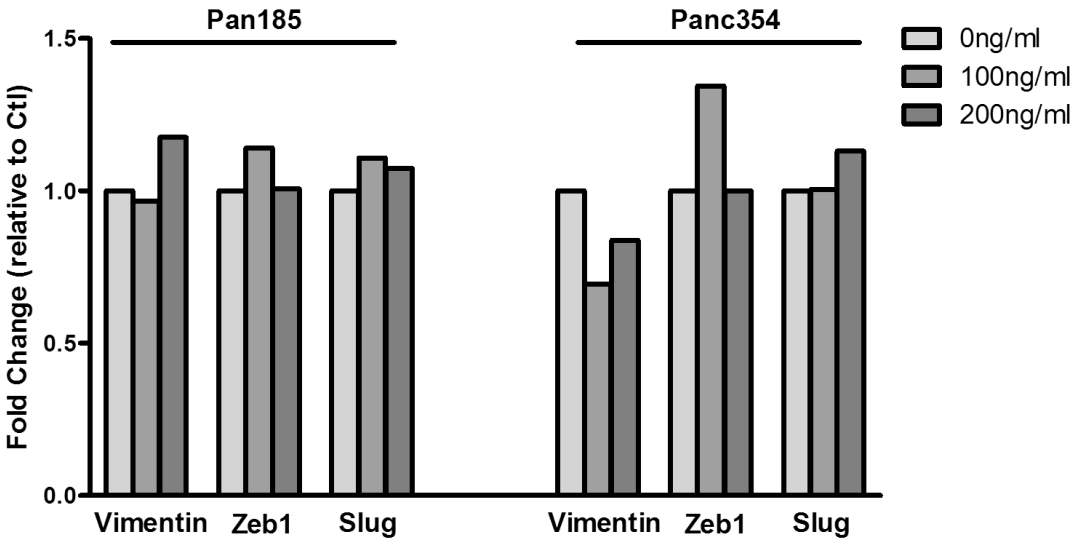


**Figure 4.4 EMT gene expression with recombinant human SerpinB3**
Panc185 and Panc354 cells treated with recombinant human SerpinB3 over 48hrs were analysed using RT qPCR for EMT gene expression (n=1). Results represent normalisation to control (0ng/ml).

This lack of effect suggested that treatment of PDAC cells with recombinant SerpinB3 protein had no effect on EMT as seen with MCM treated cells. However, it could be questioned whether the recombinant protein underwent endocytosis (to then have an intracellular effect) in our model of primary PDAC cells. Quarta *et al.* were able to demonstrate extracellular effects using recombinant human SerpinB3 protein in HepG2 cells (through immunofluorescence staining for EMT-related proteins), but also confirmed effects altering gene overexpression, indicating both an extracellular paracrine and an autocrine effect in HepG2 cells.

Therefore in order to further investigate a function of SerpinB3 in the primary PDAC model, it would be necessary to manipulate intracellular gene, and thus protein expression, through silencing and overexpression of the gene.

### 4.2.3 SerpinB3 knockdown

SerpinB3 gene silencing was performed using doxycycline inducible lentiviral SerpinB3 shRNA constructs in Panc185, 215 and 354 cells.

Sorted GFP+ cells were cultured and maintained as stably transduced populations. Expression of the SerpinB3 transcript was assessed using RT qPCR and compared to the level of gene expression in cells transduced with the non-targeting ‘scrambled’ shRNA (‘SCR shRNA’) and non-transduced cells (‘NT’) treated with MCM (Figure 4.5). Results showed a trend for knockdown of MCM induced SerpinB3 expression in all three primary transduced cells compared to non-target shRNA control, however further experiments in each cell type would need to be performed to confirm significance.

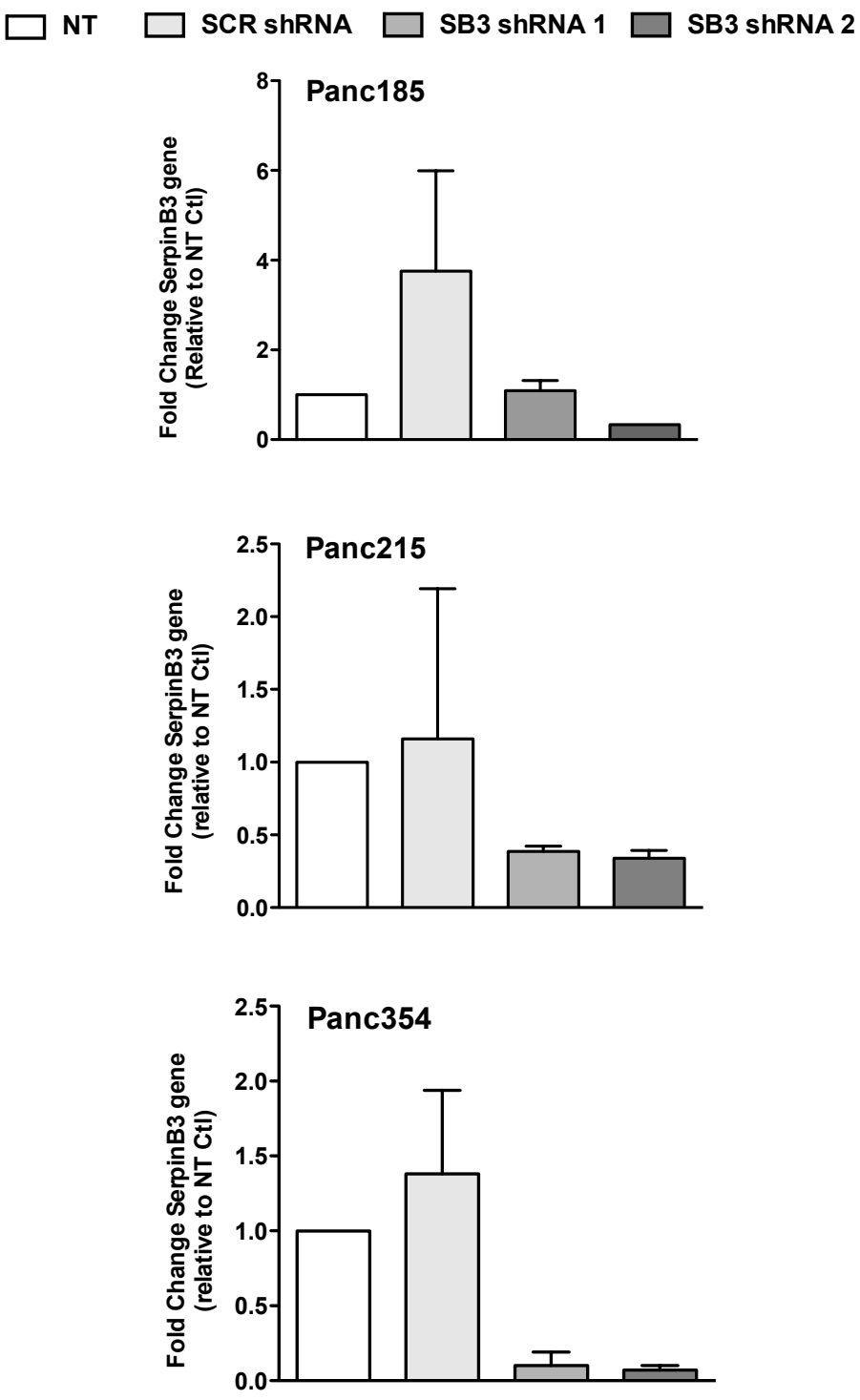


**Figure 4.5 Confirmation of SerpinB3 knockdown**
RT qPCR of SerpinB3 mRNA expression in Panc185, 215 and 354 cells (n=2 per cell type) transduced with lentiviral shRNA constructs (SB3 shRNA1 and SB3 shRNA 2) and treated with MCM for 48hrs. Comparison was made with both non-transduced control cells (NT) and non-targeting shRNA transduced cells (SCR shRNA). Results represent a compilation of duplicate experiments in each cell type, with values representing the mean (+/- SD).

#### 4.2.3.1 SerpinB3 knockdown and EMT / migration / invasion

Having shown less SerpinB3 gene in transduced primary PDAC cells, it was necessary to assess if this loss of gene resulted in a decrease of EMT genes/ migration/ invasion following MCM culture.

SerpinB3 has been shown to be critical in the process of EMT in other cells types (Quarta et al. 2010; Sheshadri et al. 2014). As PDAC cells undergo an upregulation of EMT associated genes following treatment with MCM, knockdown cells were treated with both control and MCM media, with the expectation that should SerpinB3 play an active role in the transition to a more mesenchymal state, less upregulation of EMT-related gene expression in MCM would occur. However, data showed that in Panc185 and 215 there was little difference in EMT gene expression in knockdown cells, with MCM treatment inducing increased expression of Zeb1, Vimentin and Slug in MCM in both non-transduced control cells, non-targeting shRNA transduced cells and knockdown cells (Figure 4.6A and B). In Panc354, interestingly the cells with SerpinB3 knockdown had a greater expression of EMT-related genes compared to both the non-transduced controls and the non-targeting shRNA control cells (Figure 4.6C). However, no firm conclusions can be made regarding impact of loss of SerpinB3 on EMT gene expression, and further experiments would be required to determine any or no significant differences in gene expression.

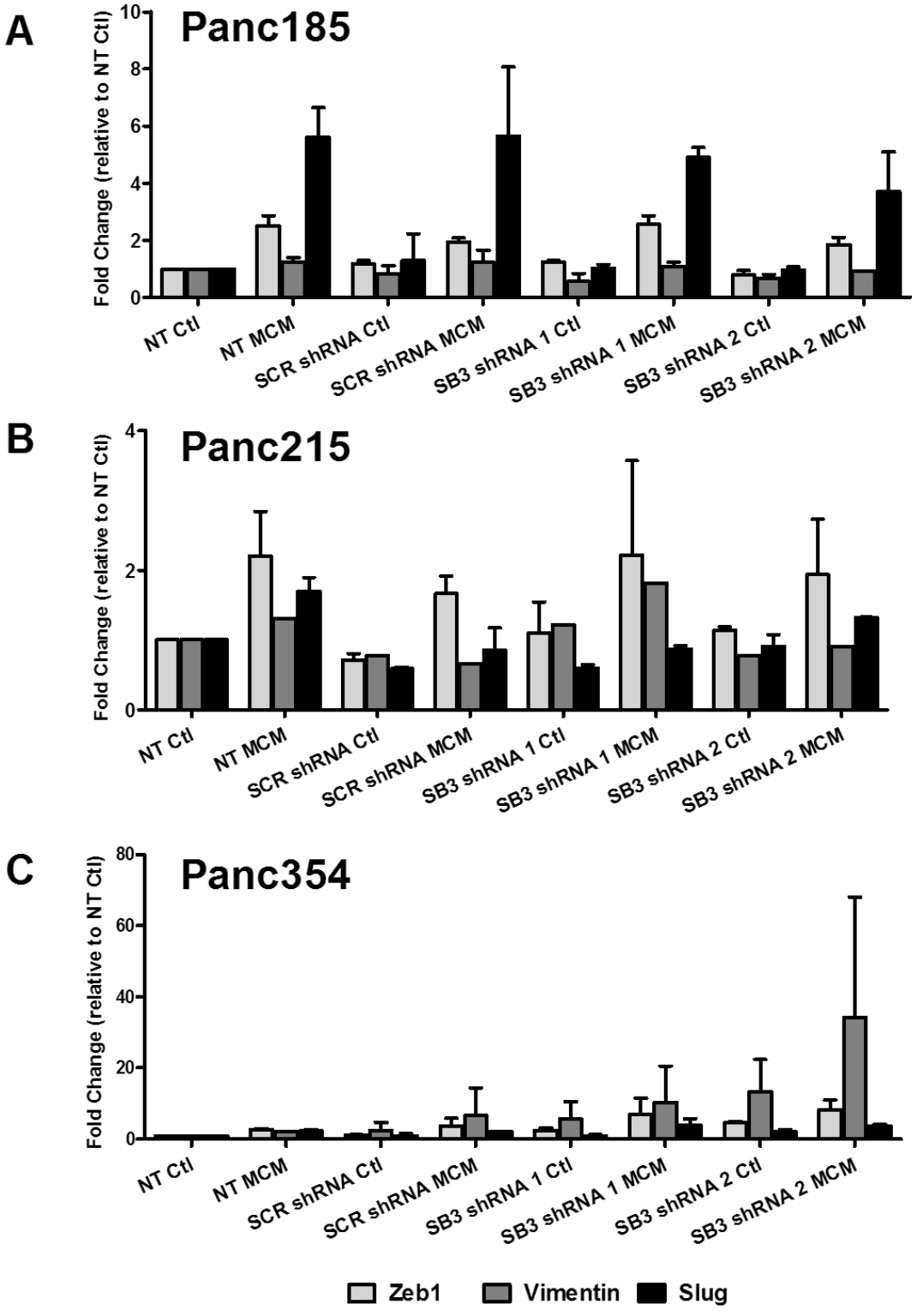


**Figure 4.6 EMT gene expression in SerpinB3 knockdown PDAC cells**
mRNA expression of zeb1, vimentin and slug in A) Panc185 (n=2), B) 215 (n=2) and C) 354 (n=2) cultured with control media and MCM for 48hrs. Results represent a compilation of experiments in each cell type, with values representing the mean (+/- SD).

Using IncuCyte ZOOM live-cell imaging, wound-healing analysis of Panc354 cells grown in MCM demonstrated a greater migratory potential in SerpinB3 shRNA knockdown over 24hrs compared to non-transduced cells. However, control non-targeting shRNA cells also showed increased migration, suggesting this effect was not specific to knockdown rather than vector transduction (Figure 4.7).

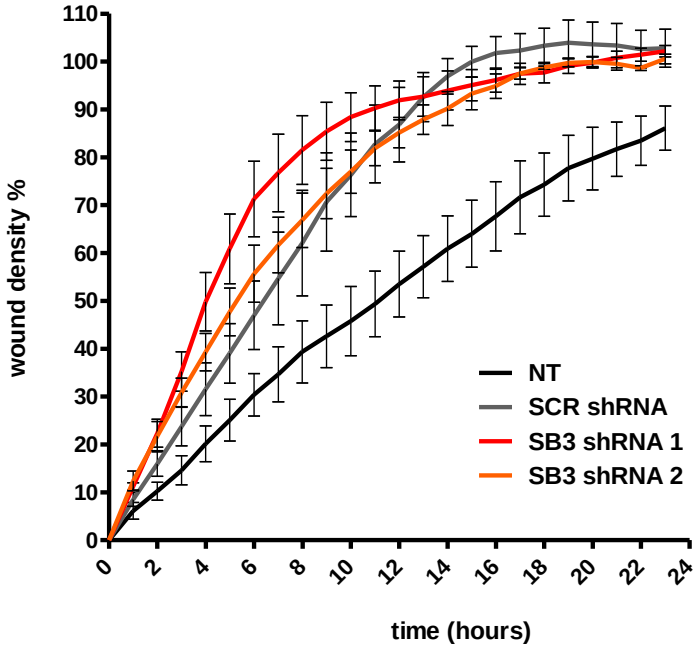


**Figure 4.7 Migration of SerpinB3 knockdown cells**
Scratch assay (n=1) was performed on Panc354 non-transduced (NT), non-targeting shRNA (SCR shRNA) and SerpinB3 knockdown transduced (SB3 shRNA 1 / SB3 shRNA 2) cells in the presence of MCM over 24hrs. Measurements from wounds made from monolayer cells were analysed for relative wound density using Incucyte Zoom software. Results represent pooled analysis of 3 technical replicates per cell type, with values representing the mean (+/- SEM).

Testing functional invasion in a '3D' system, one experiment using SerpinB3 shRNA 2 knockdown cells was performed and showed greater invasion compared to non-transduced and non-targeting shRNA cells using transwell invasion assay (Figure 4.8). However both the migration and invasion experiments would need to be repeated to determine conclusive effects.

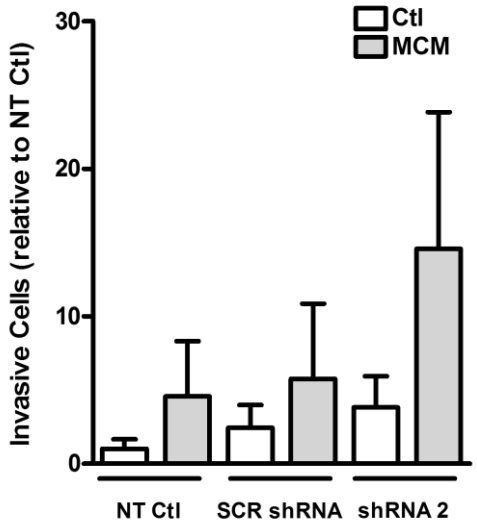


**Figure 4.8 Invasion of serpinB3 knockdown cells**
Transwell invasion assay was performed on non-transduced (NT), non-targeting shRNA (SCR shRNA) and SerpinB3 shRNA knockdown (SB3 shRNA 2) Panc354 cells seeded in MCM or control media over 16hrs (n=1). Values representing the mean count of 4x images per well (+/- SD).

### 4.2.4 SerpinB3 overexpression

To further determine the autocrine effects of SerpinB3 expression in primary PDAC cells, overexpression of the gene was next performed using lentiviral SerpinB3 constructs in Panc185 and 354 cells.

Blasticidin selected cells were cultured and maintained as stably transduced populations. Expression of the SerpinB3 transcript was assessed using RT qPCR and compared to the level of expression in non-transduced cells and with empty PLX304 vector cells (Figure 4.9). Results confirmed upregulation of SerpinB3 gene in both transduced cells types (significant in Panc185) compared to control and empty vector transduced cells.

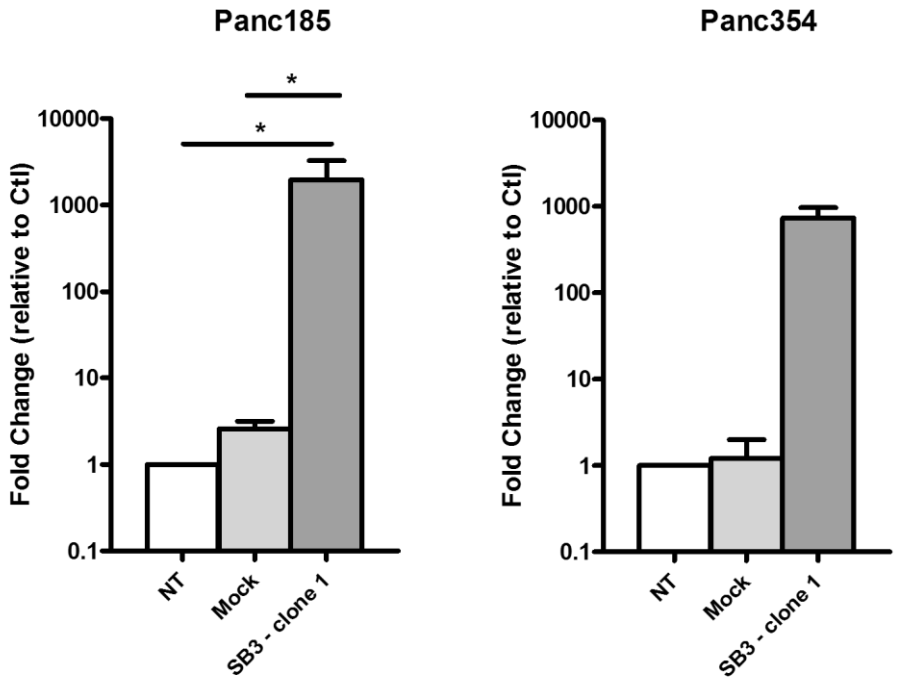


**Figure 4.9 Confirmation of serpinB3 gene overexpression**
RT qPCR of SerpinB3 mRNA expression in Panc185 (n=3) and 354 cells (n=2) transduced with lentiviral serpinB3 construct (SB3 – clone 1). Comparison was made with both non-transduced control cells (NT) and empty PLX304 vector transduced cells (Mock). Results represent a compilation of experiments in each cell type, with values representing the mean (+/- SD). Statistical significance: 1 way ANOVA * = $p<0.05$.

#### 4.2.4.1. SerpinB3 overexpression and EMT / invasion

To assess if there was a link between upregulation of SerpinB3 and EMT / invasion, cells overexpressing SerpinB3 were tested for EMT gene expression along with invasive ability.

Expression of EMT genes again showed non-specific upregulation of EMT genes with empty vector control transduced cells (Figure 4.10), although these experiments would need to be further repeated to be able to make firm conclusions on the effects of EMT gene expression in cells overexpressing SerpinB3.

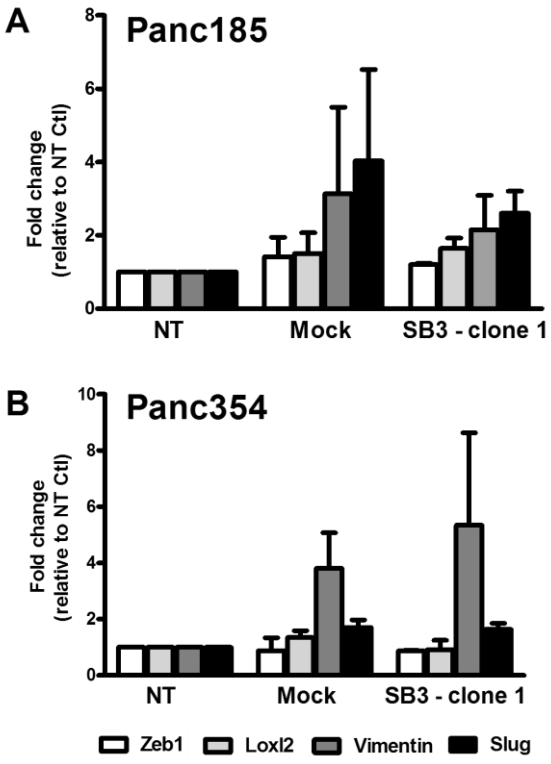


**Figure 4.10 EMT gene expression in cells overexpressing Serpin3 gene**
RT qPCR analysis of EMT genes in A) Panc185 (n=2), B) 354 (n=2) in non-transduced controls (NT), empty PLX304 vector transduced cells (Mock), or SerpinB3 construct (SB3 – clone 1). Results represent a compilation of experiments in each cell type, with values representing the mean (+/- SD).

Exploring functional activity, Panc354 cells with SerpinB3 overexpression showed greater invasion with transduction in both empty vector and SerpinB3 construct compared to wild type alone (Figure 4.11). Cells overexpressing the gene had no greater invasive ability as the empty vector control cells. However, this experiment was only performed once and would need to be repeated to deduce the effects of SerpinB3 on cell invasion.

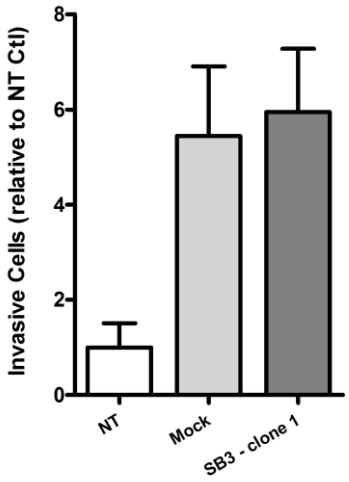


**Figure 4.11 Invasion of cells overexpressing SerpinB3 gene**
Transwell invasion assay was performed on non-transduced (NT), transduced empty PLX304 vector (Mock) and SerpinB3 overexpression (SB3- clone 1) Panc354 cells over 16hrs (n=1). Values representing the mean count of 4x images per well (+/- SD).

In conclusion, there were not enough experimental repeats to be able to make definitive conclusions on how the overexpression SerpinB3 is linked to EMT / invasion and gene expression. However the results did suggest that that cells undergoing the process of transduction, even with empty vector, are in themselves different to non-transduced populations, possibly due to the process of selection.

## 4.3 Discussion

Agilent microarray results showed significant upregulation of SerpinB3 in response to TAM secreted factors in Panc253 and 354 cells. This protein acts as a cysteine protease inhibitor in normal cells (Schick et al. 1998), however its function in cancer progression remains unclear. Cumulative data suggest both pro- and anti-tumourigenic activity of SerpinB3 in cancer cells, including mediating invasion and migration, pro-survival and treatment resistance (Table 4.1).

Initial results confirmed consistent upregulation of SerpinB3 gene and protein in MCM treated cells across different types of primary PDAC cells tested with different macrophage donors. However, recombinant SerpinB3 showed no functional effects when administered to cells. Testing with recombinant protein was based on data from Quarta *et al.* who showed intracellular effects in HepG2 cells following treatment with recombinant SerpinB3 (Quarta et al. 2010). In addition, the protein has been detected in patient plasma of various malignant and non-malignant diseases and reports suggest squamous cancer cells actively secrete it into the circulation or culture medium (Hirakawa et al. 2004; Numa et al. 1996; Tsuyama et al. 1991). Thus, one would have assumed an extracellular effect of the protein based on these data alone. However, when examining studies testing the activity of SerpinB3, only Quarta *et al.* have demonstrated an extracellular effect of the protein in HepG2 cells. Contrary to this finding, when specifically examining inhibitory cathepsin activity, Uemura *et al.* showed a lack of inhibitory activity of extracellular SerpinB3, but did detect activity within the cytosol (Uemura et al. 2000). In addition, the majority of reports in Table 4.1 describe cytoplasmic activity for SerpinB3, thus suggesting a predominant intrinsic mechanism of action. This does not explain why the protein is so abundant in the serum of patients, but Uemura *et al.* postulate that the presence of SerpinB3 in patient sera may be due to passive release rather than active secretion, especially as the protein lacks a recognisable secretory sequence.

**Table 4.1 Molecular mechanisms of action of SerpinB3**
Compiled list of publications relating to the cancer related functions of SerpinB3 and proposed molecular mechanisms of action (MOA). All cell types human unless stated. SCC = squamous cell carcinoma

| Cell type | Activity | Proposed MOA | Reference |
|---|---|---|---|
| SCC (SKG-IIIa) | Resistance to drug (7-ethyl-10-hydroxycamptothecin, etoposide), cytokine (TNFα) and effector cell (IL-2 activated NK cell) induced apoptosis | Caspase 3 and or/upstream proteases | (Suminami et al. 2000) |
| Kidney (293T) | Resistance to radiation induced apoptosis | Decreased caspase 3 and 9 activity / decreased p38 MAPK | (Murakami et al. 2001) |
| SCC (SKG-IIIA) | Tumour growth | Decreased apoptosis / Inhibition of Natural Killer cell recruitment | (Suminami et al. 2000) |
| Cervical Cancer (SiHa) | Inhibition of invasion | E1AF transcription factor activating SCCA promoter | (Iwasaki et al. 2004) |
| Hepatoma (HepG2) | Resistance to drug induced apoptosis (pro-oxidant chemotherapy) | Inhibition of ROS generation at Complex I of mitochondria | (Ciscato et al. 2014) |
| Oral SCC (MISK81-5, sMISK) | Resistance to TNFα induced death | Inhibition of cytochrome c release from mitochondria | (Tsuyama et al. 1991) |
| Cervical Cancer (CaSki, SKG-IIIa) | Cell invasion | Increased MMP9 | (Sueoka et al. 2005) |
| Mouse fibroblasts (3TC-J2) Keritanocytes (HaCaT) | Resistance of UV-induced apoptosis | Supresses c-Jun NH2- terminal kinase-1 (JNK1) | (Katagiri et al. 2006) |
| Head and Neck SCC (YCU-N) | Inhibition of tumour growth and invasion | ? inhibition of cathespins | (Nakashima et al. 2006) |
| Head and Neck SCC (HN13)<br>Prostate Cancer (DY145)<br>Mammary (MCF7)<br>Breast Cancer (231) | Cell survival | STAT3 /IL6 | (Ahmed and Darnell 2009) |
| Hepatoma (HepG2, Huh7) | Induction of EMT | Increased MMP 2 and MMP 9 | (Quarta et al. 2010) |
| Mouse kidney (BMK) | Inhibition of cell death induced by lysosomal injury (DNA alkylating agents and hypotonic shock) / Promotion of apoptosis in response to ER stress | Inhibition of cell death through blocking cathepsin activity / Promotion of apoptosis through aggregation of lysosomal caspase-8 | (Ullman, Pan, and Zong 2011) |
| Fibroblast (IMR90)<br>Pancreatic Cancer (Panc-1, CF-PAC-1, HPAF-II, L3.6, CAPAN-1) | Inflammatory cytokine production | Ras mutation / UPR dependent induction of NF-κB / IL6 | (Catanzaro et al. 2014) |
| Mammary (MCF10A) | Oncogenic transformation / Induction of EMT | UPR dependent induction of NF-κB and IL6 | (Sheshadri et al. 2014) |
| Primary human liver cirrhosis and progenitor / C57BL/6J mice | Pro-survival in progenitor cells | ?inhibition of caspase 3 | (Villano et al. 2014) |
| Hepatoma (HepG2) | Increased pro-oncogenic c-myc | Inhibition of calpain | (Turato et al. 2015) |

There is no evidence in the literature of a specific SerpinB3 receptor or that the protein has the ability to undergo endocytosis to cross the cell membrane and have intracellular effects as seen in HepG2 cells. This could therefore explain the lack of effects of recombinant protein in our primary PDAC model, as the treated cells were unlikely to have taken up SerpinB3 to then have intracellular effects.

Intrinsic function through silencing and overexpression of the SerpinB3 gene was used instead to asses function. Firm conclusions cannot be made from these experiments due to lack of experimental repeats, but the preliminary data collected here of knockdown and overexpression data of SerpinB suggest that the EMT / migratory / invasive effects were not specific to the SerpinB3 expression, but more likely due to the process of vector transduction. This is reflected in findings that control transduced cells (with non-targeting RNA in knockdown cells and empty PLX304 vector in overexpression cells), also had high EMT gene expression profile and invasive capacity despite no loss or gain in SerpinB3 gene expression.

Differences in the non-transduced versus transduced cell populations in these experiments would suggest a change in biological behaviour as a result of lentiviral gene transfer. This concept has been described in one study of Diffuse Large B Cell Lymphoma (DLBCL), in which lentiviral transduction with a control vector interfered with response to rituximab by increasing drug tolerance compared to non-transduced cells (Ranjbar et al. 2016). In this thesis, knockdown cells were treated with doxycycline and FACS sorting for GFP positivity, and overexpression cells were selected with blasticidin, a drug known to be highly toxic to mammalian cells. The processes would have applied more cellular stressors to the transduced cell populations (including control vector) than non-transduced cells. Some of these process are associated with the induction of EMT, such as mechanical compression (Tse and Kalluri 2007), potential hypoxia (Jiang, Tang, and Liang 2011) and unfolded protein response (UPR) (Dejeans et al. 2015) and therefore in turn a more invasive and migratory cancer cell population could have been induced. Thus, the experimental processes involved in transduction could have inadvertently resulted in selection of a more ‘aggressive’ cell population that was able to survive more stressors and become more mesenchymal, explaining why transduced control cells in both experiments were also seen to be functionally more invasive.

Although the data from this chapter on SerpinB3 are not robust enough to confirm the effects of SerpinB3 on EMT and invasion, its expression as a result of MCM treatment in PDAC does not have to be specifically related to this phenotype of interest and one cannot rule out other pro-tumorigenic functions for the protein yet to be discovered, especially when reviewing the many other roles it plays in other cancer types (Table 4.1). Recent data have shown a link between Serpins and responses to immunotherapy in melanoma, in which mutations of SerpinB3 and SerpinB4 are commonly seen. Patients with specific mutations derived clinical benefit from anti-CTLA4 therapy (Riaz et al. 2016). No mechanistic actions were provided for this observation, however authors speculated that because the types of mutations included missense, the protein activity could be lost, which in some autoimmune diseases results in autophagy, thereby enhancing autoantigen presentation, or leads to inflammatory aggregates formation, resulting in more immunogenic neopeptides. In our model the expression of SerpinB3 was increased, therefore based on this hypothesis one could speculate that increased SerpinB3 expression would lead to less immune aggregates and neopeptides, thus providing decreased immune cell recognition of tumour tissue as a result of macrophage driven expression. Based on the growing literature on SerpinB3 in the field of cancer biology, an as yet unknown function for this gene in tumourigenesis in PDAC is likely to emerge in the future.

# 5 CHAPTER FIVE: ONCOSTATIN M, ONCOSTATIN M RECEPTOR AND STAT3

## 5.1 Introduction and Aims

GSEA of MCM cultured Panc253 and 354 indicated enrichment of the JAK-STAT pathway and cytokine receptor gene sets. These two pathways are linked, with cytokine receptors commonly coupled with JAK kinases to allow phosphorylation of downstream STATs, thereby initiating intracellular signalling. Of the STAT family members, persistent activation of STAT3 is frequently detected in cancer cell lines and tumour tissues (Bowman et al. 2000; Buettner, Mora, and Jove 2002). In addition, STAT3 has been linked to invasion and metastasis (Huang 2007) and is implicated in PDAC tumourigenesis (Corcoran et al. 2011; Lesina et al. 2011). Crucially, targeting activation of STAT3 can inhibit tumour growth and metastasis both *in vitro* and *in vivo* without affecting normal cells (Niu et al. 1999), and JAK-STAT inhibitors are already in clinical use for treatment of patients with myeloproliferative disease (Harrison et al. 2017; Mesa et al. 2013). Therefore further investigation of STAT3 in PDAC following pathway activation by TAM secreted factors could be a valid therapeutic approach in decreasing the pro-tumourigenic effects of TAMs.

The aims of this chapter are:

- To confirm activation of the JAK-STAT3 pathway in PDAC following TAM conditioning
- To determine the likely macrophage-derived cytokines activating the JAK-STAT3 pathway in primary PDAC cultures
- To deduce whether cytokine activation of JAK-STAT3 is driving EMT, invasion and metastasis

## 5.2 Results

### 5.2.1 Microarray Gene Analysis of Panc215, 253 and 354

In addition to microarray of treated Panc253 and 354, Panc215 was also analysed. Analysis of all three cell types showed common gene upregulation in cells cultured with MCM (Figure 5.1).


**Figure 5.1 Venn diagram of microarray gene expression**
Gene expression fold change profile in Panc215, 253 and 354 comparing significantly upregulated genes in conditioned media treated cells compared to control media. Statistical significance: moderated t-test $p<0.05$.

The 7 common upregulated genes were noted between Panc215, 253 and 354 (Figure 5.2). Of note, SerpinB3 was not present in this panel; despite being significantly upregulated in Panc253 and 354, upregulation in Panc215 did not reach significance.

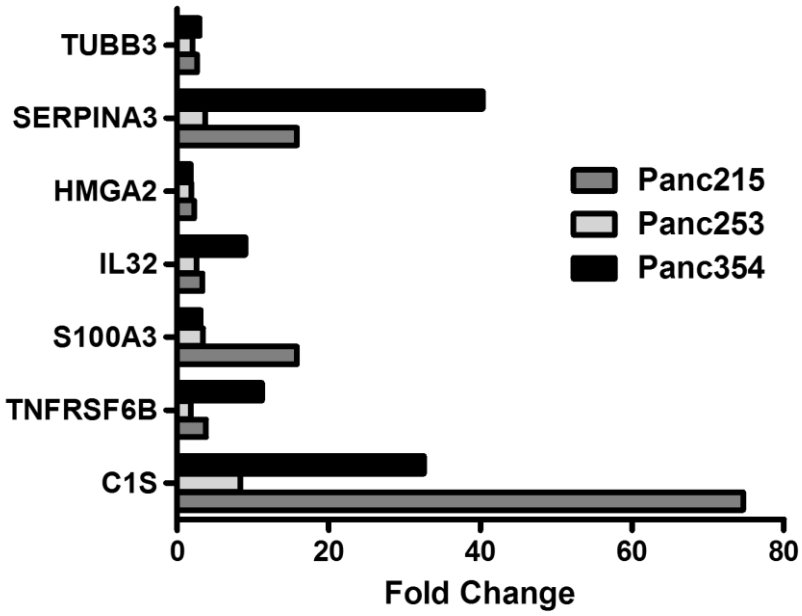


**Figure 5.2 Upregulated gene on microarray: Panc215, 253 and 354**

KEGG GSEA of collective microarray data for Panc215, 253 and 354 again revealed 10 common gene sets between the three cell types. The complement cytokine receptor and JAK-STAT gene sets had significant normalised enrichment scores (Table 5.1 and Figure 5.3).

**Table 5.1 KEGG gene set enrichment Panc215, 253 and 354**
(NES = normalised enrichment score. FDR p-val <0.25)

| KEGG GENE SET | Panc215 NES | Panc253 NES | Panc354 NES |
|---|---|---|---|
| OLFACTORY_TRANSDUCTION | 1.3116386 | 1.6780441 | 1.600173 |
| ECM_RECEPTOR_INTERACTION | 1.5504879 | 1.7152467 | 1.7317232 |
| FOCAL_ADHESION | 1.8077673 | 1.5119898 | 1.3321809 |
| HEMATOPOIETIC_CELL_LINEAGE | 1.8510597 | 1.97643 | 2.1082714 |
| COMPLEMENT_AND_COAGULATION_CASCADES | 2.0527737 | 1.4998453 | 1.7503108 |
| CYTOSOLIC_DNA_SENSING_PATHWAY | 2.0718224 | 1.6120821 | 2.0001507 |
| JAK_STAT_SIGNALING_PATHWAY | 2.1193426 | 1.7079959 | 2.1062407 |
| LEISHMANIA_INFECTION | 2.2995777 | 1.5941939 | 2.384698 |
| NOD_LIKE_RECEPTOR_SIGNALING_PATHWAY | 2.3498127 | 1.5958716 | 1.8420589 |
| CYTOKINE_CYTOKINE_RECEPTOR_INTERACTION | 2.5795727 | 1.6617507 | 2.2095013 |

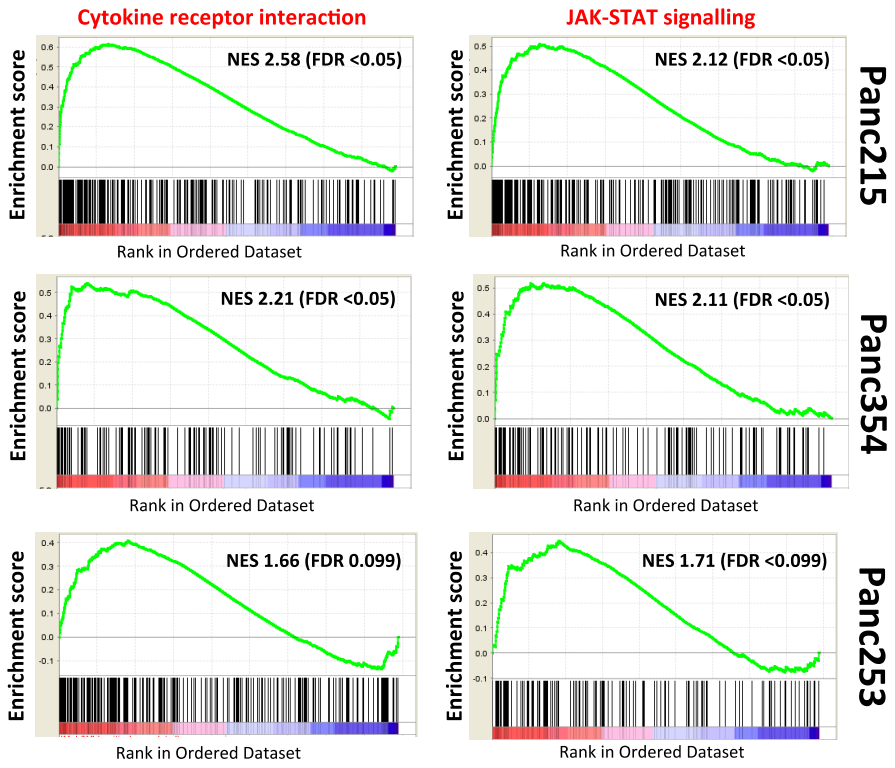


**Figure 5.3 Gene Set Enrichment Scores**

To determine which cytokines could be upstream of these genes set, the online analysis tool Ingenuity Pathway Analysis (IPA) was used with the assistance of Dr Matthieu Schoenhals; cumulative microarray results from Panc215, 253 and 354 were tested to determine candidate cytokines. Through this, several cytokines of interest

were predicted and included several interleukins and interferons. One predicted cytokine of interest was oncostatin M (OSM). Review of microarray noted that the receptor for OSM, OSMR, was a common upregulated gene in MCM treated Panc215 and 354 (Figure 5.1). Crucially, this cytokine belongs to the glycoprotein 130 (gp130) family cytokines, which are known activators of the STAT3 pathway. Thus, further investigation of OSM was taken forward.

### 5.2.2 STAT3

To confirm Agilent microarray data, western blot of pSTAT3 (specifically the Y705 residue) was performed on a panel of primary PDAC cultures treated with MCM. Phosphorylation at this site is a surrogate marker of pathway activation, leading to nuclear translocation and target gene transcription. pSTAT3 protein was consistently higher in treated cells compared to controls (Figure 5.4).

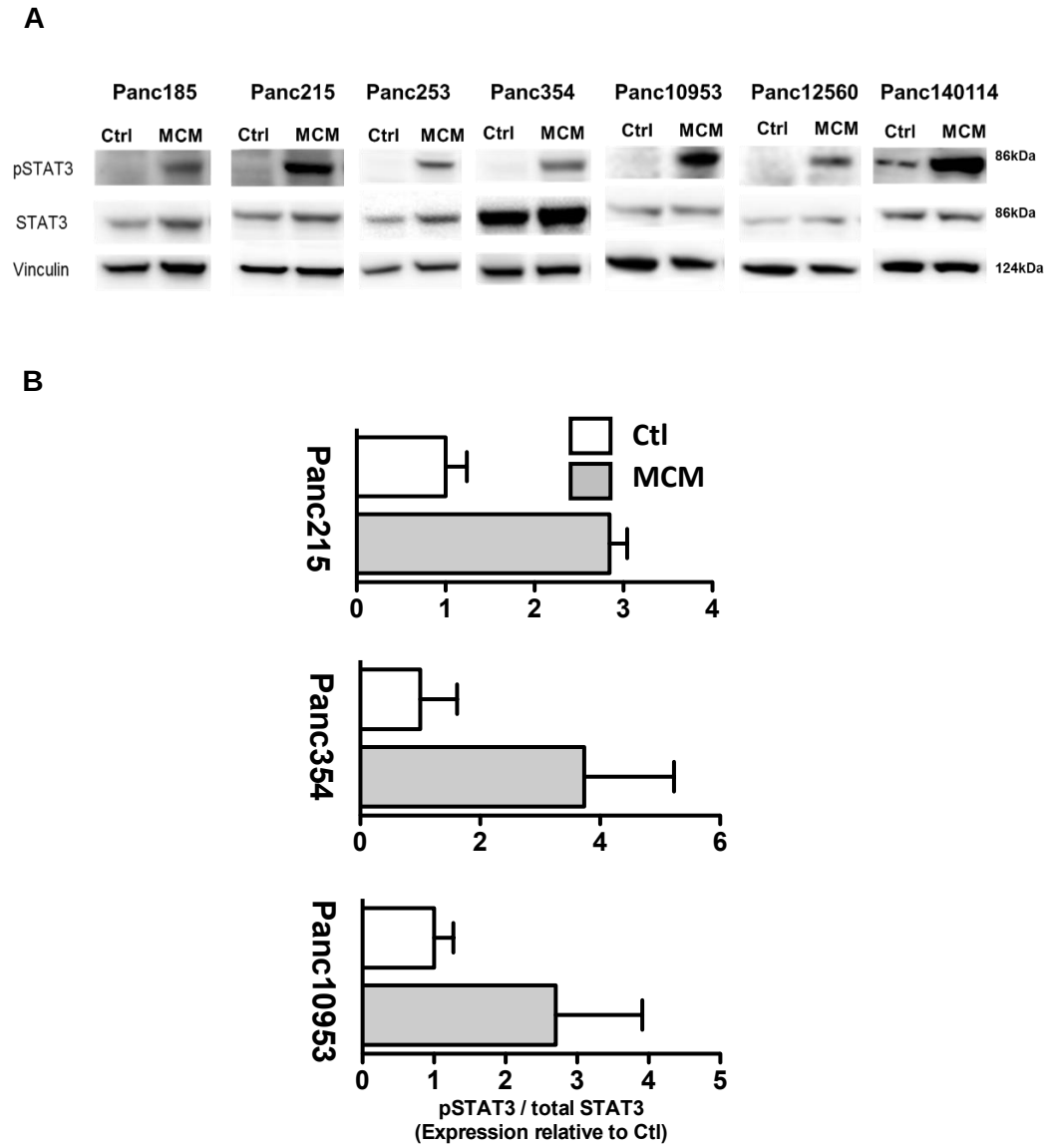


**Figure 5.4 STAT3 phosphorylation in cells cultured with MCM**

A) Representative western blots of pSTAT3 protein expression from cell lysates of PDAC cells cultured with MCM for 24hrs. B) Densitometry of pSTAT3 protein expression of Panc215, 354 and 10953 cultured for 24hrs, normalised to density of loading control (vinculin) and total STAT3. Results represent a compilation of experiments in each cell type (n=4 per cell type), with values representing the mean (+/- SD).

Phosphorylation of STAT3 was also demonstrated when direct co-culture of TAMs with PDAC cells was performed (Figure 5.5), confirming the effects were applicable upon 'direct' interaction of the two cell types. For this experiment, cell lysates were collected at 48hrs rather than 24hrs as previously described with just MCM culture alone, in view of the speculated longer 'time for tumour associated polarisation' discussed in Chapter 3 with unpolarised macrophages. Expression was not as high as with MCM. This could be due to similar reasons discussed in Chapter 3 when determining EMT gene expression in PDAC with 'direct' macrophage co-culture compared to 'indirect' with MCM.

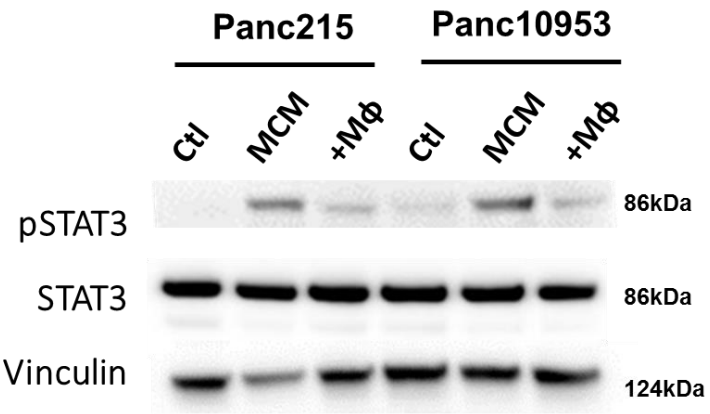


**Figure 5.5 STAT3 activation in 'direct' and 'indirect' coculture**
Western blot of pSTAT3, total STAT3 protein and control (vinculin) in Panc215 and 10953 cultured alone (Ctl), directly with unpolarised macrophages ('+MΦ') or with MCM for 48hrs.

### 5.2.3 gp130 cytokines

There are at least nine human gp130 family cytokines, so called because they all share gp130 as a common signal transducer in their receptor complex: interleukin-6 (IL6) (Taga et al. 1989), interleukin-11 (IL11) (Yin et al. 1993), interleukin-27 (IL27) (Phillips et al. 2004), leukemia inhibitory factor (LIF) (Ip et al. 1992), ciliary neurotrophic factor (CNTF) (Ip et al. 1992), OSM (Gearing et al. 1992), cardiotrophin-1 (CT1) (Gearing et al. 1992), cardiotrophin-like cytokine (CLC/ CLCF1) (Elson et al. 2000), and neuropoietin (NP) (Derouet et al. 2004).

Interest in the role of OSM in PDAC is based on IPA, suggesting this cytokine to be upstream of activated genes, and microarray gene analysis, revealing OSMR as a common upregulated factor. In addition, gp130 family members IL6 and LIF cytokine would also be important to investigate, due to their high predominance in the literature in relation to cancer and EMT (Table 5.2) and close association with the STAT3 pathway.

**Table 5.2 PubMed search for gp130 family cytokines in cancer**
Results of PubMed search (up to December 2015) for '(cytokine of interest), cancer'. In addition, a search for '(cytokine of interest), cancer, EMT' or '(cytokine of interest), cancer, PDAC' was also carried out.

| Gp130 Family Cytokine | No. publications in 'Cancer' | No. publications in 'Cancer and EMT' / 'Cancer and PDAC' | |
|---|---|---|---|
| Interleukin 6 (IL6) | 1690 | EMT | 10 |
| | | PDAC | 4 |
| Leukaemia inducing factor (LIF) | 1133 | EMT | 4 |
| | | PDAC | 2 |
| Oncostatin M (OSM) | 465 | EMT | 2 |
| | | PDAC | 0 |
| Interleukin 11 (IL11) | 426 | EMT | 6 |
| | | PDAC | 0 |
| Ciliary neurotropic factor (CNTF) | 202 | EMT | 0 |
| | | PDAC | 1 |
| Interleukin 27 (IL27) | 132 | EMT | 2 |
| | | PDAC | 0 |
| Cardiotrophin (CT) | 28 | EMT | 0 |
| | | PDAC | 0 |
| Cardiotrophin-like peptide | 6 | EMT | 0 |
| | | PDAC | 0 |
| Neuropoeietin | 1 | EMT | 0 |
| | | PDAC | 0 |

In the first instance, confirmation of STAT3 phosphorylation in the primary PDAC model with IL6, LIF and OSM was necessary. Recombinant proteins of each were used to test as per standard published doses on an expanded panel of primary PDAC cells.

Interestingly, only recombinant human OSM induced phosphorylation of STAT3 similar to that seen with MCM (Figure 5.6). When quantified for Pan215, 354 and 10953, IL6 also induced slight upregulation of protein expression (density normalised to control = 1.19), but the level was not as high or significant as with OSM (density normalised to control = 3.01 and MCM (density normalised to control = 3.41) (Figure 5.7). Of note, recombinant human interleukin 8 (IL8) was also included in the initial panel of cytokines tested, as it is known to activate EMT via the JAK/STAT3 pathway in HCC (Fu et al. 2014), but as it showed little effect on pSTAT3 expression and was not a gp130 family cytokines, further investigation was discontinued.

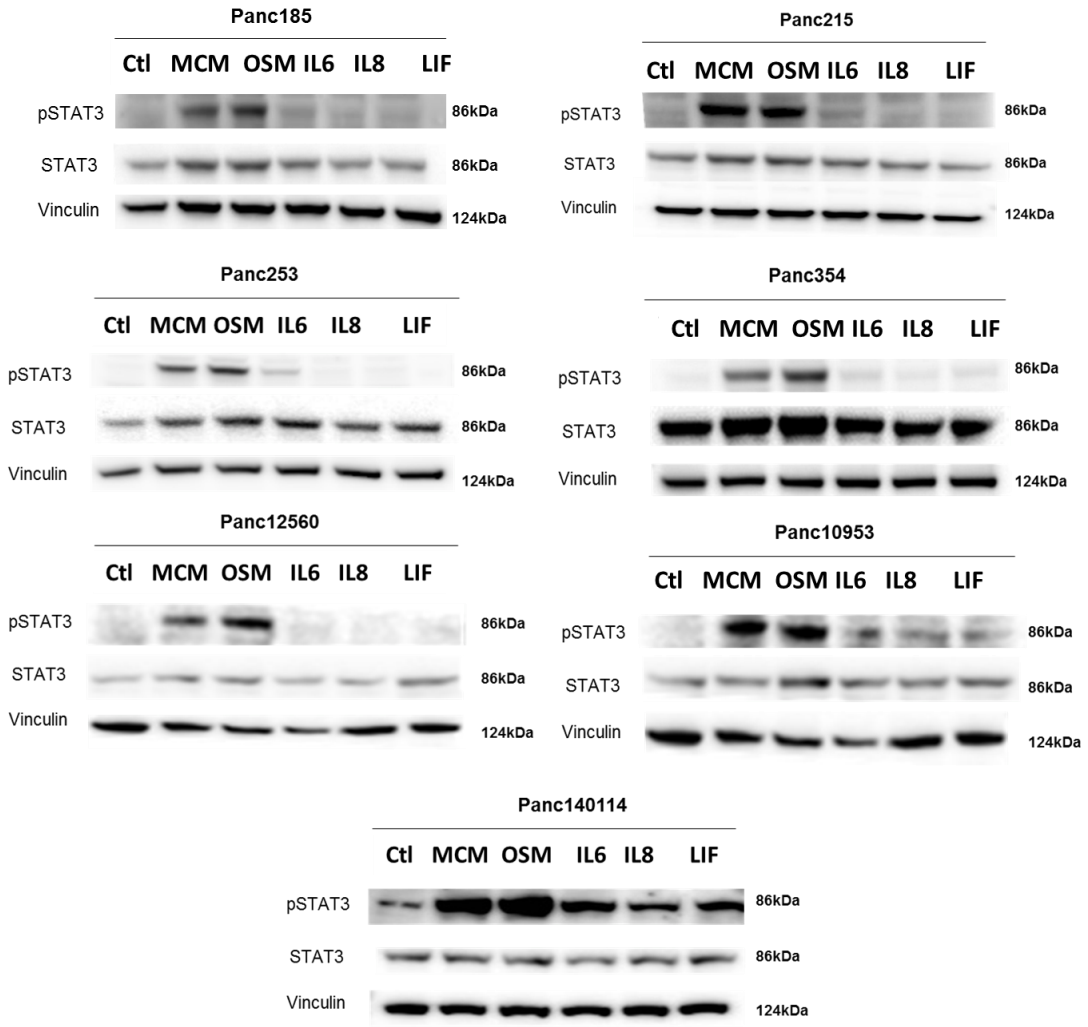


**Figure 5.6 STAT3 activation in primary PDAC cultured in MCM**
Representative western blots of pSTAT3 protein expression from cell lysates of PDAC cells cultured with control, MCM, OSM 100ng/ml, IL6 100ng/ml, IL8 100µg/ml, LIF 100ng/ml for 24hrs.

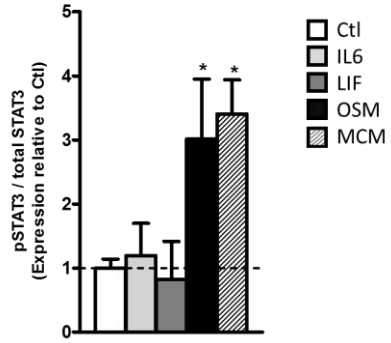


**Figure 5.7 Quantification of pSTAT3 expression Panc215, 354 and 10953**
Densitometry quantification of pSTAT3 protein expression of Panc215, 253 and 10953 cultured for 24hrs, normalised to density of loading control and total STAT3. Results represent a compilation of experiments in each cell type (n=4 per cell type), with values representing the mean (+/- SD). Statistical significance: Wilcoxian signed-rank test * = $p<0.05$. ** = $p<0.005$

Findings that OSM had greater effect on STAT3 phosphorylation compared to IL6 were surprising. This was in part because IL6 is the most well described gp130 cytokine, commonly cited as the principal activator of STAT3 in malignancy (Sansone and Bromberg 2012). An explanation of the lesser response of IL6 compared to OSM on STAT3 phosphorylation / activation in our primary PDAC model was sought.

Expression of the relative co-receptors of each cytokine was first investigated, as difference in relative receptors expression could explain increased potency of different cytokines. Activation of the JAK/STAT3 pathway by gp130 family cytokines is reliant on heterodimer formation of the relevant cytokine subunit receptor with the gp130 receptor (gp130R) (Figure 5.8).

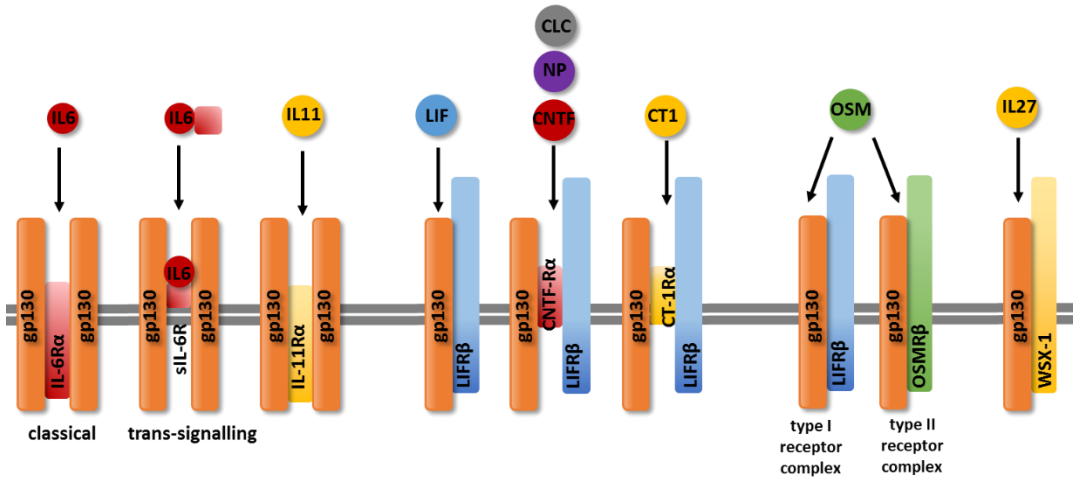


**Figure 5.8 gp130 cytokine receptors**
Classical IL6 signalling involves IL6 binding to the membrane bound IL6 receptor (IL6R) which then initiates homodimerisation of gp130 for downstream activation. In transignalling, IL6 interacts with a soluble form of IL6 receptor (sIL6R) and then activates of gp130 signalling. IL11 associates with α-receptor IL11R with homodimerized gp130. CNTFRα requires heterodimerization of gp130 and LIFRβ and is bound not only by CNTF but also NP and CLC. CT1 also utilizes the gp130/LIFRβ heterocomplex for signalling through direct binding to LIFRβ but not gp130. OSM signalling is mediated either by the gp130/LIFRβ (type I complex) or gp130/OSMRβ (type I complex) heterocomplexes. IL27 requires the association of gp130 and WSX-1 for receptor complex formation and signal transduction.

The relevant expression of the receptor genes both at baseline and following treatment with MCM were examined. For OSM, it should be noted that this cytokine can bind to both OSMR and LIFR (Figure 5.8), thus LIF could appear to have a lesser affect than OSM due to the competitive binding of both cytokines to LIFR and the ability of OSM

to bind both receptors. Basal expression of the three receptor genes was first determined in Panc215, 354 and 10953. In the case of IL6, binding is through membrane bound IL6R or soluble IL6R (sIL6R) (Figure 5.8). sIL6R is generated through either proteolysis of the membrane bound protein (Mülberg et al. 1993) or through a transcript variant which lacks the transmembrane coding regions (Lust et al. 1992). Thus, it was ensured that primers to detect mRNA of *IL6R* did not code for the transmembrane region (codon 356 – 387) and therefore detected both membrane bound and soluble receptor.

Basal OSMR gene expression was significantly higher than both *IL6R* and *LIFR* in all three cell types (Figure 5.9).

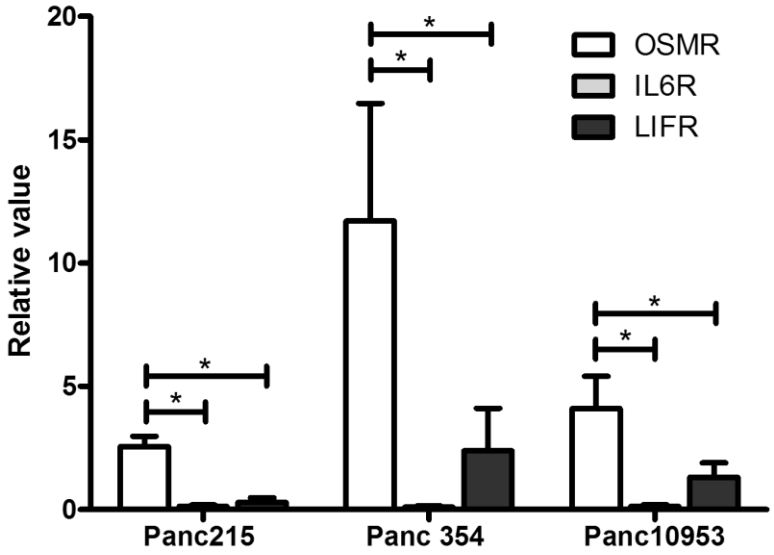


**Figure 5.9 Basal gene expression of gp130 cytokine receptors**
RT qPCR of *OSM*, *IL6* and *LIF* receptor mRNA in Panc215, 354 and 10953 (n=7 per cell type) in basal conditions (control media for 48hrs). Results represent a compilation of relative values in each cell type, with values representing the mean (+/- SEM). Statistical significance: Wilcoxian signed-rank test * $p<0.05$.

In addition, only OSMR was significantly upregulated following MCM treatment in all three cell types, and not LIFR or IL6R (Figure 5.10). In fact LIFR was actually downregulated in Panc10953 following MCM.

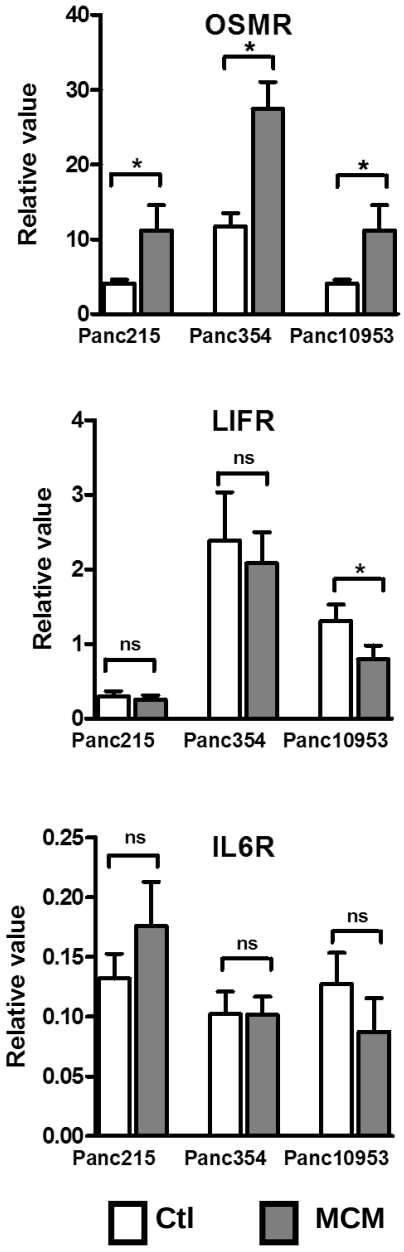


**Figure 5.10 Gene expression of gp130 cytokine receptors with MCM culture**
RT qPCR of *OSM*, *IL6* and *LIF* receptor mRNA in Panc215, 354 and 10953 (n=7 per cell type) in cells treated with control and MCM media for 48hrs. Results represent a compilation of relative values in each cell type, with values representing the mean (+/- SEM). Statistical significance: Wilcoxian signed-rank test * $p<0.05$.

These results explained the differential effect of each cytokine with regards to pSTAT3 activation following MCM treatment in primary PDAC: OSM is having a greater effect as there is more OSMR at basal levels than the other cytokine receptors, thus allowing more cytokine to initially bind compared to IL6 and LIF. The receptor also appears to be positively regulated in MCM, whereas IL6R and LIFR are not,

potentiating the effects of downstream pathway activity and allowing for sustained pSTAT3 activation seen over time. These findings support that of microarray data in which the receptor for this cytokine, OSMR, was upregulated following treatment with TAM derived factors.

Finally, to confirm the mechanism of action of pathway activation, nuclear translocation of STAT3 with both MCM and OSM were tested using immunofluorescence. Results confirmed that both MCM and OSM culture, pSTAT3 was present in the nucleus of treated cells as soon as 10 min after treatment, and was not detected with control media (Figure 5.11). A shorter time frame was used for this experiment compared to the usual 24hrs used when collecting cell lysates for western blot analysis in order to capture the initial translocation of protein to the nucleus. Therefore, activation of the signalling pathway upon cytokine receptor activation leads to nuclear translocation for gene transcription.

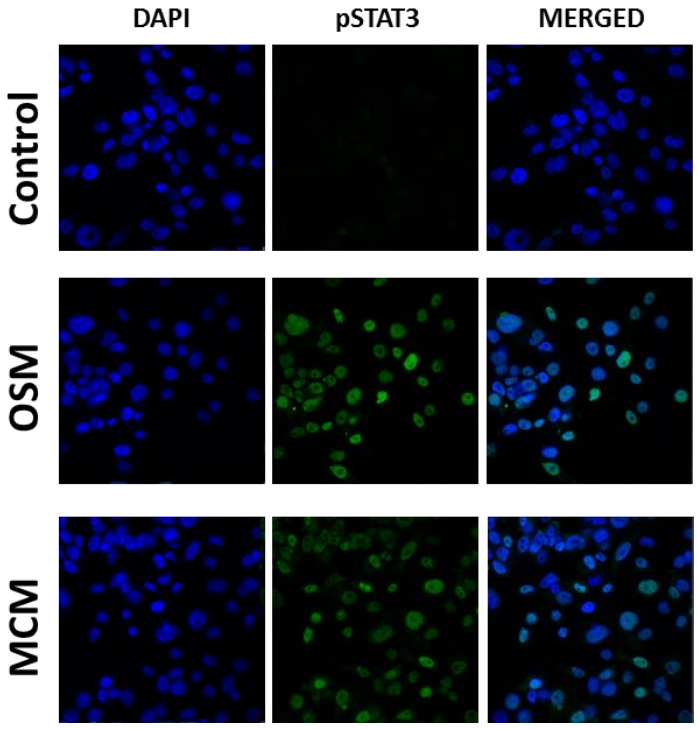


**Figure 5.11 Immunoflourescence pSTAT3**
Immunofluorescence staining of pSTAT3 in Panc354 cells following 10 minutes treatment with control / OSM / MCM.

### 5.2.4 EMT and OSM

Having confirmed pSTAT3 is upregulated and translocates to the nucleus in PDAC cells treated with OSM and MCM, confirmation of whether OSM also activates a metastatic phenotype was needed.

Initial testing of Panc354 demonstrated a similar change in cell morphology with OSM treatment and MCM (mesenchymal elongation and cell scattering) (Figure 5.12). IL6 and LIF did not appear to have these effects.

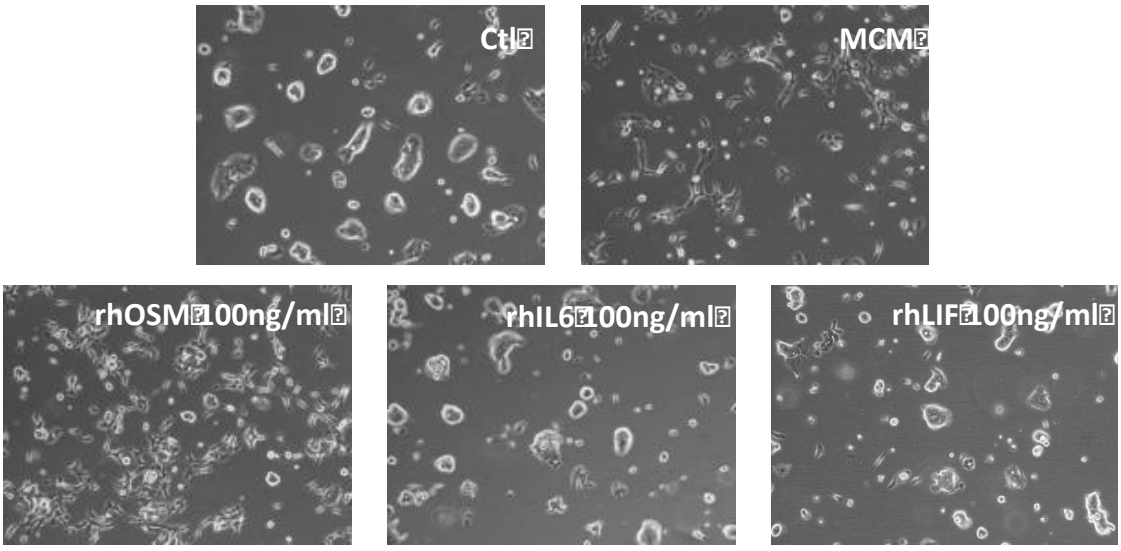


**Figure 5.12 Effects of gp130 cytokines on cell morphology**
Brightfield microscopy images of Panc354 cells treated with control media, MCM and gp130 cytokines for 48hrs

Consistent with these morphological changes, genes associated with EMT were also found to be upregulated in OSM treated cells and not with IL6 and LIF treatment (Figure 5.13).

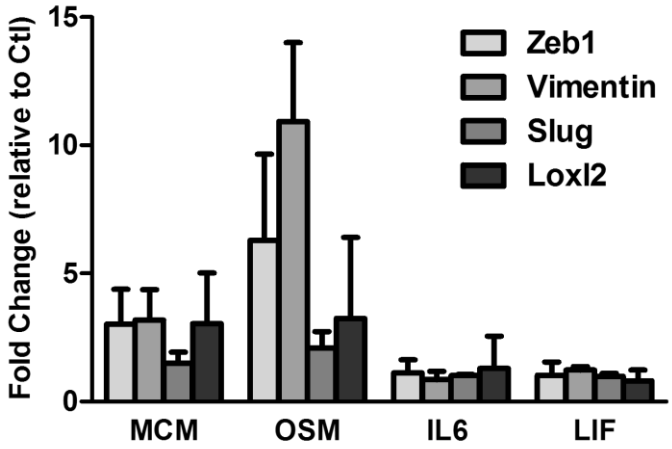


**Figure 5.13 EMT gene expression in Panc354 treated with gp130 cytokines**
RT qPCR of Panc354 (n=3) MCM and gp130 cytokines (OSM 100ng/ml, IL6 100ng/ml, LIF 100ng/ml) after 48hrs treatment. Results represent normalisation to control, with values representing the mean (+/- SEM).

To ensure the effects of OSM on gene upregulation were consistent and applicable to the other primary PDAC cell types, EMT gene expression was further analysed in Panc354, Panc215 and 10953 cells treated concurrently with OSM and MCM. Results showed upregulation of genes in a similar pattern when cells were treated simultaneously (Figure 5.14).

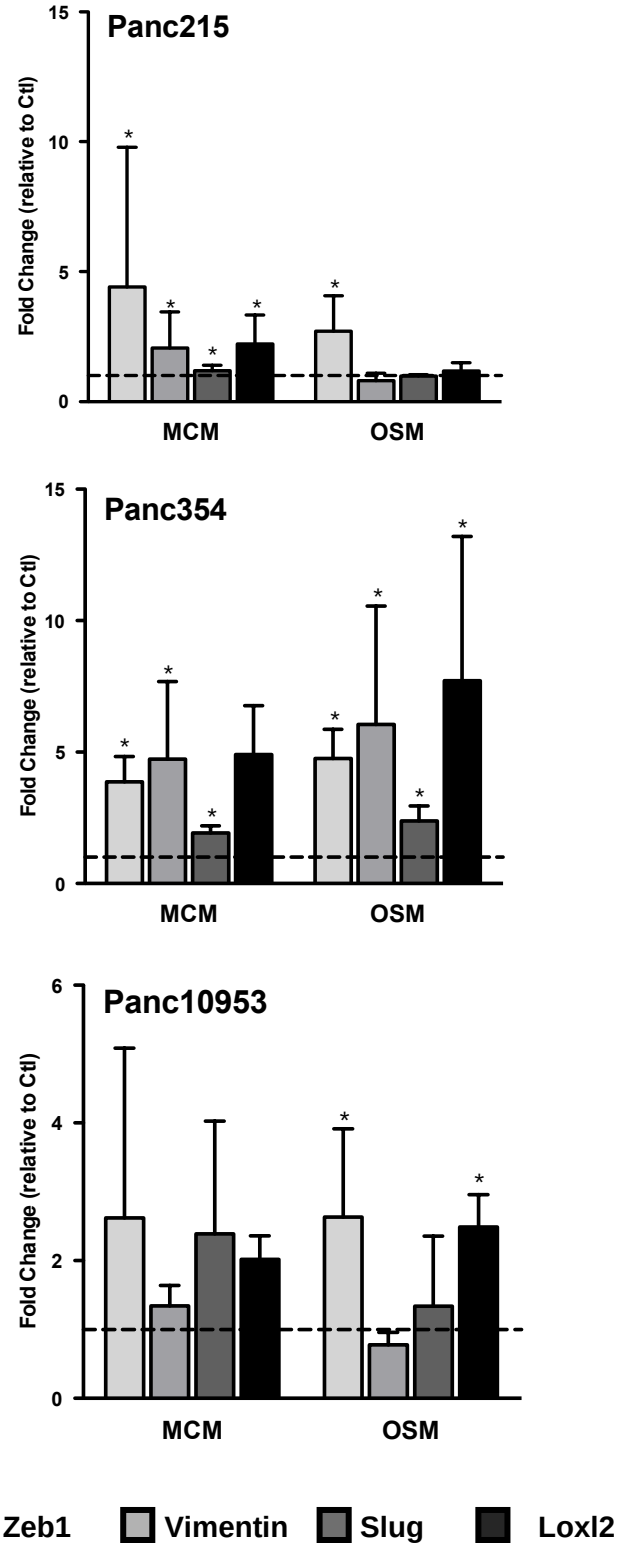


**Figure 5.14 EMT expression of OSM treated cells**
RT qPCR of EMT genes in Panc215, 354 and 10953 (n=6 per cell type) treated with control media, MCM or OSM 100ng/ml for 48hrs. Results represent a compilation of experiments normalised to control conditions, with values representing the mean (+/- SEM). Statistical significance: Wilcoxian signed-rank test * = $p<0.05$.

### 5.2.5 Invasive effects of OSM

Functional effects of OSM were tested using invasion assay. Results confirmed increased invasion of Panc215, 354 and 10953 cells pre-treated with OSM (Figure 5.15).

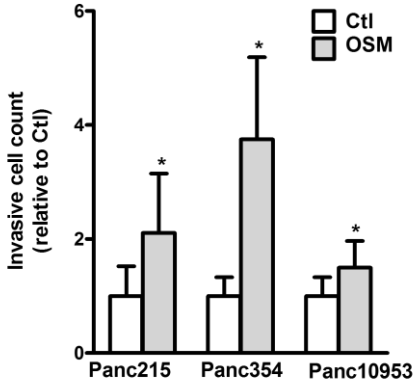


**Figure 5.15 Invasive effects of OSM**
Transwell invasion assay of Panc215, 354 and 10953 (n=6 per cell type) treated with OSM 100ng/ml for 48hrs. Results represent a compilation of experiments normalised to control, with values representing the mean (+/- SEM). Statistical significance: paired t test * = $p<0.05$.

When testing invasion of Panc354, one experiment showed less upregulation in invasion following treatment with IL6 and LIF compared to MCM and OSM (Figure 5.16), however further experimental replicates would be required to make definitive conclusions.

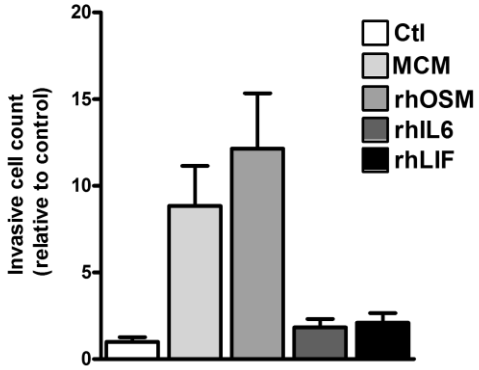


**Figure 5.16 Effects of gp130 cytokines on invasion**
Transwell invasion assay of Panc354 cells treated with control media, MCM, OSM 100ng/ml, IL6 100ng/ml and LIF 100ng/ml (n=1). Values representing the mean (+/- SD).

Taken collectively, it appeared that OSM was the most effective gp130 cytokine in activating the STAT3 signalling pathway, inducing EMT and is driving invasion in the primary PDAC cells, thus confirming its importance following initial analysis of microarray data using IPA pathway software.

#### 5.2.5.1 OSM and Macrophages

Having concluded that OSM had similar effects on PDAC phenotype as MCM, it remained to be proven that this cytokine was being secreted within the conditioned media of TAMs. Through ELISA, OSM protein was detected in different macrophage donor MCM following culture with MCSF for 4 days (Figure 5.17). Levels ranged from 232-1557pg/ml, demonstrating heterogeneity in primary macrophage OSM secretion following 4 days of polarisation.

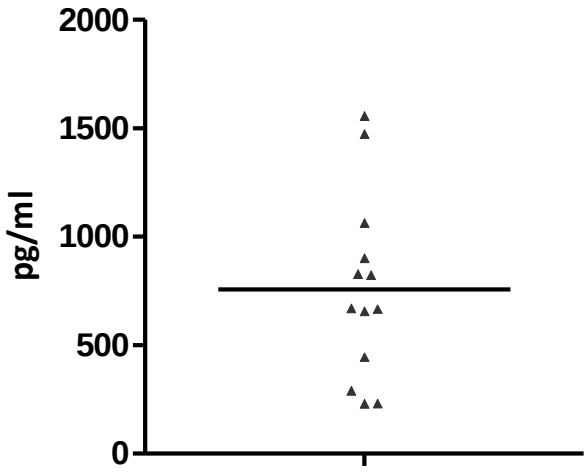


**Figure 5.17 ELISA of OSM in MCM**
ELISA of OSM protein in primary MCSF-polarised donor macrophage conditioned media (n=13). Results represent individual values with mean.

Although this result proved that OSM was being secreted by MCSF-polarised macrophages, this phenotype was artificially induced through MCSF. In other cancer models, a crosstalk between TAMs and cancer cells has been demonstrated within the TME to drive polarisation of macrophages towards a more pro-tumourigenic phenotype (Su et al. 2014). In PDAC, data from our laboratory has already shown that CSC-conditioned media can drive OSM gene expression in primary macrophages (Figure 5.18A), and it was speculated that the cytokine responsible for this was TGFβ1 (Sainz et al. 2015), which is known to be secreted in large amounts by PDAC (Massagu J. 2008) and was confirmed to be secreted by our primary PDAC culture cells (Figure 5.18B).

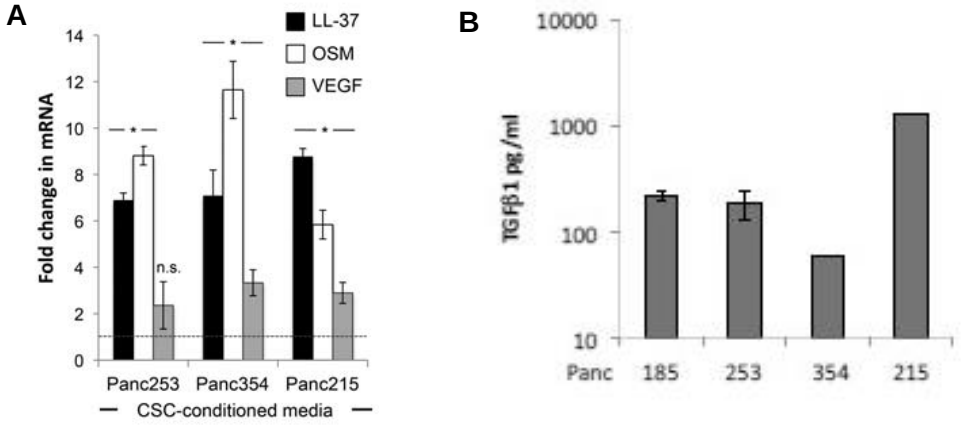


**Figure 5.18 OSM and TGFβ1 expression in primary PDAC**
A) RT qPCR analysis of *hCAP-18/LL-37, OSM* and vascular endothelial growth factor (*VEGF*) mRNA expression levels in human monocyte-derived macrophages cultured with control media or with CSC CM from three PDAC cultures *P=<0.05 B) ELISA analysis of TGFβ1 expression from primary PDAC (taken from Sainz et al. 2015).

PDAC tumours are known to harbour inactivating mutations in the TGFβ signalling pathway rendering them unresponsive (Iacobuzio-Donahue et al. 2009), therefore this cytokine, secreted from PDAC cells, is likely to act primarily on other stromal cells within the TME.

Therefore, to further test the theory that PDAC secrete TGFβ1 which then primes macrophages to be more 'tumour-associated', in turn secreting OSM, mature unpolarised macrophages were treated with either MCSF or TGFβ1 for 24 hours. Supernatant was then collected for ELISA analysis of OSM protein. Results confirmed

the previous gene expression analysis, showing protein secretion of OSM in cells treated with TGFβ1 (Figure 5.19).

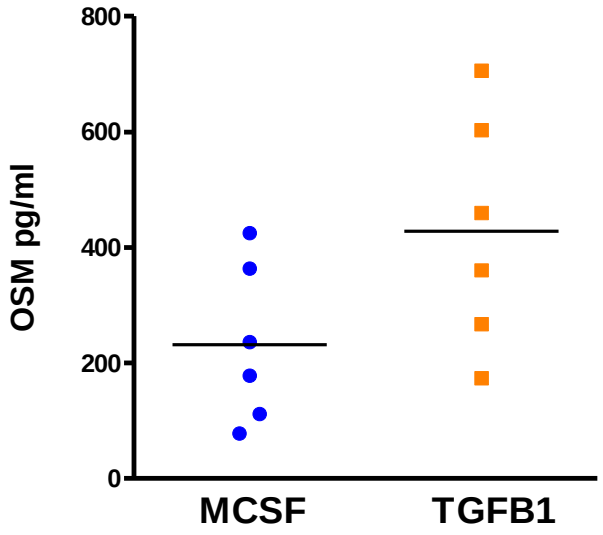


**Figure 5.19 ELISA of MCSF and TGFβ1 treatment macrophages**
ELISA of OSM protein in unpolarised macrophage treated with MCSF or TGFβ1 for 24 hours (n=6). Results represent individual values with mean.

This finding implies a potential crosstalk between cancer and immune cells that could be driving the invasive phenotype, with the PDAC associated cytokine TGFβ1 inducing OSM secretion in macrophages.

#### 5.2.5.2 Invasive effects of OSM on CSCs

Previous results have shown that CSCs are more invasive in MCM compared to non-CSCs, as defined by CD133 expression (see section 3.2.1.1). Thus, having proven that OSM mimicked the invasive effects of MCM on the 'mixed' PDAC population, effects on the CSC population were also investigated. Gene expression of Zeb1, Loxl2 and Slug were higher in CD133+ cells treated with OSM compared to treated CD133- (Figure 5.20).

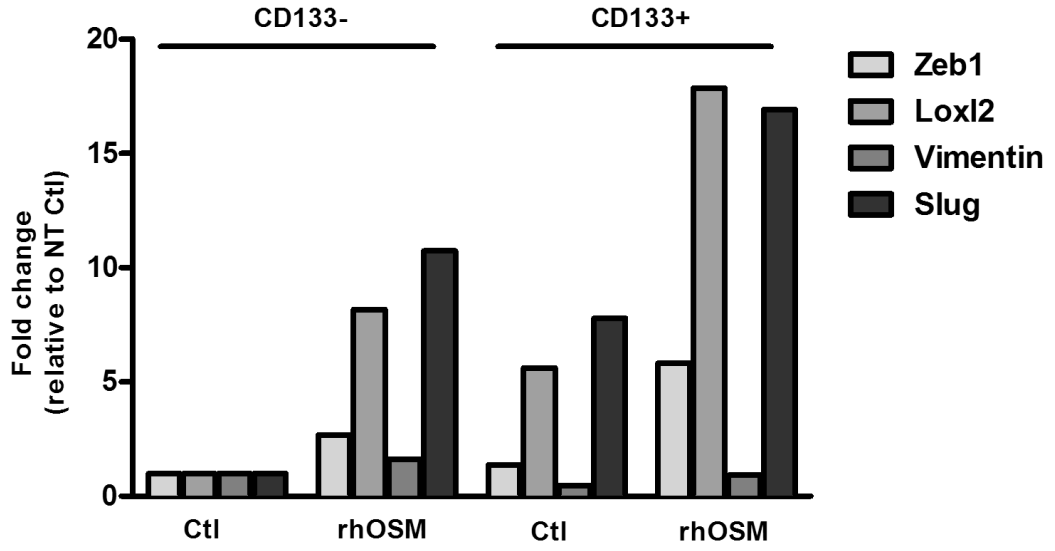


**Figure 5.20 EMT gene expression of CD133+/- cells treated with OSM**
RT qPCR of EMT genes in Panc354 CD133-/+ cells treated with control media or OSM (100ng/ml) for 48hrs (n=1).

In keeping with this finding, the most invasive cell population was the CD133+ OSM treated cells in invasion assay (Figure 5.21).

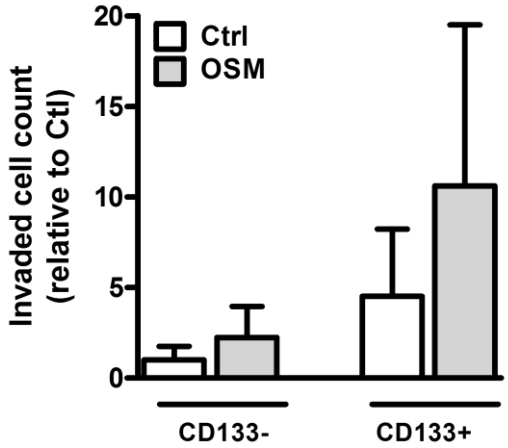


**Figure 5.21 Invasive effects of OSM on CD133+/- cells**
Transwell invasion assay of Panc354 CD133+/- cells treated with OSM (100ng/ml) (n=3). Results represent a compilation of experiments normalised to control, with values representing the mean (+/- SEM).

To determine why the CD133+ CSC population was more responsive to the invasive effects of OSM, basal gene expression of OSMR was compared in both populations immediately after sorting. The baseline expression of OSMR was significantly higher in the CSC CD133+ population compared to the non-CSC CD133- population (Figure 5.22).

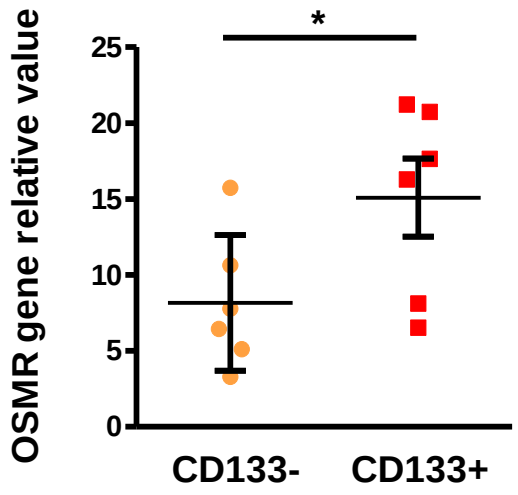


**Figure 5.22 OSMR gene expression in CSCs vs non-CSC**
RT qPCR of baseline *OSMR* mRNA in Panc354 and Panc215 (n=3 per cell type) immediately after sorting in CD133+ (CSC) compared to CD133- (non-CSC) populations. Results represent a compilation of experiments normalised to control, with values representing the mean (+/- SD). Statistical significance: Wilcoxian paired t test * = $p<0.05$.

Therefore, expression of OSMR is not only higher in the bulk population of cells compared to other gp130 cytokine receptor and positively regulated by MCM, but it is also more highly expressed in the CSC population compared to the non-CSC population at baseline. This expression leads to CSCs being the most invasive cell population in response to OSM alone or in MCM.

### 5.2.6 Stemness effects of OSM

Previous data from our group have shown that macrophage derived factors LL37 and ISG15 potentiate stemness in Panc185 and 354 cells. Based on these findings, and having shown increased invasion of stem cells with OSM, it was pertinent to test if OSM also had similar effects on inducing stemness in PDAC cells.

Panc215, 354 and 10953 were treated for 48 hours with OSM and RNA collected for analysis of the stemness genes Oct3/4, KLF and SOX2. Results showed variation in the expression of genes when normalised to control. Panc215 did not show upregulation of any genes and certainly fold change was decreased, suggesting cells were becoming less stem. In Panc354, upregulation of Oct3/4 was noted, and in Panc10953 slight increase in expression of KLF4 (Figure 5.23).

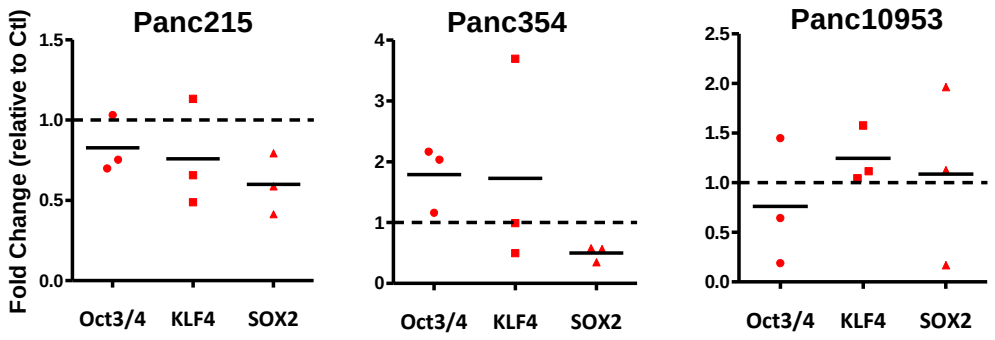


**Figure 5.23 Stemness gene expression in OSM treated cells**
RT qPCR of stemness genes in Panc215, 354 and 10953 (n=3 per cell type) following treatment with OSM 100ng/ml for 48hrs.

In addition, OSM treated Panc215 were analysed for surface expression of the stem marker, CD133. Preliminary results showed a decrease in CD133+ cells after OSM treatment when compared with control (Figure 5.24), but this would need to be repeated to make definitive conclusions.

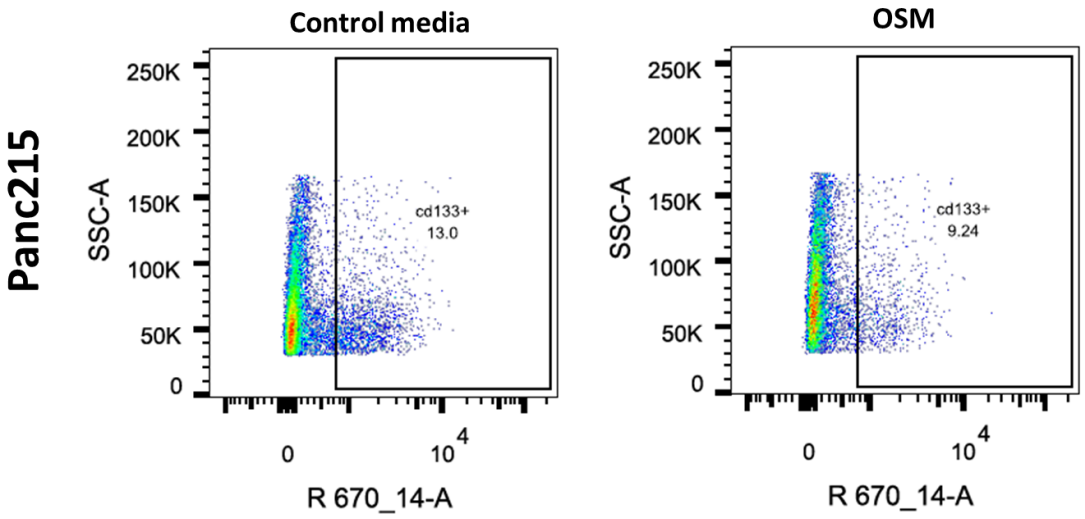


**Figure 5.24 FACS analysis of CD133 following OSM treatment**
FACS analysis of CD133 in Panc215 following 48hrs of OSM treatment (n=1).

Finally, functional assessment was undertaken using sphere formation assay. This assay measures anchorage-independent growth in sphere-like 3D structures from the proliferation of one CSC in serum free conditions. Panc354 and 10953 cells derived from primary spheres (i.e. sample already enriched for CSCs) were reseeded in the presence control media, MCM or OSM in anchorage serum free conditions. Both cell types demonstrated slight increase in sphere formation following treatment with MCM, but this experiment would require further replicates to make conclusions on the effects of sphere formation in MCM and OSM treatment (Figure 5.25).

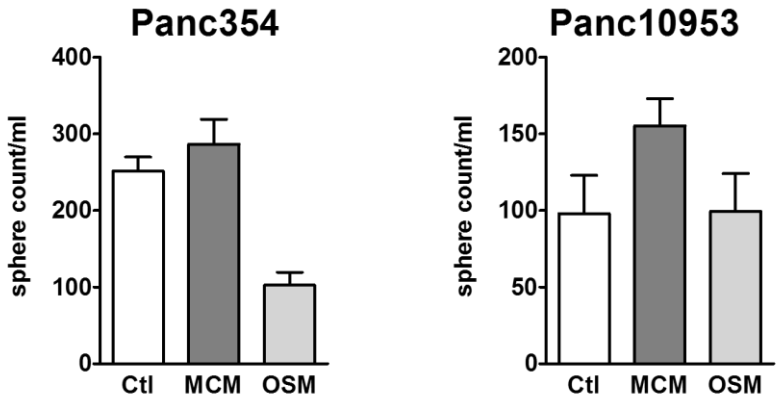


**Figure 5.25 Sphere formation assay**
Secondary sphere formation assay in MCM or OSM treated Panc354 and 10953 cells (n=2 per cell type)

Therefore, in order to definitively conclude the effects of OSM on the CSC subpopulation in PDAC, further experimental replicates would be required to gain more rigorous conclusions.

### 5.2.7 Immuno-inhibitory effects of OSM

Published data from our lab indicate culture with MCM induces immune checkpoint expression of PDL-1 in PDAC cells (Cioffi et al. 2015). Several cytokines are known to induce PDL-1 expression in various different cells types, for example IFNγ (Kondo et al. 2010). Therefore, OSM within MCM could also be having an immune modulatory effect by driving expression of PDL-1 on PDAC cells undergoing EMT to evade immune cell mediated T cell death.

Panc215, 354 and 10953 were analysed for PDL-1 expression after culture with MCM and OSM treatment for 48 hours. Results showed a consistent upregulation in PDL-1 expression compared to control treatment not only with MCM, as previously published, but also following OSM treatment (Figure 5.26A). Cumulative data of all cell cultures showed this upregulation to be significant (Figure 5.26B).

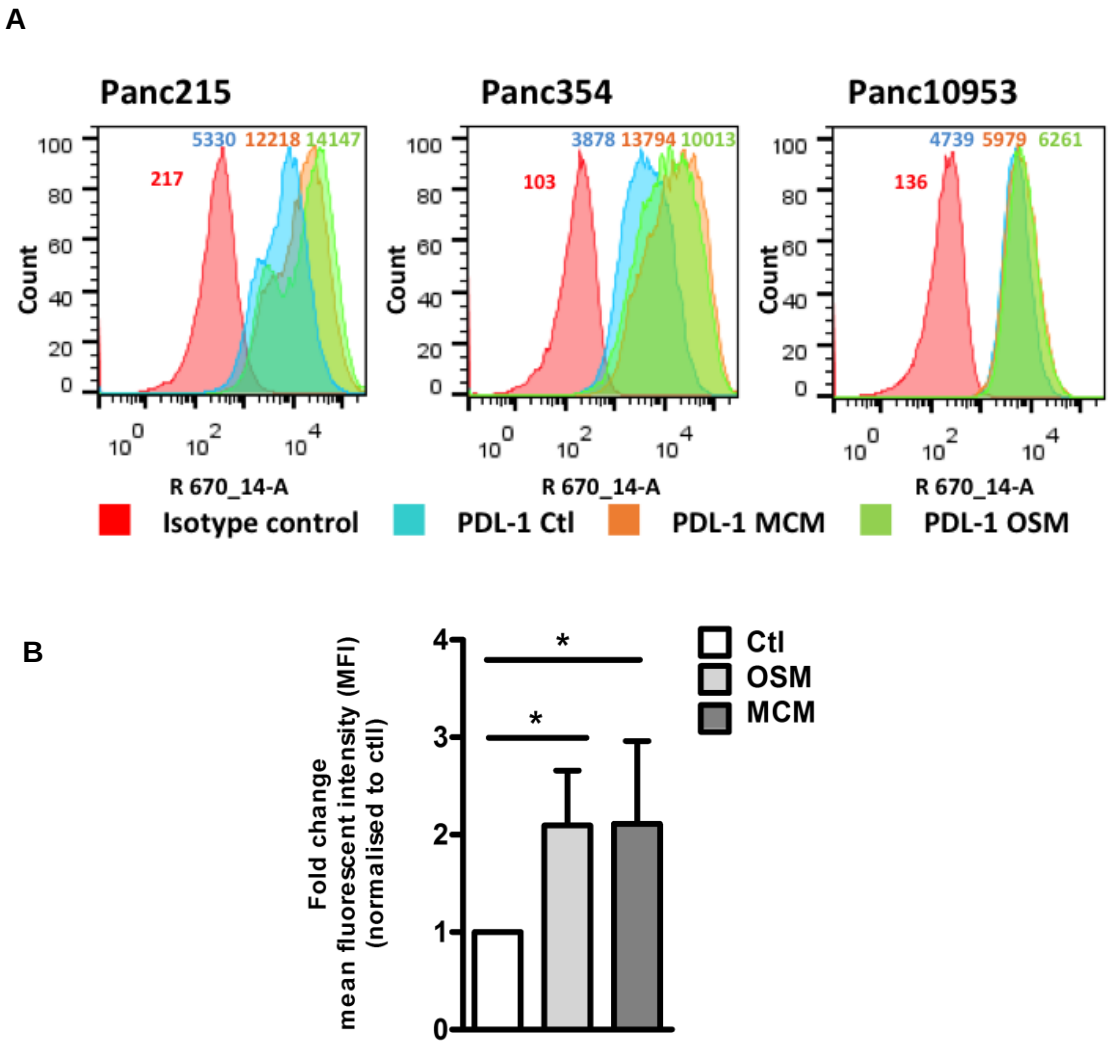


**Figure 5.26 FACS analysis of PDL-1 in PDAC**
A) Representative FACS plots of Panc215, 354 and 10953 stained with isotype control and PDL-1 antibody after 48hrs of treatment in control media or MCM. Mean fluorescent intensity (MFI) for each condition is labelled on histograms. B) Pooled MFI analysis in Panc 215 (n=2), 354 (n=2) and 10953 (n=2) treated with control media, MCM or OSM (100ng/ml). Results represent a compilation of experiments in each cell type normalised to control, with values representing the mean (+/- SD). * $p<0.05$

In PDAC tissue, PDL-1 is not only expressed on tumour cells but also infiltrating lymphocytes and stromal cells (Nomi et al. 2007). Certainly in some tumours, PDL-1 expression within the immune component (consisting of macrophages, dendritic cells and T cells) is seen as a better predictor of outcome to anti-PDL-1 blockade than the tumour component (Herbst et al. 2014). IL10 and IL6 derived from TAMs have been

shown to stimulate autocrine expression of another checkpoint inhibitor molecule, B7-H4, indicating self-governing immune suppression by TAMs (Kryczek et al. 2006, 2007). Therefore, having shown MCM and OSM induce PDL-1 expression in tumour cells, and because PDL-1 is known to be highly expressed on TAMs in PDAC (Winograd et al. 2015), PDL-1 expression on TAMs in response to OSM was analysed in case of autocrine effects. Results did not show a difference in the expression of PDL-1 by FACS analysis in control treated compared to OSM treated primary macrophages from 3 different donors (Figure 5.27).

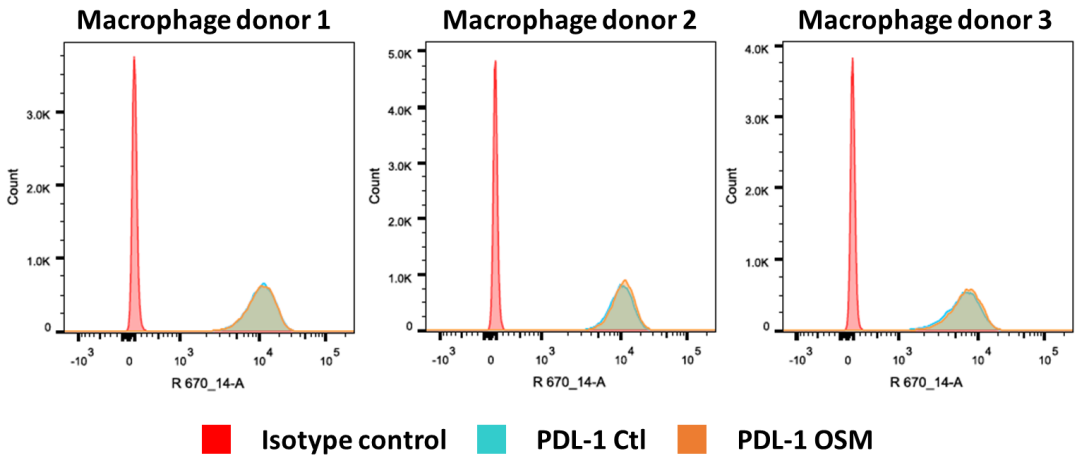


**Figure 5.27 FACS analysis of PDL-1 in TAMs**
FACS plots of three healthy primary macrophage donors, unpolarised for 4 days and then treated with control or OSM (100ng/ml) for 24hrs. Cells were stained with isotype control and PDL-1 antibody. Mean fluorescent intensity (MFI) for each condition is labelled on histograms.

Taken collectively, results show that OSM not only induce EMT and invasion, but also immune evasion of PDAC cells through regulation of PDL-1 expression. The effects of TAM derived OSM are primarily on PDAC cells, and there is no autocrine effect of OSM on PDL-1 expression in TAMs.

## 5.3 Discussion

Collective results of GSEA in Panc215, 253 and 354 confirmed enrichment of the cytokine receptor and JAK-STAT pathway gene sets in primary PDAC cells. Western blot analysis proved that TAM secreted factors were inducing activation of the STAT3 pathway via phosphorylation of Y502, and this finding was consistent across 7 primary PDAC cultures tested. Culture with MCM lead to pSTAT3 translocation to the nucleus, as shown through immunofluorescence staining, thus further confirming the postulated mechanism of action.

STAT3 is activated by growth factors and cytokine signalling. As the cytokine receptor pathway gene set was also enriched on microarray in Pan215, 253 and 354, investigation of potential cytokines secreted by TAMs that could activate STAT3 was undertaken. OSM was determined as a cytokine of interest, largely due to known links between its family of gp130 cytokines and STAT3, results of IPA analysis that predicted it to be upstream of activated genes, and because of the sigificant upregulation of its receptor gene, OSMR, in Panc253 and 354 determined by microarray analysis.

The gp130 family cytokines are linked through the following signalling pathways (Figure 5.28):

- JAK-STAT3 pathway
- Src homology 2 (SH2)-containing protein tyrosine phosphatase-2 (SHP-2)-Ras-Raf-MEK-extracellular signal-regulated kinase (ERK) pathway
  phosphoinositide 3-kinase (PI3K)-Akt pathway

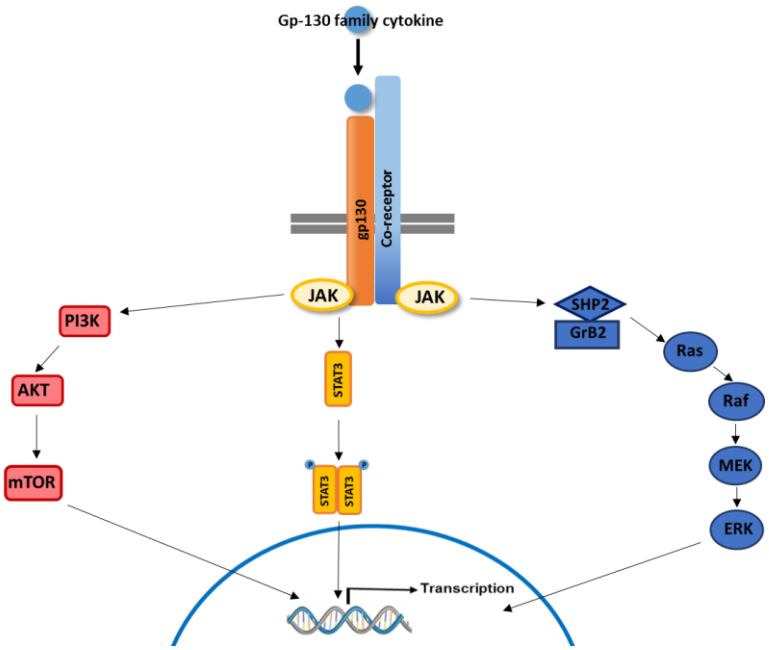


**Figure 5.28 gp130 receptor signalling pathways**

Of these pathways, STAT3 is recognised as the major signal transducer downstream of gp130 signalling (Heinrich et al. 2003). Other signalling pathways can be activated downstream of gp130 receptor complexes, for example PI3K and MAPK pathways (Figure 5.28). However it is likely that in our primary PDAC model, STAT3 is highly activated downstream of gp130 receptor, as GSEA indicated this pathway was significantly enriched in all three primary PDAC cell types tested. PI3K-AKT pathway was not enriched in any cell type, and the MAPK pathway was only significantly upregulated in Panc215, not Panc354 and 253.

Gp130 cytokines do not have intrinsic tyrosine kinase activity, therefore they engage with the receptor-associated tyrosine kinase JAK to activate phosphoyrlation of STAT3, allowing translocation of the protein to the nucleus leading to gene transcription. In cancer, gp130 receptor proteins are highly expressed in multiple tumour types, including pancreatic cancer cell lines (Corcoran et al. 2011), and are significantly associated with worse outcomes in patients (Xu and Neamati 2013).

Having proven STAT3 activation following MCM, one could not overlook other gp130 family cytokines could be secreted by TAMs and contribute to signalling

pathway induction. This was thought to be especially important as both IL6 and LIF activate STAT3 in PDAC cell lines (Corcoran et al. 2011). However, western blot data across seven primary PDAC cultures demonstrated STAT3 was being activated most strongly by OSM (similarly to MCM), to a lesser degree by IL6, and not by LIF. This pattern of STAT3 activation by each cytokine was similar to the pattern of invaision seen, with only OSM and MCM causing increased invasion of Panc354, but further replicates for this invasion assay would be required to confirm statistical significance . It was deduced the reason for this difference was due to upregulation of OSMR expression both at basal levels and in response to MCM in primary PDAC cultures compared to IL6R and LIFR, leading to a positive feedback loop and therefore greater downstream effects with OSM. One could question whether the experimental doses of recombinant protein used for each cytokine could have affected *in vitro* results. However, when referring to doses used in the literature, the most commonly used dose for all three cytokines was the same, (100ng/ml) (Klausen et al. 2000; Wang et al. 2000), therefore cytokine concentrations are unlikely to have influenced the differences seen. Certainly, our findings that OSM induced stronger STAT3 activation in PDAC compared to IL6 have also been noted in melanoma and lung, whereby higher pSTAT3 expression with OSM was found in malignant cells compared to IL6 treatment (Shien et al. 2017; Y. Wang et al. 2013).

ELISA confirmed secretion of OSM by primary TAMs in their conditioned media. Although consistently secreted, there was a large range of concentrations noted, likely because of macrophage donor heterogeneity. This varibality in OSM concerntrations could in part explain the heterogeneity in reponses, such as gene expression, that is often seen when treating primary PDAC cells in this experimental model. In the inflammatory setting, macophages secrete OSM in response to several different stimuli, for example prostoglandin E2 and pathogenic bacteria (Ganesh et al. 2012). Our results, in conjunction with previous data from the laboratory, suggest PDAC secreted TGFβ1 could be driving TAMs to secrete OSM, as demonstrated through ELISA of primary macrophages stimulated with cytokine for 24 hours. This would imply a potential crosstalk between the two cells, by which cancer cells secrete TGFβ1, which then activates TAM secretion of OSM to drive pro-tumourigenecity of PDAC.

A key finding of this chapter was the confirmation that OSM induces EMT and invasion of PDAC cells similar to that seen with MCM. This function of OSM has been noted in several different cancer types, including cervix (Kucia-Tran et al. 2016), breast (Guo et al. 2013; Lapeire et al. 2014) and lung (Argast et al. 2011). Therefore, should inhibitory mechanisms of blocking this pathway in PDAC be determined, there could be potential for application in other cancer types also.

Previous data from our lab support a crosstalk between TAM and PDAC model driving the CSC niche (Sainz et al. 2014, 2015). Transition from an epithelial-to-mesenchymal state has also been linked to stemness properties in some cancer models. Therefore, as OSM drives a more invasive phenotype in PDAC, the relationship between OSM and stemness was also investigated. No upregulation of stemness genes was seen, and further experiements would be required to confirrm the differences in surface markers or sphere formation following treatment with OSM. Current data is mixed as to whether OSM poetentiates stemness; West *et al.* show OSM not only induces EMT but also promotes stemness through SOX2 gene upregulation and CD44 surface expression in breast cancer (West, Murray, and Watson 2014), whereas in HCC the cytokine actually induces differentiation rather than stemness, defined by a decrease in AFP and CK19 expression and decrease gene expression of KRT19, AFP, TERT, BMI1 and POU5F1 (Yamashita et al. 2010). Thus, the effects of OSM on stemness may be dependent on the tissue type and markers used to define the 'stem' population. Although no conclusions can be made regarding OSM potentiating stemness, when defined by CD133 surface expression, CSCs were the most invasive in response to OSM due to higher expression of OSMR. In animal models, mesenchymal stem cells are known to be more migratory following cytokine stimulation (Naaldijk et al. 2015), however the effects of specific cytokines in the context of cancer biology (particularly of OSM) have yet to be demonstrated in current literature.

Our laboratory have already published data macrophages conditioned media induces PDL-1 expression on the surface of primary PDAC cells. A novel finding leading on from this was that OSM induces PDL-1 expression in PDAC. PDL-1 is an immune checkpoint inhibitor of great interest, as it is known to be expressed in many different tumours (Ghebeh et al. 2006; Hamanishi et al. 2007; Hino et al. 2010; Nomi et al. 2007; Ohigashi et al. 2005) and is currently targetable through antibody therapies in

the clinic. In PDAC, expression of PDL-1 correlates with worse outcomes (Nomi et al. 2007; Wang et al. 2010), and macrophages have to been linked to the regulation of PD1 and CTLA4 expression in PDAC tumours, with macrophage targeting agents enhancing the effects of checkpoint inhibitors *in vivo* (Zhu et al. 2014). PDL-1 expression is known to be mediated by several different cytokines, therefore one could speculate that macrophages are inducing checkpoint expression in tumours by cytokine secretion. IFNγ is thought to be the most potent inducer (Kondo et al. 2010). No members of the gp130 family cytokines have previously been described in driving PDL-1 expression specfically in any cell type, but IL6 has also been implicated in expression of another checkpoint inhibitor, B7-H4, on monocytes and macrophages in ovarian cancer (Kryczek et al. 2006). Therefore our findings of OSM inducing PDL-1 in PDAC cells is in keeping with a potential immune tolerance effect of this family of cytokines, but unlike IL6 the effects of OSM are only on PDAC and not TAMs. Nonetheless, it is appreciated that within the real PDAC TME it is unlikely that OSM is the only cytokine to dictate immune checkpoint inhibitor expression in malignant and stromal cells and more likely that many cytokines are inducing expression to produce an immune suppressive environment.

There are links between EMT and immune suppression programming in other tumours. Chen *et al.* have shown that Zeb1 relieves miR-200 repression of PDL-1 in tumour cells, which leads to CD8+ T cell immunsupression and metastasis in lung cancer (Chen et al. 2014). However, Hirai *et al.* found that in more mesenchymal / invasive oral squamous carcinoma cells, PDL-1 was downregulated both *in vitro* and in patient tissue, and it was stromal cells that had upregulated PDL-1 in invasive tissue rather than the tumour cells (Hirai et al. 2017). Therefore the exact link between invasion and acquisition of immune evasion in tumours is not clear, but our data support an association between the two phenotypes in tumour cells following interaction with TAM secreted factors.

Results from this chapter have so far shown upregulation of STAT3 activation and which appear to correlate with findings of more invasive and immune evasive phenotype. However, the link between STAT3 and the phenotypes described are only presumed based on previous literature and not yet directly proven. There are extesnive published data demonstrating that both invasive and immune tolerance pathways are

mediated by STAT3 (Table 5.3). In T cell lymphoma, STAT3 binds the PDL-1 gene regulators (Marzec et al. 2008) and in PDAC mouse models, ruxolitinib improved the efficacy of anti-PD-1 immunotherapy (Lu et al. 2017). In several different cancer models, STAT3 directly transcribes pro-tumourigenic genes known to contribute to metastasis in cancer such as Zeb1 and MMPs (Table 5.3). One could deduce that STAT3 activation in our model is therefore also driving EMT, as less potent activators of STAT3 (IL6 and LIF) having less EMT gene upregulation and were less functionally invasive when compared to stronger activators such as MCM and OSM. One way to confirm the involvement of this signalling pathway in TAM driven pro-tumourgenesis of PDAC is by blocking this signalling pathway to determine the effects on both phenotypes.

**Table 5.3 Cancer related genes upregulated by STAT3 in human cells**
(adapted from Carpenter and Lo 2014)

| Gene | Cell Type | Reference |
|---|---|---|
| **Transcription Factors** | | |
| c-Fos | HepG2, A431 | (Lo et al. 2007; Seidel et al. 1995; Yang et al. 2003) |
| HIF-1α | A2058 | (Niu et al. 2008) |
| c-Myc | HepG2, BAF-G277, KT-3, | (Kiuchi et al. 1999) |
| Twist | A431 | (Lo et al. 2007) |
| Zeb1 | SW1116, LoVo | (Xiong et al. 2012) |
| Oct-1 | Eca-109 | (Z. Wang et al. 2013) |
| **Apoptosis and Proliferation** | | |
| Bcl-2 | Hela | (Choi and Han 2012) |
| Mcl-1 | U266 | (Becker et al. 2014; Epling-Burnette et al. 2001) |
| Bcl-xL | U266 Myeloma | (Catlett-Falcone et al. 1999) |
| Survivin | MDA-MB-453 | (Gritsko et al. 2006) |
| Hsp70 | VSM, HeLa | (Madamanchi et al. 2001) |
| Hsp90α | Jurkat | (Chen et al. 2007) |
| Hsp90β | VSM | (Madamanchi et al. 2001) |
| Cyclin-D1 | 293T, 3YI, 2fTG | (Bromberg 2002; Leslie et al. 2006; Sinibaldi et al. 2000) |
| **Immune Suppression and Proliferation** | | |
| IL-10 | RPMI-8226 B | (Schaefer et al. 2009) |
| COX-2 | U87MG | (Lo et al. 2010) |
| PDL-1 | SUDHL-1, JB6, SUP-M2, Karpas 299, and L-82 | (Marzec et al. 2008) |
| **Metastasis** | | |
| MMP-1 | T24, HT-29 | (Itoh et al. 2006) |
| MMP-3 | HBVE | (M. Liu et al. 2013) |
| MMP-9 | MCF7 | (Song et al. 2008) |
| Fascin | 4T1 | (Snyder, Huang, and Zhang 2011) |
| Vimentin | MDA-MB-231 | (Wu et al. 2004) |
| ICAM-1 | HepG2 | (Schuringa et al. 2001) |
| NGAL | Primary Macrophages | (Jung et al. 2012) |
| SAA1 | HepG2 | (Kesanakurti et al. 2013) |
| $p21^{CIP1/WAF1}$ | MG63, A431, HT-29, WiDr, HepG2 | (Bellido et al. 1998; Chin et al. 1996; Giraud et al. 2002) |
| **Cell Signalling** | | |
| AKT | 293 | (Hung and Elliott 2001) |
| TNF-R2 | SW480 | (Hamilton et al. 2011) |
| MUC-1 | T74D, ZR-75-1 | (Ahmad et al. 2011; Gaemers et al. 2001) |
| Foxp3 | 293 | (Zorn et al. 2006) |
| **Tumour Immune Surveillance** | | |
| IFN-γ | T Cells | (Cheng et al. 2003; Kusaba et al. 2005; Wang et al. 2004) |
| RANTES | PC3 | (Cheng et al. 2003; Wang et al. 2004; Yang et al. 2007) |
| CRP | Hep3B | (Zhang et al. 1996) |
| STAT1 | MDA-MB-468 | (Han et al. 2013) |
| **Other** | | |
| TIMP-1 | HepG2, WI38, CD4+ T | (Adamson et al. 2013; Bugno et al. 1995) |
| JunB | HepG2 | (Seidel et al. 1995) |
| iNOS | A431 | (Lo et al. 2005) |
| CDC25A | HepG2, Saos Cells | (Barré, Vigneron, and Coqueret 2005) |

# 6 CHAPTER SIX: TARGETING THE ONCOSTATIN M PATHWAY

## 6.1 Introduction and Aims

Having identified upregulation in activity of the OSM/ OSMR/ STAT3 pathway in primary PDAC cells, driven by TAMs, the next aim of this thesis is to explore this pathway in the clinical setting. By determining if this pro-tumourigenic pathway is present in the clinical setting, the prospect of inhibiting it for therapeutic benefit could then be taken forward.

To date, few agents targeting TAMs specifically have reached clinical practice for treatment of solid tumours. This may be in part due the abundant presence of macrophages throughout the body, making it difficult to target TAMs specifically without causing systemic toxicity to non-malignant macrophages. Therefore, targeting the pathways activated by TAMs in cancer cells could pose a better therapeutic approach, as this would allow more specific activity towards malignant tissues.

The aims of this chapter are:

- To further explore the significance of OSM/ OSMR/ STAT3 pathway in PDAC patient samples
- Identify agents that inhibit the activation of OSM/ OSMR/ STAT3 pathway in primary PDAC cells
- Determine the effects of pathway inhibition *in vitro* and *in vivo*

## 6.2 Results

### 6.2.1 Clinical relevance of OSM in PDAC

Having demonstrated effects of OSM *in vitro* in our primary PDAC model, it was necessary to determine if this cytokine and its receptor had relevance in the clinical setting and is linked to pSTAT3 and EMT.

#### 6.2.1.1 Tissue Cancer Genome Atlas analysis of OSM

Using the TCGA, expression of OSMR, along with the other gp130 cytokine receptor genes IL6R and LIFR, was analysed in a PDAC patient population. The patient population consisted of 177 patients with a diagnosis of PDAC (Appendix 1).

Results showed expression of OSMR is prognostic in a PDAC patient cohort: patients with high gene expression had a significantly worse patient outcome than those with low expression ($p=0.01433$) (Figure 6.1). Interestingly, IL6R and LIFR expression was inversely related to survival, with high expression levels leading to better patient outcome ($p=0.0095$ and $p=0.014$ respectively).

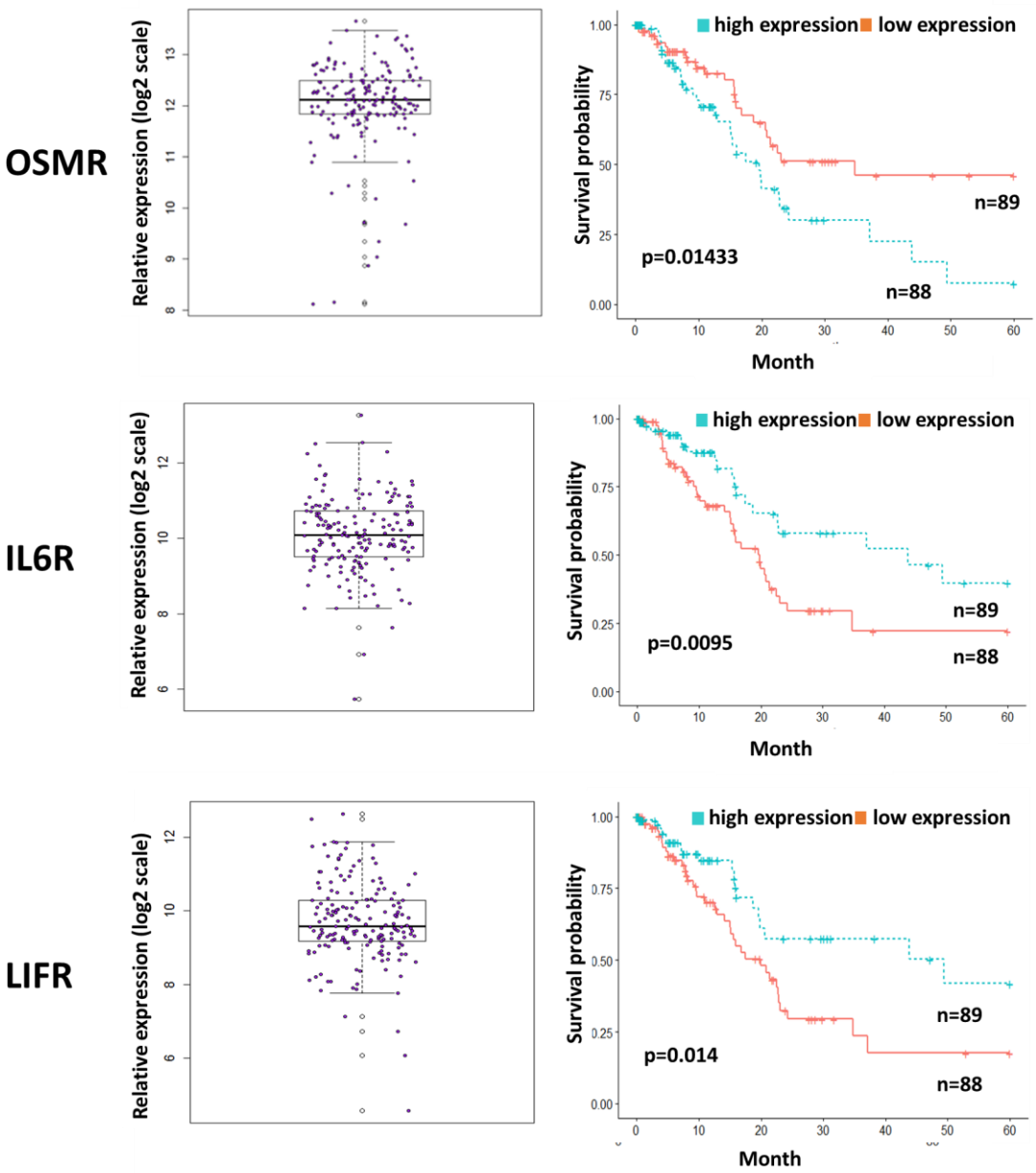


**Figure 6.1 Prognostic analysis of gp130 cytokine receptors in PDAC**
Kaplan-Meier curves of *OSMR*, *IL6R* and *LIFR* gene expression in TCGA pancreatic data set showing the overall survival analysis in patients with high and low receptor expression (median expression cut off) dichotomized at 5 years follow up.

As this patient cohort was mixed, patients were divided by stage of disease to determine of OSMR expression was relevant. Unfortunately, patient numbers were not high enough for meaningful analysis in Stage III and IV disease (n=3 and n=4 respectively). However, when analysing localised disease only i.e. stage I and II patients (n=167), patients with high OSMR expression had a significantly worse outcomes (p=0.042) (Figure 6.2). Thus, patient data suggest that OSMR is an important prognostic factor in early stage disease for inferior survival.

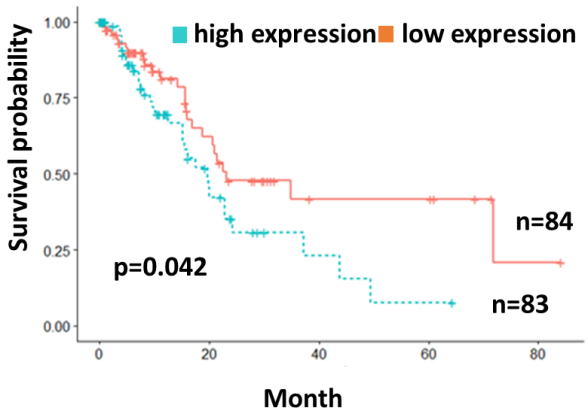


**Figure 6.2 Prognostic analysis of OSMR in Stage I and II PDAC**
Kaplan-Meier curves of *OSMR* gene expression in early stage (i.e. localized disease) in TCGA pancreatic data (n=167) showing the overall survival analysis in patients with high and low expression of *OSMR* (median expression cut off).

#### 6.2.1.2 Serum levels of OSM

In order to confirm the TCGA dataset, levels of OSM in patient serum was next tested. It was hypothesised that should OSM/ OSMR be an important pathway driving PDAC progression, then it would be elevated in patients with the disease compared to non-diseased individuals. Detectable serum levels have previously been reported in PDAC patients, whereby elevated serum levels of OSM were found to be diagnostic as part of a panel of cytokines in response to combination therapy of gemcitabine and erlotinib (Torres et al. 2014).

Levels of OSM protein were tested in treatment naïve metastatic PDAC patients and 'healthy' donor controls through ELISA (Figure 6.3). Surprisingly, results showed a

higher average level of serum OSM in healthy donor population compared to the diseased population.

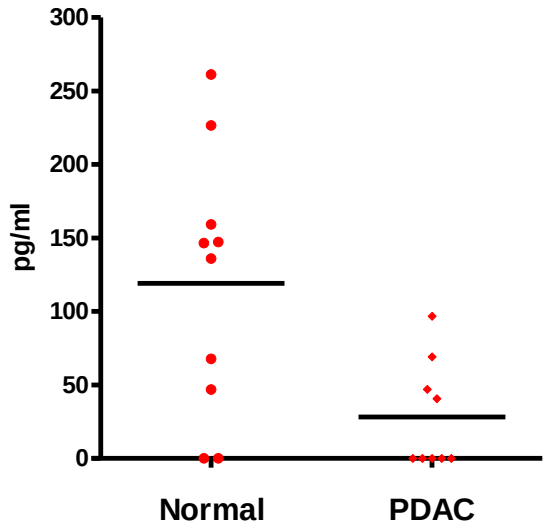


**Figure 6.3 ELISA of OSM in healthy vs. PDAC patients**
ELISA of OSM protein in healthy (n=10) vs. PDAC patient serum (n=9) macrophage conditioned media (n=13). Results represent individual values with mean.

One possible explanation for these results could be technical, as it was noted that 5/9 patients in the disease population had undetectable levels; the time to collect and process PDAC patients was longer compared to the 'healthy' donor controls. Thus, should OSM have been unstable over longer periods of time, protein levels could have appeared falsely low. In addition, baseline differences in the patient populations could have led to the differences noted. In the first instance, healthy donor and PDAC patients were not age matched, and information of disease status for healthy donor populations was not available. Thus, as OSM levels are known to vary in disease states, for example higher levels in inflammatory conditions (Richards 2013), if a donor was suffering from an inflammatory condition at the time of testing, than circulating OSM would be raised and this bias could have affected results. In addition, all of the PDAC patients tested were treatment naïve and had metastatic or locally advanced disease. Based on the TCGA analysis results, expression of OSMR is prognostic in the early stage patients and undetermined for late stage disease due to low patient numbers for analysis. Therefore, exploring circulating levels of OSM may

be more relevant in early stages of disease, rather than in this patient cohort of late stage metastatic disease.

Should these low readings of circulating OSM be true however, it could be explained that the circulating levels are not reflective of the activity at the localised tumour, especially if the cytokine is secreted by local tumour infiltrating TAMs. Thus, these findings of lower levels of serum OSM in PDAC compared to healthy controls does not necessarily reflect the activity of the pathway described thus far.

#### 6.2.1.1 Tissue Microarray

To investigate the pathway of interest at the local tumour site, TMAs of PDAC patient tissue were stained for OSMR, pSTAT3, CD68 and CK19. Zeb1 and OSM staining were also attempted, but antibodies could not be optimised for accurate analysis of IHC.

Serial staining of a TMA panel of 33 PDAC tissue cores revealed a significant positive association between the expression of nuclear pSTAT3 staining and OSMR intensity of CK19 positive cells (Figure 6.4). This result not only shows that the degree of OSMR is related to pSTAT3 activation in human tissue samples, but also confirms that OSMR protein is detectable in malignant tissue.

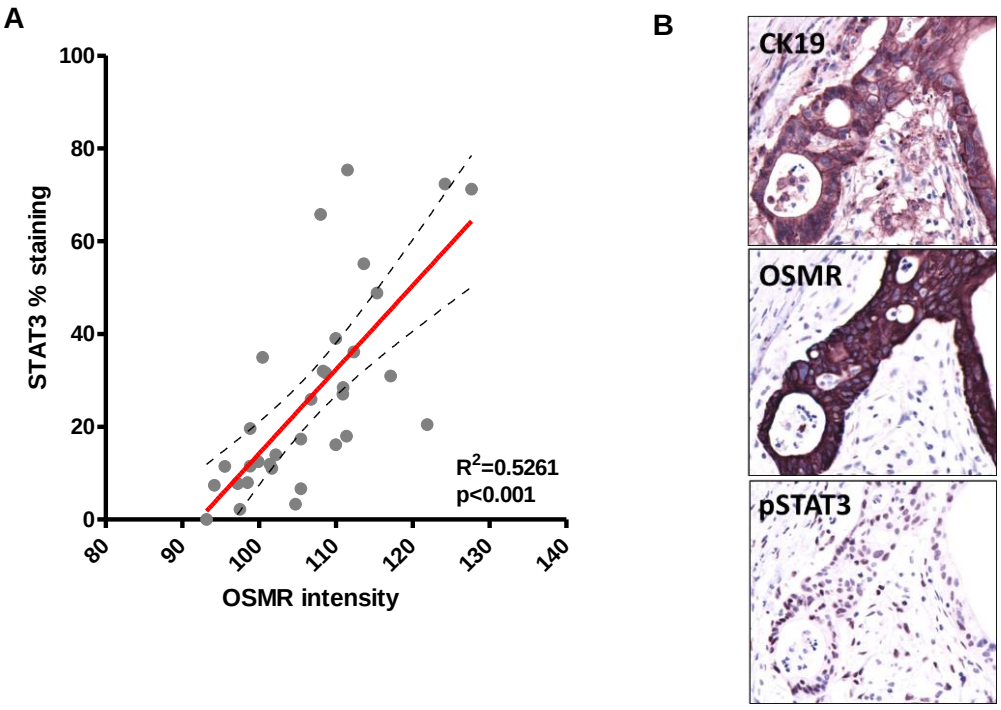


**Figure 6.4 Association of pSTAT3 and OSMR in patient tissue**
A) Correlation between nuclear pSTAT3 expression and OSMR intensity in CK19 cells of 33 PDAC tissue cores. Linear regression was conducted to evaluate the correlation between pSTAT3 percentage staining as a total CK19 cells compared to OSMR intensity in CK19 cells. Dotted lines represent the 95% confidence interval B) Representation micrographs of CK19, pSTAT3 and OSMR stained PDAC tissue cores.

Overall, this exploration of clinical data has revealed that OSMR is prognostic for worse survival in PDAC patients, and that staining of patient tissue has shown an association with this receptor and pSTAT3 in the primary tumour. These findings support *in vitro* data that OSM is likely to be initiating a pro-tumourigenic phenotype in PDAC cells via binding to its receptor, and driving STAT3 mediated pathways that lead to worse patient outcomes.

### 6.2.2 *In vitro* inhibition

To identify agents that inhibited activation of our pathway on interest, drugs had to be readily available and non-toxic to mammalian cells. In addition, a way in which to prove mechanism of action for each agent was needed. Inhibition of pSTAT3 through western blot analysis was selected for this purpose.

Based on these criteria, three inhibiting agents were selected that covered all stages of the pathway: neutralising OSM antibody (anti-OSM), antibody against the gp130 receptor (anti-gp130 antibody) and the small molecule inhibitor against JAK/STAT, ruxolitinib (Figure 6.5). It was recognised that antibody against gp130 receptor was not specific to OSM, however there is no commercial agent against OSMR therefore this antibody was selected to determine the effects of receptor inhibition.

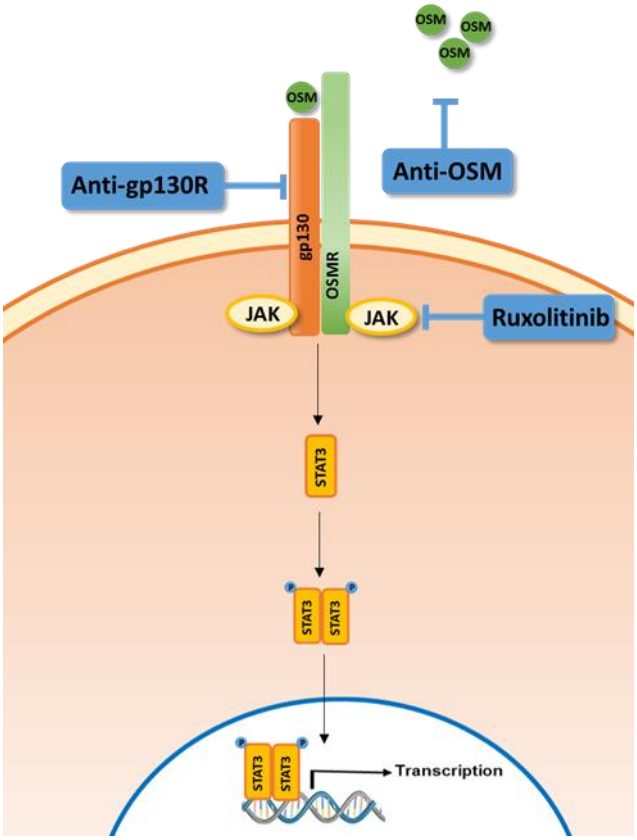


**Figure 6.5 Inhibitors of OSM / OSMR / STAT3**

### 6.2.1.2 Inhibition of STAT3 phosphorylation

Mechanism of action for each agent was confirmed through loss of STAT3 phosphorylation in both MCM treated cells (Figure 6.6). Western blot for inhibition was only performed once in each cell type, and would have to be repeated to determine significant down regulation of protein, but the trend was seen across three different primary cultures tested. Of note, inhibition appeared stronger in all three cell types with the anti-gp130 receptor antibody compared to neutralising OSM antibody in MCM. Reasons for this finding could be that at the concentrations used, OSM antibody was not completely neutralising recombinant OSM protein / secreted OSM protein present in MCM, thus some was still able to bind the receptor complex to activate the signalling pathway.

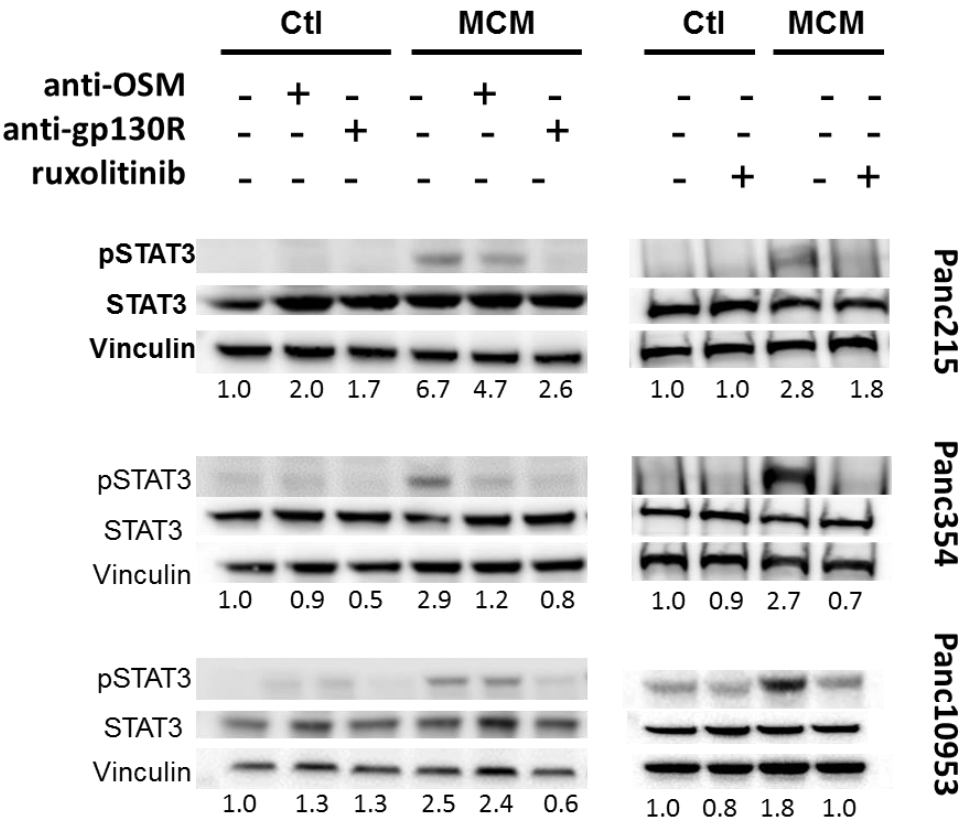


**Figure 6.6 STAT3 phosphorylation with antibody inhibition**
Western blot of pSTAT3 protein expression from cell lysates of PDAC cells cultured with MCM in the presence of anti-OSM antibody (10µg/ml), anti-gp130 receptor antibody (2µg/ml) or ruxolitinib (250nM). Relative densitometric quantification of protein bands, normalised to total STAT3 and loading control are shown below each blot.

#### 6.2.1.1 Inhibition of immune evasion

PDL-1 is known to be regulated by STAT3 in lymphomas (Marzec et al. 2008) and and in PDAC mouse model, ruxolitinib improves the efficacy of anti-PD-1 immunotherapy (Lu et al. 2017). Therefore, PDL-1 expression in PDAC could be influenced by STAT3 pathway blockade. Upregulated expression in OSM and MCM was decreased by OSM/ OSMR/ STAT3 inhibitors, confirming the hypothesis that regulation of PDL-1 in PDAC cells is STAT3 driven (Figure 6.7).

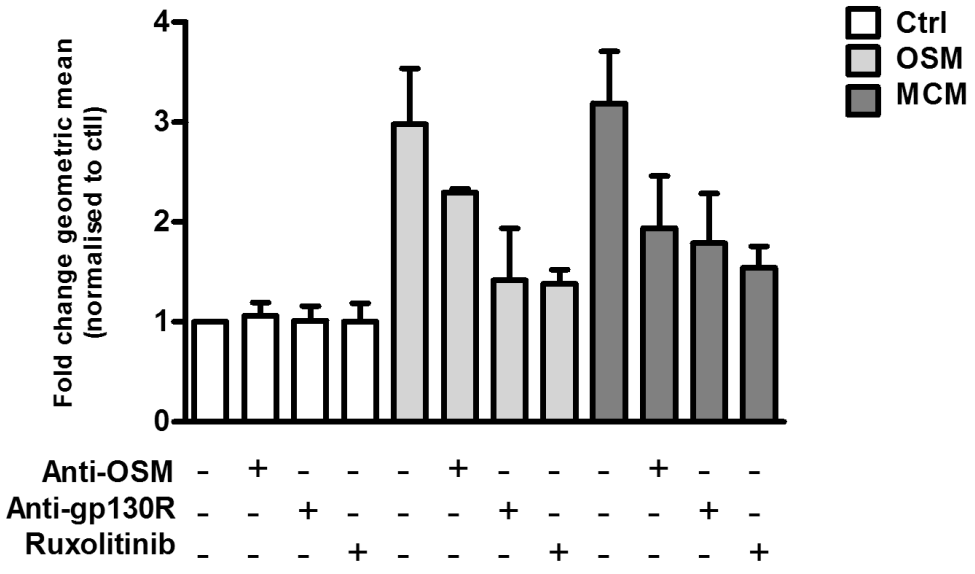


**Figure 6.7 PDL-1 expression following OSM / OSMR / STAT3 inhibitors**
Mean fluorescence intensity (MFI) analysis for Panc354 (n=2) treated with control media, MCM or OSM (100ng/ml) +/- neutralising anti-OSM (10μg/ml), anti-gp130R antibody (2μg/ml) or ruxolitinib (250nM). Results represent a compilation of experiments normalised to control media non-treated cells, with values representing the mean (+/- SD).

### 6.2.1.2 Inhibition of invasion

The effect of pathway inhibition on invasion was next determined. Treatments were applied to Panc215, 354 and 10953 and cells were subsequently used in invasion assay experiments, performed twice in each primary cell culture type (Figure 6.8). Of note, anti-gp130 receptor antibody showed the most consistent and the greatest decrease in fold change of invasion in MCM treated cells, but experiments would have to be repeated to deduce if this reduction was statistically significant.

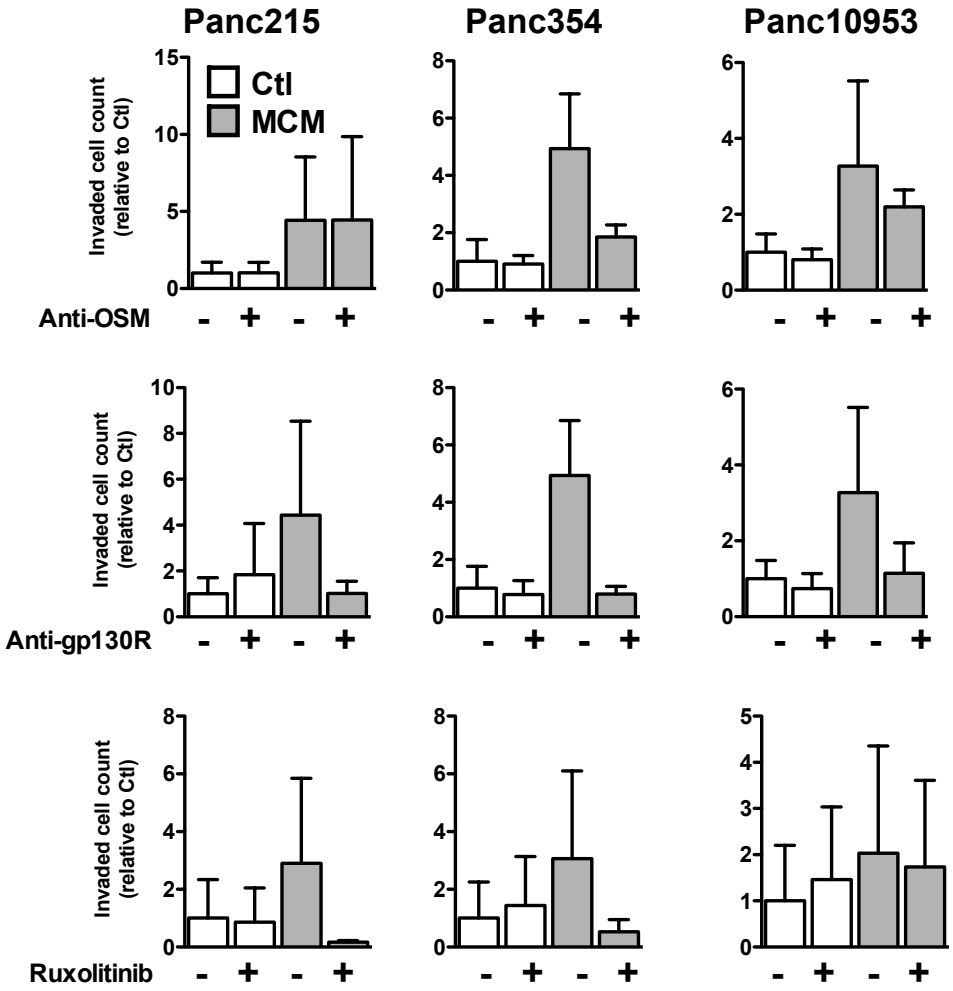


**Figure 6.8 Invasion with OSM/ OSMR/ STAT3 inhibitors**
Transwell invasion assay of Panc 215, 354 and 10953 (n=2 per cell type) pre-treated MCM for 48hrs +/- anti-OSM antibody (10μg/ml), anti-gp130 receptor antibody (2μg/ml) or ruxolitinib (250nM). Results represent a compilation of experiments normalised to control, with values representing the mean (+/- SD).

As antibody treatment against gp130 showed the strongest and most consistent downregulation in function with MCM treatment (i.e. invasion), this treatment was chosen to take forward for further testing. The effects of this antibody were confirmed in the presence of OSM treatment also, showing a decrease in EMT gene expression and invasion in the cells treated with OSM and anti-gp130 receptor antibody (Figure 6.9 and 6.10).

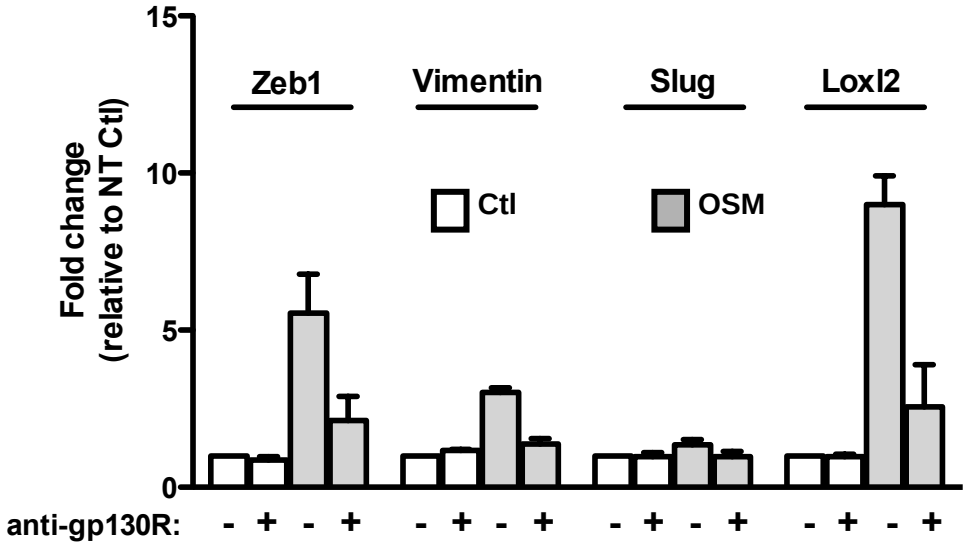


**Figure 6.9 EMT gene expression with antibody inhibition**
RT qPCR of EMT genes in Panc354 treated with OSM (100ng/ml) for 48hrs with anti-gp130 receptor antibody (2µg/ml) (n=3). Results represent normalisation to control, with values representing the mean (+/- SEM).

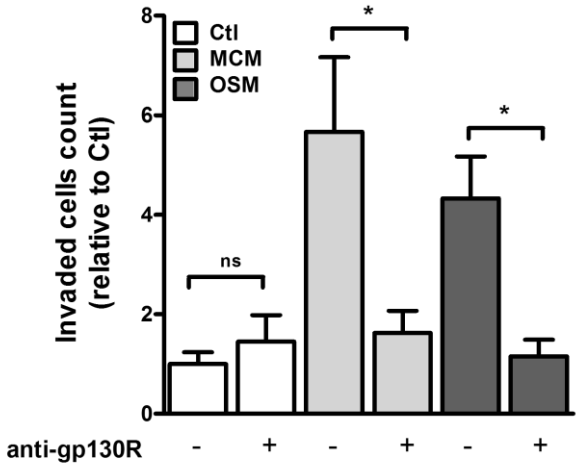


**Figure 6.10 Effect on invasion with anti-gp130 receptor**
Transwell invasion assay of Panc 215, 354 and 10953 (n=2 per cell type) pre-treated with OSM 100ng/ml and MCM for 48hrs +/- anti-gp130 receptor antibody (2µg/ml). Results represent a compilation of experiments normalised to control, with values representing the mean (+/- SEM). Statistical significance: Wilcoxian paired t test * = $p<0.05$.

In conclusion, *in vitro* testing revealed that anti-OSM antibody, anti-gp130 antibody and ruxolitinib blocked pSTAT3 expression and invasion in the presence of MCM. As anti-gp130 receptor antibody gave the most consistent downregulation in invasion with both OSM and MCM treatment cells, this agent was taken forward for inhibition in the *in vivo* setting.

### 6.2.3 *In vivo* inhibition

Prior to *in vivo* testing, it was necessary to confirm that blocking the pathway using the gp130 receptor antibody had no detrimental effects on cell growth that could influence the *in vivo* metastatic assay results or growth of a primary tumour *in situ*.

Anti-gp130 receptor antibody was tested on cells pre-treated for 48 hours with control media, MCM or OSM. After 3 days treatment, cumulative results from Panc215, 354 and 10953 demonstrated a significant decrease in proliferation of OSM treated cells compared to control treated (Figure 6.11). There was a trend for decreased proliferation in MCM as seen previously, but this was not significant. The effects on proliferation were reversed with the antibody treatment as hypothesised, but this difference was only significant in the control treated cells and not in MCM or OSM pre-treated cells.

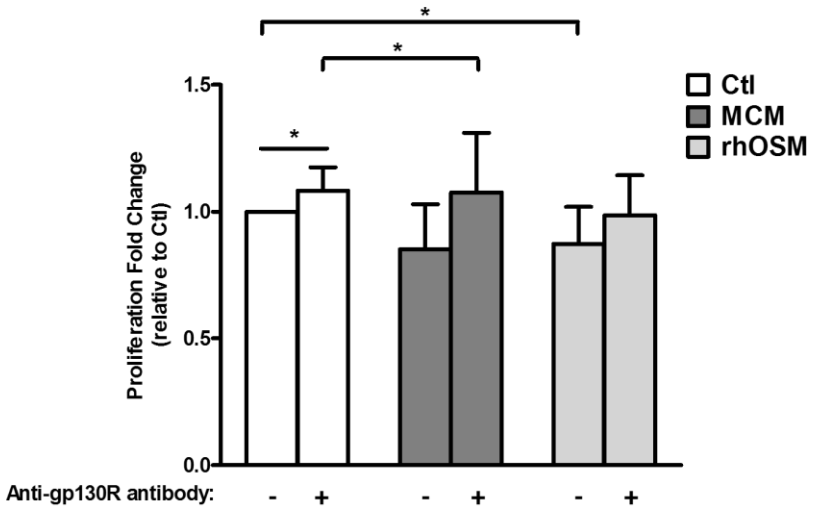


**Figure 6.11 Crystal violet proliferation with anti-gp130 receptor antibody**
Crystal violet analysis of Panc215, 354 and 10953 pre-treated with control, MCM of OSM (100ng/ml) for 48hrs, followed by 4 days treatment with corresponding media and antigp130 receptor antibody (2μg/ml) (n=2 per cell type). Staining of crystal violet was normalised to day 0 control (i.e. pre-treated cell density). Results represent a compilation of all experiments (n=6) normalised to control, with values representing the mean (+/- SD). Statistical significance: Wilcoxian paired t test * = $p<0.05$.

Applying this clinically, it would suggest that inhibiting the gp130 receptor alone in patients could theoretically lead to greater proliferation of PDAC cells within the primary tumour, especially those not under the influence of macrophage derived factors. However, independent inhibition of this pathway was never proposed, as there is no suggestion that targeting cells through this pathway would have cytotoxic effects that leads to tumour regression, an essential requirement for effective anti-cancer therapy. Thus, trying to mimic the potential clinical application of the agent, the antibody was tested in conjunction with gemcitabine in cells pre-treated with the MCM or OSM. The previous proliferative advantage seen with antibody blockade was not seen in combination treatment i.e. cells remained responsive to conventional chemotherapy when inhibiting the OSMR/ OSM/ STAT3 pathway (Figure 6.12). Therefore, when formulating a future clinical application for targeting this pathway, one would expect to give therapy in conjunction with a standard cytotoxic chemotherapy regime.

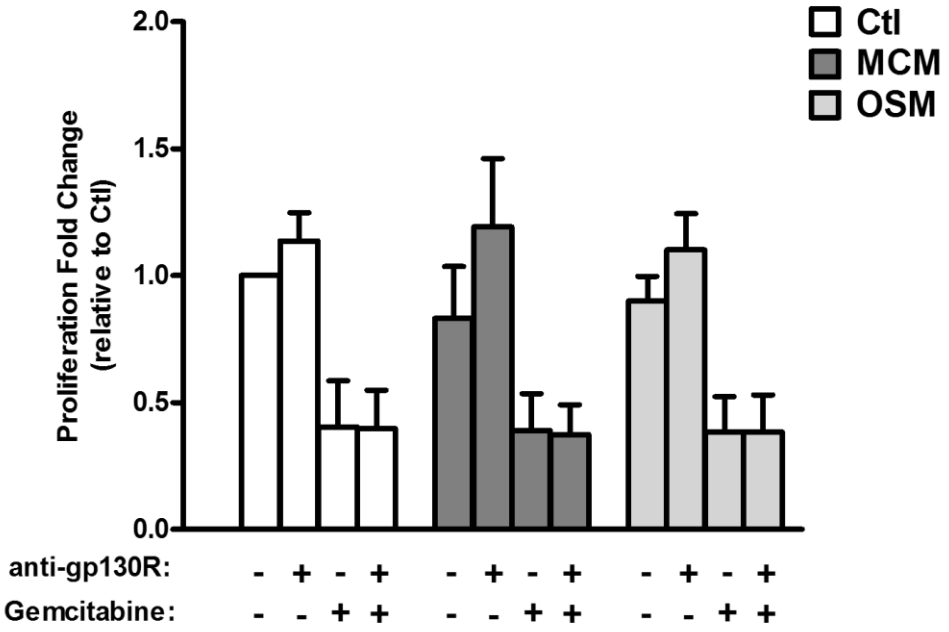


**Figure 6.12 Crystal violet proliferation with antigp130 receptor and gemcitabine**
Crystal violet analysis of Panc215, 354 and 10953 pre-treated with control, MCM of OSM (100ng/ml) for 48hrs, followed by 4 days treatment with corresponding media and antigp130 receptor antibody (2μg/ml) or gemcitibine (300nM) alone or in conjunction (n=1 per cell type). Staining of crystal violet was normalised to day 0 control (i.e. pre-treated cell density). Results represent a compilation of all experiments (n=3) normalised to control, with values representing the mean (+/- SD).

Prior to *in vivo* injection, as with MCM, effects of OSM and antibody treatment described thus far were found to be consistent in Panc354-Luc, which had undergone virus transduction and GFP sorting and therefore could have responded differently due to selection pressures. OSM treated cells displayed the typical morphological changes expected, which were reversed with antibody treatment (Figure 6.13A). pSTAT3 and invasion was upregulated with OSM treatment, and inhibited with anti-gp130 receptor antibody treatment, as with non-transduced cells (Figure 6.13B & C). These experiments were only done once for the purpose of confirming the pattern of effect was the same as those seen in non-transduced Panc354 cells (Figure 5.15 and 6.6).

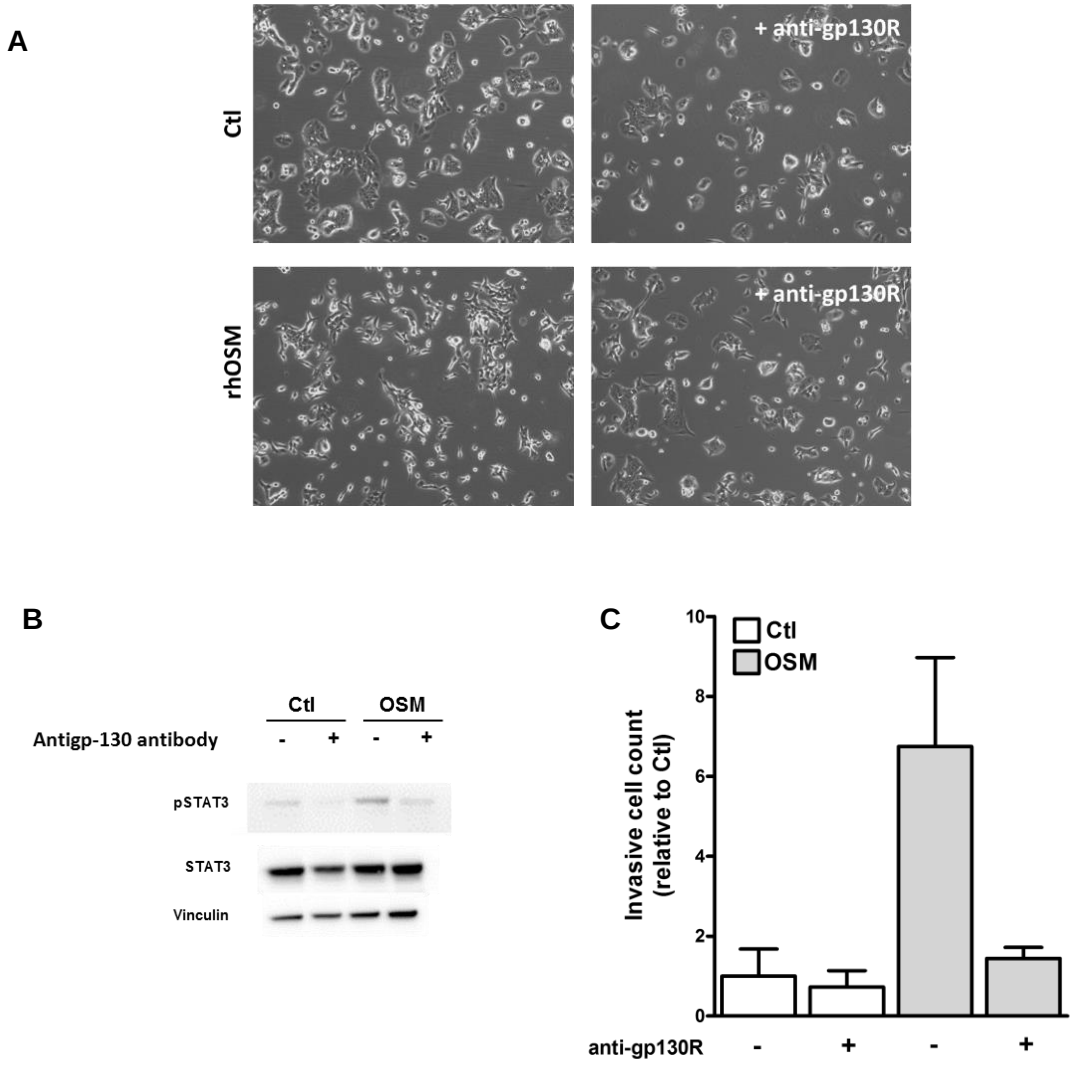


**Figure 6.13 Effects of OSM on Panc354-Luc cells**
A) Brightfield imaging of Pan354-Luc cells treated with OSM 100ng/ml +/- anti-gp130 receptor antibody 2µg/ml B) Western blot of Panc354-Luc cell lysate following treatment with OSM and antibody C) Invasion assay of Panc354-Luc cells treated with OSM and antibody inhibitors (n=1). Results represent mean cell count per image taken +/-SD.

Having confirmed OSM and inhibitory antibody effects were applicable in Panc354-Luc, further *in vivo* metastases experiments were next performed with OSM pre-treated cells. For *in vivo* experiment 'B', Panc354-Luc cells were injected to nude mice. In addition to the different mouse model used, fewer cells were injected in this experiment (50,000) compared to experiment 'A', in an attempt to avoid 'saturation' of the system in the control conditions, as 3/5 mice had liver metastases in the control group for experiment 'A'.

After 9 weeks post injection, no macrometastases were noted at the time of animal sacrifice, despite the luciferase detection criteria being met on IVIS imaging as with experiment 'A' (i.e. at least 3 mice detecting $1x10^6$ BLI signal) (Figure 6.14).

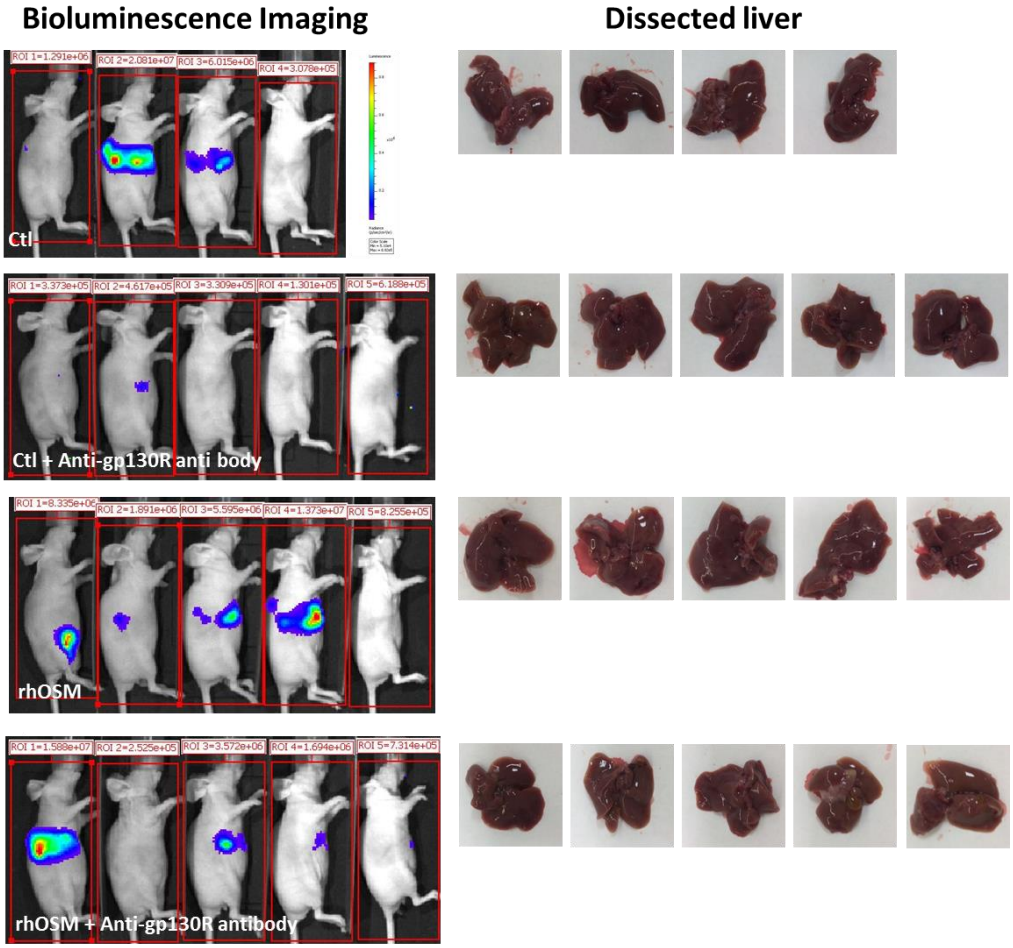


**Figure 6.14 In vivo IVIS bioluminescence imaging and liver images**
IVIS bioluminecsnce imaging of animals at 9 weeks post injection, with corresponding livers dissected the following day.

As macrometastases were not visible, livers were fixed, sectioned and serial slides were stained for CK19, using a human specific antibody, to detect micrometastases (Figure 6.15). Micrometastasis were taken as a colony of cells measuring at least 150μm in maximum diameter.

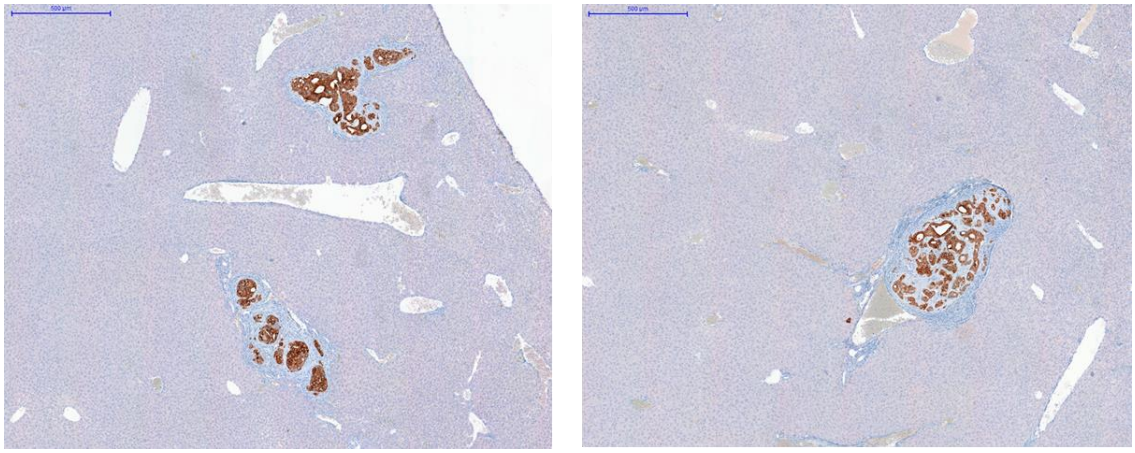

**Figure 6.15 Examples of CK19 positive micrometastases**
Examples of histology from livers sectioned from two mice injected with pre-treated OSM (100ng/ml) Panc354-Luc cells and sacrificed at 9 weeks post injection

Results of micrometastasis analysis showed that all animals in control and OSM groups had liver metastases (Table 6.1). This was unexpected, as control treated cells would not have been 'primed' to undergo EMT and be invasive as with OSM pre-treated cells. However, the antibody treatment had inhibited invasion not only in the OSM pre-treated cells but also in the control group. This finding suggested that the metastases in the control group were being driven downstream of the gp130 receptor. As no direct stimulus was being applied *in vitro* to these cells, one would assume the pathway was therefore being activated *in vivo*.

**Table 6.1 Metastasis results *in vivo***
*In vivo* metastasis results for experiment 'B'

| Pre-treatment | Positive for liver metastasis / total number of mice |
|---|---|
| Control | 4/4 |
| Control + anti-gp130R antibody | 2/5 |
| OSM | 5/5 |
| OSM + anti-gp130R antibody | 3/5 |

Reasons for a lack of visible metastases in experiment 'B' compared to 'A' could have been due to the different animal model used (NSG vs nude mice) or lower number of cells injected. Thus, for experiment 'C', NSG mice were used as per experiment 'A'. Less cells than experiment 'A' (50,000) were injected again to try to minimise the possible 'saturation' in control animals. In this experiment, animals were sacrificed at week 12, when the BLI signal was $>1x10^6$ in at least 2 mice. Visible metastases were counted (Figure 6.16). As with experiment 'A'; in livers with no visible metastases, organs were fixed, sectioned and stained with CK19 antibody. Following this, one additional liver in the OSM group stained for micrometastasis (at least 150μm) that had no visible macrometastases (Figure 6.17 and Table 6.2)

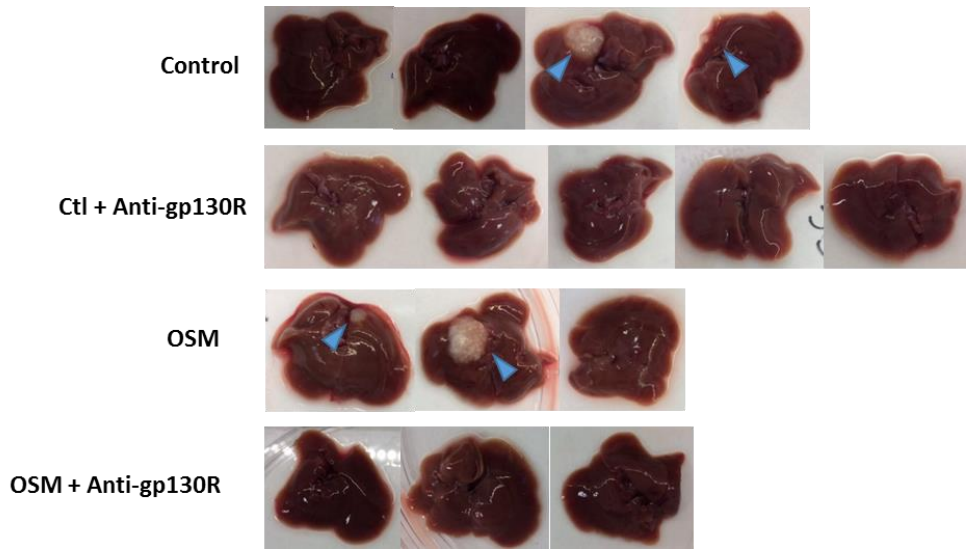


**Figure 6.16 Macrometastasis *in vivo***
Liver macrometastasis experiment 'C' following intrasplenic injection of 50,000 Panc354-Luc cells pre-treated with control, OSM (100ng/ml) +/- antigp130 receptor antibody (2μg/ml) for 48hrs *in vitro*. Animals were sacrificed and livers imaged 12 weeks post injection.

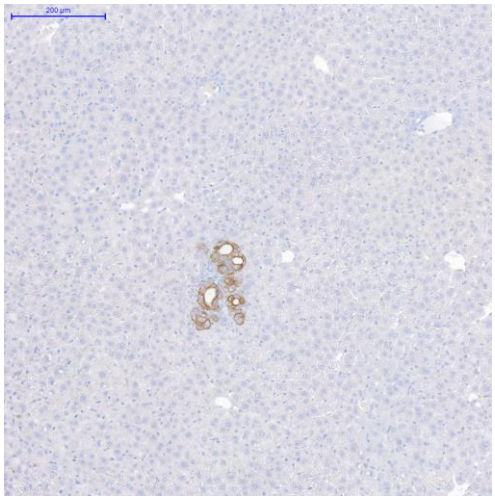

**Figure 6.17 CK19 positive micrometastases *in vivo***
Micrometastases detected through CK19 staining of serial sections in OSM pre-treated Panc354-Luc injected mouse liver negative for macrometastasis in experiment 'C'

In this third *in vivo* experiment, control cells still induced liver metastases in 2/4 mice despite less cells injected. Anti-gp130 receptor antibody again inhibited metastases formation as seen in experiment 'B', in both the control and treatment groups. OSM induced metastases in all mice (Table 6.2).

**Table 6.2 Metastasis results *in vivo***
*In vivo* metastasis results for experiment 'C'

| Pre-treatment | Positive for liver metastases / total number of mice |
|---|---|
| Control | 2/4 |
| Control + anti-gp130R antibody | 0/5 |
| OSM | 3/3 |
| OSM + anti-gp130R antibody | 0/3 |

Therefore, *in vivo* data using antibody against the gp130 receptor demonstrated a trend for a decrease in the number of mice with liver metastasis across the two models used. These data would require further experiments to be performed (in NSG mice using 50,000 cells per injection as per experiment 'C') to prove significant differences with gp130 receptor antibody treated cell conditions.

## 6.3 Discussion

The first aim of this chapter was to determine the clinical relevance of the OSM/ OSMR/ STAT3 pathway in patient samples. Analysis of the TCGA database revealed OSMR gene expression to be prognostic for poor outcome, particularly in early stage disease. This finding supports our *in vitro* data, demonstrating OSMR expression to correlate with a more pro-tumourigenic phenotype. As macrophages induce OSMR expression, and the presence of macrophages in patient tissue confers with worse patient outcome (Ino et al. 2013; Kurahara et al. 2013), this result could be extrapolated and one could speculate that higher presence of OSMR in PDAC tissue relates to a more aggressive disease.

Expression of OSM cytokine in circulation was next investigated in relation to disease. There was no correlation between levels of the cytokine in patient serum and disease status. This could have been due to technical reasons and lack of screening of 'healthy' controls for inflammatory conditions as discussed. As this thesis is investigating the effects of OSM on PDAC cells in the primary tumour tissue, staining of primary tumour was of more relevance. Unfortunately, staining of OSM and Zeb1 could not be optimised therefore a direct correlation between OSM, and the activated phenotype of interest in PDAC cells could not be determined. IHC analysis of PDAC TMAs did however establish an association between the presence of OSMR on malignant cells and pSTAT3 nuclear expression, supporting the hypothesis that upstream activation of pSTAT3 is through OSMR.

The next aim of this chapter was to test inhibitors of OSM/ OSMR/ STAT3 pathway. Inhibition of the pathway was achieved using an OSM neutralising antibody, an antibody against the gp130 receptor or the JAK-STAT inhibitor ruxolitinib, and was confirmed in each cell type by blotting for pSTAT3 in MCM treated cells *in vitro*, but further experiments would be required to ensure consistent and significant reduction. Use of these inhibitors was also found to reduce levels of PDL-1 expression in the presence of OSM and MCM. This finding is supported by *in vivo* studies in transgenic mice by Lu *et al.* whereby ruxolitinib led to more cytotoxic T cell infiltration of mouse tumours and improved the efficacy of anti-PD-1 antibody treatment (Lu et al. 2017). These *in vivo* data can now be explained by our findings that ruxolitinib treatment

leads to less PDL-1 expression on tumour cells *in vitro*. Pathway inhibitors also showed a trend for decreased invasion when tested *in vitro* when tested in each cell type (n=2), and inhibition with gp130 receptor antibody was the most consistent, but further repeats would be required to determine significance. This co-receptor is shared with other gp130 family cytokines, therefore one could argue that in the presence of MCM the effects of this antibody may not be attributed to the effect of OSM alone and thus stronger inhibition could have occurred leading to significance over other inhibitors. However, OSMR was the most highly expressed gp130 co-receptor at baseline in PDAC and the most potent activator of STAT3 compared to IL6R and LIFR, therefore one would expect that the inhibitory effects of anti-gp130R would act predominantly on OSMR activation compared to the other gp130 family cytokine receptors, and thus inhibition of these receptors influencing the results would be less important.

Panc354 cells pre-treated with OSM and anti-gp130 receptor antibody *in vitro* formed the less liver metastasis when injected *in vivo* in metastasis assay, but this would have to be definitively proven with further animal experiments. Interestingly, experiments testing the effects of this inhibitor demonstrated a large percentage of treated animals developed liver metastases even in the control groups. This had also been noted in first *in vivo* experiment 'A', in which 60% of animals in control group were positive for liver metastasis. The number of cells injected had been adjusted accordingly for subsequent experiments, however this did not appear to influence the result. This finding was unexpected, as cells injected in these control animals had not been preconditioned with factors that had not driven the process of EMT or invasion *in vitro* downstream of the gp130 receptor. Because antibody blockade in this control group led to decreased metastases forming in both animal models, it was hypothesised that the driving effect of metastasis formation therefore would have occurred *in vivo*. This can be explained by previous studies comparing tumour cells grown *in vitro* to those *in vivo* in which increased expression of genes that play a role in metastasis formation, such cell adhesion molecules and cytokines, occur *in vivo* and not *in vitro* (Creighton et al. 2003). Therefore, in animal experiments performed in this thesis, metastasis formation in the control groups could reflect non-specific pathway activation, coming from signalling from the environment for example, resulting in tumour cell dissemination that is otherwise not present *in vitro*.

Inhibitory agents against the OSM/ OSMR/ pSTAT3 pathway already exist in the clinic: ruxolitinib is currently approved for use in myeloproliferative disease (Harrison et al. 2017; Mesa et al. 2013). In PDAC, an interim analysis of phase II trial data comparing ruxolitinib plus the oral chemotherapy agent capecitabine versus capecitabine alone in refractory metastatic disease showed promise in patients with a high C-reactive protein (CRP), demonstrating better OS and PFS with combination treatment (Hurwitz et al. 2015). As CRP is a surrogate marker for systemic inflammation, this finding would support inflammatory STAT3 driven progression in PDAC. However, recruitment to the phase III trial of ruxolitinib in combination with capecitabine in metastatic PDAC patients (JANUS-2: NCT02119663) was discontinued due to an apparent lack of efficacy. Nonetheless, other agents against STAT3 are currently in testing for PDAC, for example napabucasin (BBI608). This oral agent is designed to inhibit STAT3 and is believed to specifically target cancer stemness pathways. Phase 1b/II testing in metastatic PDAC patients has shown promise, with one patient undergoing a completed response (2%) and 26 patients (43%) having partial response (Bekaii-Saab 2017). A phase III trial will conclude efficacy in combination with nab-paclitaxel plus gemcitabine in patients with metastatic pancreatic cancer (NCT02993731). Ongoing development and application of STAT3 agents in PDAC support our findings that this pathway plays an important role in tumour progression. In addition, findings from this thesis provide a mechanistic reason as to why this may be an effective therapeutic strategy.

An alternative therapeutic approach to target the OSM/ OSMR/ STAT3 pathway would be through targeting OSM. The apparent less consistent inhibitory effect with neutralising anti-OSM across the three cell types tested in this chapter could be due to low binding affinity of neutralising antibody to OSM, or that the concentrations needed for the agent to be effective were not fully optimised. A clinically developed anti-OSM antibody, GSK315234, has been tested in phase II trials in patients with rheumatoid arthritis and was deemed safe (Choy et al. 2013). However, it was noted that the antibody was not very potent, with only moderate binding affinity and rapid off-rate protein carrier effect. A more potent antibody has since been developed (GSK2330811) and is safe in healthy volunteers (Reid J, et al. 2016). A phase I trial of this agent in systemic scleroderma has been completed (NCT02386436) pending report, and a phase II is proposed (NCT03041025). Based on the findings from this

thesis, one could speculate that it would be of interest to apply these anti-OSM antibodies to the malignancy setting, particularly in PDAC.

# 7 CHAPTER SEVEN: DISCUSSION AND CONCLUSIONS

## 7.1 Discussion and Future Work

Pancreatic cancer is considered a highly desmoplastic tumour, composed of tumour and non-malignant cells within an ECM. Due to a current lack of effective treatment strategies, interest is growing in novel therapeutic interventions that target these other tumour components, such as the stromal cells (Carr and Fernandez-Zapico 2016). Tumour-associated macrophages are abundant within the PDAC TME, conferring worse survival outcomes (Ino et al. 2013; Kurahara et al. 2013). In an era of novel immunotherapies, current trials targeting TAMs in cancer have so far been limited and have failed to make real clinical impact. However, by gaining further insight into how TAMs interact with cancer cells to drive tumour progression, novel agents targeting their effects could be developed to produce better clinical efficacy.

Results from this thesis have concluded that interaction with TAMs are vital in malignant progression by driving an epithelial-to-mesenchymal phenotype, promoting invasion and increasing metastasis of primary PDAC cells. This was concluded to be due to the secretion of the gp130 family cytokine OSM. This cytokine activates STAT3 driven pathways in cancer cells that result in a pro-tumourigenic phenotype. Crosstalk between cancer and immune cells are likely to be driving this phenotype, with the PDAC associated cytokine TGFβ1 shown to induce OSM secretion by TAMs (Figure 7.1). Of note, OSM has greater effects in PDAC than other gp130 cytokine family members, such as IL6 and LIF, due to the higher presence of its receptor, OSMR, in cancer cells. For the first time the importance of this receptor has been confirmed in patient samples, whereby patients with higher gene expression had a worse OS on TCGA dataset analysis and expression in the primary tumour was shown to correlate with pSTAT3 expression in cancer cells. A higher expression of OSMR in PDAC CSCs explains the increased potency of MCM and OSM effects in this subpopulation of cells. In turn, OSM increases PDL-1 expression on PDAC, assisting in immune evasion. These two latter effects are likely to aid metastasis formation, as CSCs are believed to be key in dissemination of cancer to form heterogeneous tumours in distant sites (Hermann et al. 2007) and PDL-1 expression would protect cells from immune cell cytotoxicity when travelling away from the protective immunosuppressive PDAC TME.

Inhibition of the OSM/ OSMR/ STAT3 pathway using neutralising antibody against OSM, antibody inhibition of the gp130 co-receptor or by the JAK-STAT small molecule inhibitor ruxolitinib reversed the effects of STAT3 activation, induction of EMT, invasion and upregulation of PDL-1 by MCM and OSM *in vitro*. Confirming systemic effects of this inhibition, PDAC cells treated with anti-gp130 receptor antibody formed less metastasis *in vivo* in two mouse models tested, but further experiments would be needed to determine if this reduction was significant. Thus, preliminary data provided here shows targeting this macrophage driven pathway could have therapeutic potential.

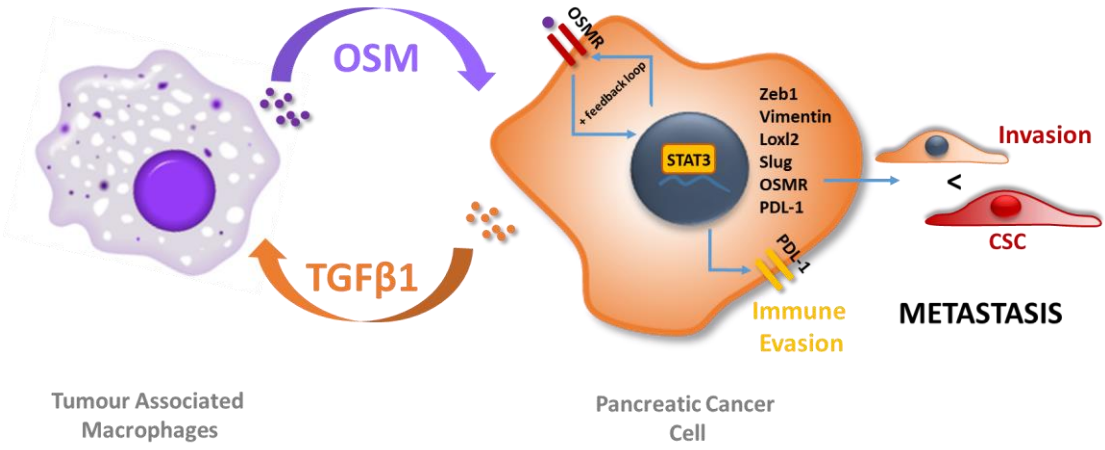


**Figure 7.1 Schematic summary of thesis**

Recent publication supports results that OSM is a key cytokine in driving PDAC tumour progression: Smigiel *et al*. have shown that OSM not only induces mesenchymal transition in PDAC cells, but also a CSC phenotype (Smigiel, Parameswaran, and Jackson 2017). Similar to our findings, authors showed OSM activation of EMT factors (Zeb1 and Snail) and pSTAT3 in PDAC cell lines (HPAC, Panc04.03, 08.13, 05.04). Also, IL6 did not drive pSTAT3 and Zeb1 expression in these PDAC cell lines, once again supporting our data. Using clinical datasets, OSMR expression was shown to be greater in PDAC tissue compared to normal. Converse to our findings however, OSM potentiated the CSC population, with CSCs being defined by expression of CD44. Our results show that stemness genes were not increased following treatment with OSM *in vitro*, but further experiments are required to

determine if there are also effects on CD133+ expression and sphere formation. Different experimental assays were used to determine stemness in Smigiel *et al*. (CD24/CD44 expression and tumourigenicity assay *in vivo*). Authors generated PDAC cells that overexpressed OSM and found they produced larger tumours *in vivo* and that these tumours were more resistant to gemcitabine. In turn, when PDAC cells were co-injected with fibroblasts overexpressing OSM *in vivo*, animals formed more metastasis and had worse survival outcomes. Overall, findings from this study support results presented in this thesis that OSM is a key cytokine in driving PDAC progression and metastasis.

In this thesis, *in vitro* and *in vivo* assays were used to explore the interactions between TAMs and PDAC. However, it should be noted that there are limitations in applying these experimental results to actual PDAC patient tumours due to the complexity of the TME that is difficult to recapitulate through *in vitro* and *in vivo* models. In the first instance, other cytokines are likely to be present within the patient TME that could also be driving EMT and invasion. However, the pleotropic activity of OSM in immune modulation and invasion, particularly on the CSC population, suggest a wide range of effects in driving metastasis formation. In turn, expression of OSMR was shown to have clinical significance. Therefore, the data presented establishes a significant role for OSM amongst the many other cytokines likely to be present in patient tumours, and one would anticipate targeting OSM would be clinically effective as it would inhibit several aspects of PDAC progression that could culminate in improved patient outcome.

Experimental findings of this thesis were based on exploring secreted factors from TAMs. However, in patient tumours cell-cell contact between macrophages and PDAC are likely to be taking place and influencing cell behaviour. This association is important in breast cancer, whereby direct binding of macrophages and CSCs potentiates the CSC niche (Lu et al. 2014). Therefore to confirm findings in more detail, it would be important to extend *in vitro* experiments to incorporate direct co-culture of macrophages and PDAC. This would investigate if juxtacrine signalling effects TAM secretion of OSM, STAT3 pathway activation and OSMR expression on PDAC. For example, this could be done by growing cells in direct co-culture, sorting them and examining gene expression (e.g. testing for OSM in macrophages and EMT

genes in PDAC cells). By performing such experiments, the speculated pathway of interest in the setting of juxtacrine signalling could be confirmed.

It is unlikely that macrophages are the only source of OSM within a patient tumour. Other cells are known to secrete OSM, such as monocytes, T cells and DCs (Richards 2013). In cancer tissue, adipose cells and CAFs have both been shown to secrete OSM in breast and lung cancer respectively (Lapeire et al. 2014; Shien et al. 2017). To determine which cells are secreting the cytokine within PDAC, further staining of TMAs could be performed. Using techniques such as RNA scope, staining of *OSM* mRNA in addition to cell specific antibodies such as *CD3* (T cells), *CD11c* (dendritic cells) and *CD68* (macrophages) could be performed. This would then help determine which stromal cell population is responsible for most OSM secretion within the primary tumour. However, even if it were found that cells other than macrophages are producing OSM, the proposed targeting of the cytokine itself or of STAT3 activation within the malignant cells rather than macrophages directly would still be an effective way to modulate tumour progression.

*In vivo* experiments of pre-treated cells suggest that targeting the OSMR-gp130R heterocomplex could decrease the metastatic effects of OSM. There are no drugs currently designed to directly bind and inhibit the gp130 co-receptor, mainly as complete inhibition could potentially cause severe side effects such as heart attack, coagulation, neuropathy and infection (Xu and Neamati 2013). No clinical agents exist against OSMR either. This receptor is expressed at high levels in normal tissue, including brain and muscle (Figure 7.2), therefore despite OSMR being overexpressed in PDAC tissue compared to normal (Smigiel et al. 2017), there would no doubt be toxicity to other organs following systemic inhibition. In addition, targeting of OSMR would not completely inhibit the STAT3 activation effects of OSM due to its ability to bind to LIFR as well.

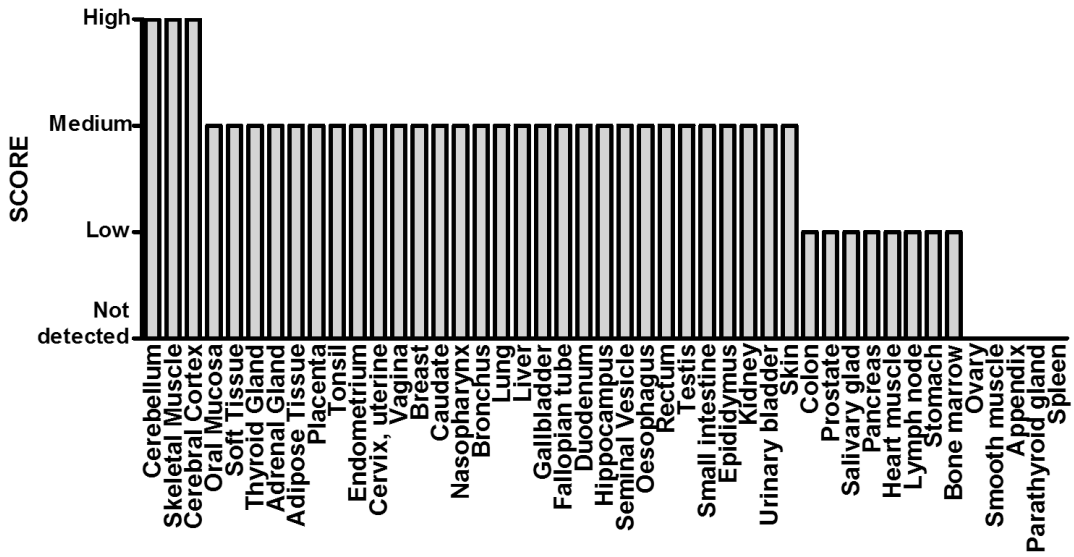


**Figure 7.2 Human Protein Atlas tissue expression of OSMR**
Taken from Human Protein Atlas (http://www.proteinatlas.org) showing protein expression data of OSMR staining for each of the 44 tissues tested.

When exploring other ways to inhibit the OSM/ OSMR/ STAT3 pathway, OSM-/- animals are viable and healthy (Hamada et al. 2007), suggesting that loss of OSM cytokine itself is not embryonically lethal and not vital for normal homeostatic activity. To date, two antibodies against OSM have been designed, GSK315234 and GSK2330811. These agents have already been safely trialled in humans (Choy et al. 2013; Reid J et al. 2016) and are proposed for further testing in inflammatory disorders. Therefore, of the therapeutic strategies suggested for targeting this pathway in cancer, neutralisation of OSM appears to be the most viable in humans. To explore the potential clinical benefits of targeting OSM in PDAC, GSK2330811 (the more potent antibody) would need to be tested in conjunction with chemotherapy *in vivo* and assessed for toxicity, effects on metastatic spread and OS in animals. The preclinical models used to test this hypothesis should ideally be genetically engineered mouse models (GEMMs). This is because *in vivo* data presented thus far has been based on the use of PDX models as an *in vivo* read out of *in vitro* treatment of PDAC primary cultures. Although these PDX models better represent intratumour heterogeneity, cancer genetics and drug responses, they exclude the participation of stromal components in tumour progression, and crucially the effects of the adaptive immune system. Therefore, due the model used, the metastatic assay does not allow

for assessment of T cell effects on disseminating tumour cells in relation to the finding of increased PDL-1 expression following cytokine treatment and do not assess systemic toxic effects of pathway inhibition because the antibody was given only with local injection of tumour cells into the spleen. Using GEMM, such as the KPC mouse model, a better representation of the clinical course of PDAC from early to late stage disease in the context of a 'true' microenvironment could be assessed. Accordingly, complementing our studies using GEMM would provide indication of the effectiveness of anti-OSM antibodies in PDAC and also provide some data on systemic drug toxicity in combination with chemotherapy. The key question that could also be answered by using these models is at what stage would administering OSM treatment be clinically effective. One could argue that early treatment prior to cancer cell dissemination, possibly in the neoadjuvant setting, would be more important in preventing metastatic recurrence. This is also supported by TCGA findings that high OSMR expression leads to worse survival outcome in early stage disease. However, OSM inhibiting agents could also be of interest in 'containing' metastatic disease progression due to its other effects on immune cell evasion and CSCs, which may lead to less metastatic growth and better OS. By following up the *in vivo* investigation of OSM pathway inhibition in both PDX and GEMM, the real benefits of clinical application could be predicted.

## 7.2 Conclusions

In this exciting era of immunotherapy in cancer medicine, novel agents targeting the inflammatory drivers of cancer progression would allow for more effective treatment strategies. Understanding the role of innate immune cells within the TME is now of interest to develop these approaches further. The work presented in this thesis indicates TAMs are driving STAT3 mediated metastatic spread of PDAC through secretion of the inflammatory cytokine, OSM. Further investigation of the clinical relevance of OSM is required, specifically whether blockade of the pleotropic effects of this cytokine inhibits tumour progression and confers with better survival outcomes.

# 8 CHAPTER EIGHT: BIBLOGRAPHY

Adamson, Adewole et al. 2013. “Tissue Inhibitor of Metalloproteinase 1 Is Preferentially Expressed in Th1 and Th17 T-Helper Cell Subsets and Is a Direct Stat Target Gene.” *PLoS ONE* 8(3).

Ahmad, Rehan et al. 2011. “MUC1-C Oncoprotein Promotes STAT3 Activation in an Autoinductive Regulatory Loop.” *Science Signaling* 4(160):ra9.

Ahmed, Simi T. and James E. Darnell. 2009. “Serpin B3/B4, Activated by STAT3, Promote Survival of Squamous Carcinoma Cells.” *Biochemical and Biophysical Research Communications* 378(4):821–25.

Almoguera, Concepcion et al. 1988. “Most Human Carcinomas of the Exocrine Pancreas Contain Mutant c-K-Ras Genes.” *Cell* 53(4):549–54.

Angevin, E. et al. 2014. “A Phase I/II, Multiple-Dose, Dose-Escalation Study of Siltuximab, an Anti-Interleukin-6 Monoclonal Antibody, in Patients with Advanced Solid Tumors.” *Clinical Cancer Research* 20(8):2192–2204.

Argast, Gretchen M. et al. 2011. “Cooperative Signaling between Oncostatin M, Hepatocyte Growth Factor and Transforming Growth Factor-β Enhances Epithelial to Mesenchymal Transition in Lung and Pancreatic Tumor Models.” *Cells Tissues Organs* 193(1–2):114–32.

Assifi, M.Mura et al. 2011. “Neoadjuvant Therapy in Pancreatic Adenocarcinoma: A Meta-Analysis of Phase II Trials.” *Surgery* 150(3):466–73.

Bailey, Peter et al. 2016. “Genomic Analyses Identify Molecular Subtypes of Pancreatic Cancer.” *Nature* 531(7592):47–52.

Balli, David, Andrew J. Rech, Ben Z. Stanger, and Robert H. Vonderheide. 2017. “Immune Cytolytic Activity Stratifies Molecular Subsets of Human Pancreatic Cancer.” *Clinical Cancer Research* 23(12):3129–38.

Bardeesy, Nabeel and Ronald a DePinho. 2002. “Pancreatic Cancer Biology and Genetics.” *Nature Reviews. Cancer* 2(12):897–909.

Barré, Benjamin, Arnaud Vigneron, and Olivier Coqueret. 2005. “The STAT3 Transcription Factor Is a Target for the Myc and Riboblastoma Proteins on the Cdc25A Promoter.” *The Journal of Biological Chemistry* 280(16):15673–81.

Beatty, Gregory L. et al. 2011. “CD40 Agnsts Alter Tumor Stroma and Show Efficacy Against Pancreatic Carcinoma in Mice and Humans.” *Science* 331(May):1612–16.

Beatty, Gregory L. et al. 2013. “A Phase I Study of an Agonist CD40 Monoclonal Antibody (CP-870,893) in Combination with Gemcitabine in Patients with

Advanced Pancreatic Ductal Adenocarcinoma." *Clinical Cancer Research* 19(22):6286–95.

Becker, T. M. et al. 2014. "Mutant B-RAF-Mcl-1 Survival Signaling Depends on the STAT3 Transcription Factor." *Oncogene* 33(9):1158–66.

Bekaii-Saab, Tanios S. 2017. "A Phase Ib/II Study of Cancer Stemness Inhibitor Napabucasin (BBI-608) in Combination with Gemcitabine (Gem) and Nab-Paclitaxel (nabPTX) in Metastatic Pancreatic Adenocarcinoma (mPDAC) Patients (Pts)." *J Clin Oncol* 35((suppl; abstr 4106)).

Bellido, T., C. A. O'Brien, P. K. Roberson, and S. C. Manolagas. 1998. "Transcriptional Activation of the p21(WAF1,CIP1,SDI1) Gene by Interleukin-6 Type Cytokines. A Prerequisite for Their pro- Differentiating and Anti-Apoptotic Effects on Human Osteoblastic Cells." *J Biol Chem* 273(33):21137–44.

Bellmunt, Joaquim et al. 2017. "Pembrolizumab as Second-Line Therapy for Advanced Urothelial Carcinoma." *New England Journal of Medicine* 376(11):1015–26.

Von Bernstorff, Wolfram et al. 2001. "Systemic and Local Immunosuppression in Pancreatic Cancer Patients." *Clinical Cancer Research* 7(11 SUPPL.).

Biankin, Andrew V et al. 2012. "Pancreatic Cancer Genomes Reveal Aberrations in Axon Guidance Pathway Genes." *Nature* 491(7424):399–405.

Bingle, L., N. J. Brown, and C. E. Lewis. 2002. "The Role of Tumour-Associated Macrophages in Tumour Progression: Implications for New Anticancer Therapies." *Journal of Pathology* 196(3):254–65.

Biswas, Subhra K. and Alberto Mantovani. 2010. "Macrophage Plasticity and Interaction with Lymphocyte Subsets : Cancer as a Paradigm." *Nature Immunology* 11(10):889–96.

Bonde, Anne-Katrine, Verena Tischler, Sushil Kumar, Alex Soltermann, and Reto a Schwendener. 2012. "Intratumoral Macrophages Contribute to Epithelial-Mesenchymal Transition in Solid Tumors." *BMC Cancer* 12(1):35.

Borghaei, Hossein et al. 2015. "Nivolumab versus Docetaxel in Advanced Nonsquamous Non–Small-Cell Lung Cancer." *New England Journal of Medicine* 373(17):1627–39.

Bowman, Tammy, Roy Garcia, James Turkson, and Richard Jove. 2000. "STATs in Oncogenesis." *Oncogene* 19(21):2474–88.

Brabletz, T. et al. 2001. "Variable -Catenin Expression in Colorectal Cancers Indicates

Tumor Progression Driven by the Tumor Environment." *Proceedings of the National Academy of Sciences* 98(18):10356–61.

Brahmer, Julie R. et al. 2010. "Phase I Study of Single-Agent Anti-Programmed Death-1 (MDX-1106) in Refractory Solid Tumors: Safety, Clinical Activity, Pharmacodynamics, and Immunologic Correlates." *Journal of Clinical Oncology* 28(19):3167–75.

Brana, Irene et al. 2015. "Carlumab, an Anti-C-C Chemokine Ligand 2 Monoclonal Antibody, in Combination with Four Chemotherapy Regimens for the Treatment of Patients with Solid Tumors: An Open-Label, Multicenter Phase 1b Study." *Targeted Oncology* 10(1):111–23.

Bromberg, Jacqueline. 2002. "Stat Proteins and Oncogenesis." *Journal of Clinical Investigation* 109(9):1139–42.

Bromberg, Jacqueline F. et al. 1999. "Stat3 as an Oncogene." *Cell* 98(3):295–303.

Buettner, Ralf, Linda B. Mora, and Richard Jove. 2002. "Activated STAT Signaling in Human Tumors Provides Novel Molecular Targets for Therapeutic Intervention." *Clinical Cancer Research* 8(4).

Bugno, M. et al. 1995. "Identification of the Interleukin-6/oncostatin M Response Element in the Rat Tissue Inhibitor of Metalloproteinases-1 (TIMP-1) Promoter." *Nucleic Acids Research* 23(24):5041–47.

Burris 3rd, H. A. et al. 1997. "Improvements in Survival and Clinical Benefit with Gemcitabine as First-Line Therapy for Patients with Advanced Pancreas Cancer: A Randomized Trial." *J Clin Oncol* 15(6):2403–13.

Byrne, Katelyn T., Robert H. Vonderheide, Elizabeth M. Jaffee, and Todd D. Armstrong. 2015. "Special Conference on Tumor Immunology and Immunotherapy: A New Chapter." *Cancer Immunology Research* 3(6):590–97.

Cancer Research UK. 2017. "CANCER RESEARCH UK." Retrieved (http://www.cancerresearchuk.org).

Di Caro, Giuseppe et al. 2015. "Dual Prognostic Significance of Tumour-Associated Macrophages in Human Pancreatic Adenocarcinoma Treated or Untreated with Chemotherapy." *Gut* (November 2016):gutjnl-2015-309193.

Carpenter, Richard L. and Hui Wen Lo. 2014. "STAT3 Target Genes Relevant to Human Cancers." *Cancers* 6(2):897–925.

Carr, Ryan M. and Martin E. Fernandez-Zapico. 2016. "Pancreatic Cancer Microenvironment, to Target or Not to Target?" *EMBO Molecular Medicine*

8(2):80–82.

Cassier, Philippe A. et al. 2015. “CSF1R Inhibition with Emactuzumab in Locally Advanced Diffuse-Type Tenosynovial Giant Cell Tumours of the Soft Tissue: A Dose-Escalation and Dose-Expansion Phase 1 Study.” *The Lancet Oncology* 16(8):949–56.

Catanzaro, Joseph M. et al. 2014. “Oncogenic Ras Induces Inflammatory Cytokine Production by Upregulating the Squamous Cell Carcinoma Antigens SerpinB3/B4.” *Nature Communications* 5:3729.

Catlett-Falcone, R. et al. 1999. “Constitutive Activation of Stat3 Signaling Confers Resistance to Apoptosis in Human U266 Myeloma Cells.” *Immunity* 10(1):105–15.

Chen, Jingqi et al. 2011. “CCL18 from Tumor-Associated Macrophages Promotes Breast Cancer Metastasis via PITPNM3.” *Cancer Cell* 19(4):541–55.

Chen, Limo et al. 2014. “Metastasis Is Regulated via microRNA-200/ZEB1 Axis Control of Tumour Cell PD-L1 Expression and Intratumoral Immunosuppression.” *Nature Communications* 5:5241.

Chen, Xue-song et al. 2007. “Diverse Effects of Stat1 on the Regulation of hsp90alpha Gene under Heat Shock.” *Journal of Cellular Biochemistry* 102(4):1059–66.

Cheng, Fengdong et al. 2003. “A Critical Role for Stat3 Signaling in Immune Tolerance.” *Immunity* 19:425–36.

Chin, Y. E. et al. 1996. “Cell Growth Arrest and Induction of Cyclin-Dependent Kinase Inhibitor p21 WAF1/CIP1 Mediated by STAT1.” *Science (New York, N.Y.)* 272(5262):719–22.

Choi, Hye-Jin and Joong-Soo Han. 2012. “Overexpression of Phospholipase D Enhances Bcl-2 Expression by Activating STAT3 through Independent Activation of ERK and p38MAPK in HeLa Cells.” *Biochimica et Biophysica Acta (BBA) - Molecular Cell Research* 1823(6):1082–91.

Choy, Ernest H. et al. 2013. “Safety, Tolerability, Pharmacokinetics and Pharmacodynamics of an Anti- Oncostatin M Monoclonal Antibody in Rheumatoid Arthritis: Results from Phase II Randomized, Placebo-Controlled Trials.” *Arthritis Research & Therapy* 15(5):R132.

Cioffi, Michele et al. 2015. “The miR-17-92 Cluster Counteracts Quiescence and Chemoresistance in a Distinct Subpopulation of Pancreatic Cancer Stem Cells.” *Gut* 64(12):1936–48.

Cioffi, Michele et al. 2017. “The miR-25-93-106b Cluster Regulates Tumor Metastasis and Immune Evasion via Modulation of CXCL12 and PD-L1.” *Oncotarget* 8(13):21609–25.

Ciscato, Francesco et al. 2014. “SERPINB3 Protects from Oxidative Damage by Chemotherapeutics through Inhibition of Mitochondrial Respiratory Complex I.” *Oncotarget* 5(9):2418–27.

Clark, C. E. et al. 2007. “Dynamics of the Immune Reaction to Pancreatic Cancer from Inception to Invasion.” *Cancer Research* 67(19):9518–27.

Clarke, Michael F. et al. 2006. “Cancer Stem Cells - Perspectives on Current Status and Future Directions: AACR Workshop on Cancer Stem Cells.” Pp. 9339–44 in *Cancer Research*, vol. 66.

Collisson, Eric A. et al. 2011. “Subtypes of Pancreatic Ductal Adenocarcinoma and Their Differing Responses to Therapy.” *Nature Medicine* 17(4):500–503.

Colotta, Francesco, Paola Allavena, Antonio Sica, Cecilia Garlanda, and Alberto Mantovani. 2009. “Cancer-Related Inflammation, the Seventh Hallmark of Cancer: Links to Genetic Instability.” *Carcinogenesis* 30(7):1073–81.

Conroy, T. et al. 2011. “FOLFIRINOX versus Gemcitabine for Metastatic Pancreatic Cancer.” *N Engl J Med* 364(19):1817–25.

Corcoran, Ryan B. et al. 2011. “STAT3 Plays a Critical Role in KRAS-Induced Pancreatic Tumorigenesis.” *Cancer Research* 71(14):5020–29.

Coward, J. et al. 2011. “Interleukin-6 as a Therapeutic Target in Human Ovarian Cancer.” *Clinical Cancer Research* 17(18):6083–96.

Craene, Bram De and Geert Berx. 2013. “Regulatory Networks Defining EMT during Cancer Initiation and Progression.” *Nature Reviews Cancer* 13(2):97–110.

Creighton, Chad et al. 2003. “Profiling of Pathway-Specific Changes in Gene Expression Following Growth of Human Cancer Cell Lines Transplanted into Mice.” *Genome Biology* 4(7):R46.

Dejeans, Nicolas, Kim Barroso, Martin E. Fernandez-Zapico, Afshin Samali, and Eric Chevet. 2015. “Novel Roles of the Unfolded Protein Response in the Control of Tumor Development and Aggressiveness.” *Seminars in Cancer Biology* 33:67–73.

Demetri, George D. et al. 2016. “Efficacy and Safety of Trabectedin or Dacarbazine for Metastatic Liposarcoma or Leiomyosarcoma after Failure of Conventional Chemotherapy: Results of a Phase III Randomized Multicenter Clinical Trial.”

*Journal of Clinical Oncology* 34(8):786–93.

Derouet, Damien et al. 2004. "Neuropoietin, a New IL-6-Related Cytokine Signaling through the Ciliary Neurotrophic Factor Receptor." *Proceedings of the National Academy of Sciences of the United States of America* 101(14):4827–32.

Dorff, T. B. et al. 2010. "Clinical and Correlative Results of SWOG S0354: A Phase II Trial of CNTO328 (Siltuximab), a Monoclonal Antibody against Interleukin-6, in Chemotherapy-Pretreated Patients with Castration-Resistant Prostate Cancer." *Clinical Cancer Research* 16(11):3028–34.

Drysdale, B. E., C. M. Zacharchuk, and H. S. Shin. 1983. "Mechanism of Macrophage-Mediated Cytotoxicity: Production of a Soluble Cytotoxic Factor." *The Journal of Immunology* 131(5).

Ducreux, M. et al. 2015. "Cancer of the Pancreas: ESMO Clinical Practice Guidelines for Diagnosis, Treatment and Follow-Up." *Annals of Oncology* 26(5):56–68.

Dyck, Helen G. et al. 1996. "Autonomy of the Epithelial Phenotype in Human Ovarian Surface Epithelium: Changes with Neoplastic Progression and with a Family History of Ovarian Cancer." *International Journal of Cancer* 69(6):429–36.

Eggermont, Alexander M. M. et al. 2015. "Adjuvant Ipilimumab versus Placebo after Complete Resection of High-Risk Stage III Melanoma (EORTC 18071): A Randomised, Double-Blind, Phase 3 Trial." *The Lancet Oncology* 16(5):522–30.

Elson, G. C. et al. 2000. "CLF Associates with CLC to Form a Functional Heteromeric Ligand for the CNTF Receptor Complex." *Nature Neuroscience* 3:867–72.

Epelman, Slava, Kory J. Lavine, and Gwendalyn J. Randolph. 2014. "Origin and Functions of Tissue Macrophages." *Immunity* 41(1):21–35.

Epling-Burnette, P. K. et al. 2001. "Inhibition of STAT3 Signaling Leads to Apoptosis of Leukemic Large Granular Lymphocytes and Decreased Mcl-1 Expression." *Journal of Clinical Investigation* 107(3):351–61.

Evans, R. and P; Alexander. 1970. "Cooperation of Immune Lymphoid Cells with Macrophages in Tumour Immunity." *Nature* 228(24):361–62.

Faris, Jason E. et al. 2013. "FOLFIRINOX in Locally Advanced Pancreatic Cancer: The Massachusetts General Hospital Cancer Center Experience." *The Oncologist* 18(5):543–48.

Fehrenbacher, Louis et al. 2016. "Atezolizumab versus Docetaxel for Patients with Previously Treated Non-Small-Cell Lung Cancer (POPLAR): A Multicentre, Open-Label, Phase 2 Randomised Controlled Trial." *Lancet (London, England)*

387(10030):1837–46.

Feng, Xi et al. 2015. “Loss of CX3CR1 Increases Accumulation of Inflammatory Monocytes and Promotes Gliomagenesis.” *Oncotarget* 6(17):15077–94.

Ferlay, J. et al. 2014. “GLOBOCAN 2012 v1.1, Cancer Incidence and Mortality Worldwide: IARC CancerBase No. 11 [Internet]. Lyon, France: International Agency for Research on Cancer;” Retrieved (http://globocan.iarc.fr).

Fesinmeyer, Megan Dann, Melissa A. Austin, Christopher I. Li, Anneclaire J. De Roos, and Deborah J. Bowen. 2005. “Differences in Survival by Histologic Type of Pancreatic Cancer.” *Cancer Epidemiology and Prevention Biomarkers* 14(7).

Fischer, Richard et al. 2012. “Early Recurrence of Pancreatic Cancer after Resection and during Adjuvant Chemotherapy.” *Saudi Journal of Gastroenterology : Official Journal of the Saudi Gastroenterology Association* 18(2):118–21.

Frank, David A. 2007. “STAT3 as a Central Mediator of Neoplastic Cellular Transformation.” *Cancer Letters* 251(2):199–210.

Fu, Xiu-Tao et al. 2014. “Macrophage-Secreted IL-8 Induces Epithelial-Mesenchymal Transition in Hepatocellular Carcinoma Cells by Activating the JAK2/STAT3/Snail Pathway.” *International Journal of Oncology*.

Gaemers, Ingrid C., Hans L. Vos, Haukeline H. Volders, Sylvia W. Van der Valk, and John Hilkens. 2001. “A STAT-Responsive Element in the Promoter of the Episialin/MUC1 Gene Is Involved in Its Overexpression in Carcinoma Cells.” *Journal of Biological Chemistry* 276(9):6191–99.

Gal, A. et al. 2008. “Sustained TGFβ Exposure Suppresses Smad and Non-Smad Signalling in Mammary Epithelial Cells, Leading to EMT and Inhibition of Growth Arrest and Apoptosis.” *Oncogene* 27(9):1218–30.

Ganesh, Kasturi et al. 2012. “Prostaglandin E2 Induces Oncostatin M Expression in Human Chronic Wound Macrophages through Axl Receptor Tyrosine Kinase Pathway.” *The Journal of Immunology* 189(5).

Garon, Edward B. et al. 2015. “Pembrolizumab for the Treatment of Non–Small-Cell Lung Cancer.” *New England Journal of Medicine* 372(21):2018–28.

Gearing, D. P. et al. 1992. “The IL-6 Signal Transducer, gp130: An Oncostatin M Receptor and Affinity Converter for the LIF Receptor.” *Science (New York, N.Y.)* 255(5050):1434–37.

Germano, Giovanni et al. 2010. “Antitumor and Anti-Inflammatory Effects of Trabectedin on Human Myxoid Liposarcoma Cells.” *Cancer Research*

70(6):2235–44.

Ghebeh, Hazem et al. 2006. “The B7-H1 (PD-L1) T Lymphocyte-Inhibitory Molecule Is Expressed in Breast Cancer Patients with Infiltrating Ductal Carcinoma: Correlation with Important High-Risk Prognostic Factors.” *Neoplasia* 8(3):190–98.

Gillen, Sonja, Tibor Schuster, Christian Meyer zum Büschenfelde, Helmut Friess, and Jörg Kleeff. 2010. “Preoperative/Neoadjuvant Therapy in Pancreatic Cancer: A Systematic Review and Meta-Analysis of Response and Resection Percentages” edited by C. Seiler. *PLoS Medicine* 7(4):e1000267.

Gillet, J. P. et al. 2011. “Redefining the Relevance of Established Cancer Cell Lines to the Study of Mechanisms of Clinical Anti-Cancer Drug Resistance.” *Proceedings of the National Academy of Sciences* 108(46):18708–13.

Giraud, Sandrine et al. 2002. “Functional Interaction of STAT3 Transcription Factor with the Coactivator NcoA/SRC1a.” *Journal of Biological Chemistry* 277(10):8004–11.

Glass, George, Jason A. Papin, and James W. Mandell. 2009. “SIMPLE: A Sequential Immunoperoxidase Labeling and Erasing Method.” *The Journal of Histochemistry and Cytochemistry : Official Journal of the Histochemistry Society* 57(10):899–905.

Godinho, Susana A. et al. 2014. “Oncogene-like Induction of Cellular Invasion from Centrosome Amplification.” *Nature* 510(7503):167–71.

Gordon, Siamon and Fernando O. Martinez. 2010. “Alternative Activation of Macrophages: Mechanism and Functions.” *Immunity* 32(5):593–604.

Gordon, Siamon and Philip R. Taylor. 2005. “Monocyte and Macrophage Heterogeneity.” *Nature Reviews. Immunology* 5(12):953–64.

Greaves, Paul et al. 2013. “Expression of FOXP3, CD68, and CD20 at Diagnosis in the Microenvironment of Classical Hodgkin Lymphoma Is Predictive of Outcome.” *Journal of Clinical Oncology : Official Journal of the American Society of Clinical Oncology* 31(2):256–62.

Gritsko, Tanya et al. 2006. “Persistent Activation of Stat3 Signaling Induces Survivin Gene Expression and Confers Resistance to Apoptosis in Human Breast Cancer Cells.” *Clinical Cancer Research* 12(1):11–19.

Guerra, Carmen et al. 2007. “Chronic Pancreatitis Is Essential for Induction of Pancreatic Ductal Adenocarcinoma by K-Ras Oncogenes in Adult Mice.” *Cancer Cell* 11(3):291–302.

Guo, L. et al. 2013. “Stat3-Coordinated Lin-28–let-7–HMGA2 and miR-200–ZEB1 Circuits Initiate and Maintain Oncostatin M-Driven Epithelial–mesenchymal Transition.” *Oncogene* 32(45):5272–82.

Gupta, Piyush B. et al. 2009. “Identification of Selective Inhibitors of Cancer Stem Cells by High-Throughput Screening.” *Cell* 138(4):645–59.

Halama, Niels et al. 2016. “Tumoral Immune Cell Exploitation in Colorectal Cancer Metastases Can Be Targeted Effectively by Anti-CCR5 Therapy in Cancer Patients.” *Cancer Cell* 29(4):587–601.

Hamada, Tetsuhiro et al. 2007. “Oncostatin M Gene Therapy Attenuates Liver Damage Induced by Dimethylnitrosamine in Rats.” *The American Journal of Pathology* 171(3):872–81.

Hamanishi, J. et al. 2007. “Programmed Cell Death 1 Ligand 1 and Tumor-Infiltrating CD8+ T Lymphocytes Are Prognostic Factors of Human Ovarian Cancer.” *Proceedings of the National Academy of Sciences* 104(9):3360–65.

Hamid, Omid et al. 2013. “Safety and Tumor Responses with Lambrolizumab (Anti–PD-1) in Melanoma.” *New England Journal of Medicine* 369(2):134–44.

Hamilton, Kathryn E., James G. Simmons, Shengli Ding, Laurianne Van Landeghem, and P.Kay Lund. 2011. “Cytokine Induction of Tumor Necrosis Factor Receptor 2 Is Mediated by STAT3 in Colon Cancer Cells.” *Molecular Cancer Research : MCR* 9(12):1718–31.

Han, Woody, Richard L. Carpenter, Xinyu Cao, and Hui Wen Lo. 2013. “STAT1 Gene Expression Is Enhanced by Nuclear EGFR and HER2 via Cooperation With STAT3.” *Molecular Carcinogenesis* 52(12):959–69.

Hanahan, Douglas and Robert A. Weinberg. 2011. “Hallmarks of Cancer: The next Generation.” *Cell* 144(5):646–74.

Harrison, C. N. et al. 2017. “Long-Term Findings from COMFORT-II, a Phase 3 Study of Ruxolitinib vs Best Available Therapy for Myelofibrosis.” *Leukemia* 31(3):775–775.

Harrison, M. L. et al. 2007. “Tumor Necrosis Factor Alpha as a New Target for Renal Cell Carcinoma: Two Sequential Phase II Trials of Infliximab at Standard and High Dose.” *J Clin Oncol* 25(29):4542–49.

Heery, Christopher R. et al. 2017. “Avelumab for Metastatic or Locally Advanced Previously Treated Solid Tumours (JAVELIN Solid Tumor): A Phase 1a, Multicohort, Dose-Escalation Trial.” *The Lancet Oncology* 18(5):587–98.

Heinrich, Peter C. et al. 2003. “Principles of Interleukin (IL)-6-Type Cytokine Signalling and Its Regulation.” *The Biochemical Journal* 374(Pt 1):1–20.

Helm, Ole et al. 2014. “Tumor-Associated Macrophages Exhibit pro- and Anti-Inflammatory Properties by Which They Impact on Pancreatic Tumorigenesis.” *International Journal of Cancer* 135(4):843–61.

Herbst, Roy S. et al. 2014. “Predictive Correlates of Response to the Anti-PD-L1 Antibody MPDL3280A in Cancer Patients.” *Nature* 515(7528):563–67.

Hermann, Patrick C. et al. 2007. “Distinct Populations of Cancer Stem Cells Determine Tumor Growth and Metastatic Activity in Human Pancreatic Cancer.” *Cell Stem Cell* 1(3):313–23.

Hidalgo, Manuel et al. 2014. “Patient-Derived Xenograft Models: An Emerging Platform for Translational Cancer Research.” *Cancer Discovery*.

Hino, Ryosuke et al. 2010. “Tumor Cell Expression of Programmed Cell Death-1 Ligand 1 Is a Prognostic Factor for Malignant Melanoma.” *Cancer* 116(7):1757–66.

Hirai, Mariko et al. 2017. “Regulation of PD-L1 Expression in a High-Grade Invasive Human Oral Squamous Cell Carcinoma Microenvironment.” *International Journal of Oncology* 50(1):41–48.

Hirakawa, Hiroshi et al. 2004. “Regulation of Squamous Cell Carcinoma Antigen Production by E-Cadherin Mediated Cell-Cell Adhesion in Squamous Cell Carcinoma Cell Line.” *Oncology Reports* 11(2):415–19.

Hodi, F.Stephen et al. 2010. “Improved Survival with Ipilimumab in Patients with Metastatic Melanoma.” *New England Journal of Medicine* 363(8):711–23.

Von Hoff, Daniel D. et al. 2013. “Increased Survival in Pancreatic Cancer with Nab-Paclitaxel plus Gemcitabine.” *The New England Journal of Medicine* 369(18):1691–1703.

Hong, David S. et al. 2014. “MABp1, a First-in-Class True Human Antibody Targeting Interleukin-1α in Refractory Cancers: An Open-Label, Phase 1 Dose-Escalation and Expansion Study.” *The Lancet. Oncology* 15(6):656–66.

Huang, Suyun. 2007. “Regulation of Metastases by Signal Transducer and Activator of Transcription 3 Signaling Pathway: Clinical Implications.” *Clinical Cancer Research* 13(5).

Hudes, Gary et al. 2013. “A Phase 1 Study of a Chimeric Monoclonal Antibody against Interleukin-6, Siltuximab, Combined with Docetaxel in Patients with

Metastatic Castration-Resistant Prostate Cancer." *Investigational New Drugs* 31(3):669–76.

Hung, W. and B. Elliott. 2001. "Co-Operative Effect of c-Src Tyrosine Kinase and Stat3 in Activation of Hepatocyte Growth Factor Expression in Mammary Carcinoma Cells." *The Journal of Biological Chemistry* 276(15):12395–403.

Hurwitz, Herbert I. et al. 2015. "Randomized, Double-Blind, Phase II Study of Ruxolitinib or Placebo in Combination With Capecitabine in Patients With Metastatic Pancreatic Cancer for Whom Therapy With Gemcitabine Has Failed." *Journal of Clinical Oncology* 33(34):4039–47.

Iacobuzio-Donahue, Christine A. et al. 2009. "DPC4 Gene Status of the Primary Carcinoma Correlates With Patterns of Failure in Patients With Pancreatic Cancer." *Journal of Clinical Oncology* 27(11):1806–13.

Ino, Y. et al. 2013. "Immune Cell Infiltration as an Indicator of the Immune Microenvironment of Pancreatic Cancer." *British Journal of Cancer* 108(4):914–23.

Ip, Nancy Y. et al. 1992. "CNTF and LIF Act on Neuronal Cells via Shared Signaling Pathways That Involve the IL-6 Signal Transducing Receptor Component gp130." *Cell* 69(7):1121–32.

Itoh, M. et al. 2006. "Requirement of STAT3 Activation for Maximal Collagenase-1 (MMP-1) Induction by Epidermal Growth Factor and Malignant Characteristics in T24 Bladder Cancer Cells." *Oncogene* 25(8):1195–1204.

Iwasaki, Masahiro et al. 2004. "E1AF/PEA3 Reduces the Invasiveness of SiHa Cervical Cancer Cells by Activating Serine Proteinase Inhibitor Squamous Cell Carcinoma Antigen." *Experimental Cell Research* 299(2):525–32.

Jiang, Jian, Ya-ling Tang, and Xin-hua Liang. 2011. "EMT: A New Vision of Hypoxia Promoting Cancer Progression." *Cancer Biology & Therapy* 11(8):714–23.

Jones, Siân et al. 2008. "Core Signaling Pathways in Human Pancreatic Cancers Revealed by Global Genomic Analyses." *Science* 321(5897).

Jung, M. et al. 2012. "Interleukin-10-Induced Neutrophil Gelatinase-Associated Lipocalin Production in Macrophages with Consequences for Tumor Growth." *Molecular and Cellular Biology* 32(19):3938–48.

Kalluri, Raghu and Robert A. Weinberg. 2009. "The Basics of Epithelial-Mesenchymal Transition." *The Journal of Clinical Investigation* 119(6):1420–28.

Katagiri, Chika, Jotaro Nakanishi, Kuniko Kadoya, and Toshihiko Hibino. 2006.

"Serpin Squamous Cell Carcinoma Antigen Inhibits UV-Induced Apoptosis via Suppression of c-JUN NH2-Terminal Kinase." *Journal of Cell Biology* 172(7):983–90.

Kato, H. and T. Torigoe. 1977. "Radioimmunoassay for Tumor Antigen of Human Cervical Squamous Cell Carcinoma." *Cancer* 40(4):1621–28.

Kesanakurti, D., C. Chetty, D. Rajasekhar Maddirela, M. Gujrati, and J. S. Rao. 2013. "Essential Role of Cooperative NF-κB and Stat3 Recruitment to ICAM-1 Intronic Consensus Elements in the Regulation of Radiation-Induced Invasion and Migration in Glioma." *Oncogene* 32(43):5144–55.

Kiuchi, N. et al. 1999. "STAT3 Is Required for the gp130-Mediated Full Activation of the c-Myc Gene." *The Journal of Experimental Medicine* 189(1):63–73.

Klausen, Pia, Lone Pedersen, Jesper Jurlander, and Heinz Baumann. 2000. "Oncostatin M and Interleukin 6 Inhibit Cell Cycle Progression by Prevention of p27kip1 Degradation in HepG2 Cells." *Oncogene* 19(32):3675–83.

Kleeff, Jorg et al. 2016. "Pancreatic Cancer." *Nature Reviews Disease Primers* 2:16022.

Kondo, A. et al. 2010. "Interferon- and Tumor Necrosis Factor- Induce an Immunoinhibitory Molecule, B7-H1, via Nuclear Factor- B Activation in Blasts in Myelodysplastic Syndromes." *Blood* 116(7):1124–31.

Krebs, Angela M. et al. 2017. "The EMT-Activator Zeb1 Is a Key Factor for Cell Plasticity and Promotes Metastasis in Pancreatic Cancer." *Nature Cell Biology* 19(5):518–29.

Kreso, Antonija and John E. Dick. 2014. "Evolution of the Cancer Stem Cell Model." *Cell Stem Cell* 14(3):275–91.

Kryczek, I. et al. 2007. "Relationship between B7-H4, Regulatory T Cells, and Patient Outcome in Human Ovarian Carcinoma." *Cancer Research* 67(18):8900–8905.

Kryczek, Ilona et al. 2006. "B7-H4 Expression Identifies a Novel Suppressive Macrophage Population in Human Ovarian Carcinoma." *The Journal of Experimental Medicine* 203(4):871–81.

Kuang, Dong-Ming et al. 2009. "Activated Monocytes in Peritumoral Stroma of Hepatocellular Carcinoma Foster Immune Privilege and Disease Progression through PD-L1." *The Journal of Experimental Medicine* 206(6):1327–37.

Kucia-Tran, Justyna A. et al. 2016. "Overexpression of the Oncostatin-M Receptor in Cervical Squamous Cell Carcinoma Is Associated with Epithelial–mesenchymal

Transition and Poor Overall Survival." *British Journal of Cancer* 115(2):212–22.

Kurahara, Hiroshi et al. 2013. "M2-Polarized Tumor-Associated Macrophage Infiltration of Regional Lymph Nodes Is Associated with Nodal Lymphangiogenesis and Occult Nodal Involvement in pN0 Pancreatic Cancer." *Pancreas* 42(1):155–59.

Kurzrock, R. et al. 2013. "A Phase I, Open-Label Study of Siltuximab, an Anti-IL-6 Monoclonal Antibody, in Patients with B-Cell Non-Hodgkin Lymphoma, Multiple Myeloma, or Castleman Disease." *Clinical Cancer Research* 19(13):3659–70.

Kusaba, Hitoshi et al. 2005. "Interleukin-12-Induced Interferon-Gamma Production by Human Peripheral Blood T Cells Is Regulated by Mammalian Target of Rapamycin (mTOR)." *The Journal of Biological Chemistry* 280(2):1037–43.

Lapeire, Lore et al. 2014. "Cancer-Associated Adipose Tissue Promotes Breast Cancer Progression by Paracrine Oncostatin M and Jak/STAT3 Signaling." *Cancer Research* 74(23).

Larkin, J. M. G. et al. 2010. "A Phase I/II Trial of Sorafenib and Infliximab in Advanced Renal Cell Carcinoma." *British Journal of Cancer* 103(8):1149–53.

Larkin, James et al. 2015. "Combined Nivolumab and Ipilimumab or Monotherapy in Untreated Melanoma." *New England Journal of Medicine* 373(1):23–34.

Lesina, Marina et al. 2011. "Stat3/Socs3 Activation by IL-6 Transsignaling Promotes Progression of Pancreatic Intraepithelial Neoplasia and Development of Pancreatic Cancer." *Cancer Cell* 19(4):456–69.

Leslie, Kenneth et al. 2006. "Cyclin D1 Is Transcriptionally Regulated by and Required for Transformation by Activated Signal Transducer and Activator of Transcription 3." *Cancer Research* 66(5):2544–52.

Li, D. H., K. P. Xie, R. Wolff, and J. L. Abbruzzese. 2004. "Pancreatic Cancer." *Lancet* 363:1049–57.

Liang, Chun-Chi, Ann Y. Park, and Jun-Lin Guan. 2007. "In Vitro Scratch Assay: A Convenient and Inexpensive Method for Analysis of Cell Migration in Vitro." *Nature Protocols* 2(2):329–33.

Lin, E. Y. et al. 2006. "Macrophages Regulate the Angiogenic Switch in a Mouse Model of Breast Cancer." *Cancer Research* 66(23):11238–46.

Lin, E. Y., A. V Nguyen, R. G. Russell, and J. W. Pollard. 2001. "Colony-Stimulating Factor 1 Promotes Progression of Mammary Tumors to Malignancy." *The*

*Journal of Experimental Medicine* 193(6):727–40.

Lin, Elaine Y. et al. 2007. "Vascular Endothelial Growth Factor Restores Delayed Tumor Progression in Tumors Depleted of Macrophages." *Molecular Oncology* 1(3):288–302.

Liu, Bingyan et al. 2016. "Tumor-Associated Macrophage-Derived CCL20 Enhances the Growth and Metastasis of Pancreatic Cancer." *Acta Biochimica et Biophysica Sinica* 48(12):1067–74.

Liu, Chao-Ying et al. 2013. "M2-Polarized Tumor-Associated Macrophages Promoted Epithelial–mesenchymal Transition in Pancreatic Cancer Cells, Partially through TLR4/IL-10 Signaling Pathway." *Laboratory Investigation* 93(7):844–54.

Liu, Mingli, Nana O. Wilson, Jacqueline M. Hibbert, and Jonathan K. Stiles. 2013. "STAT3 Regulates MMP3 in Heme-Induced Endothelial Cell Apoptosis." *PLoS ONE* 8(8).

Lo, H. W. et al. 2007. "Epidermal Growth Factor Receptor Cooperates with Signal Transducer and Activator of Transcription 3 to Induce Epithelial-Mesenchymal Transition in Cancer Cells via up-Regulation of TWIST Gene Expression." *Cancer Research* 67(19):9066–76.

Lo, Hui-Wen, Xinyu Cao, Hu Zhu, and Francis Ali-Osman. 2010. "Cyclooxygenase-2 Is a Novel Transcriptional Target of the Nuclear EGFR-STAT3 and EGFRvIII-STAT3 Signaling Axes." *Molecular Cancer Research : MCR* 8(2):232–45.

Lo, Hui Wen et al. 2005. "Nuclear Interaction of EGFR and STAT3 in the Activation of the iNOS/NO Pathway." *Cancer Cell* 7(6):575–89.

Lu, Chunwan, Asif Talukder, Natasha M. Savage, Nagendra Singh, and Kebin Liu. 2017. "JAK-STAT-Mediated Chronic Inflammation Impairs Cytotoxic T Lymphocyte Activation to Decrease Anti-PD-1 Immunotherapy Efficacy in Pancreatic Cancer." *OncoImmunology* 6(3):e1291106.

Lu, Haihui et al. 2014. "A Breast Cancer Stem Cell Niche Supported by Juxtacrine Signalling from Monocytes and Macrophages." *Nature Cell Biology* 16(11):1105–17.

Lust, J. A. et al. 1992. "Isolation of an mRNA Encoding a Soluble Form of the Human Interleukin-6 Receptor." *Cytokine* 4(2):96–100.

Madamanchi, N. R., S. Li, C. Patterson, and M. S. Runge. 2001. "Thrombin Regulates Vascular Smooth Muscle Cell Growth and Heat Shock Proteins via the JAK-STAT Pathway." *The Journal of Biological Chemistry* 276(22):18915–24.

Madhusudan, Srinivasan et al. 2004. "A Phase II Study of Etanercept (Enbrel), a Tumor Necrosis Factor Alpha Inhibitor in Patients with Metastatic Breast Cancer." *Clinical Cancer Research : An Official Journal of the American Association for Cancer Research* 10(19):6528–34.

Madhusudan, Srinivasan et al. 2005. "Study of Etanercept, a Tumor Necrosis Factor-Alpha Inhibitor, in Recurrent Ovarian Cancer." *Journal of Clinical Oncology : Official Journal of the American Society of Clinical Oncology* 23(25):5950–59.

Malka, D. et al. 2002. "Risk of Pancreatic Adenocarcinoma in Chronic Pancreatitis." *Gut* 51(6):849–52.

Mani, Sendurai A. et al. 2008. "The Epithelial-Mesenchymal Transition Generates Cells with Properties of Stem Cells." *Cell* 133(4):704–15.

Mantovani, Alberto et al. 1979. "Effects on in Vitro Tumor Growth of Macrophages Isolated from Human Ascitic Ovarian Tumors." *International Journal of Cancer* 23(2):157–64.

Mantovani, Alberto et al. 2008. "Cancer-Related Inflammation." *Nature* 454(7203):436–44.

Mantovani, Alberto, Federica Marchesi, Alberto Malesci, Luigi Laghi, and Paola Allavena. 2017. "Tumour-Associated Macrophages as Treatment Targets in Oncology." *Nature Reviews Clinical Oncology*.

Martinez, Fernando O. and Siamon Gordon. 2014. "The M1 and M2 Paradigm of Macrophage Activation: Time for Reassessment." *F1000Prime Reports* 6.

Marzec, M. et al. 2008. "Oncogenic Kinase NPM/ALK Induces through STAT3 Expression of Immunosuppressive Protein CD274 (PD-L1, B7-H1)." *Proceedings of the National Academy of Sciences* 105(52):20852–57.

Massagu, Joan. 2008. "TGFbeta in Cancer." *Cell* 134(2):215–30.

McWhorter, F. Y., T. Wang, P. Nguyen, T. Chung, and W. F. Liu. 2013. "Modulation of Macrophage Phenotype by Cell Shape." *Proceedings of the National Academy of Sciences* 110(43):17253–58.

Medema JP, Vermeulen L. 2011. "Microenvironmental Regulation of Stem Cells in Intestinal Homeostasis and Cancer." *Nature* 474(7351):318–26.

Meng, Fanbin et al. 2015. "CCL18 Promotes Epithelial-Mesenchymal Transition, Invasion and Migration of Pancreatic Cancer Cells in Pancreatic Ductal Adenocarcinoma." *International Journal of Oncology* 46(3):1109–20.

Mesa, Ruben A. et al. 2013. “Effect of Ruxolitinib Therapy on Myelofibrosis-Related Symptoms and Other Patient-Reported Outcomes in COMFORT-I: A Randomized, Double-Blind, Placebo-Controlled Trial.” *Journal of Clinical Oncology* 31(10):1285–92.

Mikiko, Kawata et al. 2012. “TGF-β-Induced Epithelial-Mesenchymal Transition of A549 Lung Adenocarcinoma Cells Is Enhanced by pro-Inflammatory Cytokines Derived from RAW 264.7 Macrophage Cells.” *Journal of Biochemistry*.

Mitchem, Jonathan B. et al. 2013. “Targeting Tumor-Infiltrating Macrophages Decreases Tumor-Initiating Cells, Relieves Immunosuppression, and Improves Chemotherapeutic Responses.” *Cancer Research* 73(3):1128–41.

Moffitt, Richard A. et al. 2015. “Virtual Microdissection Identifies Distinct Tumor- and Stroma-Specific Subtypes of Pancreatic Ductal Adenocarcinoma.” *Nature Genetics* 47(10):1168–78.

Morel, Anne-Pierre et al. 2008. “Generation of Breast Cancer Stem Cells through Epithelial-Mesenchymal Transition.” *PloS One* 3(8):e2888. Retrieved (http://www.pubmedcentral.nih.gov/articlerender.fcgi?artid=2492808&tool=pmcentrez&rendertype=abstract).

Motzer, Robert J. et al. 2015. “Nivolumab versus Everolimus in Advanced Renal-Cell Carcinoma.” *New England Journal of Medicine* 373(19):1803–13.

Mueller, Maria-Theresa et al. 2009. “Combined Targeted Treatment to Eliminate Tumorigenic Cancer Stem Cells in Human Pancreatic Cancer.” *Gastroenterology* 137(3):1102–13.

Mukherjee, Somnath et al. 2013. “Gemcitabine-Based or Capecitabine-Based Chemoradiotherapy for Locally Advanced Pancreatic Cancer (SCALOP): A Multicentre, Randomised, Phase 2 Trial.” *The Lancet Oncology* 14(4):317–26.

Mülberg, Jürgen et al. 1993. “The Soluble Interleukin-6 Receptor Is Generated by Shedding.” *European Journal of Immunology* 23(2):473–80.

Murakami, a et al. 2001. “Squamous Cell Carcinoma Antigen Suppresses Radiation-Induced Cell Death.” *British Journal of Cancer* 84:851–58.

Murray, Peter J. et al. 2014. “Macrophage Activation and Polarization: Nomenclature and Experimental Guidelines.” *Immunity* 41(1):14–20.

Murray, Peter J. and Thomas A. Wynn. 2011. “Protective and Pathogenic Functions of Macrophage Subsets.” *Nature Reviews Immunology* 11(11):723–37.

Naaldijk, Yahaira et al. 2015. “Migrational Changes of Mesenchymal Stem Cells in

Response to Cytokines, Growth Factors, Hypoxia, and Aging." *Experimental Cell Research* 338(1):97–104.

Nakashima, Torahiko et al. 2006. "Role of Squamous Cell Carcinoma Antigen 1 Expression in the Invasive Potential of Head and Neck Squamous Cell Carcinoma." *Head & Neck* 28(1):24–30.

NCCN. 2015. "National Comprehensive Cancer Network. NCCN Guidelines: Pancreatic Adenocarcinoma." Retrieved (http://www.nccn.org.).

Neoptolemos, J. P. et al. 2001. "Adjuvant Chemoradiotherapy and Chemotherapy in Resectable Pancreatic Cancer: A Randomised Controlled Trial." *Lancet (London, England)* 358(9293):1576–85.

Neoptolemos, John P. et al. 2010. "Adjuvant Chemotherapy With Fluorouracil Plus Folinic Acid vs Gemcitabine Following Pancreatic Cancer Resection." *JAMA* 304(10):1073.

Neoptolemos, John P. et al. 2017. "Comparison of Adjuvant Gemcitabine and Capecitabine with Gemcitabine Monotherapy in Patients with Resected Pancreatic Cancer (ESPAC-4): A Multicentre, Open-Label, Randomised, Phase 3 Trial." *The Lancet* 389(10073):1011–24.

Nielsen, Sebastian R. and Michael C. Schmid. 2017. "Macrophages as Key Drivers of Cancer Progression and Metastasis." *Mediators of Inflammation* 2017:1–11.

Niu, Guilian et al. 1999. "Gene Therapy with Dominant-Negative Stat3 Suppresses Growth of the Murine Melanoma B16 Tumor in Vivo." *Cancer Research* 59(20).

Niu, Guilian et al. 2008. "Signal Transducer and Activator of Transcription 3 Is Required for Hypoxia-Inducible Factor-1alpha RNA Expression in Both Tumor Cells and Tumor-Associated Myeloid Cells." *Molecular Cancer Research : MCR* 6(7):1099–1105.

Nomi, T. et al. 2007. "Clinical Significance and Therapeutic Potential of the Programmed Death-1 Ligand/Programmed Death-1 Pathway in Human Pancreatic Cancer." *Clinical Cancer Research* 13(7):2151–57.

Noy, Roy and Jeffrey W. Pollard. 2014. "Tumor-Associated Macrophages: From Mechanisms to Therapy." *Immunity* 41(1):49–61.

Numa, F. et al. 1996. "Tumor Necrosis Factor-Alpha Stimulates the Production of Squamous Cell Carcinoma Antigen in Normal Squamous Cells." *Tumour Biology : The Journal of the International Society for Oncodevelopmental Biology and Medicine* 17(2):97–101.

Nywening, Timothy M. et al. 2016. “Targeting Tumour-Associated Macrophages with CCR2 Inhibition in Combination with FOLFIRINOX in Patients with Borderline Resectable and Locally Advanced Pancreatic Cancer: A Single-Centre, Open-Label, Dose-Finding, Non-Randomised, Phase 1b Trial.” *The Lancet Oncology* 17(5):651–62.

Oettle, H. et al. 2007. “Adjuvantchemo- Therapy with Gemcitabine vs Observation Inpatients Undergoing Curative-Intent Resection of Pancreatic Cancer: A Randomized Controlled Trial.” *JAMA* 297:267–77.

Oettle, Helmut et al. 2013. “Adjuvant Chemotherapy with Gemcitabine and Long-Term Outcomes among Patients with Resected Pancreatic Cancer: The CONKO-001 Randomized Trial.” *JAMA : The Journal of the American Medical Association* 310(14):1473–81.

Ohigashi, Y. et al. 2005. “Clinical Significance of Programmed Death-1 Ligand-1 and Programmed Death-1 Ligand-2 Expression in Human Esophageal Cancer.” *Clinical Cancer Research* 11(8):2947–53.

Ojalvo, Laureen S., William King, Dianne Cox, and Jeffrey W. Pollard. 2009. “High-Density Gene Expression Analysis of Tumor-Associated Macrophages from Mouse Mammary Tumors.” *The American Journal of Pathology* 174(3):1048–64.

Paget, S. 1989. “The Distribution of Secondary Growths in Cancer of the Breast. 1889.” *Cancer Metastasis Reviews* 8(2):98–101.

De Palma, Michele et al. 2005. “Tie2 Identifies a Hematopoietic Lineage of Proangiogenic Monocytes Required for Tumor Vessel Formation and a Mesenchymal Population of Pericyte Progenitors.” *Cancer Cell* 8(3):211–26.

Phillips, Robert A.Kastelein et al. 2004. “WSX-1 and Glycoprotein 130 Constitute a Signal-Transducing Receptor for IL-27.” *J. Immunol* 172:2225–31.

Pienta, Kenneth J. et al. 2013. “Phase 2 Study of Carlumab (CNTO 888), a Human Monoclonal Antibody against CC-Chemokine Ligand 2 (CCL2), in Metastatic Castration-Resistant Prostate Cancer.” *Investigational New Drugs* 31(3):760–68.

Plimack, Elizabeth R. et al. 2017. “Safety and Activity of Pembrolizumab in Patients with Locally Advanced or Metastatic Urothelial Cancer (KEYNOTE-012): A Non-Randomised, Open-Label, Phase 1b Study.” *The Lancet. Oncology* 18(2):212–20.

Postow, Michael A. et al. 2015. “Nivolumab and Ipilimumab versus Ipilimumab in Untreated Melanoma.” *New England Journal of Medicine* 372(21):2006–17.

Powles, Thomas et al. 2014. “MPDL3280A (Anti-PD-L1) Treatment Leads to Clinical

Activity in Metastatic Bladder Cancer." *Nature* 515(7528):558–62.

Quarta, S. et al. 2010. "SERPINB3 Induces Epithelial-Mesenchymal Transition." *The Journal of Pathology* 221(3):343–56.

Rahib, Lola et al. 2014. "Projecting Cancer Incidence and Deaths to 2030: The Unexpected Burden of Thyroid, Liver, and Pancreas Cancers in the United States." *Cancer Research* 74(11):2913–21.

Ranjbar, Benyamin et al. 2016. "Anti-Apoptotic Effects of Lentiviral Vector Transduction Promote Increased Rituximab Tolerance in Cancerous B-Cells." *PloS One* 11(4):e0153069.

Reid J, Zamuner S, Edwards K, Rumley S, Sully K, Feeney M, Kumar S, Fernando D, Wisniacki N. T. 2016. "Targeting Oncostatin M in the Target Tissue: Assessment of in-Vivo Affinity and Target Engagement of an Anti-OSM Monoclonal Antibody By Combining Blood and Skin Blister Fluid Data [Abstract]." *Arthritis Rheumatol.* 68 (suppl.

Rhim, Andrew D. et al. 2012. "EMT and Dissemination Precede Pancreatic Tumor Formation." *Cell* 148(1–2):349–61.

Riaz, Nadeem et al. 2016. "Recurrent SERPINB3 and SERPINB4 Mutations in Patients Who Respond to Anti-CTLA4 Immunotherapy." *Nature Genetics* 48(11):1327–29.

Richards, Carl D. and Carl D. 2013. "The Enigmatic Cytokine Oncostatin M and Roles in Disease." *ISRN Inflammation* 2013:512103.

Ries, Carola H. et al. 2014. "Targeting Tumor-Associated Macrophages with Anti-CSF-1R Antibody Reveals a Strategy for Cancer Therapy." *Cancer Cell* 25(6):846–59.

Rishi, Arvind, Michael Goggins, Laura D. Wood, and Ralph H. Hruban. 2015. "Pathological and Molecular Evaluation of Pancreatic Neoplasms." *Seminars in Oncology* 42(1):28–39.

Robert, Caroline et al. 2011. "Ipilimumab plus Dacarbazine for Previously Untreated Metastatic Melanoma." *New England Journal of Medicine* 364(26):2517–26.

Robert, Caroline et al. 2014. "Anti-Programmed-Death-Receptor-1 Treatment with Pembrolizumab in Ipilimumab-Refractory Advanced Melanoma: A Randomised Dose-Comparison Cohort of a Phase 1 Trial." *The Lancet* 384(9948):1109–17.

Robert, Caroline et al. 2015. "Pembrolizumab versus Ipilimumab in Advanced Melanoma." *New England Journal of Medicine* 372(26):2521–32.

Rodriguez, P. C. et al. 2004. “Arginase I Production in the Tumor Microenvironment by Mature Myeloid Cells Inhibits T-Cell Receptor Expression and Antigen-Specific T-Cell Responses.” *Cancer Research* 64(16):5839–49.

Rossi, J. F. et al. 2010. “A Phase I/II Study of Siltuximab (CNTO 328), an Anti-Interleukin-6 Monoclonal Antibody, in Metastatic Renal Cell Cancer.” *British Journal of Cancer* 103(8):1154–62.

Royal, Richard E. et al. 2010. “Phase 2 Trial of Single Agent Ipilimumab (Anti-CTLA-4) for Locally Advanced or Metastatic Pancreatic Adenocarcinoma.” *Journal of Immunotherapy* 33(8):828–33.

Ruffell, Brian and Lisa M. Coussens. 2015. “Macrophages and Therapeutic Resistance in Cancer.” *Cancer Cell* 27(4):462–72.

Sainz, B. et al. 2015. “Microenvironmental hCAP-18/LL-37 Promotes Pancreatic Ductal Adenocarcinoma by Activating Its Cancer Stem Cell Compartment.” *Gut* 0:1–15.

Sainz, Bruno, Beatriz Martín, Marianthi Tatari, Christopher Heeschen, and Susana Guerra. 2014. “ISG15 Is a Critical Microenvironmental Factor for Pancreatic Cancer Stem Cells.” *Cancer Research* 74(24):7309–20.

Sakaguchi, S. et al. 2001. “Immunologic Tolerance Maintained by CD25+ CD4+ Regulatory T Cells: Their Common Role in Controlling Autoimmunity, Tumor Immunity, and Transplantation Tolerance.” *Immunol Rev* 182(8):18–32.

Salgado, M. et al. 2017. “Management of Unresectable, Locally Advanced Pancreatic Adenocarcinoma.” *Clinical and Translational Oncology* 1–6.

Sandhu, Shahneen K. et al. 2013. “A First-in-Human, First-in-Class, Phase I Study of Carlumab (CNTO 888), a Human Monoclonal Antibody against CC-Chemokine Ligand 2 in Patients with Solid Tumors.” *Cancer Chemotherapy and Pharmacology* 71(4):1041–50.

Sansone, Pasquale and Jacqueline Bromberg. 2012. “Targeting the Interleukin-6/Jak/stat Pathway in Human Malignancies.” *Journal of Clinical Oncology : Official Journal of the American Society of Clinical Oncology* 30(9):1005–14.

Schaefer, Annette et al. 2009. “Mechanism of Interferon-Gamma Mediated down-Regulation of Interleukin-10 Gene Expression.” *Molecular Immunology* 46(7):1351–59.

Schick, Charles et al. 1998. “Cross-Class Inhibition of the Cysteine Proteinases Cathepsins K, L, and S by the Serpin Squamous Cell Carcinoma Antigen 1: A Kinetic Analysis †.” *Biochemistry* 37(15):5258–66.

Scholz, Arne et al. 2003. "Activated Signal Transducer and Activator of Transcription 3 (STAT3) Supports the Malignant Phenotype of Human Pancreatic Cancer." *Gastroenterology* 125(3):891–905.

Schuringa, J. J., H. Timmer, D. Luttickhuizen, E. Vellenga, and W. Kruijer. 2001. "C-Jun and c-Fos Cooperate with STAT3 in IL-6-Induced Transactivation of the IL-6 Respone Element (IRE)." *Cytokine* 14(2):78–87.

SEER. 2017. "SEER DATABASE: Pancreatic Cancer Statistics." Retrieved (https://seer.cancer.gov/statfacts/html/pancreas.html).

Seidel, H. M. et al. 1995. "Spacing of Palindromic Half Sites as a Determinant of Selective STAT (Signal Transducers and Activators of Transcription) DNA Binding and Transcriptional Activity." *Proceedings of the National Academy of Sciences of the United States of America* 92(7):3041–45.

Shen, Zhanlong et al. 2013. "Macrophage Coculture Enhanced Invasion of Gastric Cancer Cells via TGF-β and BMP Pathways." *Scandinavian Journal of Gastroenterology* 48(4):466–72.

Sheshadri, Namratha et al. 2014. "SCCA1/SERPINB3 Promotes Oncogenesis and Epithelial-Mesenchymal Transition via the Unfolded Protein Response and IL6 Signaling." *Cancer Research* 74(21):6318–29.

Shien, Kazuhiko et al. 2017. "JAK1/STAT3 Activation through a Proinflammatory Cytokine Pathway Leads to Resistance to Molecularly Targeted Therapy in Non-Small Cell Lung Cancer."

Sinibaldi, D. et al. 2000. "Induction of p21WAF1/CIP1 and Cyclin D1 Expression by the Src Oncoprotein in Mouse Fibroblasts: Role of Activated STAT3 Signaling." *Oncogene* 19(48):5419–27.

Smigiel, Jacob M., Neetha Parameswaran, and Mark W. Jackson. 2017. "Potent EMT and CSC Phenotypes Are Induced by Oncostatin-M in Pancreatic Cancer." *Molecular Cancer Research*.

Snyder, M., X. Y. Huang, and J. J. Zhang. 2011. "Signal Transducers and Activators of Transcription 3 (STAT3) Directly Regulates Cytokine-Induced Fascin Expression and Is Required for Breast Cancer Cell Migration." *The Journal of Biological Chemistry* 286(45):38886–93.

Song, Yuhua et al. 2008. "Fra-1 and Stat3 Synergistically Regulate Activation of Human MMP-9 Gene." *Molecular Immunology* 45(1):137–43.

Steeg, Patricia S. 2016. "Targeting Metastasis." *Nature Reviews. Cancer* 16(4):201–18.

Stein, M., S. Keshav, N. Harris, and S. Gordon. 1992. “Interleukin 4 Potently Enhances Murine Macrophage Mannose Receptor Activity: A Marker of Alternative Immunologic Macrophage Activation.” *The Journal of Experimental Medicine* 176(1):287–92.

Su, S. et al. 2014. “A Positive Feedback Loop between Mesenchymal-like Cancer Cells and Macrophages Is Essential to Breast Cancer Metastasis.” *Cancer Cell* 25(5):605–20.

Sueoka, Kotaro et al. 2005. “Tumor-Associated Serpin, Squamous Cell Carcinoma Antigen Stimulates Matrix Metalloproteinase-9 Production in Cervical Squamous Cell Carcinoma Cell Lines.” *International Journal of Oncology* 27(5):1345–53.

Suminami, Y. et al. 2000. “Inhibition of Apoptosis in Human Tumour Cells by the Tumour-Associated Serpin, SCC Antigen-1.” *British Journal of Cancer* 82(4):981–89.

Taga, T. et al. 1989. “Interleukin-6 Receptor and a Unique Mechanism of Its Signal Transduction.” Pp. 713–22 in *Cold Spring Harbor Symposia on Quantitative Biology*, vol. 54.

Techasen, Anchalee et al. 2012. “Cytokines Released from Activated Human Macrophages Induce Epithelial Mesenchymal Transition Markers of Cholangiocarcinoma Cells.” *Asian Pacific Journal of Cancer Prevention* 13(SUPPL.1):115–18.

Thiery, Jean Paul. 2002. “Epithelial-Mesenchymal Transitions in Tumour Progression.” *Nature Reviews. Cancer* 2(6):442–54.

Thiery, Jean Paul, Hervé Acloque, Ruby Y. J. Huang, and M.Angela Nieto. 2009. “Epithelial-Mesenchymal Transitions in Development and Disease.” *Cell* 139(5):871–90.

Torres, Carolina et al. 2014. “Serum Cytokine Profile in Patients With Pancreatic Cancer.” *Pancreas* 43(7):1042–49.

Torroella-Kouri, M. et al. 2009. “Identification of a Subpopulation of Macrophages in Mammary Tumor-Bearing Mice That Are Neither M1 nor M2 and Are Less Differentiated.” *Cancer Research* 69(11):4800–4809.

Tsai, Jeff H., Joana L. Donaher, Danielle A. Murphy, Sandra Chau, and Jing Yang. 2012. “Spatiotemporal Regulation of Epithelial-Mesenchymal Transition Is Essential for Squamous Cell Carcinoma Metastasis. TL - 22.” *Cancer Cell* 22 VN-r(6):725–36.

Tse, Joyce C. and Raghu Kalluri. 2007. “Mechanisms of Metastasis: Epithelial-to-

Mesenchymal Transition and Contribution of Tumor Microenvironment." *Journal of Cellular Biochemistry* 101(4):816–29.

Tsuyama, S. et al. 1991. "Different Behaviors in the Production and Release of SCC Antigen in Squamous-Cell Carcinoma." *Tumour Biology : The Journal of the International Society for Oncodevelopmental Biology and Medicine* 12(1):28–34.

Turato, Cristian et al. 2015. "SerpinB3 and Yap Interplay Increases Myc Oncogenic Activity." *Scientific Reports* 5:17701.

Uemura, Y. et al. 2000. "Circulating Serpin Tumor Markers SCCA1 and SCCA2 Are Not Actively Secreted but Reside in the Cytosol of Squamous Carcinoma Cells." *International Journal of Cancer* 89(4):368–77.

Ullman, E., J. A. Pan, and W. X. Zong. 2011. "Squamous Cell Carcinoma Antigen 1 Promotes Caspase-8-Mediated Apoptosis in Response to Endoplasmic Reticulum Stress While Inhibiting Necrosis Induced by Lysosomal Injury." *Molecular and Cellular Biology* 31(14):2902–19.

Vidalino, Laura et al. 2009. "SERPINB3, Apoptosis and Autoimmunity." *Autoimmunity Reviews* 9(2):108–12.

Villano, Gianmarco et al. 2014. "Hepatic Progenitor Cells Express SerpinB3." *BMC Cell Biology* 15(1):5.

Vincent, A., J. Herman, R. Schulick, R. H. Hruban, and M. Goggins. 2011. "Pancreatic Cancer." *Lancet* 378(9791):607–20.

Wachsmann, M. B., L. M. Pop, and E. S. Vitetta. 2012. "Pancreatic Ductal Adenocarcinoma: A Review of Immunologic Aspects." *Journal of Investigative Medicine* 60(4):643–63.

Waddell, Nicola et al. 2015. "Whole Genomes Redefine the Mutational Landscape of Pancreatic Cancer." *Nature* 518(7540):495–501.

Wang-Gillam, Andrea et al. 2016. "Nanoliposomal Irinotecan with Fluorouracil and Folinic Acid in Metastatic Pancreatic Cancer after Previous Gemcitabine-Based Therapy (NAPOLI-1): A Global, Randomised, Open-Label, Phase 3 Trial." *The Lancet* 387(10018):545–57.

Wang, Liancai et al. 2010. "Clinical Significance of B7-H1 and B7-1 Expressions in Pancreatic Carcinoma." *World Journal of Surgery* 34(5):1059–65.

Wang, T. et al. 2004. "Regulation of the Innate and Adaptive Immune Responses by Stat-3 Signaling in Tumor Cells." *Nat Med* 10(1):48–54.

Wang, Xingyuan et al. 2017. “Bladder Cancer Cells Induce Immunosuppression of T Cells by Supporting PD-L1 Expression in Tumour Macrophages Partially through Interleukin 10.” *Cell Biology International* 41(2):177–86.

Wang, Y. et al. 2000. “Receptor Subunit-Specific Action of Oncostatin M in Hepatic Cells and Its Modulation by Leukemia Inhibitory Factor.” *Journal of Biological Chemistry* 275(33):25273–85.

Wang, Yuxin, Anette H. H. van Boxel-Dezaire, HyeonJoo Cheon, Jinbo Yang, and George R. Stark. 2013. “STAT3 Activation in Response to IL-6 Is Prolonged by the Binding of IL-6 Receptor to EGF Receptor.” *Proceedings of the National Academy of Sciences of the United States of America* 110(42):16975–80.

Wang, Zhipeng et al. 2013. “STAT3 Is Involved in Esophageal Carcinogenesis through Regulation of Oct-1.” *Carcinogenesis* 34(3):678–88.

Weber, Jeffrey S. et al. 2015. “Nivolumab versus Chemotherapy in Patients with Advanced Melanoma Who Progressed after Anti-CTLA-4 Treatment (CheckMate 037): A Randomised, Controlled, Open-Label, Phase 3 Trial.” *The Lancet Oncology* 16(4):375–84.

Weizman, N. et al. 2014. “Macrophages Mediate Gemcitabine Resistance of Pancreatic Adenocarcinoma by Upregulating Cytidine Deaminase.” *Oncogene* 33(29):3812–19.

West, N. R., J. I. Murray, and P. H. Watson. 2014. “Oncostatin-M Promotes Phenotypic Changes Associated with Mesenchymal and Stem Cell-like Differentiation in Breast Cancer.” *Oncogene* 33(12):1485–94.

White, R. R. et al. 2001. “Neoadjuvant Chemoradiation for Localized Adenocarcinoma of the Pancreas.” *Annals of Surgical Oncology* 8(10):758–65.

Winograd, R. et al. 2015. “Induction of T-Cell Immunity Overcomes Complete Resistance to PD-1 and CTLA-4 Blockade and Improves Survival in Pancreatic Carcinoma.” *Cancer Immunology Research* 3(4):399–411.

Wörmann, S. M., K. N. Diakopoulos, M. Lesina, and H. Algül. 2014. “The Immune Network in Pancreatic Cancer Development and Progression.” *Oncogene* 33(23):2956–67.

Wu, Christina et al. 2013. “Disrupting Cytokine Signaling in Pancreatic Cancer: A Phase I/II Study of Etanercept in Combination with Gemcitabine in Patients with Advanced Disease.” *Pancreas* 42(5):813–18.

Wu, Yongzhong, Iman Diab, Xueping Zhang, Elena S. Izmailova, and Zendra E. Zehner. 2004. “Stat3 Enhances Vimentin Gene Expression by Binding to the

Antisilencer Element and Interacting with the Repressor Protein, ZBP-89." *Oncogene* 23(1):168–78.

Wyckoff, Jeffrey et al. 2004. "A Paracrine Loop between Tumor Cells and Macrophages Is Required for Tumor Cell Migration in Mammary Tumors." *Cancer Research* 64(19):7022–29.

Xiong, Hua et al. 2012. "Roles of STAT3 and ZEB1 Proteins in E-Cadherin Down-Regulation and Human Colorectal Cancer Epithelial-Mesenchymal Transition." *Journal of Biological Chemistry* 287(8):5819–32.

Xu, Shili and Nouri Neamati. 2013. "gp130: A Promising Drug Target for Cancer Therapy." *Expert Opinion on Therapeutic Targets* 17(11):1303–28.

Yamashita, T. et al. 2010. "Oncostatin M Renders Epithelial Cell Adhesion Molecule-Positive Liver Cancer Stem Cells Sensitive to 5-Fluorouracil by Inducing Hepatocytic Differentiation." *Cancer Research* 70(11):4687–97.

Yang, Edward, Lorena Lerner, Daniel Besser, and James E. Darnell. 2003. "Independent and Cooperative Activation of Chromosomal c-Fos Promoter by STAT3." *Journal of Biological Chemistry* 278(18):15794–99.

Yang, Jinbo et al. 2007. "Unphosphorylated STAT3 Accumulates in Response to IL-6 and Activates Transcription by Binding to NF??B." *Genes and Development* 21(11):1396–1408.

Yeo, Theresa Pluth. 2015. "Demographics, Epidemiology, and Inheritance of Pancreatic Ductal Adenocarcinoma." *Seminars in Oncology* 42(1):8–18.

Yin, T. et al. 1993. "Involvement of IL-6 Signal Transducer gp130 in IL-11-Mediated Signal Transduction." *Journal of Immunology (Baltimore, Md. : 1950)* 151(5):2555–61.

Yu, H., H. Lee, A. Herrmann, R. Buettner, and R. Jove. 2014. "Revisiting STAT3 Signalling in Cancer: New and Unexpected Biological Functions." *Nat Rev Cancer* 14(11):736–46.

Zavoral, Miroslav, Petra Minarikova, Filip Zavada, Cyril Salek, and Marek Minarik. 2011. "Molecular Biology of Pancreatic Cancer." *World Journal of Gastroenterology* 17(24):2897–2908.

Zhang, D., M. Sun, D. Samols, and I. Kushner. 1996. "STAT3 Participates in Transcriptional Activation of the C-Reactive Protein Gene by Interleukin-6." *The Journal of Biological Chemistry* 271(16):9503–9.

Zhang, Jia et al. 2015. "Regulation of Epithelial-Mesenchymal Transition by Tumor-

Associated Macrophages in Cancer." *American Journal of Translational Research* 7(10):1699–1711.

Zheng, Xiaofeng et al. 2015. "Epithelial-to-Mesenchymal Transition Is Dispensable for Metastasis but Induces Chemoresistance in Pancreatic Cancer." *Nature* 527(7579):525–30.

Zhu, Y. et al. 2014. "CSF1/CSF1R Blockade Reprograms Tumor-Infiltrating Macrophages and Improves Response to T-Cell Checkpoint Immunotherapy in Pancreatic Cancer Models." *Cancer Research* 74(18):5057–69.

Zhu, Yu et al. 2017. "Tissue-Resident Macrophages in Pancreatic Ductal Adenocarcinoma Originate from Embryonic Hematopoiesis and Promote Tumor Progression." *Immunity* 47(2):323–338.e6.

Zorn, Emmanuel et al. 2006. "IL-2 Regulates FOXP3 Expression in Human CD4+CD25+ Regulatory T Cells through a STAT-Dependent Mechanism and Induces the Expansion of These Cells in Vivo." *Blood* 108(5):1571–79.

# Appendix

### Appendix 1. TCGA PDAC patient details

| Gender | Grade | Stage | T | N | M | Status | Follow Up (months) |
|---|---|---|---|---|---|---|---|
| MALE | G1 | 0 | 0 | N0 | MX | 0 | 52.99726 |
| MALE | G1 | 0 | TX | NX | MX | 0 | 47.21096 |
| FEMALE | G2 | 0 | T3 | N1 | MX | 0 | 12.75616 |
| FEMALE | G2 | IA | T1 | N0 | MX | 0 | 28.73425 |
| MALE | G1 | IB | T2 | N0 | MX | 0 | 60.95342 |
| FEMALE | G1 | I | T1 | 0 | MX | 0 | 84.09863 |
| FEMALE | G2 | IB | T2 | NX | MX | 0 | 68.51507 |
| FEMALE | G1 | IB | T2 | N0 | MX | 0 | 38.26849 |
| MALE | G1 | IB | T2 | N0 | MX | 0 | 30.6411 |
| FEMALE | G1 | IB | T2 | N0 | MX | 0 | 31.79178 |
| MALE | G2 | IA | T1 | N0 | MX | 0 | 29.62192 |
| MALE | G3 | IB | T2 | N0 | M0 | 0 | 2.465753 |
| MALE | G2 | IA | T1 | N0 | MX | 1 | 8.021918 |
| MALE | G2 | IB | T2 | N0 | MX | 0 | 0 |
| MALE | G3 | IA | T1 | N0 | MX | 0 | 0.09863 |
| FEMALE | GX | IA | T1 | N0 | MX | 0 | 2.991781 |
| MALE | G1 | IB | T2 | N0 | MX | 0 | 0.230137 |
| MALE | G3 | IB | T2 | N0 | M0 | 1 | 19.66027 |
| FEMALE | G2 | IB | T2 | N0 | M0 | 1 | 7.2 |
| FEMALE | G2 | IB | T2 | N0 | M0 | 1 | 4.734247 |
| FEMALE | G1 | IB | T3 | N1 | MX | 0 | 3.090411 |
| FEMALE | G2 | IB | T2 | N0 | M0 | 0 | 0.29589 |
| MALE | G2 | IB | T2 | N0 | M0 | 0 | 31.26575 |
| FEMALE | G2 | IB | T2 | N0 | M0 | 0 | 23.67123 |
| MALE | G3 | IIB | T3 | N1 | M0 | 1 | 2.169863 |
| MALE | G2 | IIB | T2 | N1 | M0 | 0 | 23.96712 |
| MALE | G2 | IIA | T3 | N0 | M0 | 1 | 9.632877 |
| MALE | G3 | IIB | T3 | N1 | M0 | 0 | 2.630137 |
| FEMALE | G1 | IIB | T3 | N1 | M0 | 1 | 20.6137 |
| MALE | G2 | IIB | T3 | N1 | M0 | 1 | 19.95616 |
| MALE | G2 | IIA | T3 | N0 | M0 | 0 | 21.79726 |
| MALE | G3 | IIB | T3 | N1 | M0 | 1 | 22.71781 |
| MALE | G3 | IIA | T3 | N0 | M0 | 0 | 22.06027 |
| FEMALE | G3 | IIA | T3 | N0 | M0 | 0 | 10.84932 |
| MALE | G2 | IIB | T3 | N1 | M0 | 0 | 15.91233 |
| MALE | G2 | IIB | T3 | N1 | M0 | 0 | 11.34247 |
| FEMALE | G4 | IIB | T3 | N1 | M0 | 0 | 11.67123 |
| FEMALE | G3 | IIA | T3 | N0 | M0 | 0 | 10.75068 |
| FEMALE | G2 | IIB | T3 | N1 | M0 | 0 | 10.48767 |
| MALE | G3 | IIB | T3 | N1 | M0 | 1 | 9.106849 |
| MALE | G4 | IIB | T3 | N1 | M0 | 1 | 21.43562 |
| MALE | G2 | IIB | T3 | N1 | MX | 1 | 4.70137 |
| MALE | G2 | IIB | T3 | N1 | M0 | 1 | 22.48767 |
| MALE | G3 | IIB | T3 | N1 | MX | 1 | 3.386301 |
| MALE | G3 | IIB | T3 | N1 | MX | 1 | 9.6 |
| MALE | G1 | IIB | T3 | N1 | MX | 0 | 30.04932 |
| MALE | G2 | IIB | T3 | N1 | MX | 0 | 23.60548 |
| MALE | G2 | IIA | T3 | N0 | MX | 1 | 20.84384 |
| FEMALE | G3 | IIB | T3 | N1 | MX | 1 | 7.364384 |
| FEMALE | G2 | IIB | T3 | N1 | MX | 1 | 24.26301 |
| MALE | G3 | IIB | T3 | N1 | MX | 1 | 15.05753 |
| MALE | G2 | IIB | T3 | N1 | MX | 1 | 10.12603 |
| MALE | G2 | IIB | T3 | N1 | MX | 0 | 12.39452 |
| MALE | G3 | IIB | T3 | N1 | MX | 0 | 71.40822 |
| MALE | G2 | IIA | T3 | N0 | MX | 1 | 71.73699 |
| MALE | G2 | IIB | T3 | N1 | M0 | 1 | 10.98082 |
| MALE | G1 | IIB | T3 | N1 | M0 | 0 | 9.69863 |
| MALE | G3 | IIB | T3 | N1 | M0 | 0 | 11.83562 |
| MALE | G1 | IIB | T3 | N1 | M0 | 1 | 7.10137 |
| FEMALE | G2 | IIB | T3 | N1 | M0 | 0 | 5.030137 |
| MALE | G2 | IIA | T3 | N0 | M0 | 0 | 5.194521 |
| MALE | G3 | IIB | T3 | N1 | M0 | 1 | 3.123288 |
| MALE | G2 | IIA | T3 | N0 | M0 | 0 | 5.490411 |
| FEMALE | G2 | IIB | T3 | N1 | MX | 0 | 0.131507 |
| MALE | G1 | IIB | T3 | N1 | MX | 0 | 0.230137 |
| FEMALE | G2 | IIB | T3 | N1 | M0 | 0 | 0.032877 |
| FEMALE | G2 | IIB | T3 | N1 | M0 | 0 | 0.032877 |
| MALE | G2 | IIA | T3 | NX | M0 | 0 | 5.457534 |
| MALE | G3 | IIB | T3 | N1 | MX | 1 | 15.94521 |
| MALE | G2 | IIB | T3 | N1 | MX | 1 | 37.15068 |
| FEMALE | G2 | IIB | T2 | N1 | MX | 0 | 7.49589 |
| FEMALE | G2 | IIA | T3 | N0 | MX | 1 | 12.52603 |
| MALE | G2 | IIB | T2 | N1 | MX | 1 | 34.81644 |

| | | | | | | | |
|---|---|---|---|---|---|---|---|
| MALE | G3 | IIB | T2 | N1 | MX | 0 | 7.430137 |
| MALE | G3 | IIA | T3 | N0 | MX | 1 | 15.55068 |
| MALE | G2 | IIB | T3 | N1 | MX | 1 | 4.043836 |
| FEMALE | G3 | IIB | T3 | N1 | MX | 1 | 5.030137 |
| FEMALE | G2 | IIB | T3 | N1 | MX | 1 | 1.019178 |
| FEMALE | G3 | IIB | T3 | N1 | M0 | 0 | 5.950685 |
| FEMALE | G3 | IIB | T3 | N1 | MX | 0 | 7.660274 |
| MALE | G2 | IIA | T3 | N0 | MX | 0 | 13.01918 |
| MALE | G2 | IIA | T3 | NX | MX | 1 | 4.208219 |
| FEMALE | G2 | IIA | T3 | N0 | MX | 0 | 7.627397 |
| FEMALE | G2 | IIB | T3 | N1 | M0 | 0 | 9.50137 |
| FEMALE | G1 | IIB | T3 | N1b | M0 | 0 | 64.20822 |
| MALE | G2 | IIA | T3 | N0 | MX | 0 | 8.284932 |
| MALE | GX | IIB | T3 | N1 | M0 | 0 | 28.2411 |
| MALE | G3 | IIB | T3 | N1 | MX | 0 | 29.91781 |
| FEMALE | G2 | IIB | T2 | N1 | MX | 1 | 17.49041 |
| MALE | G1 | IIB | T3 | N1 | MX | 0 | 7.890411 |
| MALE | G3 | IIB | T3 | N1 | M0 | 0 | 0.920548 |
| FEMALE | G2 | IIB | T3 | N1 | M0 | 0 | 0.657534 |
| FEMALE | G1 | IIB | T3 | N1 | MX | 0 | 0.131507 |
| MALE | G2 | IIA | T3 | N0 | MX | 0 | 0.263014 |
| FEMALE | G2 | IIA | T3 | N0 | MX | 0 | 12.13151 |
| MALE | G2 | IIB | T3 | N1 | MX | 0 | 11.86849 |
| MALE | G1 | IIB | T3 | N1 | MX | 0 | 0.263014 |
| MALE | G2 | IIB | T3 | N1 | MX | 0 | 0.789041 |
| FEMALE | G2 | IIB | T3 | N1 | MX | 0 | 0.690411 |
| MALE | G3 | IIB | T3 | N1 | MX | 1 | 3.945205 |
| FEMALE | G2 | IIA | T3 | N0 | MX | 0 | 0.920548 |
| FEMALE | G1 | IIB | T3 | N1 | MX | 0 | 0.526027 |
| FEMALE | G3 | IIB | T3 | N1 | MX | 0 | 0 |
| FEMALE | G2 | IIB | T2 | N1 | MX | 0 | 0.756164 |
| FEMALE | G2 | IIB | T3 | N1 | MX | 0 | 0.953425 |
| MALE | G2 | IIB | T3 | N1 | MX | 0 | 0 |
| MALE | G3 | IIB | T3 | N1b | MX | 0 | 6.378082 |
| MALE | G3 | IIB | T3 | N1 | MX | 0 | 1.512329 |
| FEMALE | G2 | IIB | T2 | N1 | MX | 0 | 0.361644 |
| MALE | G1 | IIB | T3 | N1 | MX | 0 | 0.427397 |
| FEMALE | G2 | IIB | T3 | N1 | MX | 0 | 1.084932 |
| MALE | G1 | IIB | T3 | N1 | MX | 0 | 0 |
| FEMALE | G1 | IIB | T3 | N1 | M0 | 1 | 49.38082 |
| MALE | G2 | IIB | T3 | N1 | M0 | 1 | 4.767123 |
| FEMALE | G2 | IIB | T3 | N1 | M0 | 1 | 15.35342 |
| FEMALE | G2 | IIB | T3 | N1 | M0 | 1 | 19.82466 |
| FEMALE | G2 | IIB | T3 | N1 | M0 | 0 | 15.64932 |
| MALE | G2 | IIB | T2 | N1 | M0 | 1 | 15.64932 |
| FEMALE | G2 | IIB | T3 | N1 | M0 | 0 | 27.97808 |
| MALE | G3 | IIB | T3 | N1 | M0 | 1 | 4.043836 |
| FEMALE | G2 | IIB | T3 | N1 | M0 | 1 | 3.616438 |
| FEMALE | G2 | IIA | T3 | N0 | M0 | 1 | 43.79178 |
| FEMALE | G1 | IIB | T3 | N1 | M0 | 1 | 15.8137 |
| FEMALE | G1 | IIB | T3 | N1 | M0 | 0 | 16.04384 |
| MALE | G3 | IIA | T3 | N0 | M0 | 1 | 3.846575 |
| FEMALE | G2 | IIB | T3 | N1 | M0 | 1 | 15.97808 |
| MALE | G2 | IIB | T3 | N1 | M0 | 0 | 6.378082 |
| MALE | G2 | IIB | T3 | N1 | M0 | 0 | 10.81644 |
| MALE | G2 | IIA | T3 | N0 | M0 | 0 | 9.863014 |
| FEMALE | G3 | IIB | T3 | N1 | M0 | 1 | 15.12329 |
| FEMALE | G2 | IIB | T3 | N1 | M0 | 0 | 0.263014 |
| MALE | G2 | IIB | T3 | N1 | M0 | 0 | 8.153425 |
| MALE | G3 | IIB | T3 | N1 | M0 | 1 | 1.347945 |
| MALE | G2 | IIB | T3 | N1 | MX | 1 | 8.219178 |
| MALE | G3 | IIB | T3 | N1 | MX | 0 | 5.950685 |
| MALE | G3 | IIB | T2 | N1 | M0 | 0 | 0.263014 |
| FEMALE | G3 | IIB | T3 | N1 | M0 | 1 | 7.857534 |
| MALE | G2 | IIB | T3 | N1 | M0 | 0 | 9.534247 |
| MALE | G2 | IIB | T3 | N1 | M0 | 1 | 6.016438 |
| MALE | G1 | IIB | T3 | N1 | M0 | 0 | 4.208219 |
| FEMALE | G2 | IIB | T3 | N1 | M0 | 0 | 5.884932 |
| MALE | G1 | IIB | T2 | N1 | M0 | 0 | 6.180822 |
| MALE | G3 | IIB | T3 | N1 | M0 | 0 | 5.030137 |
| MALE | G2 | IIB | T3 | N1 | M0 | 0 | 7.528767 |
| FEMALE | G3 | IIB | T3 | N1 | M0 | 0 | 5.884932 |
| FEMALE | G3 | IIB | T3 | N1 | M0 | 0 | 5.391781 |
| FEMALE | G2 | IIB | T3 | N1 | MX | 0 | 4.175342 |
| FEMALE | G1 | IIA | T3 | N0 | MX | 0 | 1.150685 |
| FEMALE | G3 | IIB | T3 | N1 | MX | 0 | 5.09589 |
| FEMALE | G2 | IIA | T3 | N0 | M0 | 0 | 19.2 |
| MALE | G1 | IIA | T3 | N0 | M0 | 0 | 3.616438 |
| FEMALE | G3 | IIB | T3 | N1 | MX | 0 | 8.120548 |
| MALE | G2 | IIB | T3 | N1 | MX | 0 | 3.452055 |
| FEMALE | G2 | IIB | T3 | N1 | MX | 0 | 1.183562 |

| | | | | | | | |
|---|---|---|---|---|---|---|---|
| MALE | G3 | IIB | T1 | N1 | MX | 0 | 1.380822 |
| MALE | G3 | IIB | T3 | N1 | MX | 0 | 13.05205 |
| FEMALE | G2 | IIB | T3 | N1 | MX | 0 | 6.476712 |
| FEMALE | G3 | IIB | T3 | N1 | MX | 1 | 23.07945 |
| FEMALE | G3 | IIB | T3 | N1 | MX | 1 | 22.84932 |
| MALE | G2 | IIA | T3 | N0 | MX | 0 | 27.74795 |
| FEMALE | G1 | IIB | T3 | N1b | MX | 1 | 16.8 |
| MALE | G3 | IIB | T3 | N1 | MX | 1 | 14.13699 |
| MALE | G2 | IIB | T3 | N1 | MX | 1 | 0.394521 |
| FEMALE | G2 | IIB | T3 | N1b | MX | 1 | 18.67397 |
| FEMALE | G2 | IIB | T3 | N1 | M0 | 0 | 5.391781 |
| FEMALE | G2 | IIB | T3 | N1 | MX | 0 | 6.641096 |
| MALE | G2 | IIA | T3 | N0 | MX | 0 | 6.180822 |
| MALE | G2 | IIB | T3 | N1 | MX | 0 | 5.260274 |
| FEMALE | G3 | IIB | T3 | N1 | MX | 0 | 60.29589 |
| FEMALE | G1 | IIA | T3 | N0 | M0 | 0 | 0.690411 |
| FEMALE | G2 | III | T4 | N0 | MX | 1 | 12.95342 |
| MALE | G2 | III | T4 | N0 | MX | 0 | 0.624658 |
| FEMALE | G1 | III | T4 | N1 | M0 | 0 | 0.558904 |
| FEMALE | G3 | IV | T3 | N0 | M1 | 0 | 0.164384 |
| MALE | G2 | IV | T3 | N0 | M1 | 0 | 19.82466 |
| FEMALE | G2 | IV | T3 | N1 | M1 | 0 | 11.40822 |
| FEMALE | G2 | IV | T3 | N1 | M1 | 0 | 5.293151 |